NKS-475
ISBN 978-87-7893-570-0

Source Term and Timing Uncertainty in Severe accidents NKS-STATUS Phase 2 report

Sergey Galushin[1]

Govatsa Acharya[2], Dmitry Grischenko[2], Pavel Kudinov[2]

Sara Ojalehto[3], Tuomo Sevón[3], Ilona Lindholm[3]

Patrick Isaksson[4], Elisabeth Tengborn[4]

Naeem Ul-Syed[5]

[1] Vysus Sweden AB

[2] KTH Royal Institute of Technology

[3] VTT Technical Research Centre of Finland Ltd

[4] SSM Swedish Radiation Safety Authority

[5] DSA Norwegian Radiation and Nuclear Safety Authority

July 2023

Abstract

The overall goal of the project is to generate a body of knowledge regarding the uncertainty in the magnitude of fission products release in case of a potential severe accident in Nordic nuclear power plants. The work aims to provide insights into the effect of various types of uncertainty on the source term predictions. Results of the work will be useful both for probabilistic and deterministic safety assessments as well as for emergency response applications.

Within the second phase of the project sensitivity and uncertainty analyses were performed for a set of risk significant accident scenarios identified by the review of PSA L2 for a typical Nordic BWR within the first phase of the project. These scenarios include accident sequences that lead to filtered containment venting in case of a transient or LOCA, and accident sequences that lead to containment failure due to ex-vessel phenomena in case of a transient or LOCA.

To perform sensitivity and uncertainty analyses, a review of available methods and tools for sensitivity analysis and uncertainty quantification was performed, selected methods were implemented in the simulation tools used in the project.

Sensitivity analysis was performed to identify the most influential MELCOR code modelling parameters for selected accident scenarios. These parameters involved in the modelling of core degradation and relocation, fission products release from fuel, debris behaviour in the core region and vessel lower head, vessel lower head failure, fission products behaviour in the RCS and the containment, as well as modelling of the filter trapping, containment sprays and pool scrubbing.

The most influential MELCOR code modelling parameters were then considered in quantification of uncertainty in the magnitude and timing of the fission products release to the environment.

Key words

Severe accident, uncertainty quantification, MELCOR, Nordic BWR, fission products, source term

NKS-475
ISBN 978-87-7893-570-0
Electronic report, July 2023
NKS Secretariat
P.O. Box 49
DK - 4000 Roskilde, Denmark
Phone +45 4677 4041
www.nks.org
e-mail nks@nks.org

Source Term and Timing Uncertainty in Severe accidents

Final Report from the NKS-R STATUS activity
(Contract: AFT/NKS-R(22)133/3)

Sergey Galushin[1],

Govatsa Acharya[2], Dmitry Grischenko[2], Pavel Kudinov[2]

Sara Ojalehto[3], Tuomo Sevón[3], Ilona Lindholm[3]

Patrick Isaksson[4], Elisabeth Tengborn[4]

Naeem Ul-Syed[5]

[1] Vysus Sweden AB

[2] KTH Royal Institute of Technology

[3] VTT Technical Research Centre of Finland Ltd

[4] SSM Swedish Radiation Safety Authority

[5] DSA Norwegian Radiation and Nuclear Safety Authority

NKS conveys its gratitude to all organizations and persons who by means of financial support or contributions in kind have made the work presented in this report possible.

Table of contents

1. Introduction

Analyzing and estimating risks is an integral part of both the industrial use and the public debate on nuclear power. At the same time, global climate change is increasing the demand for low-carbon sources of electricity, and the nuclear industry strives to maintain and expand its share of the global energy production. With these observations in mind it is reasonable to expect that the need for technological advances and reduction of uncertainties in both financial and radiological risks related to nuclear power will be as big as ever in the coming decades.

An important part of the risk profile of nuclear power relates to so-called severe accidents – i.e. events leading to a partly or fully damaged (melted) reactor core. State-of-the-art assessments of radiological risks related to such events relies on estimations of two fundamental quantities; their frequency and their consequence. As simple as these notions may seem, their quantification depends heavily on input data as well as on scope and complexity in the mathematical modelling used.

In so-called level 2 probabilistic safety assessments (L2 PSA), the main frequency estimate of interest is the large release frequency, (LRF), or sometimes the large early release frequency, (LERF). Assessing these frequencies based on summation over a large number of possible event sequences implies, among other things, that radioactive releases (the source term) need to be calculated for a set of representative scenario classes and compared to a pre-defined threshold to classify them as large or not large. These assessments are typically performed with integral plant response codes, such as ASTEC, MAAP or MELCOR, and are in themselves subject to uncertainty, both regarding the accident scenarios (aleatory uncertainty) and in the modelling of phenomena (epistemic uncertainty). Aleatory uncertainty arises from the natural variability of stochastic processes and cannot be reduced beyond this level, while epistemic uncertainty relates to our knowledge on systems, processes or parameters and can therefore be reduced by gathering more knowledge.

Typically, the source term evaluation is performed for a limited set of accident scenarios, using point-estimate values of epistemic uncertain parameters in the code used. Furthermore, such analyses typically do not consider the effect of epistemic uncertainty on interactions between physical phenomena or processes and transient accident scenarios, i.e. when different samples on the epistemic uncertainty range can significantly affect the course of the accident progression.

For some accident sequences, the standard practice, for the sake of conservatism, is to define the source term as everything escaping the containment. This creates a situation where a potentially very diverse family of realistic scenarios is represented by a set of assumed sequences that may contribute substantially to the LRF in a typical PSA L2. In this case, the uncertainty lies in the level of applied conservatism.

In both cases described above, source term uncertainty presents a challenge for any attempt to develop, use or increase the level of detail in L2 PSA results and merits targeted research solely on the basis of this.

Within the field of nuclear emergency preparedness towards severe accidents, the main goal is ultimately to be able to perform relevant and efficient actions to protect the public. The International Atomic Energy Agency (IAEA) states on the one hand that decisions on these actions should be based on observations of plant conditions, and on the other hand that decisions or protective actions should not be delayed by attempts to perform detailed source term estimates [1][2]. It is acknowledged that performing source term assessments with integral plant response codes is sufficiently complicated outside of accident conditions, which creates a need for simpler and faster tools for assessment of plant condition and source term estimation. One such tool is the Rapid Source Term Prediction (RASTEP) methodology, developed by Vysus Group. This method relies on a database on pre-calculated source term scenarios together with a probabilistic Bayesian Belief Network (BBN) model. The tool has the ability to take observed plant conditions and rescale results from L1-L2 PSA using conditional probabilities, logical relations and expert judgements. The output is a complete list of scenarios ranked by likelihoods, which is continuously updated with any new observations. In this way, current plant conditions can always be mapped to a representative class of scenarios. A problem arises if a RASTEP model (or any approach based on pre-calculated source terms) is used with overly conservative or uncertain data. Within emergency preparedness planning, source term uncertainties therefore also come with an operational aspect, directly impacting decisions taken in a stressful situation.

Within this project, the analysis of severe accident progression and fission products release to the environment are performed using MELCOR. MELCOR is a fully integrated, engineering-level computer code that models the progression of severe accidents in light water reactor nuclear power plants. A broad spectrum of severe accident phenomena in both boiling and pressurized water reactors is treated in MELCOR in a unified framework. These include thermal-hydraulic response in the reactor coolant system, reactor cavity, containment, and confinement buildings; core heatup, degradation, and relocation; core-concrete attack; hydrogen production, transport, and combustion; fission product release and transport behavior. Current uses of MELCOR include estimation of severe accident source terms and their sensitivities and uncertainties in a variety of applications [6][7].

It is our hope that this project will be able to shine some light on all of the abovementioned aspects of the source term uncertainty, limited to nordic Boiling Water Reactors (BWR).

2. Project scope and goals

The overall goal of the project is to generate a body of knowledge regarding the uncertainty in the magnitude of fission products release in case of a potential severe accident in Nordic nuclear power plants. The work aims to provide insights into the effect of various types of uncertainty on the source term predictions. Results of the work will be useful both for probabilistic and deterministic safety assessments as well as for emergency response applications.

Within the first phase of the project (see [23]) the participating organizations performed the analysis of the safety design of Swedish and Finnish Nordic BWRs and respective MELCOR modelling, review of the PSA L2 for a typical Nordic BWR design and identification of risk significant accident sequences, as well as the state-of-the-art review of the modelling of severe accident phenomena and identification of possible sources of uncertainty in severe accident progression and the source term. These uncertain parameters are involved in the modelling of core degradation and relocation, fission products release from fuel, debris behaviour in the core region and vessel lower head, vessel lower head failure, fission products behaviour in the RCS and the containment, as well as modelling of the filter trapping, containment sprays and pool scrubbing. A bounding assessment was performed for seven accident scenarios, that, according to the PSA L2 lead to acceptable (mitigated sequences and sequences with filtered release) and unacceptable (unmitigated sequences with failed containment isolation and containment failure due to ex-vessel phenomena) releases to the environment. The analysis identified the MELCOR code uncertain parameters that have significant effect on the code response, and one accident scenario where release category can change owing to uncertainties in the accident progression. Based on the results five accident scenarios were chosen for more detailed analysis in the second phase of the project.

The goal of the second phase of the project will be evaluation of the sensitivity of the magnitude of the fission products release in different accident scenarios (aleatory uncertainty) to the variability in deterministic modelling parameters (epistemic uncertainty), identification of the major contributors to the uncertainty, as well as quantification of the uncertainty in the results, and include the following tasks:

- Review of available methods for sensitivity analysis and uncertainty quantification and implementation of selected methods in the simulation platform.
- Sensitivity analysis of the MELCOR code predictions of the magnitude of fission products release to the environment in Swedish and Finnish plant configurations to variability in MELCOR modelling parameters identified in the first phase of the project.
- Review of available literature and experimental evidences regarding the most influential parameters and associated distribution.
- Quantification of the uncertainty in the magnitude of fission products release to the environment in Finnish and Swedish plant configurations due to variability of the most influential MELCOR modelling parameters.

The main outcome of the abovementioned tasks will be the evaluation of the sensitivity of the magnitude of the fission products release in different accident scenarios to the variability in deterministic modelling parameters (epistemic uncertainty), identification of the major contributors to the uncertainty, as well as quantification of the uncertainty in the results.

3. Background on Nordic Boiling Water Reactors

Designed by ASEA/ABB Atom, a total of 10 BWRs have been commissioned in Sweden and Finland since the first unit, Oskarshamn 1, was brought online in 1972. Two of the original design families, BWR69 and BWR75, are in operation today, distributed as four units in Sweden and two units in Finland, all with planned lifetimes extending to around 2040.

Over time, these reactors have evolved in partly different directions. The configurations of the sister reactors Forsmark 1/2 as well as Olkiluoto 1/2 are still more or less identical within the sites, while the differences between the sites are more marked.

3.1. Safety design

The Nordic Boiling Water Reactor (NBWR) will hereby be used as a common name for ~3300 MW_{th} BWRs designed by ASEA/ABB Atom. A summary of main technical data for the currently operational NBWRs is given in [3].

Table 3-1. Main technical data for operating NBWRs, some numbers rounded.

	O3/F3 (BWR75)	**F1/2 (BWR69)**	**OL1/2 (BWR69)**
Thermal power [MW]	3900/3300	3000/3250	2500
Reactor operating pressure [MPa]	7.0	7.0	7.0
Number of fuel elements [-]	700	676	500
Number of control rods [-]	169	161	121
Gas volume in containment [m^3]	8300/8500	6800	7600
Capacity of system [kg/s]:			
Containment drywell spray	300	360	250
Containment wetwell spray	400	N/A	120
Containment design pressure [MPa]	0.6	0.5	0.5
Containment operating pressure [MPa]	<0.1	<0.1	<0.1
Filtered containment venting pressure setpoint [MPa]	0.5	0.57	0.2/0.5-0.6*
Unfiltered containment venting pressure setpoint [MPa]	0.65		
Containment rupture pressure [MPa]	~1	~1	~1

*For wetwell venting in OL1/2, the drywell pressure needs to exceed the defined overpressure that depends on drywell gas temperature (total pressure 0.5-0.6 MPa). The drywell venting takes place if the water level in the wetwell is too high to allow venting from there, and the drywell pressure is higher than 0.2 MPa.

The safety design of the NBWRs is described further in the following.

The reactor pressure vessel (RPV) consists of carbon steel clad by stainless steel on the inside. The reactor containment is of the pressure suppression (PS) type with vertical blowdown pipes, and its outer cylindrical shell is made of pre-stressed concrete. It is sealed at the top by a large steel cupola which sits at the bottom of the reactor service pool. The containment also functions as a radiological shield to the environment. During normal operation, the containment gas volume is filled with nitrogen to prevent ignition of hydrogen if generated during a severe accident.

Details on the NBWR safety systems relevant for severe accident progression (and source term) are provided below:

- Hydraulic control rod insertion: The hydraulic actuating power shut-off system gives full insertion of all control rods within a few seconds after initiation. Should this system fail, an electromechanic system inserts the rods within a few minutes. If this also fails, boric acid can be added to the reactor vessel via a dedicated injection system.
- Pressure control and relief system: This system has several operating modes and can operate with battery backup only:
    - TA Function: The spring-operated part of the overpressure protection system will open valves stepwise, starting at slightly above 7 MPa to release steam and protect the RPV from catastrophic failure. After a properly controlled pressure transient, the system will continue to control the pressure to around 7 MPa.
    - TB Function (ADS): Activation of TB initiates steam discharge into the wetwell (WW) on setpoint 1 m below top of active fuel (TAF). The pressure is reduced to a level sufficient for water injection by the emergency core cooling system (ECCS) or the independent core cooling system. The TB function is at the same time leading to coolant being lost from the primary system quite rapidly, which leads to core uncover.
- Emergency core cooling system (ECCS): This is an AC power driven, low-pressure coolant injection system comprised of four independent trains, which can pump water to the reactor from the suppression pool. The system has activation setpoints on water level 2 m above TAF and low reactor pressure. Actual water injection will not occur unless the pressure difference between WW and downcomer (DC) is less than 1.25 MPa and the injection capacity is, in general, dependent on this pressure difference.
- Independent core cooling system: This is, in the Swedish configuration, an AC power driven injection system comprised of one independent train with one or several separate water sources as well as a dedicated diesel generator. In the Finnish configuration, this is a separate steam turbine driven injection system, taking suction from water storage tanks in the system for distribution of demineralised water.
- Auxiliary feedwater system (AFW): This is an AC power driven high-pressure coolant injection system comprised of four independent trains, which provides water to the reactor from the wetwell or from a separate storage tank into the downcomer. The system activation logics includes several different setpoints. Water injection is more or less independent of reactor pressure.
- Drywell flooding system: Flooding of drywell from the wetwell is initiated to provide cooling of melt fragmentation and debris in case of melt release from the reactor pressure vessel. The system is typically actuated on downcomer water level 2 m below the TAF for more than 10 minutes, or 30 minutes after containment isolation, depending on plant.
- Non-filtered containment venting system: This is a pressure relief directly to the ambient atmosphere designed for LOCA events with failing PS function. It is activated by the opening of a rupture disc at around 0.65 MPa containment pressure. The line is automatically closed by a shut-off valve 20 minutes after containment isolation signal. It should be noted that this containment isolation signal is triggered individually by any of the typical conditions that are indicative of a serious

event e.g. low reactor water level, high containment temperature, high containment pressure or triggered TB function.

- Filtered containment venting system: In the Swedish configuration, this is achieved from the upper drywell to the atmosphere via a multi-venturi scrubbing system situated in a separate building, equipped with a dedicated stack. Venting is activated by a rupture disc opening around 0.55 MPa containment pressure. In parallel with this rupture disc, two valves for manual depressurization are also installed for cases where additional capacity is required, e.g. when manual operation of the filtered venting is an option due to for instance favourable weather conditions.

  In the Finnish configuration, filtered venting can be done both from the wetwell and drywell to the atmosphere via a SAM-scrubber placed inside the reactor building. Wetwell venting is possible if the water level is below 14.5 m. The drywell pressure needs to exceed the defined overpressure that depends on drywell gas temperature. At a drywell temperature of 293 K, the threshold overpressure is 0.5 MPa.
  The drywell venting through a rupture disk takes place if the water level in the wetwell has been higher than 14.5 m for longer than a specified time (which precludes possibility of venting from wetwell) and the drywell pressure is higher than 0.2 MPa.

- Suppression pool: The suppression pool, located in the wetwell, is an inherently passive system designed to limit the containment pressure by use of the so-called PS function; Steam leaking or blown out from the primary system to the drywell will be pushed through blowdown pipes ending in the wetwell pool where the steam is condensed. Vacuum valves in large pipes between wetwell and lower drywell ensure that the wetwell pressure will not be higher than that of the drywell.
- Residual heat removal and containment spray system (RHR and CSS): This is an AC power driven system, comprised of four independent trains with heat exchangers, all recirculating water from the suppression pool. All four loops are connected to feed spray nozzles located in the containment. The safety functions of the system are to reduce the containment pressure by condensing steam in case of a LOCA, to remove heat from the suppression pool through a series of heat exchangers and to provide scrubbing of airborne fission products from the containment atmosphere in case of core damage.
- Independent containment heat removal and spray system: This is an EOP/SAMG spray system in the upper drywell (UDW) that takes water from an independent external water source. It can be used to reduce pressure in the containment as well as to provide scrubbing of airborne fission products. Water level control is provided in order to not damage the containment.

3.2.MELCOR models

3.2.1. Swedish MELCOR modelling of NBWR

The MELCOR model of NBWR used in this project is the further development of the input deck originally developed for the analysis of accidents in power uprated plants [4], mainly maintained by KTH. In this model, the core is represented by five non-uniform radial rings and eight axial levels. The 6^{th} ring represents the downcomer region (Figure 3-1).

The reactor pressure vessel (Figure 3-2) and the containment (Figure 3-3) are represented by 27 control volumes (CV), connected with 45 flow paths (FL) and 73 heat structures (HS). The vessel is represented by 6 rings and 19 axial levels, with the first 10 axial levels representing the lower plenum; the 11th axial level represents the core support plate; levels 12 and 19 represent the core inlet and outlet regions and structures; and levels 13-18 represent the active core region. Lower head penetrations for 66 instrumentation guide tubes (IGTs) are distributed between rings 1-5 proportionally to the cross-sectional area of these rings. Containment leakage is modelled from the drywell directly to the environment.

The containment is subdivided into control volumes for upper and lower drywell, wetwell, blowdown pipes and overflow pipes from lower drywell to wetwell.

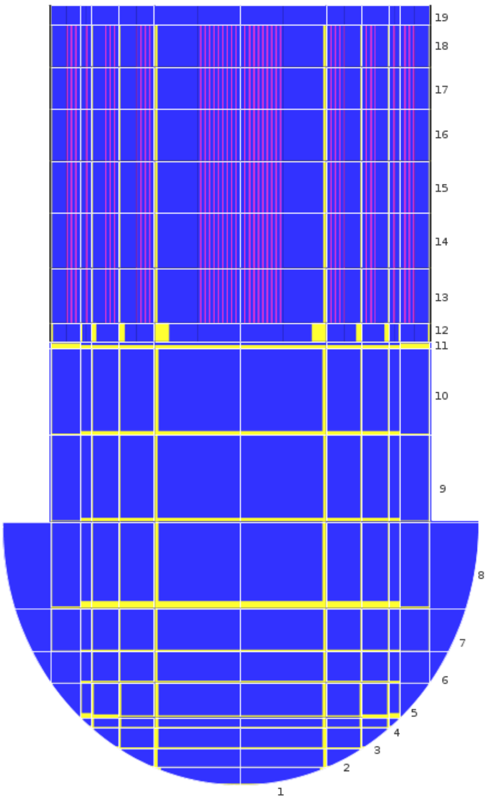

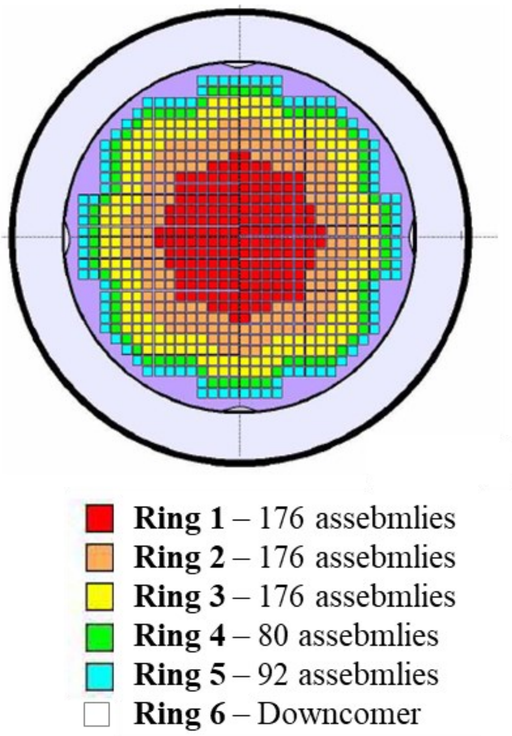

Figure 3-1. Swedish NBWR model COR nodalization.

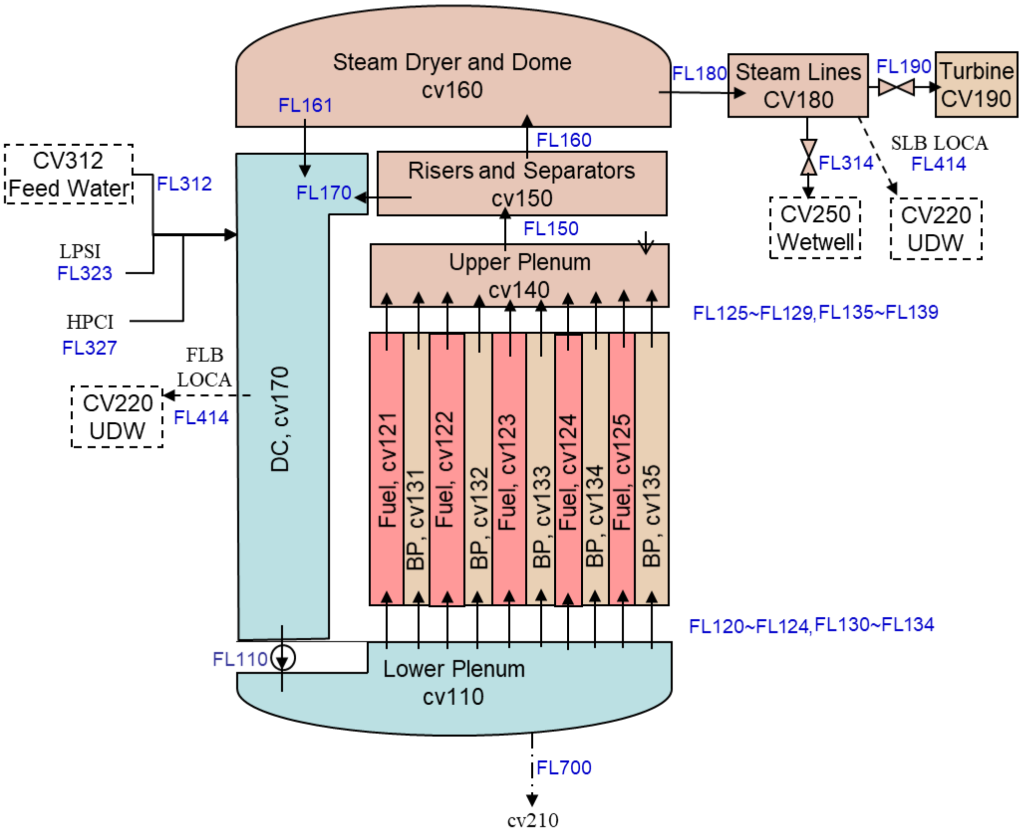

Figure 3-2. Swedish NBWR model CVH nodalization of the core.

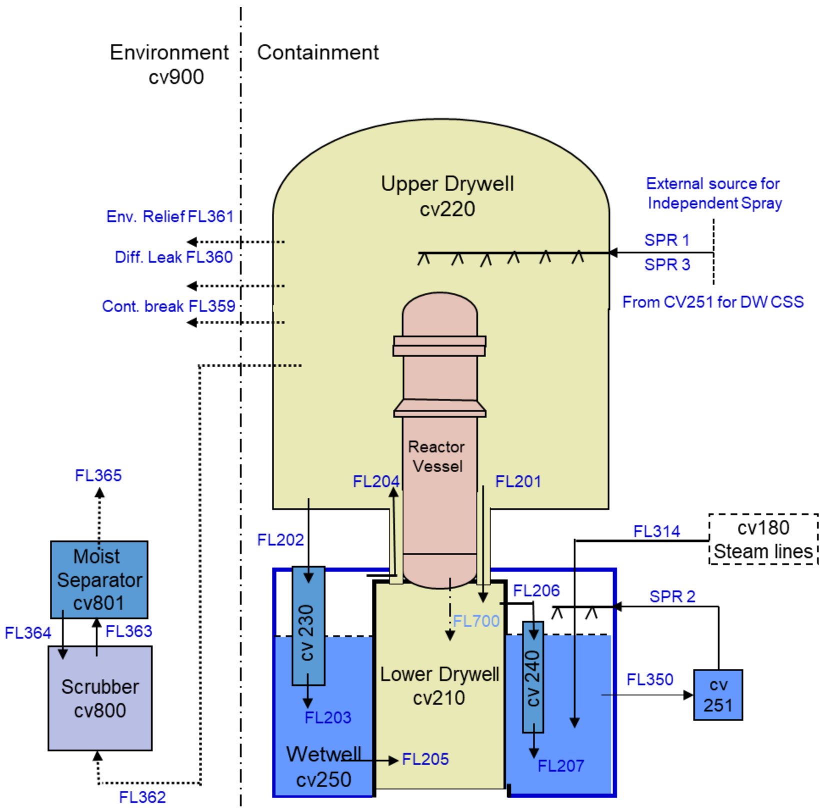

Figure 3-3. Swedish NBWR model containment nodalization.

The following safety systems are implemented in the model:

- Hydraulic control rod insertion
    - The effect of this system is modeled in MELCOR by fission power decrease (during 3.5 s) according to a tabular function at time zero.
- Pressure control and relief system
    - Both TA and TB valves as well as pipelines are implemented as a single flow path (FL314) from the steamlines to the wetwell, controlled by a set of control and tabular functions. SPARC pool scrubbing model is activated at the pool discharge end of the 314-pipes.
- Emergency core cooling system
    - All 4 trains are modeled by a single flow path (FL323) to the downcomer, with the number of trains and flow managed by a set of control functions. Flow rate vs. back pressure is controlled by a tabular function. The wetwell is used as water source for the system in the model and the injection is stopped on high suppression pool temperature.
- Auxiliary feedwater system.
    - All 4 trains are modeled by a single flow path (FL171) to the downcomer, with the number of trains and flow managed by a set of control functions. It is assumed that the system injects water with constant flow rate of 26 kg/s regardless of the pressure difference between DW and WW. The wetwell is used as water source for the system in the model and the injection is stopped on high suppression pool temperature.
- Drywell flooding system.
    - The system is implemented as a single flow path (FL205) from the wetwell to the lower drywell; the valves are controlled by a set of control functions. Together with the drywell flooding system an overflow pipe is modelled connecting the lower drywell and the wetwell to prevent lower drywell overfilling.
- Drywell blowdown pipes
    - A total of 24 drywell blowdown pipes are modelled from the drywell floor to the suppression pool. The diameter of the pipes is about 60 cm. The SPARC pool scrubbing model is activated at wetwell discharge at the end of the blowdown pipe. The blowdown pipes are purposed for the LOCA situations, when rapid and large steam release is able to clear the water in the pipes, and steam is driven into the suppression pool for condensation.
- Vacuum breakers
    - Vacuum breakers are modelled as a single flow path (FL204) that connects wetwell gas space with upper drywell to prevent wetwell pressure exceeding the drywell pressure.
- Non-filtered containment venting system.
    - Implemented as a single flow path (FL361) from the upper drywell to the environment, the rupture disk and shut-off valves are modelled as a set of control functions.
- Filtered containment venting system.

- Implemented by a set of flow paths and control volumes (c.f. Figure 3-3). The rupture disk and valves are controlled by a set of control functions. The actual filtering of substances containing radionuclides is modelled by simple filter factors based on system requirements.

- Residual heat removal and containment spray system.
  - Currently modelled as two sprays (SPR2 in the wetwell and SPR3 in the drywell). The wetwell spray (SPR2) represents up to 4 trains of the containment spray system with 100 kg/s per train, with a possibility to reroute up to 3 spray trains to the upper drywell. Control volume CV251 represents the heat exchangers in the residual heat removal system and used as a water (and temperature) source by the containment spray system and enthalpy source for the residual heat removal system.
- Independent containment spray system
  - Implemented as a single train system with flow path (SPR1) ending in the upper drywell. The capacity is 100 kg/s assuming a constant water source temperature at 293.15 K.

The MELCOR model does not include the newly implemented independent core cooling system. As the aim is to study source terms of severe accidents, i.e. cases where all core cooling fails, this is judged to be acceptable.

The MELCOR model is not built to treat cases with failing hydraulic control rod insertion, as sequences with failing reactor shutdown also require the electromechanical insertion and the boron injection to fail, thereby rendering this core damage mode a very small contributor in the PSA.

Note that steam lines, condenser and turbine plant are not modelled, as is also the case for the reactor building and its ventilation system. This implies that containment rupture or bypass cases will be conservative in terms of the source term, as any retention and delay in the turbine system or building structures will not be taken into account.

In the last few years, KTH has developed and demonstrated a systematic approach to quantification of uncertainty in severe accident scenarios and phenomena based on the Risk Oriented Accident Analysis Methodology framework (ROAAM+). The approach combines the most recent development in the areas of sensitivity analysis, uncertainty quantification and surrogate modeling approaches. In the previous ROAAM+ work the focus was on the quantification of uncertainty in containment failure probability. The next step in the ROAAM+ development is application to quantification of uncertainty in the source term.

3.2.2. Finnish MELCOR modelling of NBWR

VTT's MELCOR model of Olkiluoto 1&2 was developed for code version 1.8.2 in 1994. The model has been updated several times when new code versions have been taken into use. The latest update was made in 2017 by Magnus Strandberg who converted the model to MELCOR 2.1 with funding from the SAFIR2018 research program [5]. Systematic checking of the input deck or comparisons to current plant configuration have not been made for at least 19 years. The model is somewhat outdated because it does not follow current best modelling practices, and plant modifications are not included in the model.

The core nodalization is presented in Figure 3-4 (left). The core is modelled with five uniform radial rings; the sixth ring represents the downcomer region. The first three axial levels represent the lower plenum; the fourth axial level represents the core support plate; levels 5–14 represent the active core region; and level 15 represents the core outlet region.

The reactor thermal-hydraulic nodalization is presented in Figure 3-4 (right). There are 7 control volumes and 10 flow paths, plus one flow path from the core to the bypass that is opened upon failure of the channel boxes. The steam lines are not modelled as a separate volume. Instead, the steam to the safety relief valves is taken directly from the downcomer volume. The instrument guide tube penetrations in the lower head were added to the model during the current project.

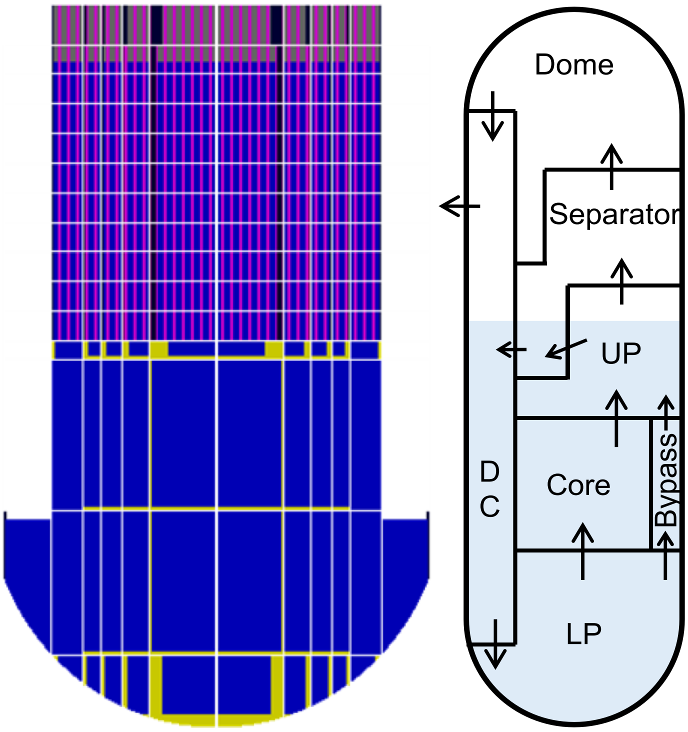

Figure 3-4. Finnish NBWR core model COR (left) and CVH (right) nodalization.

The containment is modelled with four control volumes, see Figure 3-5. The biological shield volume represents the space between the RPV and the concrete wall around it. The RPV lower head is interfaced with the biological shield volume. In addition, the model has six volumes representing rooms in the reactor building and a time-independent volume representing the environment. The control volumes of the reactor building represent major potential leakage routes from the containment to the reactor building and were purposed for hydrogen spreading and combustion analyses. The reactor building model is not purposed to model the entire complex RB configuration. Containment leakage is modelled from the drywell to the reactor building.

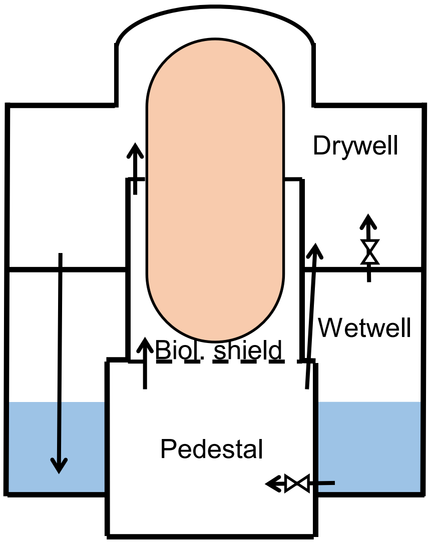

Figure 3-5. Finnish NBWR model containment nodalization.

The following systems are implemented in the Finnish NBWR MELCOR model:

- Hydraulic control rod insertion
  - Reactor scram is assumed to take place at time zero.
- Containment isolation
  - Closure of the main steam isolation valves (system 311) is activated by I-isolation or at a predefined time.
- Reactor main recirculation,
  - Modelled as a coast-down curve during the first 9.1 s of the calculation
- Pressure control and relief system
  - Relief valves controlled by downcomer pressure are modelled to discharge from the RPV downcomer to the suppression pool in the wetwell as four different groups: Group 1 opens when the downcomer pressure exceeds 8 MPa and closes when the pressure decreases below 7.4 MPa. The second group opens at 7.4 MPa and close at 7.1 MPa, the third group of valves opens at 8.5 MPa and closes at 7.6 MPa and the fourth group is open at pressure higher than 7.0 MPa and otherwise closed. The vertical discharge lines are submerged 4.5 meters in the suppression pool. SPARC pool scrubbing model is activated at the pool discharge end of the 314-pipes.
  - Automatic depressurization system of the reactor (314-ADS)

    Automatic depressurization is initiated on any of the following three signals:

    1) automatic TB signal

    2) manual TB signal

    3) on L4 signal lasting for the delay of 906 s.

    The automatic TB signal is generated if L4 signal is obtained and drywell pressure simultaneously exceeds 95 kPa and the drywell pressure increases faster than 130 Pa/s. The valve opening generates a delay of 15 s. The ADS blowdown takes place from the downcomer to the suppression pool at water submergence of 4.5 m. SPARC model is activated at the pool discharge end of the 314 pipes by input parameter.

- Emergency core cooling system
  - The system 323 injects water to the Upper Plenum (UP node) and takes suction from the suppression pool. The injection starts when L4 signal is obtained (downcomer water level goes below 28.25 m (0.5 meters above TAF)) and the 323 pumps run until the water level in the downcomer reaches 32.25 m (= 4.5 meters above TAF). There are four (4) pumps with each having the capacity ranging from a maximum of 115 kg/s to zero at respective downcomer counter pressure range from 0.1 MPa to 1.0 MPa. The initiation of 323 injection to core spray requires also that suppression pool heat removal recirculation mode (system 322) is first locked-off.
- Auxiliary feedwater system
  - System 327 injects coolant to downcomer (50%) and to upper plenum via core spray spargers (50%). The system incorporates four (4) piston-driven pumps that produce constant water flow rate of 25 kg/s per pump independently of counter-pressure up to the pressure 2.0 MPa. The signals L2 and L3 are received when the collapsed water level in the downcomer becomes less than 2.9 m and less than 1.8 m above the top of active fuel (TAF), respectively (i.e. DC water height is less than 30.65 m and 29.55 m). Two 327 pumps start to inject water to downcomer when L2 signal is reached and a 10-s pump delay has elapsed. The DC injection continues until the collapsed water height in the DC reaches 4.0 meters above TAF. The 327 injection with two pumps through core spray spargers initiates from L3 signal with a 10-s pump delay and continues until the DC collapsed level reaches 4.5 meters above TAF.
- Failure of reactor lower head
  - A flow path from the reactor lower plenum to the pedestal is opened when MELCOR calculates lower head failure. The flow area is determined by MELCOR.
- Vacuum breaker between wetwell and drywell
  - Vacuum breakers are modelled as valves between the wetwell and the drywell near the ceiling of the wetwell. The vacuum breakers are purposed to relief wetwell pressure in situations where non-condensable gases accumulate in the wetwell thus diminishing steam suppression in the wetwell pool. The valves open when the pressure in 10 kPa higher in the wetwell than in the drywell. After pressure balancing to the level 1000 Pa the valves are fully closed.
- Drywell-wetwell leak
  - A small leakage between the wetwell and drywell is modelled, the leak area is assumed to increase with drywell pressure being at least 0.01 m2 at drywell pressure higher than 0.5 MPa.
- Drywell blowdown pipes
  - A total of 16 drywell blowdown pipes are modelled from the drywell floor to the suppression pool with a submergence depth of 6.5 m. The diameter of the pipes is about 60 cm. The SPARC pool scrubbing model is activated at wetwell discharge at the end of the blowdown pipe. The 316 pipes are purposed for the LOCA

situations, when rapid and large steam release is able to clear the water in the pipes, and steam is driven into the suppression pool for condensation.

- Containment heat removal and spray system
  - Drywell spray starts on I-isolation signal or by manual activation of the operator. The 322 system is also used for wetwell pool cooling in recirculation mode. A heat exchanger aligned in the 322 recirculation loop removes 172 kJ/K/kg from the pool water with flow capacity of 45 kg/s. The cut-off pool temperature for recirculation cooling is 291 K. Manual starting of spray requires that the water level in the drywell is lower than 2.5 m. The drywell spray flow rate is 60 kg/s.
  - The 322 spray can also be aligned to sprinkle wetwell airspace. The flow rate is then 30 kg/s. The initiation signal is I-isolation or manual start.
- Drywell flooding.
  - Assumed within 30 minutes in a station blackout situation.
- Filtered containment venting system
  - Wetwell venting is possible if the water level is below 14.5 m. The vent line elevation in the wetwell is 17.5 m. The drywell pressure needs to exceed the defined overpressure (to ambient pressure) that depends on drywell gas temperature in the following way: at a drywell temperature of 293 K, the threshold overpressure is 0.5 MPa and at 453 K the threshold is 0.4 MPa. The actual filtering of substances containing radionuclides is modelled by simple filter factors based on system requirements.
  - The drywell venting through a rupture disk takes place if the water level in the wetwell has been higher than 14.5 m for longer than a specified time (which precludes possibility of venting from wetwell) and the drywell pressure is higher than 0.2 MPa.
- Reactor building blow-off panel
  - opening at a pressure difference of 2.5 kPa to the environment.

4. Methods and Tools for Sensitivity and Uncertainty Analysis with MELCOR code

4.1.Methods used for sensitivity and uncertainty analysis

4.1.1. Sensitivity analysis

The sources of uncertainty in analysis of severe accident progression are numerous and it is impractical to address all of them quantitatively. Experience in performing uncertainty studies of severe accident phenomena (e.g. [15][16][17][18]) suggests that the effects of uncertainties from some sources are larger and more dominant than the effects of uncertainties from other sources. In an integral sense, then, the aggregate uncertainty in main figures of merit (FOMs) can be estimated by selecting the dominant sources of uncertainty and treating them in detail. The dominant sources of uncertainty should be identified by sensitivity analysis.

A review of global sensitivity analysis methods (see [12] for more details) presents a brief summary on a great variety of different sensitivity analysis methods. Figure 4-1 provides a synthesis of SA methods presented in the paper.

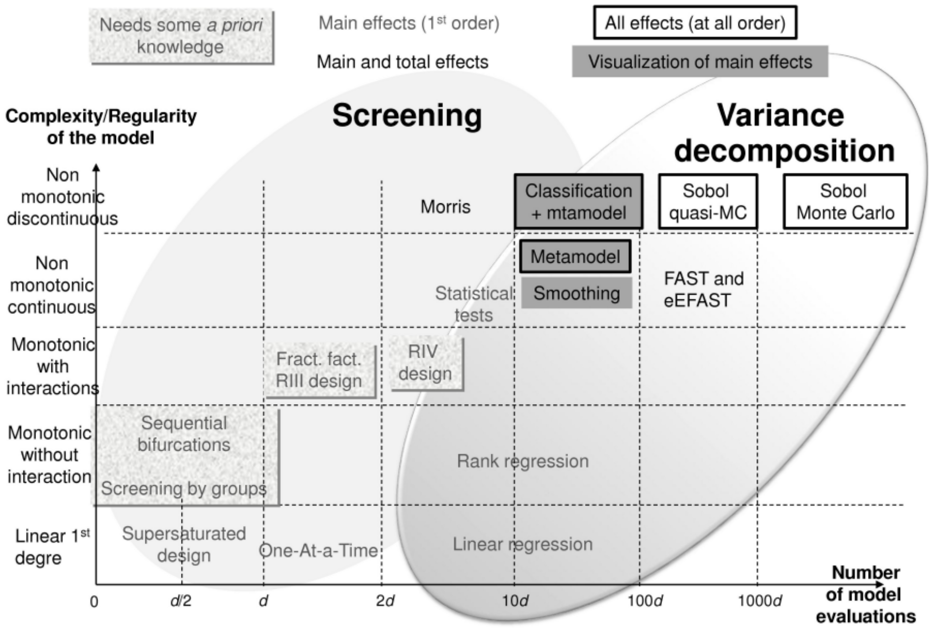

Figure 4-1. SA methods graphical synthesis [12].

Based on the review, the Morris method has been selected as an appropriate tool to perform sensitivity analysis. The Morris method is a screening method that can be applied to models with non-monotonic and discontinuous behavior. Furthermore, based on [8][12] the Morris method should give reasonable results given relatively low computational effort (from approximately *2d* to *10d* model evaluations, where *d* is the number of uncertain parameters).

4.1.1.1. Morris method for sensitivity analysis

The Morris method [9] is a global sensitivity analysis method. The Morris method performs analysis of the model outputs along different trajectories in the input space where parameters are varied "one-factor-at-a-time" (OAT) and the effect of changing every parameter is evaluated through elementary effects - $d_i(x^j)$ calculated by:

$$d_i(x^j) = \frac{[f(x^{i+1}) - f(x^i)]}{\Delta} \tag{1}$$

where $f(x)$ – is the model function, x^j – j-th input vector, Δ - variation step, which is linked to the number of levels (p) as follows:

$$\Delta = \frac{p}{2(p-1)} \tag{2}$$

The number of levels - p and number of elementary effects – r, are defined by a user. The large values of p will require large number of r to be calculated to have reasonable coverage on input domain. Based on [8] the recommended choice for the number of elementary effects is $r = 10$ (or at least $r \geq 4$), and the number of levels should be equal to $p = 4$.

When r – elementary effects are calculated for each input parameter, two sensitivity measures are used:

$$\mu_i = \sum_{i=1}^{r} \frac{|d_i|}{r}; \sigma_i = \sqrt{\sum_{i=1}^{r} (d_i - \mu)^2 / r} \tag{3}$$

where the values of μ_i , substantially different from zero, indicate significant overall influence of i^{th} input; and large values of σ_i indicate possible interactions with other input parameters and non-linear behaviour of the output with respect to the input.

The number of model evaluations to be performed is calculated by

$$N = r * (k + 1) \tag{4}$$

where k is the number of input factors and r is the number of elementary effects.

The Morris method for SA is available in the Dakota package [10]. A pyDakota coupling interface for Morris SA has been developed and implemented in pyMELCOR simulation platform (see section 4.1.3). It performs processing of the user input and generation of the sampling set, as well as processing of the results and generation of sensitivity analysis results.

4.1.1.2.One-way ANOVA

One-way ANOVA can be used to perform analysis of variance in the data set produced by Morris method for SA. The levels p and variation step Δ divide the space of the model input parameters into the subsets where each parameter has an unique fixed value. The variance within each subset can be analyzed whether the subsets means are equal (null hypothesis).

The F-statistic can be used to judge the effect/importance of the parameter in question, i.e., as F-value is defined as variation between sample means vs. variation within the samples, large F>>1 values can indicate that the parameter has significant effect on the results.

4.1.2. Uncertainty analysis

Uncertainty quantification (UQ) is the process of determining the effect of input uncertainties on model responses. These input uncertainties may be characterized as either aleatory uncertainties, which are irreducible variabilities inherent in nature, or epistemic uncertainties, which are reducible uncertainties resulting from a lack of knowledge. Since sufficient data is generally available for aleatory uncertainties, probabilistic methods are commonly used for computing response distribution statistics based on input probability distribution specifications. Conversely, for epistemic uncertainties, data is generally sparse, making the use of probability theory questionable and often leading to non-probabilistic methods based on e.g., interval specifications (Dempster-Shafer evidence theory) [10].

The objective of evidence theory is to model the effects of epistemic uncertainties. Epistemic uncertainty refers to the situation where one does not know enough to specify a probability distribution on a variable. Sometimes epistemic uncertainty is referred to as subjective, reducible, or lack of knowledge uncertainty. In Dempster-Shafer theory of evidence, the uncertain input variables are modelled as sets of intervals. The user assigns a basic probability assignment (BPA) to each interval, indicating how likely it is that the uncertain input falls within the interval. The intervals may be overlapping, contiguous, or have gaps. The intervals and their associated BPAs are then propagated through the simulation to obtain cumulative distribution functions on belief and plausibility. Belief is the lower bound on a probability estimate that is consistent with the evidence, and plausibility is the upper bound on a probability estimate that is consistent with the evidence [10][14].

Alternatively, ROAAM+ methods can be employed, which make use of the second order probabilities [13]. The ROAAM+ framework for Nordic BWR employs the concept of second-order probability in quantification of the conditional containment failure probability. The need for the second-order probabilities comes from the realization of the nature of epistemic uncertainties in prediction of failure probability (i.e., partial probabilistic knowledge). Epistemic uncertain parameters in ROAAM+ framework is separated into two groups, depending on the degree of knowledge:

- Model deterministic parameters – complete probabilistic knowledge (i.e., range and probability distribution).
- Model intangible parameters – incomplete or no probabilistic knowledge, one can only speculate regarding the possible range.

Based on ROAAM+ formulation, since probabilities are designed to handle uncertainty, it would be logical to consider representing uncertain probabilities with probabilities. Thus, in order to assess the importance of the missing information about the distributions of intangible parameters the distributions itself are considered as uncertain (i.e., parameters that characterize distributions, as in hierarchical Bayesian models).

4.1.2.1.Sampling-based uncertainty propagation

An analysis outcome of a model will have an uncertainty structure that derives from the uncertainty structure of the model input parameters. For uncertainty propagation through a model, it is important that the sampling set of model input parameters provides an adequate coverage of the space of these parameters. Adequate coverage of the uncertainty space of model input parameters depends on various factors, such as the number of samples, selected probability distributions as well as the choice of sampling approach.

4.1.2.2.Number of samples

Wilks' non-parametric method for setting tolerance limits is one of the common choices to determine tolerance limits with some confidence level for input parameters with unknown distributions in computational applications in the nuclear industry. The advantage of Wilks' method is the required sample size is independent of the number of input parameters and all input parameters can be sampled simultaneously.

Table 4-1 provides the minimum sample size N required to obtain various tolerance/confidence upper bounds (one sided) and intervals (two-sided) for ranks from 1 to 10. It shows that larger sample sizes N are required to increase the tolerance and the confidence. In addition, higher rank order statistics require an increase in the number of samples [19].

Table 4-1. Minimum sample size required for tolerance/confidence Wilks tolerance limits and bounds. Results are shown for four common tolerance/confidence combinations for ranks from 1 to 10 [19].

r	95%/95%		95%/99%		99%/95%		99%/99%	
	Bound	Interval	Bound	Interval	Bound	Interval	Bound	Interval
1	59	93	90	130	299	473	459	662
2	93	153	130	198	473	773	662	1001
3	124	208	165	259	628	1049	838	1307
4	153	260	198	316	773	1312	1001	1596
5	181	311	229	371	913	1568	1157	1874
6	208	361	259	425	1049	1818	1307	2144
7	234	410	288	478	1182	2064	1453	2409
8	260	458	316	529	1312	2306	1596	2669
9	286	506	344	580	1441	2546	1736	2925
10	311	554	371	631	1568	2784	1874	3179

Higher rank Wilks' estimates correspond to using more centrally located order statistics to estimate the desired tolerance limit. These estimates require larger sample sizes but estimate the same tolerance with approximately equal confidence [19].

4.1.2.3.Random and LHS Sampling

Random sampling is a part of the sampling technique in which each sample has an equal probability of being chosen.

A sample chosen randomly is meant to be an unbiased representation of the total population. Latin hypercube sampling (LHS) is a statistical method for generating a near-random sample of parameter values from a multidimensional distribution. When sampling a function of N variables, the range of each variable is divided into M equally probable intervals. M sample points are then placed to satisfy the Latin hypercube requirements; this forces the number of divisions, M, to be equal for each variable. This sampling scheme does not require more samples for more dimensions (variables); this independence is one of the main advantages of this sampling scheme. Another advantage is that random samples can be taken one at a time, remembering which samples were taken so far.

Both random and LHS sampling techniques are available in the Dakota[1] package [10]. A pyDakota interface for random and LHS sampling in Dakota has been developed. It performs user input processing (parameters, ranges and distributions) and generation of the sampling set. Currently, the interface supports truncated normal, truncated lognormal, uniform, loguniform, triangular, exponential, beta, gamma and Weibull distributions, as well as discrete real and integer sets with predefined probabilities. Furthermore, the sampling accounts for correlations among the variables, which can be defined by a user-supplied correlation matrix.

[1] Dakota is an open-source Multilevel Parallel Object-Oriented Framework for Design Optimization, Parameter Estimation, Uncertainty Quantification, and Sensitivity Analysis developed by SNL.

4.1.2.4. Importance sampling

Importance sampling is a method that allows one to estimate statistical quantities such as failure probabilities in a way that is more efficient than Monte Carlo sampling. The core idea in importance sampling is that one generates samples that are preferentially placed in important regions of the space (e.g. in or near the failure region or user-defined region of interest), then appropriately weights the samples to obtain an unbiased estimate of the failure probability [10].

Importance sampling technique can be applied when performing post-processing of the uncertainty analysis results, to assess the effect of missing information regarding probability distributions of intangible parameters (see section 4.1.2).

4.1.3. MELCOR simulation platform

A simulation platform (pyMELCOR) has been developed in Python to perform sensitivity and uncertainty analysis with MELCOR code.

Based on the user input, the pyDakota interface generates an input file for sensitivity/uncertainty analysis using Dakota [10]. The simulation driver (pyMELCOR) generates a set of MELCOR input decks and performs parallel execution of the MELCOR code. In case of code convergence issues and crashes, pyMELCOR performs adaptive refinement of the maximum time step and restarting in case of crashed simulations. The plot data (FOMs and other MELCOR code plot variables defined by the user) is extracted using the pyPTF extraction script, written in Python based on the MELCOR plot file format described in [11]. The extracted data is stored in the MELCOR database of solutions, while FOMs are analyzed in the Dakota package [10].

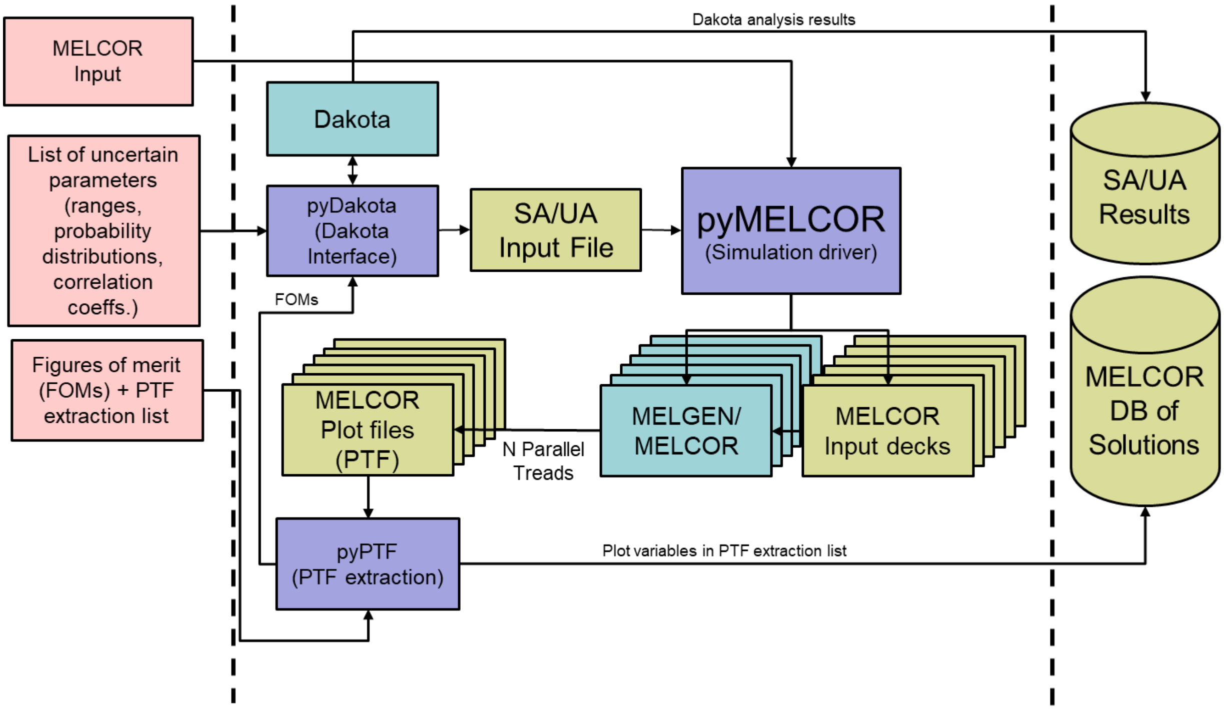

Figure 4-2. pyMELCOR simulation platform.

4.2. Methods used for sensitivity and uncertainty analysis by VTT

VTT's method of choice for both the sensitivity and uncertainty analyses was Dakota SNAP plug-in, which was used to sample the model parameters and to post-process majority of the results.

SNAP (Symbolic Nuclear Analysis Package) is an analysis tool developed by ISL (Information Systems Laboratories), and it consists of multiple integrated analysis code applications such as MELCOR, CONTAIN, and TRACE. It enables the creation and editing of model inputs, as well as setting up job streams and running the models and the other codes. SNAP also provides a robust visualization of the models [37].

Dakota (Design Analysis Kit for Optimization and Terascale Applications) toolkit has been developed by Sandia National Laboratories (SNL) for optimization and uncertainty quantification [38]. The SNAP plug-in for Dakota enables the addition of the uncertainty step in the job stream in SNAP. The main tasks of the uncertainty step are parameter sampling according to the user-input data (sampling method, target probability and confidence levels, bounds of the parameter values, probability distributions) of which Dakota calculates the adequate number of samples using the Wilks method mentioned in chapter 4.1.2.2, and post-processing of the results into a report form.

Using Dakota with SNAP is not necessarily straightforward. One well-known issue with the plug-in is that if even one of the generated MELCOR input files fail during the MELGEN step, no Dakota report is generated at the end of the simulation run. Crashes during the MELCOR step might not prevent Dakota from generating the report. It should however be noted, that "wrong" results resulting from code crashes will affect the final results of the sensitivity and uncertainty studies.

Moreover, even though the SNAP plug-in for Dakota uses the actual Dakota code, the features within SNAP are rather limited. For example, there seems not to be an intuitive way to use Morris method for sensitivity analysis. For this reason, the traditional one-at-time method (called OAT, too), in which the parameters are varied one at time while the others are kept constant, is used. The strengths of OAT method are its simplicity, easy interpretability of its results and easy isolation of individual parameter effects. However, OAT leans heavily on the assumption of linearity, and it assesses only the effect of individual input parameters, ignoring nonlinearities and the possible interactions between multiple parameters. This has arisen concerns about its reliability [39]

Dakota calculates multiple correlation coefficients that can be used in assessing the sensitivity of the model against the input parameters. The first one is called simple correlation coefficient in Dakota, but it is also known as Pearson correlation coefficient. It measures the linear correlation between two datasets, in this case between the parameter and the FOM. Pearson correlation between variables x and y can be calculated with [38].

$$Corr(x,y) = \frac{\sum_i (x_i - \bar{x})(y_i - \bar{y})}{\sqrt{\sum_i (x_i - \bar{x})^2 \sum_i (y_i - \bar{y})^2}} \tag{5}$$

The second coefficient is called partial correlation coefficient. In addition to the linear correlation between two variables, it also considers the effect of the other parameters. In OAT sensitivity study this coefficient is not very relevant. Both coefficients also have a rank form. The rank form of Pearson correlation coefficient is called simple rank correlation coefficient in Dakota and Spearman correlation coefficient elsewhere. The difference between the original correlation and rank correlation is that instead of actual values, rank correlation coefficients are calculated from the ranks of the datasets. This way, the effect of possible outliers in datasets can be minimized.

Uncertainty study is performed in a similar way as the sensitivity analysis, using SNAP with Dakota plug-in. Instead of OAT method, all the interesting parameters are varied simultaneously. The LHS sampling is done with Dakota, calculation itself with MELCOR in SNAP, and post processing with Dakota.

5. Results

5.1.Sensitivity analysis RC4 – Swedish plant configuration

During the first phase of the project KTH performed best estimate and bounding calculations for RC4A (unmitigated LOCA with containment failure due to ex-vessel phenomena at RPV melt-through) and RC4B (unmitigated SBO with containment failure due to ex-vessel phenomena at RPV melt-through) with splinter scenarios, considering solid debris ejection mode ON (IDEJ0) or OFF (IDEJ1). The same procedure of performing sensitivity and uncertainty analysis for 2 scenarios each of RC4A and RC4B is followed here.

The calculations performed in the first phase were limited to the first 24h after initiating event. It was observed that the environmental releases of CS and I2 (FOMs) were largely increasing without reaching a steady state, and hence the calculations were rerun for 72h after initiating event. Of the initial 73 cases, parameters that significantly affected the FOM (<-50% and >50% from the best estimate case) were identified and are listed in Table 5-1. Out of 50 parameters, 26 were screened to be of importance to the release fraction. Of them 19 parameters were identified to be significant to LOCA, while 15 were identified to be significant to SBO.

Table 5-1. Selected MELCOR parameters for SA and their ranges.

No	Model	Parameter name	Range	Units	Scenario
1	Fission product release from fuel	SC710641	241000 - 381400	J/kg-mole	LOCA/SBO
2		SC710651	0.000006 - 0.00001	M	SBO
3	Core degradation and relocation	TUO2ZRO2	2450 - 2800	K	LOCA
4		FCELRA	0.1 - 0.25		LOCA
5		HFRZSS	1000 - 2500	W/m2-K	LOCA
6		SC11312	2100 - 2500	K	LOCA/SBO
7	RPV lower head failure	TPFAIL	1273 - 1600	K	SBO
8		HDBPN	100 - 1000	W/m2-K	LOCA/SBO
9	Fission product and aerosol dynamics	GAMMA	1 - 3		LOCA/SBO
10		STICK	0.5 - 1		LOCA
11		RHONOM	1000 - 4900	kg/m3	SBO
12		TURBDS	0.00075 - 0.00125	m2/s3	LOCA/SBO
13		SC7111I1	4.2347 - 5.7293	A	LOCA
14		SC7111I2	467.5 - 632.5	K	LOCA/SBO
15		SC7111CS1	3.0745 - 4.1595	A	SBO
16		SC7111CS2	82.45 - 111.55	K	LOCA
17		SC7170CS	3.3575 - 4.5425	kg/kg H2O	SBO
18		SC7170CSI3	0.374 - 0.506	kg/kg H2O	SBO
19		SC7170CSI4	1.9125 - 2.5875	kg/kg H2O	LOCA
20		SC7170CSM	0.5695 - 0.7705	kg/kg H2O	LOCA/SBO
21		SC71521	0.005 - 0.008	m	LOCA

No	Model	Parameter name	Range	Units	Scenario
22	Spray and pool scrubbing, and filters trapping	SC71531	6.6946 - 9.0574	cm/s	LOCA
23		SC71551	1.523 - 2.0606		LOCA
24		SC71555	0.9681 - 1.3098		SBO
25		SC71542	0.0025593 - 0.0034626	I-s/cm2	LOCA/SBO
26		SC3210	1 - 1.15		LOCA

The bounding analysis showed that CORSOR-Booth diffusion model for high burnup oxide fuel is a significant parameter affecting release of CS and I2 during LOCA. Additional analysis is required to ascertain its effect on accident progression, and in this study the default value of ICRLSE = -5 on RN1_FP00 card is used in further analysis. Coefficients in the candling model and intercell radiation model showed high effects to CS and I2 release during LOCA, while debris formation and relocation models showed least effects, and thus not be considered for LOCA analysis. Effects of aerosol dynamics and vapour diffusivity models on releases were high during SBO and coefficients of eutectics model, intercell radiation model, debris formation and relocation models were of lesser significance. These models are not considered for further SA for SBO.

For the Morris analysis based on [8], valuable results can be obtained for 4 levels and repetitions *r* in the range of 4-10. In this study with many variables, 20 repetitions and at 6 levels were considered for effective coverage in input space. Based on Equation (4) a total of 400 simulations were run for LOCA in IDEJ0 and IDEJ1 scenarios and 320 simulations were run for SBO in IDEJ0 and IDEJ1 scenarios. The sampling for the Morris analysis was performed using Dakota. The primary FOMs considered were CS and I2 releases.

5.1.1. Results

Figure 5-1 and Figure 5-2 show the combined distributions of CS and I2 release fractions for the 4 scenarios. Figure 5-3 shows the TLHF for the 4 scenarios. The effect of mode of debris ejection can be clearly seen in the release fractions. Only liquid melt ejection to the cavity leads to higher releases. While for LOCA, large amounts of CS is released compared to SBO, this does not hold for I2 release, which sees comparable or even larger release in SBO than in LOCA, indicating that the most severe accident (LOCA) counterintuitively may not be as severe from the perspective of I2 release. This will need further analysis of the mechanism and the driving phenomena and will be addressed in a future study. TLHF behaves expectedly, with mean timings of 1.723h for LOCA-IDEJ0 and 1.694h for LOCA-IDEJ1 being quicker than 2.968h for SBO-IDEJ0 and 2.951h for SBO-IDEJ1.

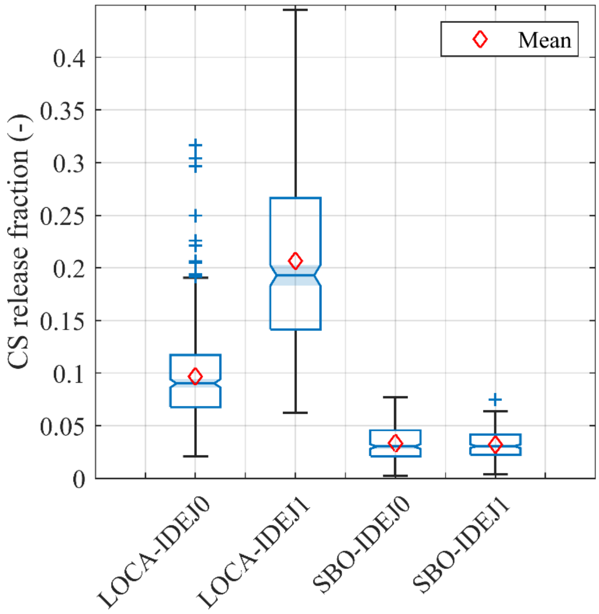

Figure 5-1 CS release fraction**s** to the environment during LOCA (400 runs each for IDEJ0 and IDEJ1) and SBO (320 runs each for IDEJ0 and IDEJ1)**.**

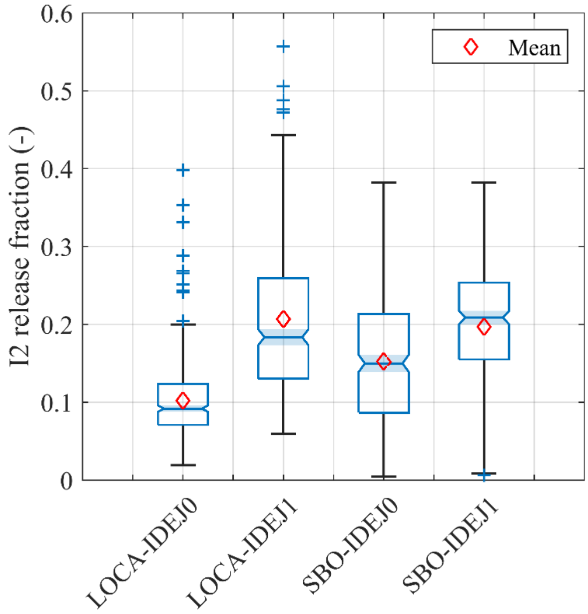

Figure 5-2 I2 release fractions to the environment during LOCA (400 runs each for IDEJ0 and IDEJ1) and SBO (320 runs each for IDEJ0 and for IDEJ0 and IDEJ1).

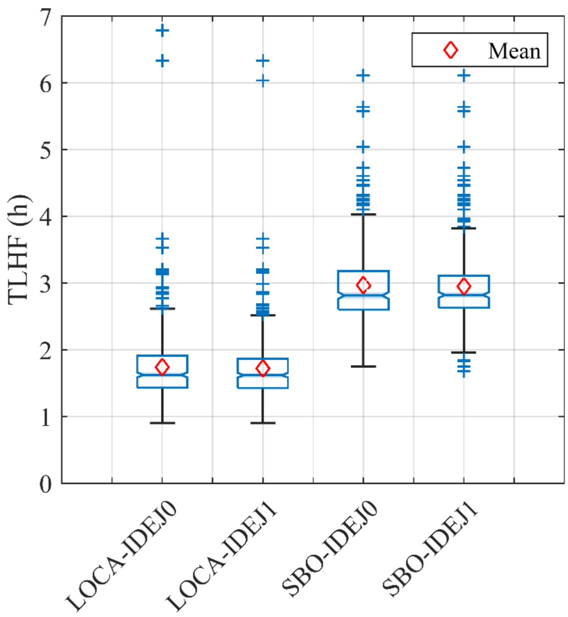

Figure 5-3 Time of lower head failure (TLHF) distributions during LOCA (400 runs each for IDEJ0 and IDEJ1) and SBO (320 runs each for IDEJ0 and IDEJ1).

The results of Morris analysis for the scenarios are given below. Note that amongst the 640 runs of SBO, no code crashes were reported, however amongst the 800 runs of LOCA, 9 runs did not converge. The partial results of the crashed runs were extrapolated and considered in the study. The values of sensitivity coefficients presented here are calculated at the 72h mark. The time evolution of Morris sensitivity indices for the 4 scenarios is provided in Appendix B.

5.1.1.1. Release category RC4A – LOCA

5.1.1.1.1. RC4A – LOCA-IDEJ0

Cesium release fraction

The Morris diagram for the CS release during LOCA-IDEJ0 is shown in Figure 5-4. Higher Morris modified mean corresponds to higher parameter importance. SC11312, SC710641 and SC71531 of the candling model, CORSOR-Booth diffusion model and SPARC-90 bubble rise velocity model respectively, are the most important, while SC7111CS2, TUO2ZRO2 and FCELRA of the vapour diffusivity model, eutectics model and intercell radiation model respectively, are the least important. Higher Morris standard deviation implies non-monotonic and/or nonlinear interaction between the parameters and the output. Correlation coefficients (Pearson and Spearman rank) are shown in Figure 5-5. A parameter might be positively/negatively correlated to the output, but not necessarily important (Ex: HDBPN) and vice-versa, important but not linearly correlated (Ex: GAMMA).

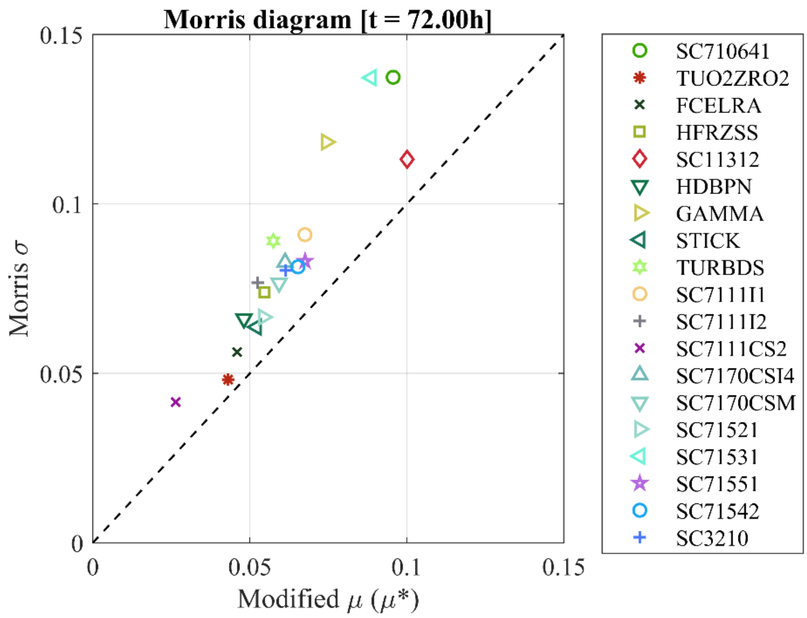

Figure 5-4 Morris diagram for the CS release fraction to the environment (LOCA-IDEJ0).

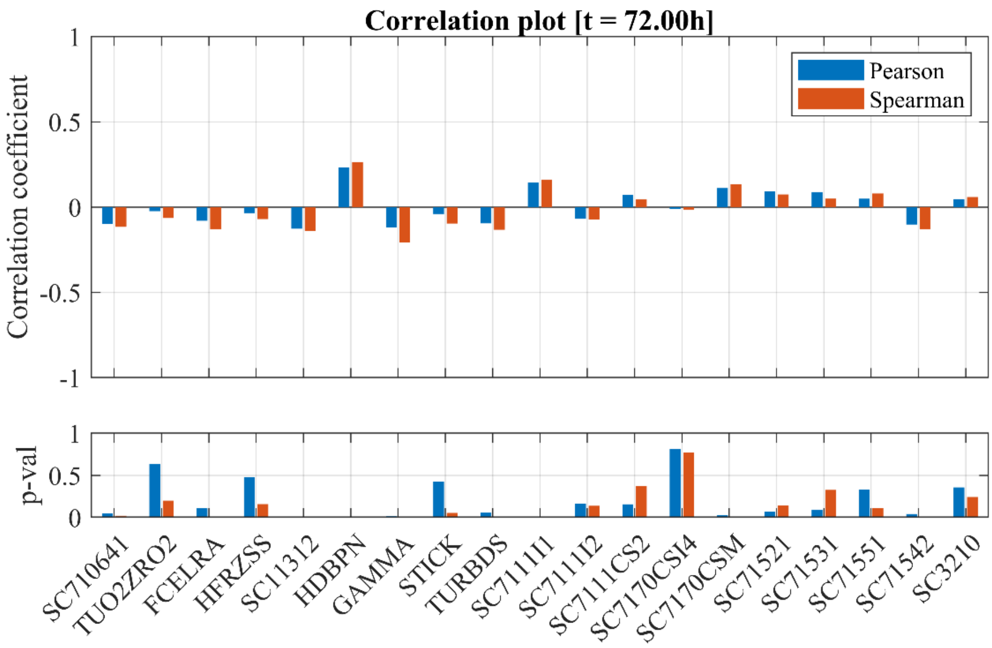

Figure 5-5 Correlation coefficients of the CS release fraction to the environment (LOCA-IDEJ0).

The results of one way ANOVA analysis for LOCA-IDEJ0 are summarised in Table 5-2 and the boxplots for the first 2 influential parameters are shown in Figure 5-6 and Figure 5-7.

Table 5-2 One way ANOVA results for CS release fraction to the environment (LOCA-IDEJ0).

	LOCA-IDEJ0	
	F	p
SC710641	4.149E+00	1.102E-03
TUO2ZRO2	7.805E-01	5.642E-01
FCELRA	1.076E+00	3.730E-01
HFRZSS	2.292E+00	4.507E-02
SC11312	2.696E+00	2.067E-02
HDBPN	5.947E+00	2.569E-05
GAMMA	2.868E+00	1.476E-02
STICK	4.225E-01	8.330E-01
TURBDS	5.951E+00	2.546E-05
SC7111I1	4.590E+00	4.416E-04
SC7111I2	1.444E+00	2.075E-01
SC7111CS2	2.230E+00	5.066E-02
SC7170CSI4	2.172E+00	5.651E-02
SC7170CSM	1.798E+00	1.121E-01
SC71521	1.907E+00	9.214E-02
SC71531	4.006E+00	1.478E-03
SC71551	8.359E-01	5.248E-01
SC71542	3.991E+00	1.524E-03
SC3210	1.630E+00	1.508E-01

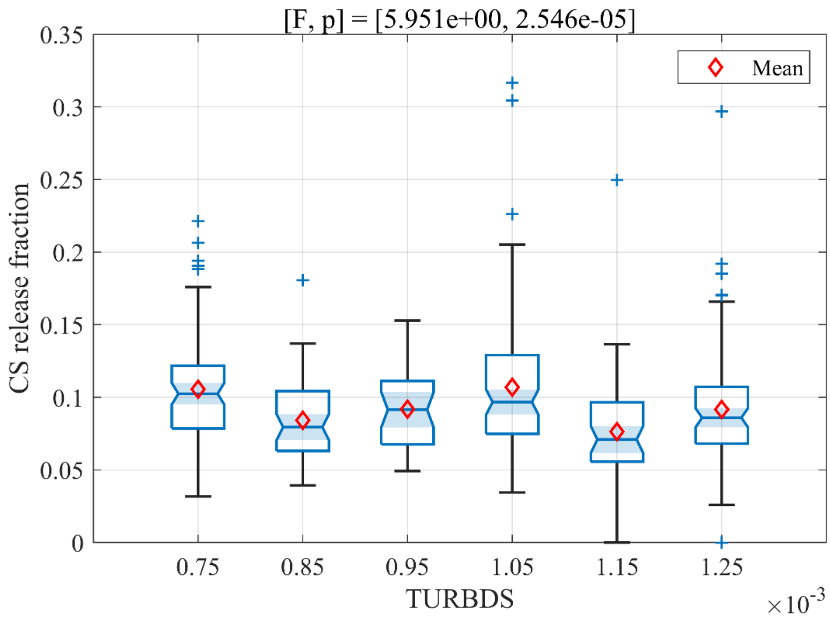

Figure 5-6 Boxplot for CS release fraction vs TURBDS (LOCA-IDEJ0).

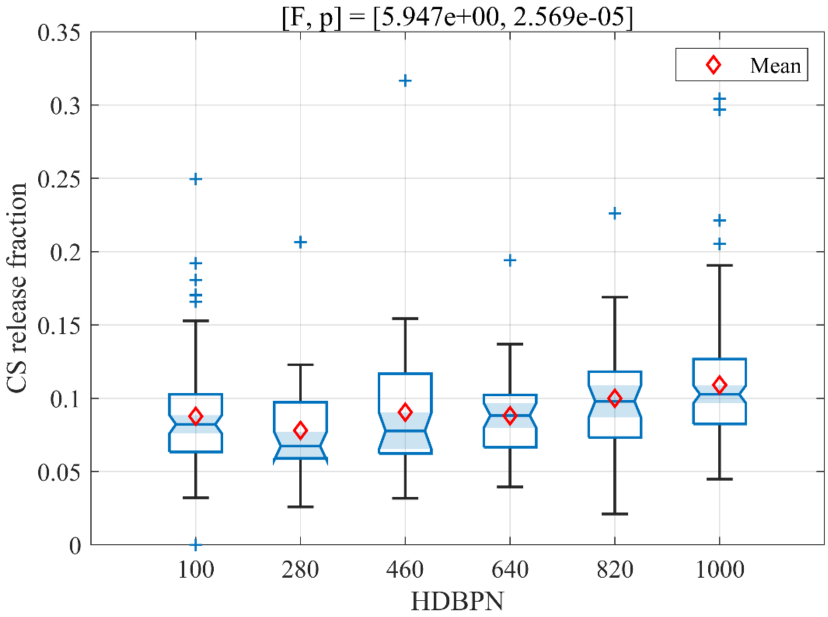

Figure 5-7 Boxplot for CS release fraction vs HDBPN (LOCA-IDEJ0).

Iodine release fraction

The Morris diagram for the I2 release during LOCA-IDEJ0 is shown in Figure 5-8. SC710641, SC11312 and GAMMA of the CORSOR-Booth diffusion model, candling model and aerosol dynamics model respectively, are the most important, while SC7111CS2, FCELRA and HDBPN of the vapour diffusivity model, intercell radiation model and vessel failure model respectively, are the least important. Correlation coefficients (Pearson and Spearman rank) are shown in Figure 5-9.

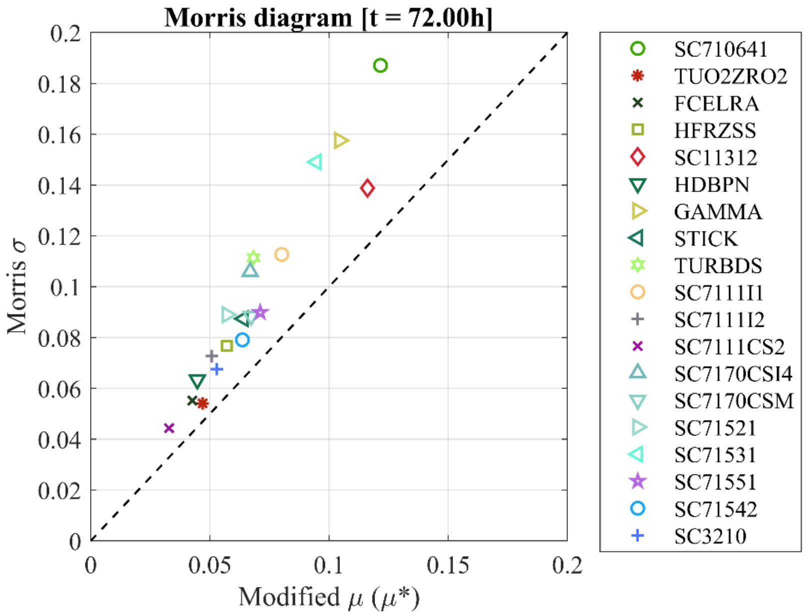

Figure 5-8 Morris diagram for the I2 release fraction to the environment (LOCA-IDEJ0).

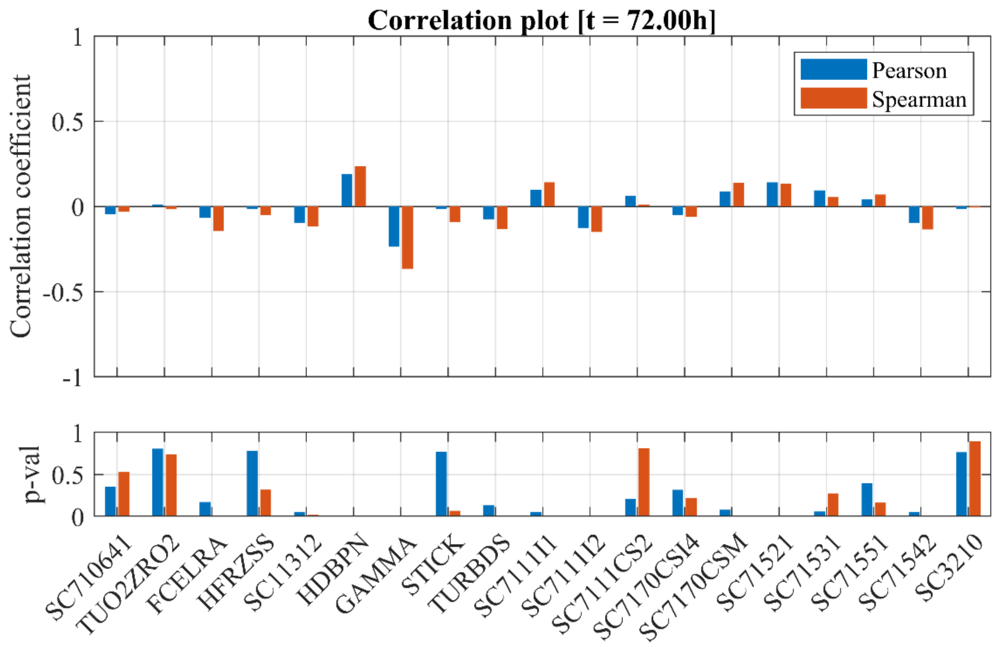

Figure 5-9 Correlation coefficients of the I2 release fraction to the environment (LOCA-IDEJ0).

The results of one way ANOVA analysis for LOCA-IDEJ0 are summarised in Table 5-3 and the boxplots for the first 2 influential parameters are shown in Figure 5-10 and Figure 5-11.

Table 5-3 One way ANOVA results for I2 release fraction to the environment (LOCA-IDEJ0).

	LOCA-IDEJ0	
	F	**p**
SC710641	2.060E+00	6.962E-02
TUO2ZRO2	1.238E+00	2.903E-01
FCELRA	1.761E+00	1.199E-01
HFRZSS	1.732E+00	1.262E-01
SC11312	3.858E+00	2.002E-03
HDBPN	4.074E+00	1.284E-03
GAMMA	6.735E+00	4.873E-06
STICK	6.194E-01	6.851E-01
TURBDS	5.452E+00	7.270E-05
SC7111I1	1.990E+00	7.923E-02
SC7111I2	1.521E+00	1.821E-01
SC7111CS2	2.266E+00	4.732E-02
SC7170CSI4	2.144E+00	5.950E-02
SC7170CSM	1.900E+00	9.333E-02
SC71521	2.633E+00	2.339E-02
SC71531	3.429E+00	4.802E-03
SC71551	7.933E-01	5.549E-01
SC71542	1.974E+00	8.157E-02
SC3210	1.679E+00	1.384E-01

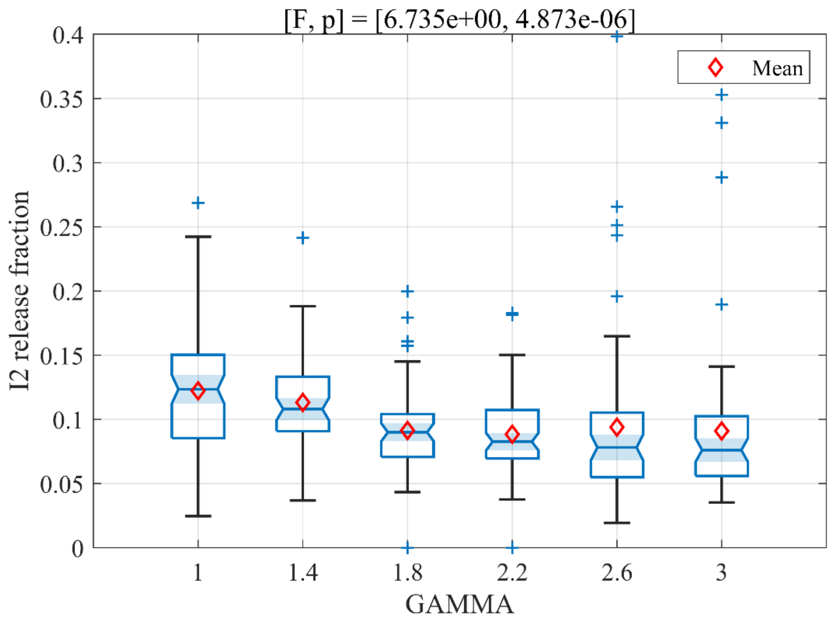

Figure 5-10 Boxplot for I2 release fraction vs GAMMA (LOCA-IDEJ0).

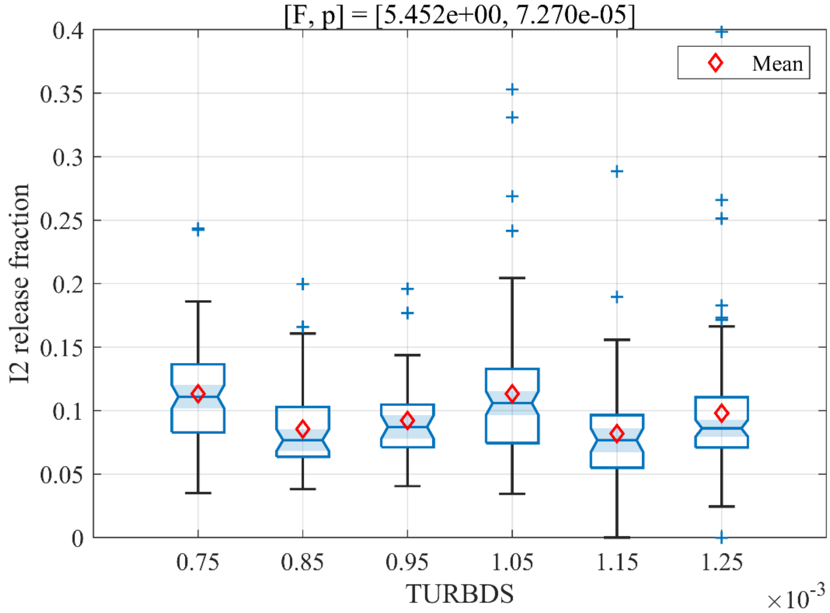

Figure 5-11 Boxplot for I2 release fraction vs TURBDS (LOCA-IDEJ0).

5.1.1.1.2. RC4A – LOCA-IDEJ1

Cesium release fraction

The Morris diagram for the CS release during LOCA-IDEJ1 is shown in Figure 5-12. FCELRA, SC71521 and SC710641 of the intercell radiation model, SPARC-90 bubble shape model and CORSOR-Booth diffusion model respectively, are the most important, while SC7170CSM, HDBPN and TUO2ZRO2 of the hygroscopic aerosol model, vessel failure model and eutectics model respectively, are the least important. Correlation coefficients (Pearson and Spearman rank) are shown in Figure 5-13.

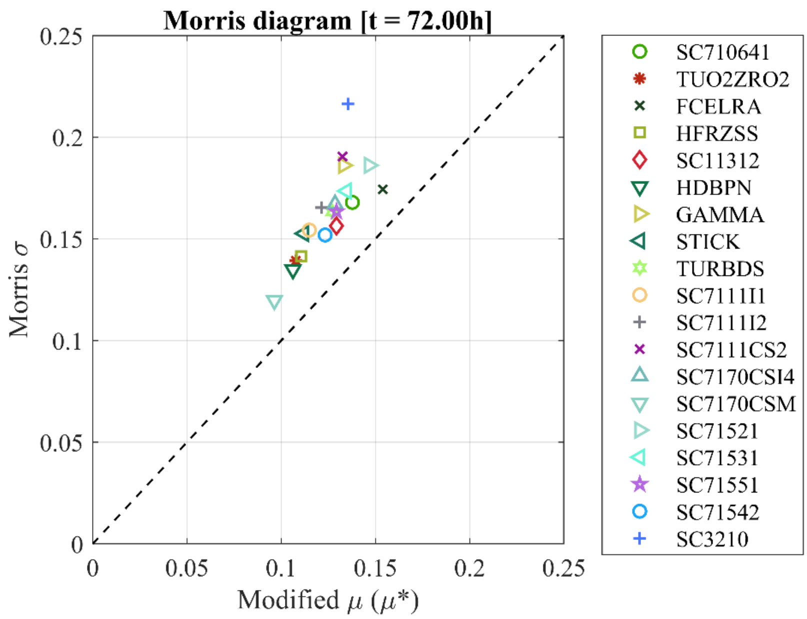

Figure 5-12 Morris diagram for the CS release fraction to the environment (LOCA-IDEJ1).

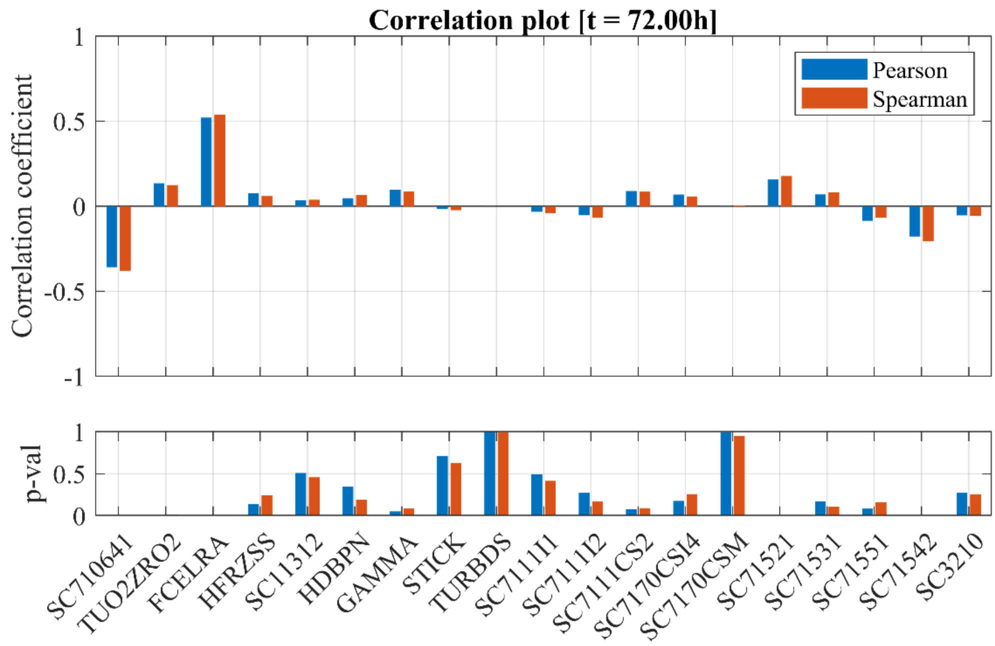

Figure 5-13 Correlation coefficients of the CS release fraction to the environment (LOCA-IDEJ1).

The results of one way ANOVA analysis for LOCA-IDEJ1 are summarised in Table 5-4 and the boxplots for the first 2 influential parameters are shown in Figure 5-14 and Figure 5-15.

Table 5-4 One way ANOVA results for CS release fraction to the environment (LOCA-IDEJ1).

	LOCA-IDEJ1	
	F	**p**
SC710641	1.458E+01	4.006E-13
TUO2ZRO2	2.816E+00	1.634E-02
FCELRA	3.164E+01	4.351E-27
HFRZSS	6.784E+00	4.389E-06
SC11312	3.759E+00	2.454E-03
HDBPN	1.486E+01	2.290E-13
GAMMA	1.820E+00	1.079E-01
STICK	3.134E+00	8.700E-03
TURBDS	3.380E-01	8.898E-01
SC7111I1	4.960E+00	2.041E-04
SC7111I2	4.998E-01	7.764E-01
SC7111CS2	1.164E+00	3.262E-01
SC7170CSI4	2.473E+00	3.186E-02
SC7170CSM	1.882E+00	9.636E-02
SC71521	3.053E+00	1.023E-02
SC71531	8.244E-01	5.328E-01
SC71551	1.808E+00	1.102E-01
SC71542	7.310E+00	1.447E-06
SC3210	3.270E+00	6.615E-03

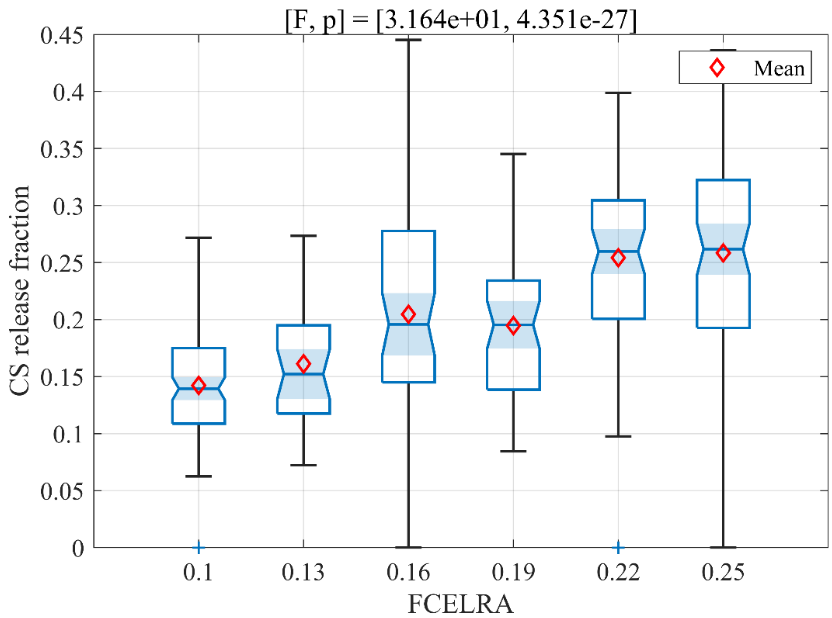

Figure 5-14 Boxplot for CS release fraction vs FCELRA (LOCA-IDEJ1).

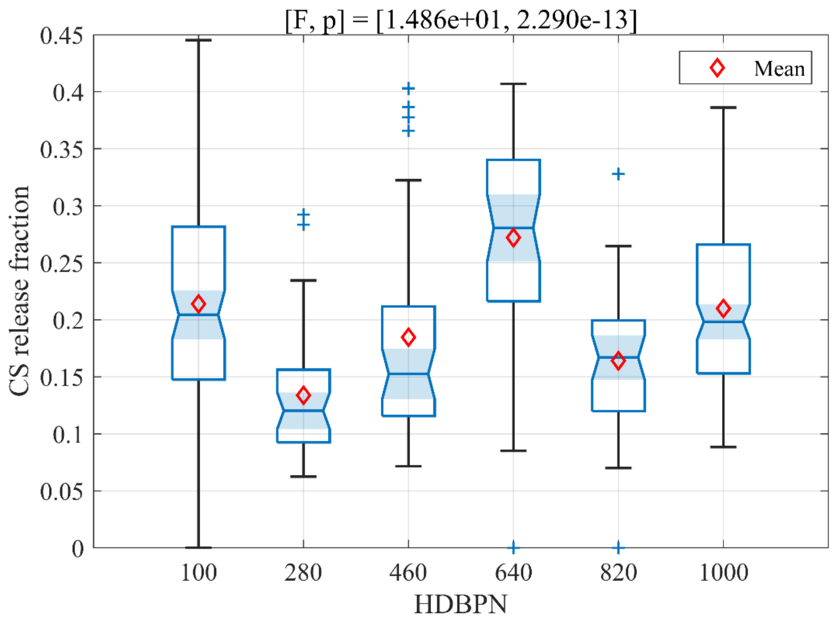

Figure 5-15 Boxplot for CS release fraction vs HDBPN (LOCA-IDEJ1).

Iodine release fraction

The Morris diagram for the I2 release during LOCA-IDEJ1 is shown in Figure 5-16. FCELRA, SC71521 and SC71531 of the intercell radiation model, SPARC-90 bubble shape model and SPARC-90 bubble rise velocity model respectively, are the most important, while HFRZSS, SC7170CSM and SC7111CS2 of the candling model, hygroscopic aerosol model and vapour diffusivity model respectively, are the least important. Correlation coefficients (Pearson and Spearman rank) are shown in Figure 5-17.

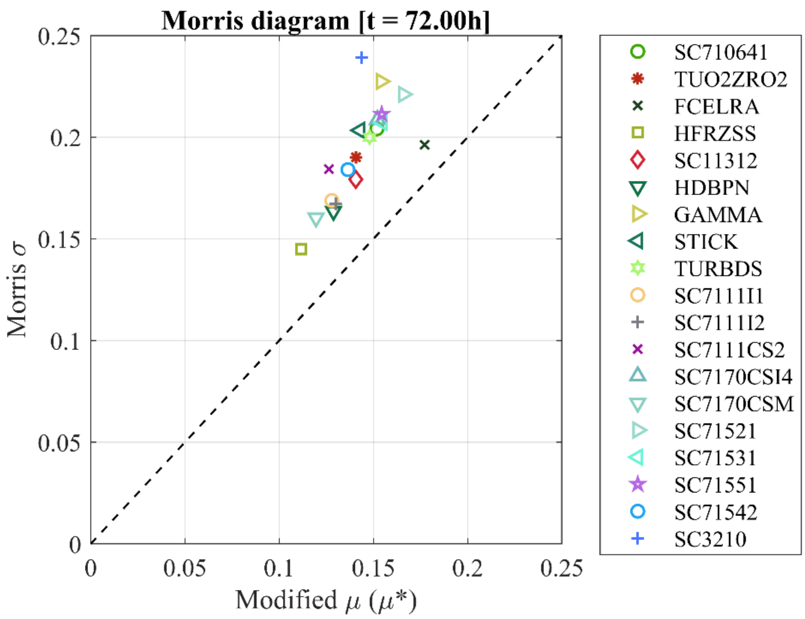

Figure 5-16 Morris diagram for the I2 release fraction to the environment (LOCA-IDEJ1).

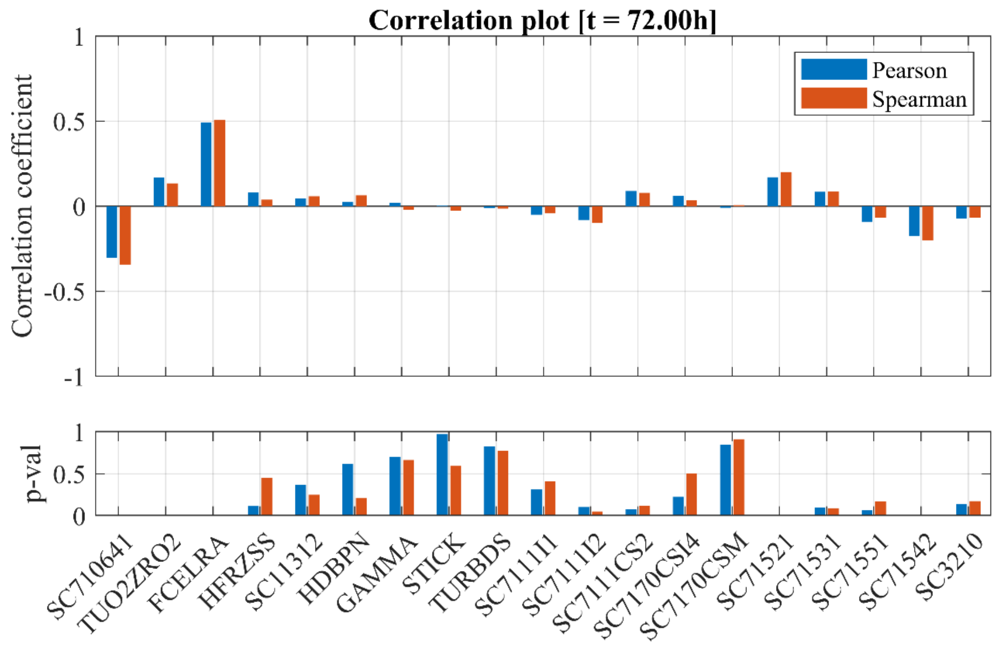

Figure 5-17 Correlation coefficients of the I2 release fraction to the environment (LOCA-IDEJ1).

The results of one way ANOVA analysis for LOCA-IDEJ1 are summarised in Table 5-5 and the boxplots for the first 2 influential parameters are shown in Figure 5-18 and Figure 5-19.

Table 5-5 One way ANOVA results for I2 release fraction to the environment (LOCA-IDEJ1).

	LOCA-IDEJ1	
	F	p
SC710641	1.062E+01	1.394E-09
TUO2ZRO2	3.676E+00	2.904E-03
FCELRA	2.747E+01	7.268E-24
HFRZSS	6.110E+00	1.822E-05
SC11312	4.289E+00	8.233E-04
HDBPN	1.112E+01	4.853E-10
GAMMA	1.067E+00	3.779E-01
STICK	2.452E+00	3.317E-02
TURBDS	3.218E-01	8.998E-01
SC7111I1	3.853E+00	2.024E-03
SC7111I2	7.364E-01	5.965E-01
SC7111CS2	1.593E+00	1.611E-01
SC7170CSI4	2.622E+00	2.389E-02
SC7170CSM	2.028E+00	7.391E-02
SC71521	3.365E+00	5.467E-03
SC71531	9.497E-01	4.487E-01
SC71551	2.101E+00	6.452E-02
SC71542	7.072E+00	2.392E-06
SC3210	3.584E+00	3.504E-03

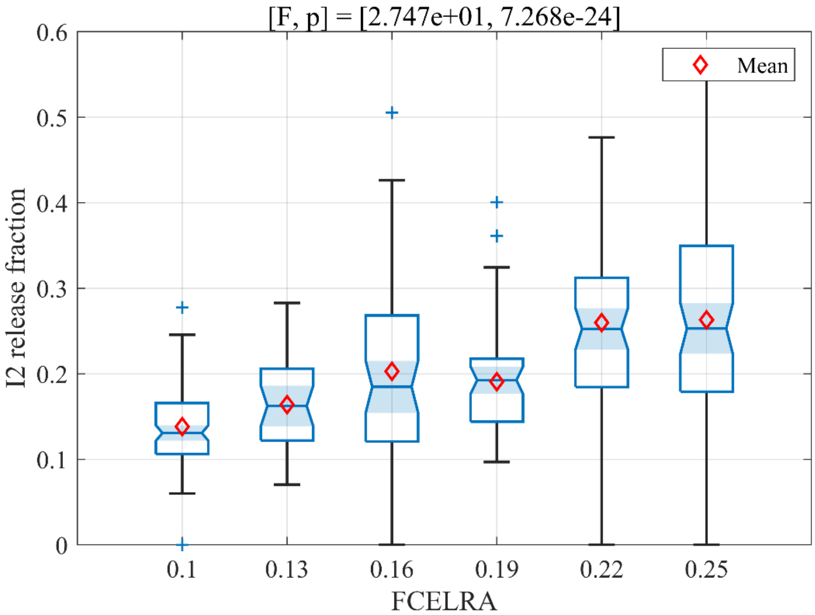

Figure 5-18 Boxplot for I2 release fraction vs FCELRA (LOCA-IDEJ1).

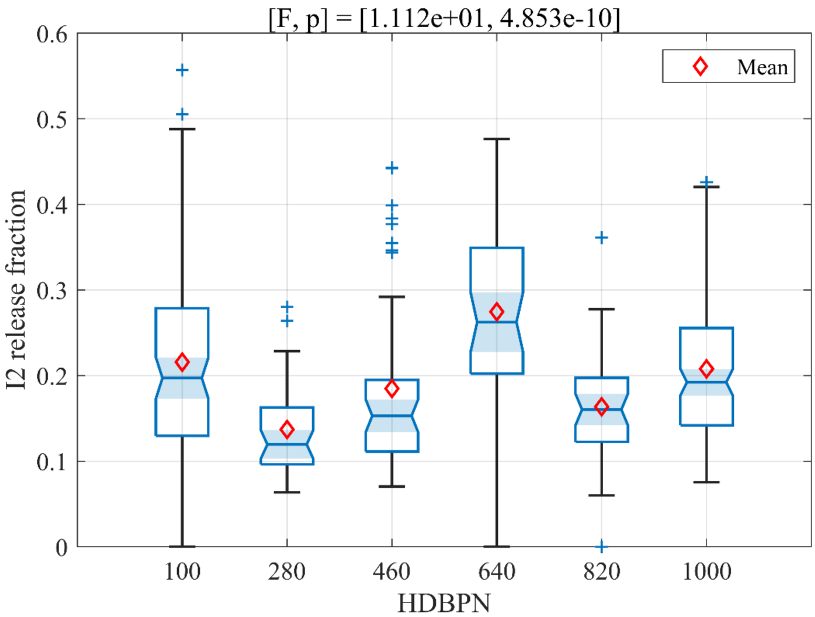

Figure 5-19 Boxplot for I2 release fraction vs HDBPN (LOCA-IDEJ1).

The combined correlation matrix of linear and rank coefficients for LOCA scenario is shown in Figure 5-20. The values in the matrix were computed separately for CS and I2 releases in IDEJ0 and IDEJ1 are combined to a single heatmap. The correlations between any 2 among the 19 different input parameters do not vary with scenarios, if the model order does not vary. This enables representing the correlations between the input and output on a single map.

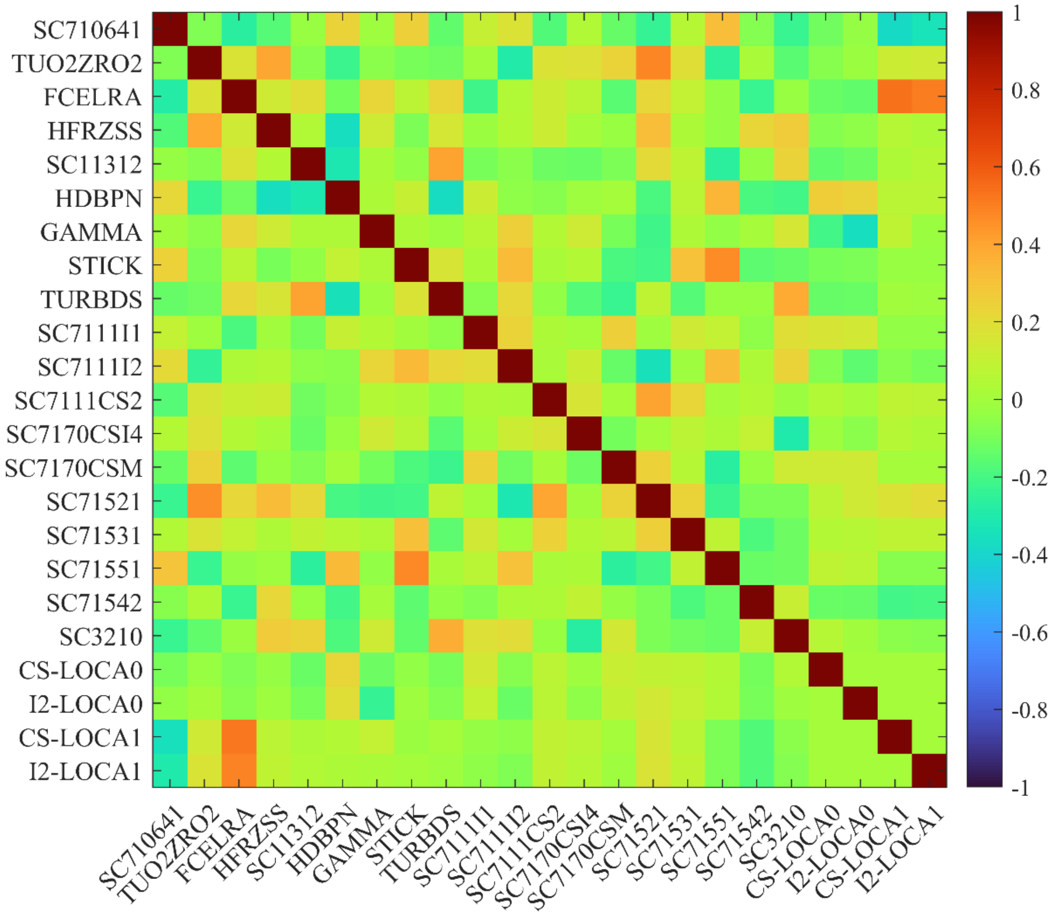

Figure 5-20 Correlation matrix for LOCA scenario. The lower left triangle of the matrix represents Pearson linear correlation coefficients and the upper right triangle represents Spearman rank correlation coefficients. (CS-LOCA0 notation represents CS release during LOCA-IDEJ0).

5.1.1.2.Release category RC4B – SBO

5.1.1.2.1. RC4B – SBO-IDEJ0

Cesium release fraction

The Morris diagram for the CS release during SBO-IDEJ0 is shown in Figure 5-21. GAMMA, SC7111CS1 and SC7170CS of the aerosol dynamics model, vapour diffusivity model and hygroscopic aerosol model respectively, are the most important, while SC7111I2, TPFAIL and HDBPN of the vapour diffusivity model and vessel failure model respectively, are the least important. GAMMA is an almost monotonically influential parameter and can also be observed in the correlation values. Correlation coefficients (Pearson and Spearman rank) are shown in Figure 5-22.

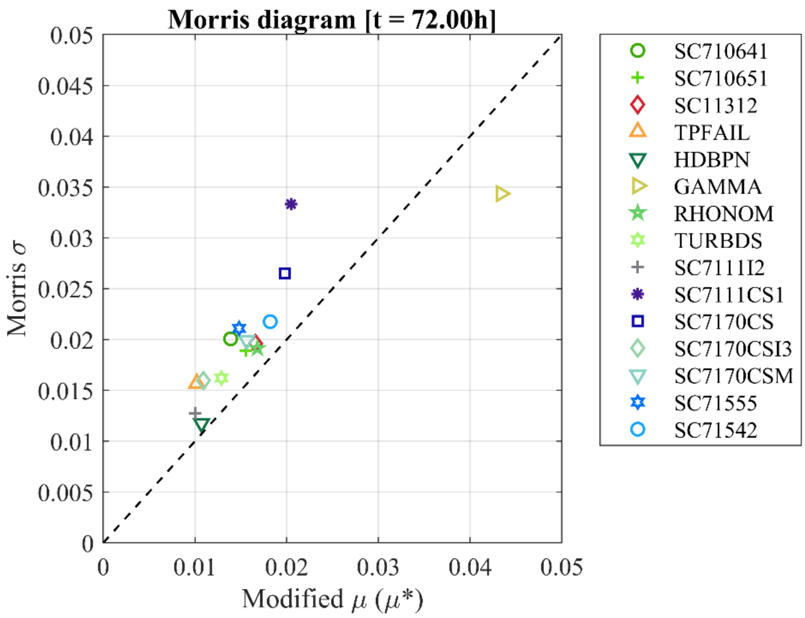

Figure 5-21 Morris diagram for the CS release fraction to the environment (SBO-IDEJ0).

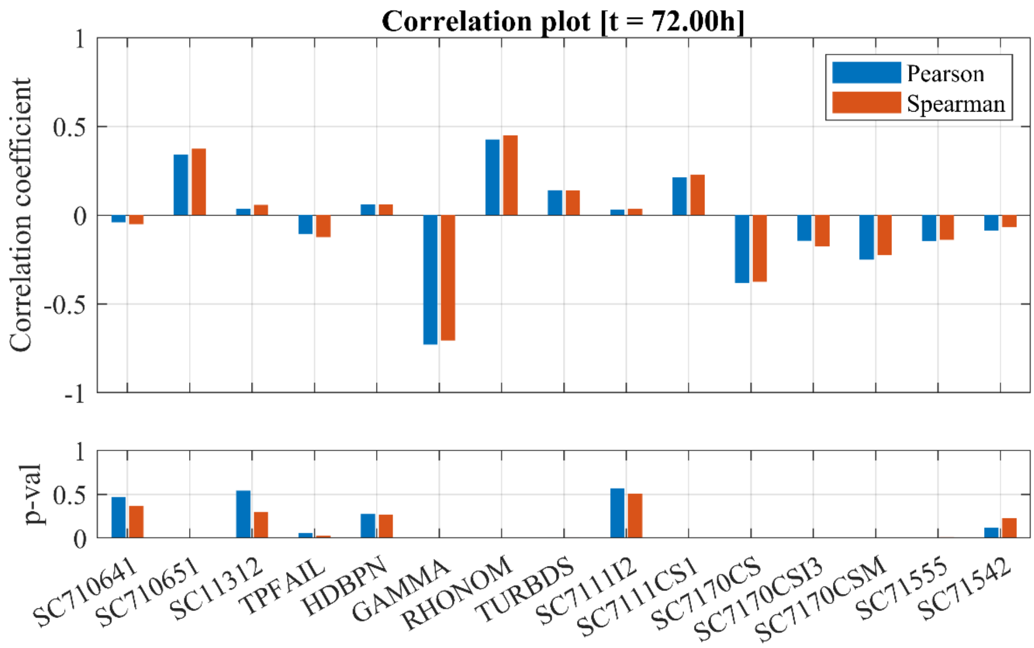

Figure 5-22 Correlation coefficients of the CS release fraction to the environment (SBO-IDEJ0).

The results of one way ANOVA analysis for SBO-IDEJ0 are summarised in Table 5-6 and the boxplots for the first 2 influential parameters are shown in Figure 5-23 and Figure 5-24.

Table 5-6 One way ANOVA results for CS release fraction to the environment (SBO-IDEJ0).

	SBO-IDEJ0	
	F	**p**
SC710641	2.352E+00	4.068E-02
SC710651	1.557E+01	1.093E-13
SC11312	1.010E+00	4.116E-01
TPFAIL	1.353E+01	5.852E-12
HDBPN	9.824E+00	9.744E-09
GAMMA	8.943E+01	2.870E-58
RHONOM	1.540E+01	1.507E-13
TURBDS	5.013E+00	1.960E-04
SC7111I2	1.536E+00	1.782E-01
SC7111CS1	7.029E+00	3.033E-06
SC7170CS	1.419E+01	1.580E-12
SC7170CSI3	2.153E+00	5.915E-02
SC7170CSM	8.799E+00	7.905E-08
SC71555	5.518E+00	6.914E-05
SC71542	2.618E+00	2.446E-02

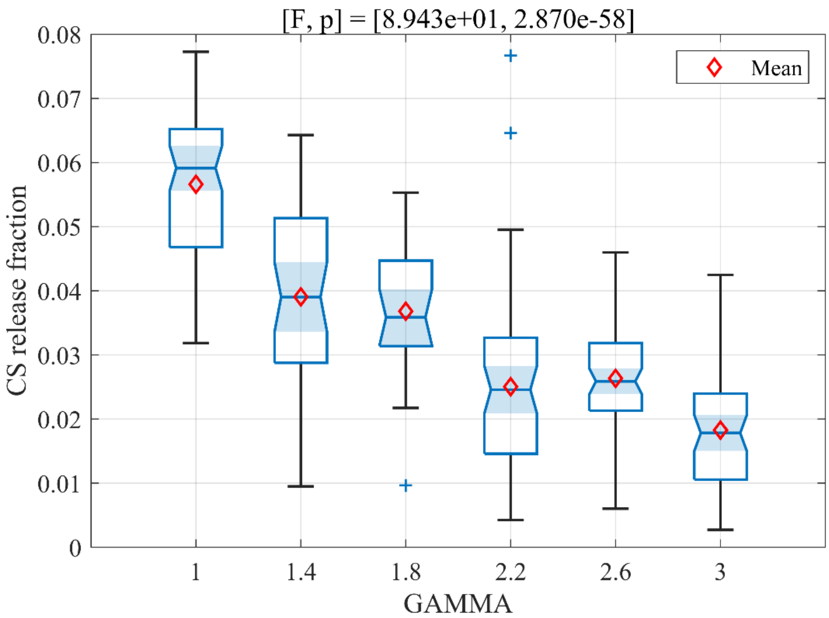

Figure 5-23 Boxplot for CS release fraction vs GAMMA (SBO-IDEJ0).

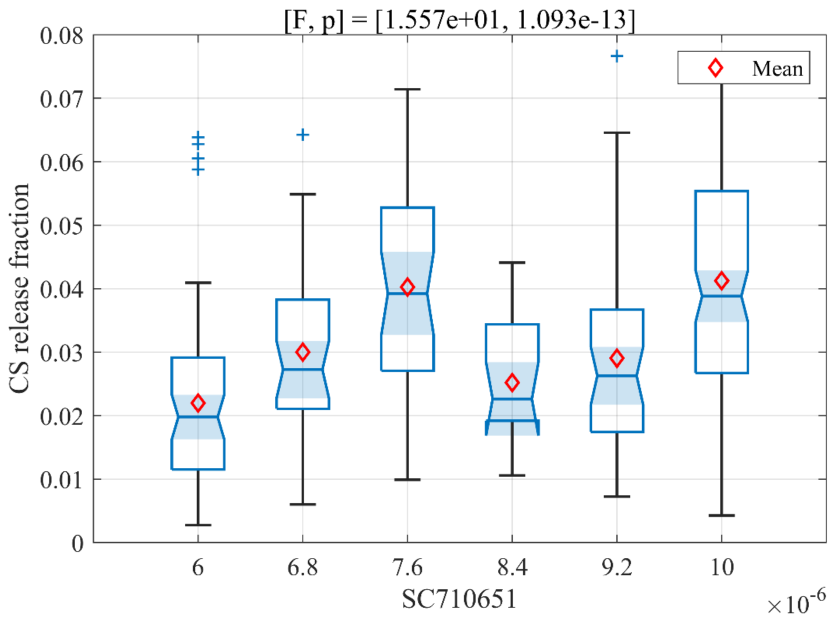

Figure 5-24 Boxplot for CS release fraction vs SC710651 (SBO-IDEJ0).

Iodine release fraction

The Morris diagram for the I2 release during SBO-IDEJ0 is shown in Figure 5-25. GAMMA, SC7170CS and SC7111CS1 of the aerosol dynamics model, hygroscopic aerosol model and vapour diffusivity model respectively, are the most important, while TPFAIL, HDBPN and TURBDS of the vessel failure model and aerosol dynamics model respectively, are the least important. GAMMA is observed to be almost linearly influential parameter. Correlation coefficients (Pearson and Spearman rank) are shown Figure 5-26.

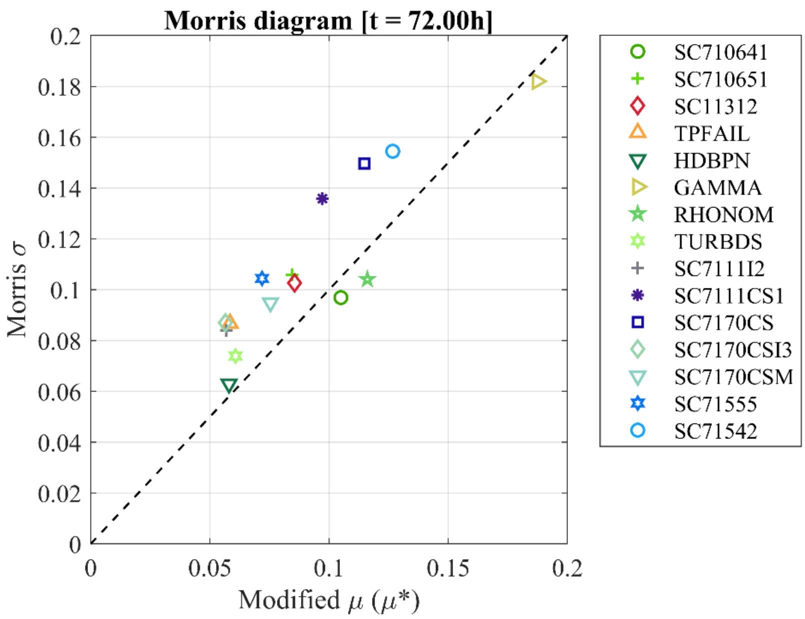

Figure 5-25 Morris diagram for the I2 release fraction to the environment (SBO-IDEJ0).

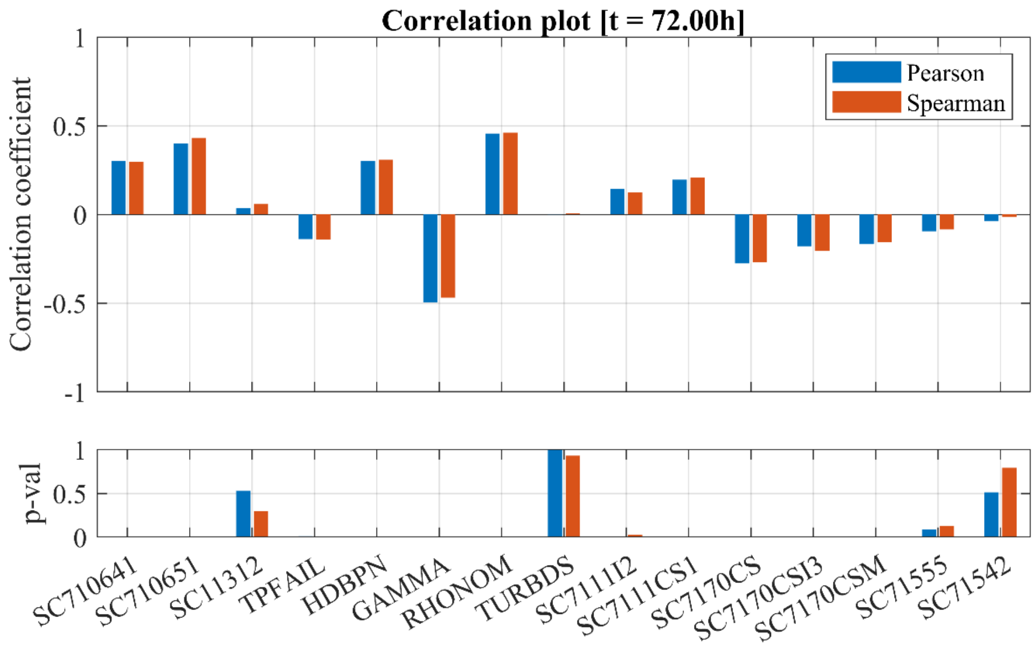

Figure 5-26 Correlation coefficients of the I2 release fraction to the environment (SBO-IDEJ0).

The results of one way ANOVA analysis for SBO-IDEJ0 are summarised in Table 5-7 and the boxplots for the first 2 influential parameters are shown in Figure 5-27 and Figure 5-28.

Table 5-7 One way ANOVA results for I2 release fraction to the environment (SBO-IDEJ0).

	SBO-IDEJ0	
	F	**p**
SC710641	8.101E+00	3.321E-07
SC710651	2.407E+01	1.690E-20
SC11312	1.634E+00	1.506E-01
TPFAIL	1.312E+01	1.302E-11
HDBPN	1.522E+01	2.143E-13
GAMMA	2.760E+01	3.718E-23
RHONOM	1.956E+01	5.783E-17
TURBDS	5.498E+00	7.205E-05
SC7111I2	5.040E+00	1.855E-04
SC7111CS1	8.131E+00	3.121E-07
SC7170CS	7.387E+00	1.447E-06
SC7170CSI3	3.574E+00	3.701E-03
SC7170CSM	4.482E+00	5.847E-04
SC71555	4.487E+00	5.789E-04
SC71542	1.615E+00	1.557E-01

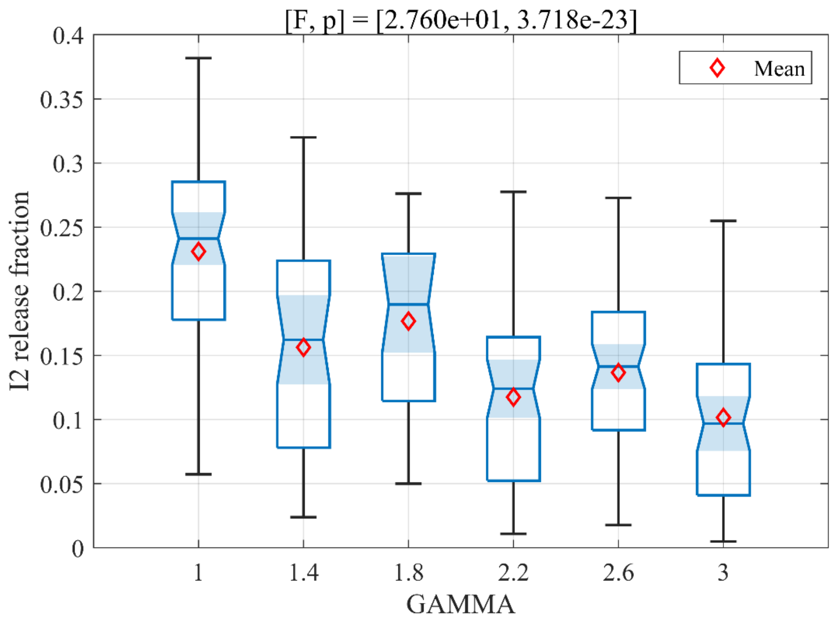

Figure 5-27 Boxplot for I2 release fraction vs GAMMA (SBO-IDEJ0).

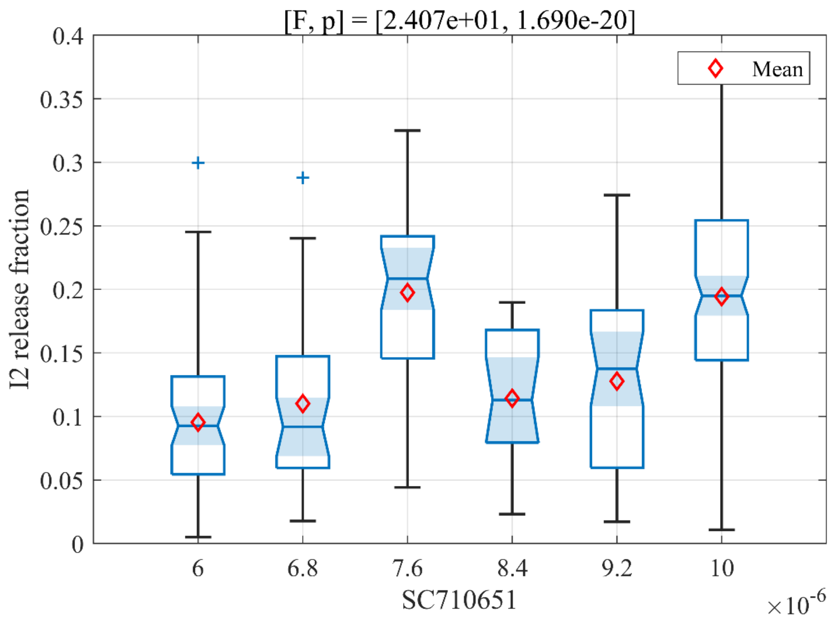

Figure 5-28 Boxplot for I2 release fraction vs SC710651 (SBO-IDEJ0).

5.1.1.2.2. RC4B – SBO-IDEJ1

Cesium release fraction

The Morris diagram for the CS release during SBO-IDEJ1 is shown in Figure 5-29. GAMMA, SC7111CS1 and SC7170CS of the aerosol dynamics model, vapour diffusivity model and hygroscopic aerosol model respectively, are the most important, while TPFAIL, HDBPN and TURBDS of the vessel failure model and aerosol dynamics model respectively, are the least important. SC7111CS1 is largely a non-monotonic/nonlinear parameter and GAMMA is an almost monotonically influential parameter, which can also be observed in the correlation values. Correlation coefficients (Pearson and Spearman rank) are shown in Figure 5-30.

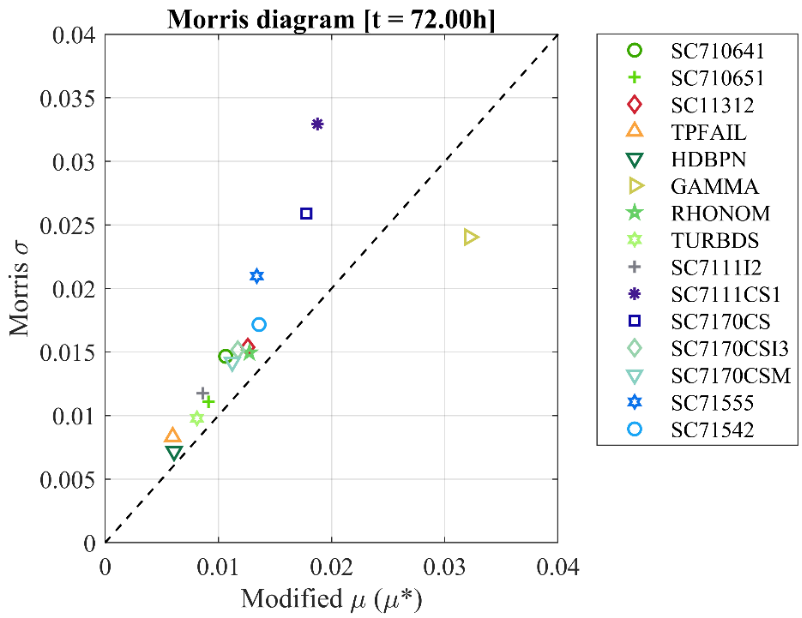

Figure 5-29 Morris diagram for the CS release fraction to the environment (SBO-IDEJ1).

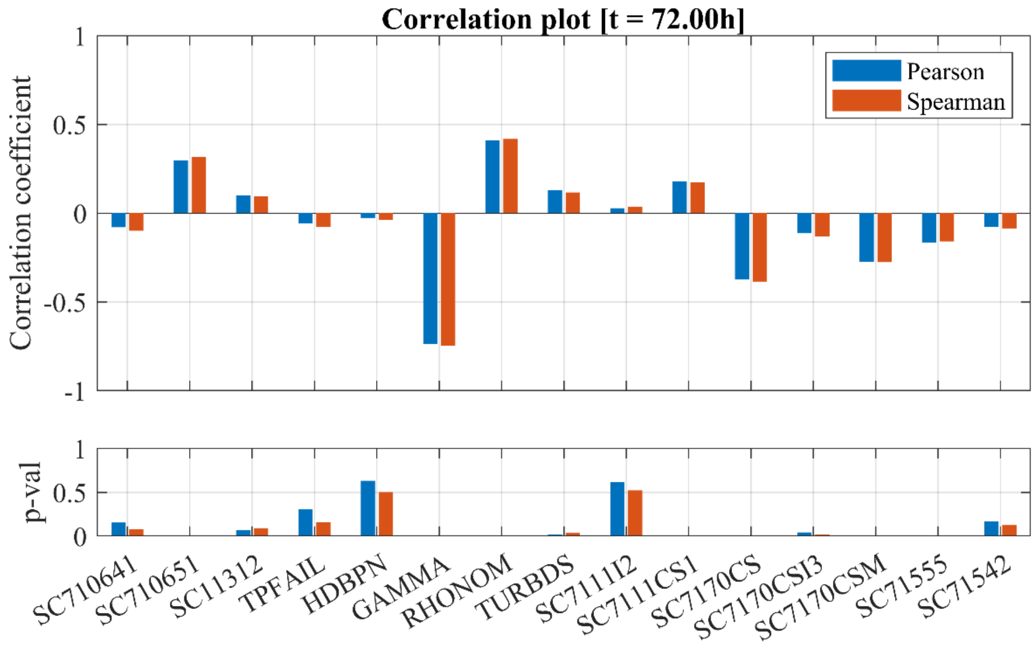

Figure 5-30 Correlation coefficients of the CS release fraction to the environment (SBO-IDEJ1).

The results of one way ANOVA analysis for SBO-IDEJ1 are summarised in Table 5-8 and the boxplots for the first 2 influential parameters are shown in Figure 5-31 and Figure 5-32.

Table 5-8 One way ANOVA results for CS release fraction to the environment (SBO-IDEJ1).

	SBO-IDEJ1	
	F	**p**
SC710641	4.126E+00	1.209E-03
SC710651	1.159E+01	2.746E-10
SC11312	1.875E+00	9.835E-02
TPFAIL	1.485E+01	4.427E-13
HDBPN	6.843E+00	4.454E-06
GAMMA	8.362E+01	1.246E-55
RHONOM	1.347E+01	6.585E-12
TURBDS	4.360E+00	7.497E-04
SC7111I2	9.861E-01	4.263E-01
SC7111CS1	5.528E+00	6.771E-05
SC7170CS	1.321E+01	1.095E-11
SC7170CSI3	1.629E+00	1.520E-01
SC7170CSM	1.050E+01	2.457E-09
SC71555	5.587E+00	5.997E-05
SC71542	4.415E+00	6.702E-04

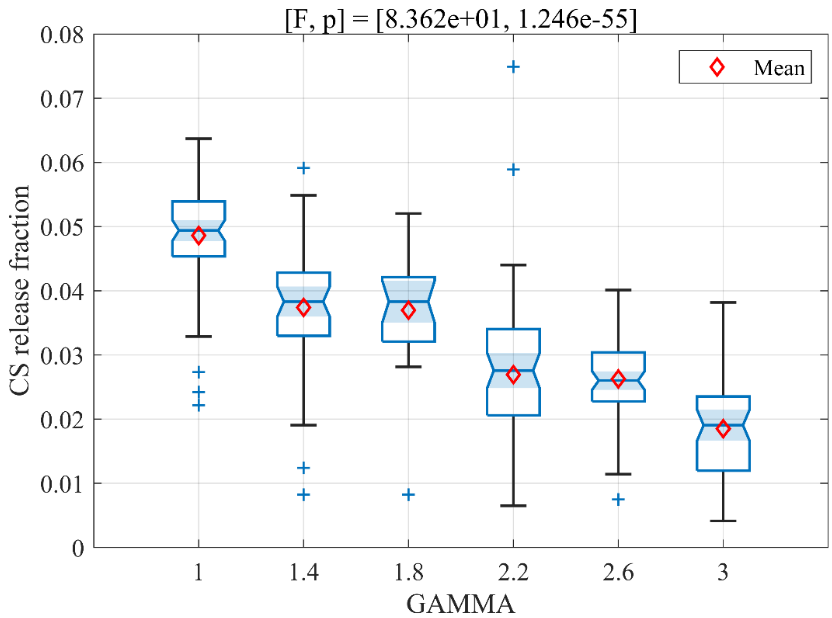

Figure 5-31 Boxplot for CS release fraction vs GAMMA (SBO-IDEJ1).

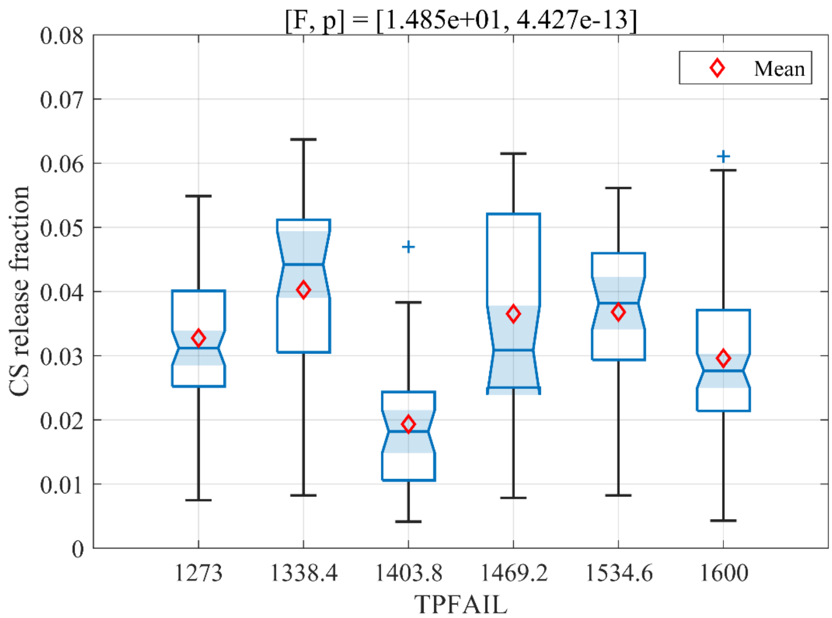

Figure 5-32 Boxplot for CS release fraction vs TPFAIL (SBO-IDEJ1).

5.1.1.2.2.1. Iodine release fraction

The Morris diagram for the I2 release during SBO-IDEJ1 is shown in Figure 5-33. GAMMA, SC7170CS and SC7111CS1 of the aerosol dynamics model, hygroscopic aerosol model and vapour diffusivity model respectively, are the most important, while TPFAIL, HDBPN and TURBDS of the vessel failure model and aerosol dynamics model respectively, are the least important. Correlation coefficients (Pearson and Spearman rank) are shown in Figure 5-34Figure 5-30.

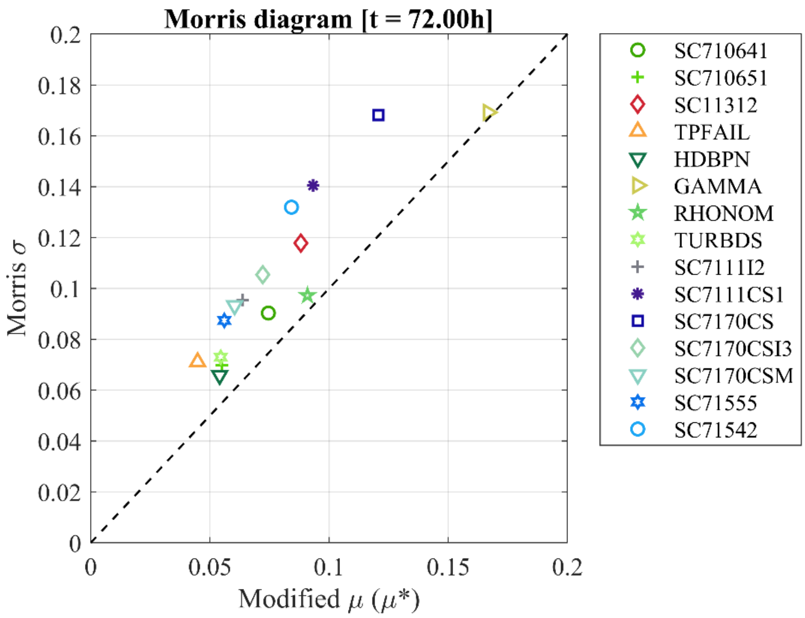

Figure 5-33 Morris diagram for the I2 release fraction to the environment (SBO-IDEJ1).

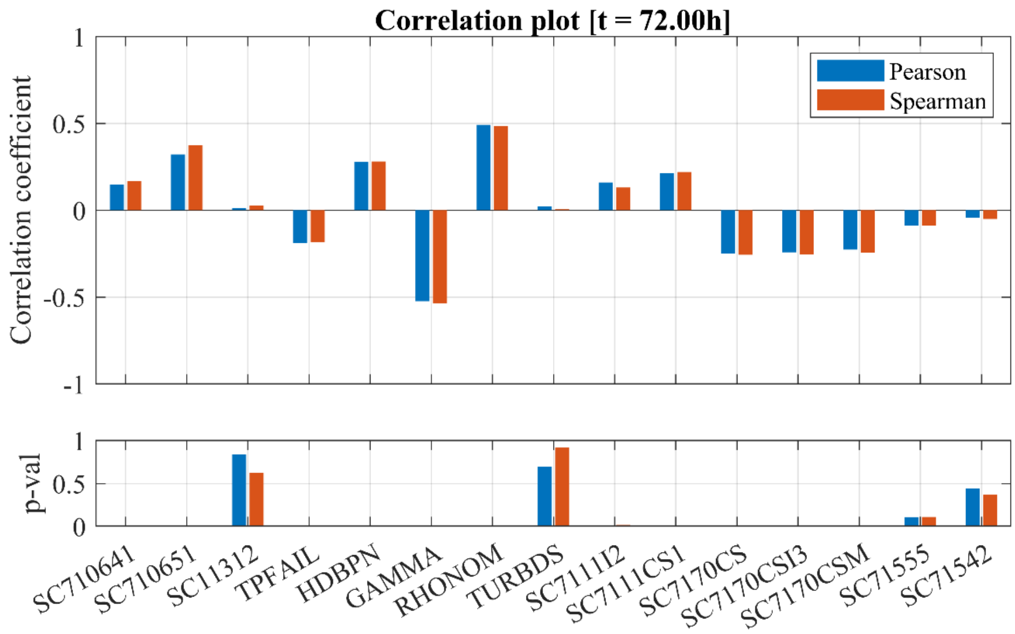

Figure 5-34 Correlation coefficients of the I2 release fraction to the environment (SBO-IDEJ1).

The results of one way ANOVA analysis for SBO-IDEJ1 are summarised in Table 5-9 and the boxplots for the first 2 influential parameters are shown in Figure 5-35 and Figure 5-36.

Table 5-9 One way ANOVA results for I2 release fraction to the environment (SBO-IDEJ1).

	SBO-IDEJ1	
	F	**p**
SC710641	4.251E+00	9.371E-04
SC710651	1.547E+01	1.313E-13
SC11312	2.996E+00	1.172E-02
TPFAIL	2.192E+01	7.831E-19
HDBPN	1.636E+01	2.368E-14
GAMMA	3.693E+01	1.005E-29
RHONOM	2.447E+01	8.334E-21
TURBDS	5.721E+00	4.549E-05
SC7111I2	4.028E+00	1.476E-03
SC7111CS1	8.139E+00	3.071E-07
SC7170CS	5.697E+00	4.780E-05
SC7170CSI3	5.335E+00	1.009E-04
SC7170CSM	8.694E+00	9.814E-08
SC71555	3.421E+00	5.031E-03
SC71542	2.526E+00	2.919E-02

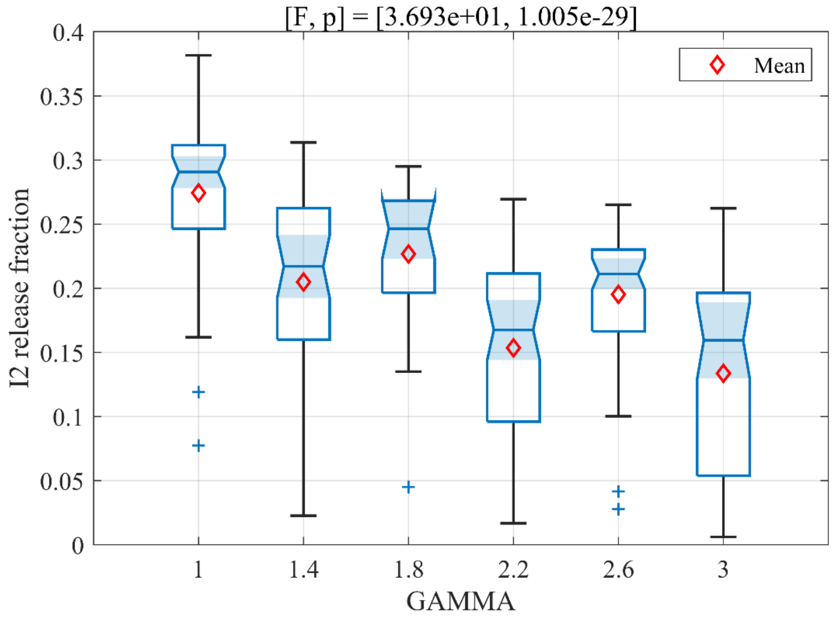

Figure 5-35 Boxplot for I2 release fraction vs GAMMA (SBO-IDEJ1).

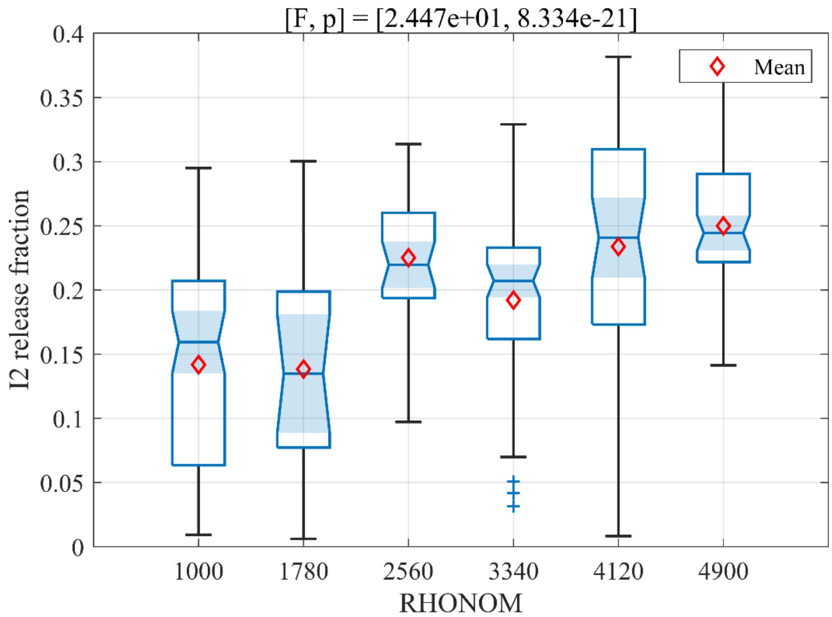

Figure 5-36 Boxplot for I2 release fraction vs RHONOM (SBO-IDEJ1).

The combined correlation matrix of linear and rank coefficients for SBO scenario is shown in Figure 5-37. The correlations between any 2 among the 15 different input parameters do not vary with scenarios if the model order does not vary. This enables representing the correlations between the input and output on a single map.

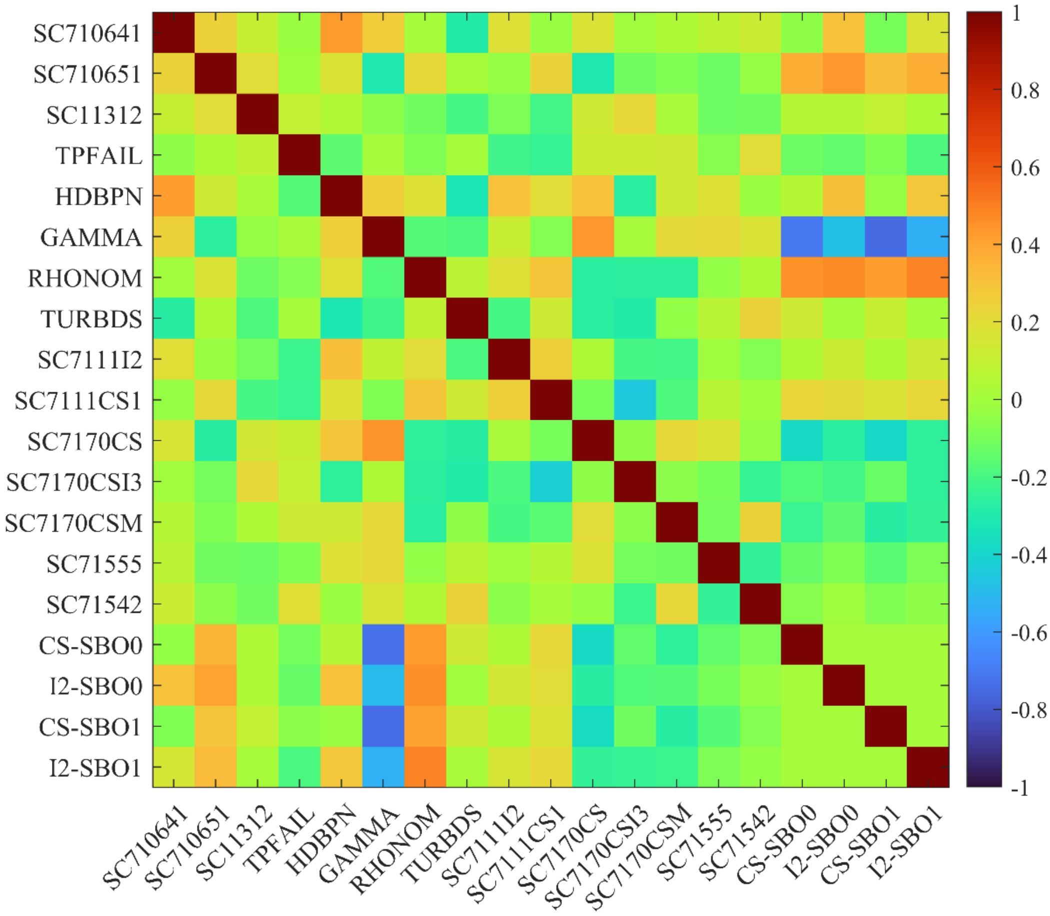

Figure 5-37 Correlation matrix for SBO scenario. The lower left triangle of the matrix represents Pearson linear correlation coefficients and the upper right triangle represents Spearman rank correlation coefficients. (CS-SBO0 notation represents CS release during SBO-IDEJ0).

5.2.Sensitivity analysis RC7 – Swedish plant configuration

Withing the second phase of the project VG focused on scenarios within the RC7 release category (acceptable releases - Filtered containment venting). The analysis performed within the first phase of the project indicated that in case of unmitigated LB-LOCA for some MELCOR calculations the fraction of Cs core inventory released to the environment exceeds the design criterion. The main purpose of sensitivity analysis is to identify the most influential MELCOR code parameters to consider in uncertainty analysis. The analysis will be performed for RC7B release category (unmitigated LB-LOCA in feedwater line that leads to filtered containment venting (LOCA-MVSS)) and RC7A release category (unmitigated SBO that leads to filtered containment venting (SBO-MVSS)).

5.2.1. Parameter selection

The results of the bounding analysis for RC7 performed during the first phase of the project indicate that the maximum time step has quite significant effect on the code response, which makes direct interpretation of the results quite challenging, without proper statistical treatment.

Based on the results, all parameters varied between the min and max values and produced no effect of the code response were excluded from further sensitivity and uncertainty analysis (e.g., *TFFAIL, SC7157, DIAMO*).

Analysis of the Cs and I fuel release fractions showed that the CORSOR-Booth SC7106 sensitivity coefficients have smaller effects compared to the effect of other uncertain modelling parameters (e.g., *HFRZSS, HFRZZR*) and modelling switches (selection of CORSOR-Booth model *ICRLSE* on *RN1_FP00* card). Thus, sensitivity and uncertainty analysis will be performed with the revised CORSOR-BOOTH for high burnup fuel, which can be achieved by enabling *ICRLSE=-7* on *RN1_FP00* card. Other parameters related to FP release kinetics from the fuel will be excluded from further analysis.

The results of the bounding analysis show that the mode of debris ejection from the vessel (*IDEJ*) has the dominant effect on the code predictions of the fractions of Cs and I_2 released to the environment. Since it is impossible to treat this parameter probabilistically, due to lack of knowledge, this parameter will be considered as a phenomenological splinter[2]. Furthermore, the analysis of the effect of the mode of debris ejection on the containment and environmental source terms showed the importance of the filtering of fission products vapors. Since the current MELCOR model of Nordic BWR employs a simple filtering model with constant decontamination factor for aerosols (DF=500), without proper treatment of scrubbing of gaseous fission products in the scrubber system, an additional simple filtering model for the fission products vapors will be considered in the analysis. The simple filtering model will use constant decontamination factor MVSSDFV = 1(-) with uncertainty range [1-500](-), the filtering will be applied for all RN groups except noble gases (Xe). Additional analysis is necessary to establish proper values of decontamination factors for gaseous fission products.

To reduce computational burden, the parameters that control radial debris spreading (SC1020-1 for solid and SC1020-2 for molten materials) we be considered in the analysis together, by a

---

[2] In ROAAM formulation a splinter scenario is a phenomenological scenario where relevant epistemic uncertainties are *beyond the reach of any reasonably verifiable quantification*.

multiplication factor SC1020 = [1-4] (-), as follows: SC1020*180 (s) for SC1020-1 and SC1020*30 (s) for SC1020-2.

The velocity of falling debris (VFALL) showed relatively low effect on the code predictions of Cs and I2 release fractions. On the other hand, the analysis performed in [22], suggests that this parameter can have significant effect on the code response when using IDEJ=1 (only molten materials can be ejected at RPV penetrations failure). Thus, the parameter will be considered in the study with slightly extended range [0.01-0.5] (m/s) based on [22].

Other parameters and respective models related to early and late in-vessel phases of severe accident progression, vessel lower head failure and modelling parameters related to transport and deposition of FPs in the RCS and the containment will be included in further analysis if they contribute significantly to the main FOMs.

Furthermore, the bounding analysis results indicate that the importance of the multiplier on the tabular function used in the time-at-temperature fuel rod collapse model in the MELCOR code is very low, and detailed analysis of the results show that the main mechanisms for fuel rod collapse are (i) CL temperature exceeds TRDFAI = 2800K (represented by SC1132-1 – oxidized fuel rod collapse temperature) or (ii) the remaining thickness of unoxidized CL component in a core cell is reduced below the user defined threshold *DRZRMN=0.0001*. Therefore, the uncertainty in the modelling of fuel rod collapse will be addressed by considering SC1132-1 = 2800K with the following [2500-2800K], which is based on the fuel collapse temperatures of VERCORS and VERDON tests [21].

Table 5-10 summarize the parameters and respective ranges selected for the sensitivity analysis.

Table 5-10. Parameter selection for SA

N	Parameter name	Default value	Range	Units
1	TZRSSINC	1210	[1210, 1700]	K
2	TUO2ZRO2	2450	[2450, 2800]	K
3	FCELRA[3]	0.25	[0.1, 0.25]	-
4	PDPOR	0.3	[0.3, 0.5]	-
5	CORNSBLD	1520	[1520, 1700]	K
6	VFALL	0.01	[0.01, 0.5]	m/s
7	SC1020[4]	2	[1,4]	-
8	HFRZSS	1000	[1000, 2500]	W/m2-K
9	HFRZZR	1000	[1000, 7500]	W/m2-K
10	SC11312	2400	[2100, 2500]	K
11	SC11412	0.2	[0.2, 2.0]	kg/m-s
12	DHYPDLP	0.002	[0.002, 0.005]	m
13	HDBH2O	100	[200, 2000]	W/m2-K
14	TPFAIL	1273	[1273, 1600]	K

[3] Parameter used as an input for radiative exchange factors FCELR (radial) and FCELA (axial)on COR_RF card.

[4] Multiplication factor on SC1020-1 = 180 s and SC1020-2 = 30 s.

N	Parameter name	Default value	Range	Units
15	HDBPN	1000	[100, 1000]	W/m2-K
16	CHI	1	[1.0, 3.0]	-
17	GAMMA	1	[1.0, 3.0]	-
18	STICK	1	[0.5, 1]	-
19	RHONOM	1000	[1000, 4900]	kg/m3
20	NUMSEC	10	[10, 20]	0
21	TURBDS	0.001	[7.5E-4, 1.25E-3]	m2/s3
22	SC7111I1	4.982	[4.2347, 5.7293]	Å
23	SC7111I2	550	[467.50, 632.50]	K
24	SC7111CS1	3.617	[3.0745,4.1595]	Å
25	SC7111CS2	97	[82.450,111.550]	K
26	SC7170CS	3.95	[3.3575, 4.5425]	kg/kg H2O
27	SC7170CSI3	0.44	[0.374, 0.5060]	kg/kg H2O
28	SC7170CSI4	2.25	[1.9125, 2.5875]	kg/kg H2O
29	SC7170CSM	0.67	[0.5695, 0.7705]	kg/kg H2O
30	SC715010	1	[1,3]	-
31	SC71521	0.007	[5.E-3, 8.E-3]	m
32	SC71531	7.876	[6.6946, 9.0574]	cm/s
33	SC71551	1.79182	[1.5230, 2.0606]	-
34	SC71555	1.13893	[0.9681, 1.3098]	-
35	SC71542	0.003011	[2.5593E-03, 3.4626E-03]	l-s/cm2
36	SC71568	-0.00232	[-2.6691e-03, -1.9728e-03]	-
37	OXM[5]	1	[1,2,3,4]	-
38	MVSSDFA	500	[100, 500]	-
39	SC3210	1	[1, 1.15]	-
40	SC11321	2800	[2500-2800]	K
41	MVSSDFV	1	[1-500]	-

The amount of code evaluations in the Morris sensitivity analysis is determined by equation (4) in section 4.1.1.1. If we consider the number of elementary effects equal to 11, it will require 462 code runs for every splinter scenario (i.e., 2x462 to address the uncertainty in the modelling of melt/debris ejection from the vessel represented by IDEJ modelling switch).

5.2.2. Results

Results of MELCOR sensitivity analysis performed by VG during the project are described in the following sections. The following accident sequences have been studied:

- RC7A – Unmitigated Station blackout, leading to filtered venting,

[5] Modelling switch, see [23] for details.

- RC7B – Unmitigated feedwater line LOCA, leading to filtered venting.

The mode of debris ejection from the vessel IDEJ0 or IDEJ1 was considered as a splinter scenario, i.e., sensitivity analysis has been performed separately 0for:

- RC7A-IDEJ0 – 462 MELCOR code evaluations.
- RC7A-IDEJ1 – 462 MELCOR code evaluations.
- RC7B-IDEJ0 – 462 MELCOR code evaluations.
- RC7B-IDEJ1 – 462 MELCOR code evaluations.

5.2.2.1.Release category RC7A - SBO-MVSS

5.2.2.1.1. RC7A - SBO-MVSS IDEJ1

Table 5-11 illustrates the range as well as the mean and 0.05/0.5/0.95 quantiles of the distributions of the main FOMs analyzed in sensitivity study.

Table 5-11. Summary of SA analysis results for SBO-MVSS IDEJ1 (RC7A IDEJ1)

	Range		Mean	Median	5%	95%
MVSS Time [h]	3.73	16.72	7.30	6.90	5.43	11.42
LHF Time [h]	1.34	9.42	2.63	2.44	1.76	4.45
MVSS-LHF Time[h]	1.39	12.43	4.67	4.39	2.58	8.30
H2 Mass in COR [kg]	432.39	895.12	570.59	568.33	465.40	685.00
CS Release fraction [-]	1.19E-06	7.73E-05	1.18E-05	9.10E-06	2.24E-06	3.59E-05
I Release fraction [-]	1.99E-06	3.59E-03	4.77E-04	8.02E-05	4.85E-06	2.10E-03

Figures 5-38 - 5-43 show the Morris diagrams, where the x-axis represents the Morris modified mean and y-axis shows the Morris standard deviation. Morris modified mean values substantially different from zero, indicate significant overall influence of the parameter, while large values of Morris standard deviation indicate possible interactions with other input parameters and non-linear behavior of the output with respect to the input.

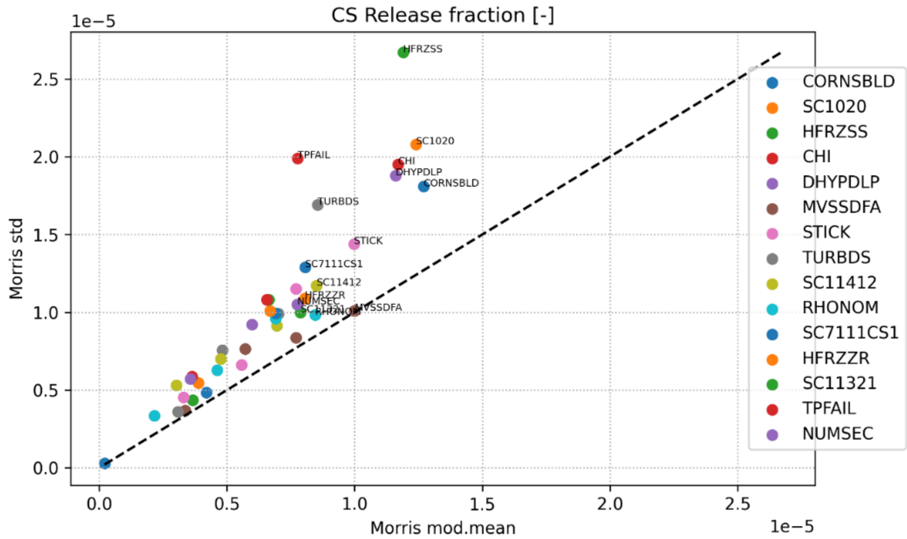

Figure 5-38 Morris diagram for the fraction of Cs released to the environment [-]

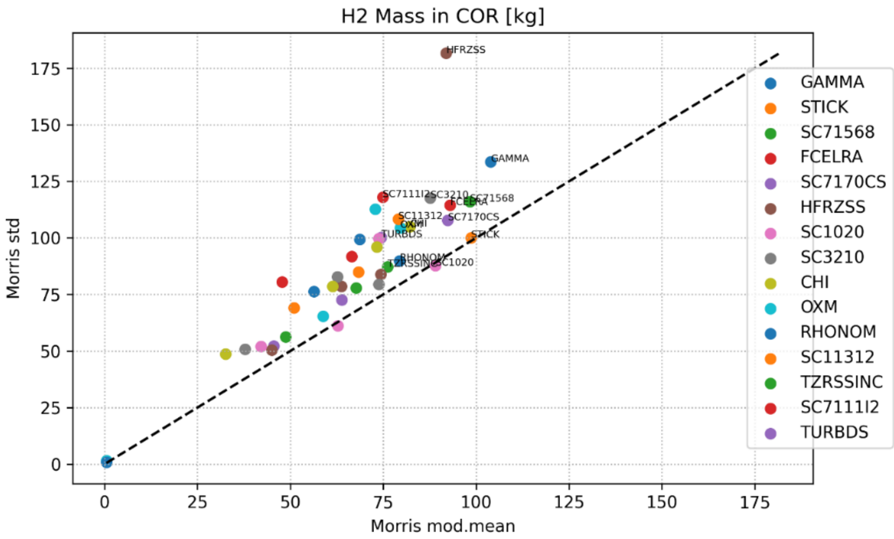

Figure 5-39 Morris diagram for the H2 mass generated in the COR package [kg]

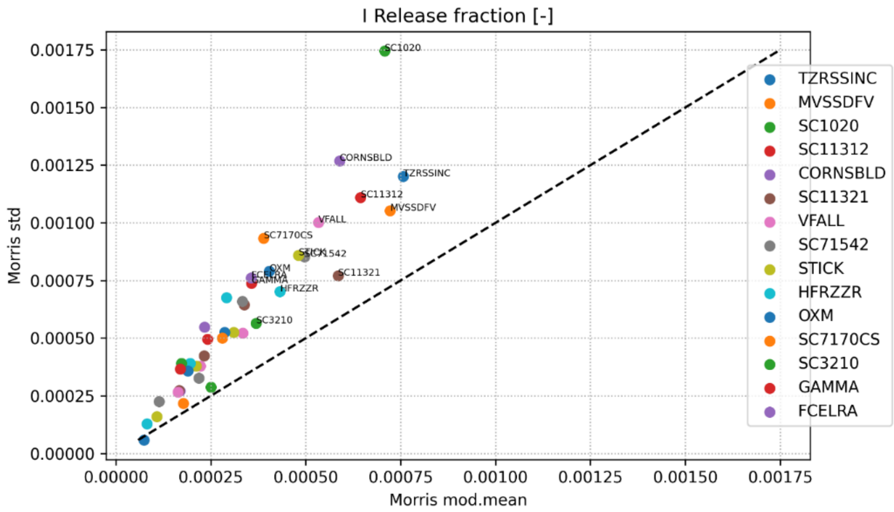

Figure 5-40 Morris diagram for the fraction of I released to the environment [-]

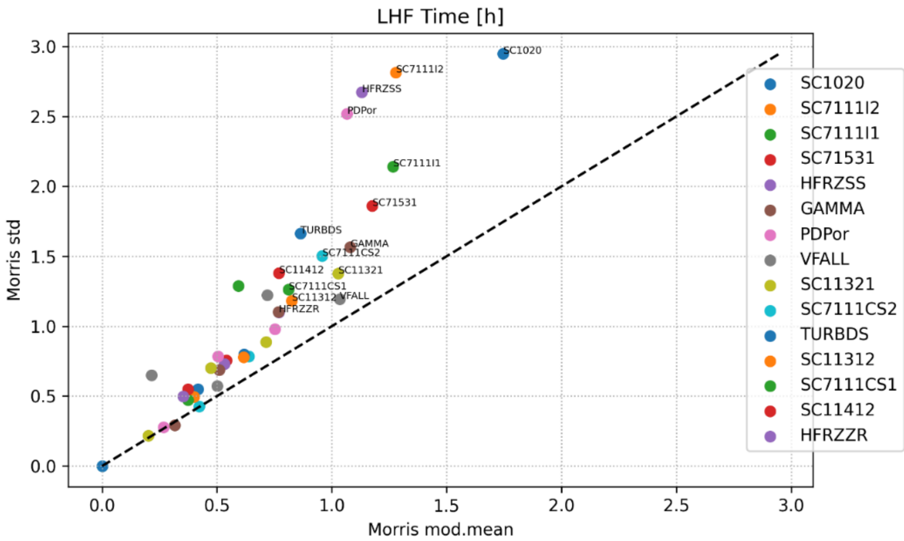

Figure 5-41 Morris diagram for the lower head failure time [h]

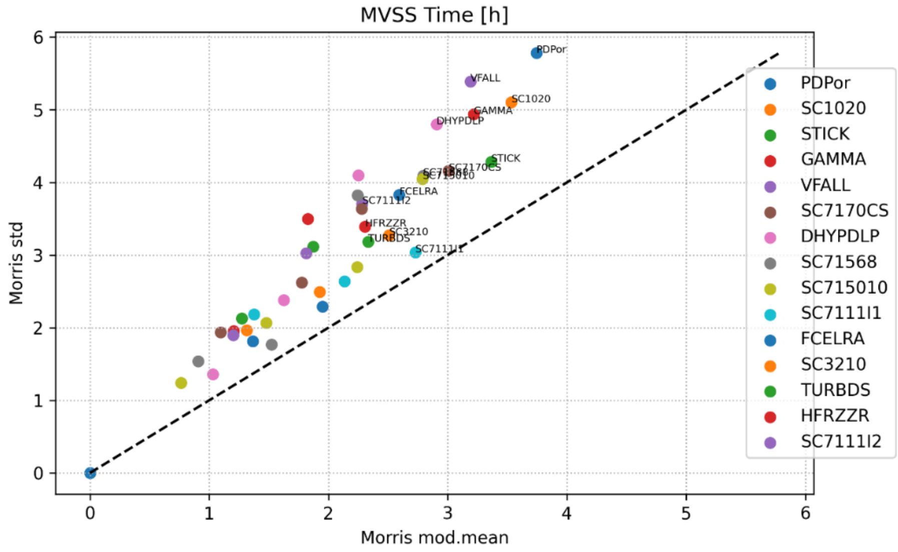

Figure 5-42 Morris diagram for MVSS opening time [h]

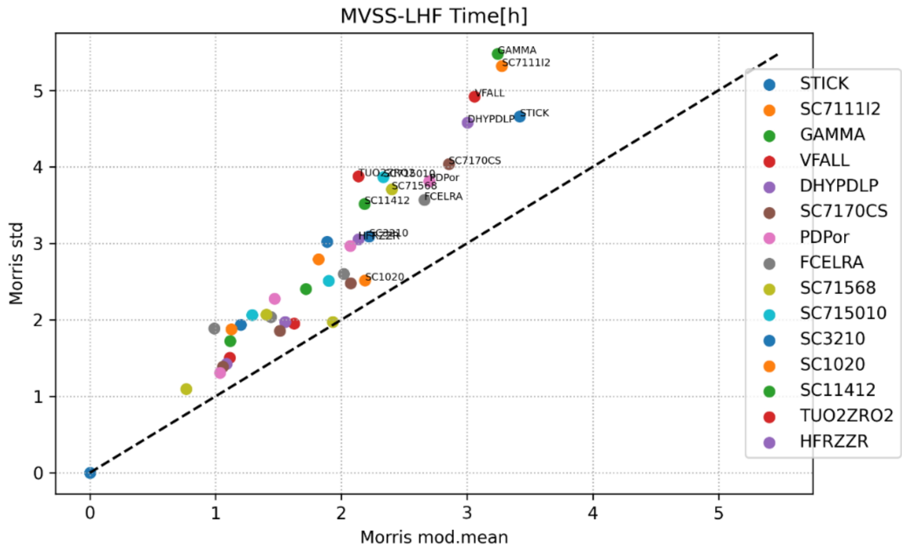

Figure 5-43 Morris diagram for the difference between the time of MVSS opening and vessel lower head failure [h]

One-way ANOVA analysis was performed on the data set generated by the Morris method for SA, the results of the analysis are summarized in Table 5-12. Figures 5-44-5-47 show the box-and-whisker plots for the fraction of Cs released to the environment and timing of MVSS venting vs. the most influential parameters identified by ANOVA.

Table 5-12. One-way ANOVA results for SBO-MVSS IDEJ1

Cs release fraction [-]			**MVSS Time [h]**		
variable	**F-value**	**p-value**	**variable**	**F-value**	**p-value**
MVSSDFA	149.04	2.15E-67	SC7111I2	11.27	3.81E-07
GAMMA	129.55	9.08E-61	SC7170CS	9.94	2.32E-06
SC7111I1	42.42	3.31E-24	SC71555	8.91	9.51E-06
SC71551	37.96	6.30E-22	VFALL	8.39	1.94E-05
SC11321	31.90	9.71E-19	SC7111I1	8.09	2.92E-05
SC71555	29.67	1.51E-17	MVSSDFA	7.04	1.23E-04
SC7111I2	26.86	5.08E-16	SC11321	6.88	1.54E-04

Cs release fraction [-]		
variable	**F-value**	**p-value**
SC7170CSM	26.79	5.56E-16
OXM	26.35	9.72E-16
RHONOM	26.01	1.48E-15
SC3210	22.44	1.43E-13
HDBPN	21.18	7.25E-13
HFRZZR	21.12	7.85E-13
MVSSDFV	20.34	2.18E-12
SC7170CS	20.04	3.19E-12
VFALL	17.01	1.73E-10
SC7170CSI4	15.86	7.89E-10
STICK	15.19	1.93E-09
TPFAIL	14.75	3.49E-09
HDBH2O	14.55	4.56E-09
SC71531	14.10	8.38E-09
DHYPDLP	13.06	3.37E-08
SC7111CS1	12.01	1.39E-07
SC11312	11.70	2.12E-07
TURBDS	11.43	3.07E-07
SC71521	9.49	4.29E-06
NUMSEC	8.53	1.61E-05
SC71542	8.45	1.78E-05
SC71568	8.13	2.77E-05
CHI	7.00	1.29E-04
SC715010	6.91	1.47E-04
TZRSSINC	6.21	3.87E-04
PDPor	6.06	4.72E-04
FCELRA	5.63	8.50E-04
SC1020	5.55	9.56E-04
CORNSBLD	4.06	7.29E-03
SC7170CSI3	3.32	1.97E-02
SC7111CS2	2.89	3.51E-02
SC11412	2.65	4.84E-02
HFRZSS	2.41	6.60E-02
TUO2ZRO2	0.52	6.65E-01

MVSS Time [h]		
variable	**F-value**	**p-value**
NUMSEC	6.86	1.58E-04
SC7170CSI4	6.41	2.91E-04
SC11312	6.41	2.94E-04
SC11412	5.71	7.60E-04
SC71568	5.02	1.97E-03
DHYPDLP	4.83	2.55E-03
PDPor	4.35	4.91E-03
SC7111CS1	4.16	6.37E-03
CORNSBLD	4.15	6.40E-03
SC7170CSM	4.09	6.98E-03
SC3210	4.03	7.60E-03
GAMMA	3.96	8.32E-03
SC7111CS2	3.90	9.00E-03
TPFAIL	3.90	9.03E-03
SC1020	3.87	9.40E-03
SC71521	3.87	9.41E-03
TURBDS	3.61	1.34E-02
SC715010	3.38	1.82E-02
CHI	3.34	1.92E-02
SC7170CSI3	3.09	2.67E-02
SC71531	2.91	3.44E-02
TUO2ZRO2	2.66	4.75E-02
FCELRA	2.62	5.01E-02
HFRZSS	2.54	5.56E-02
HDBPN	2.43	6.42E-02
OXM	2.16	9.25E-02
HFRZZR	2.15	9.34E-02
SC71551	1.93	1.23E-01
SC71542	1.51	2.11E-01
STICK	1.29	2.79E-01
TZRSSINC	1.25	2.91E-01
MVSSDFV	0.66	5.75E-01
HDBH2O	0.63	5.95E-01
RHONOM	0.25	8.62E-01

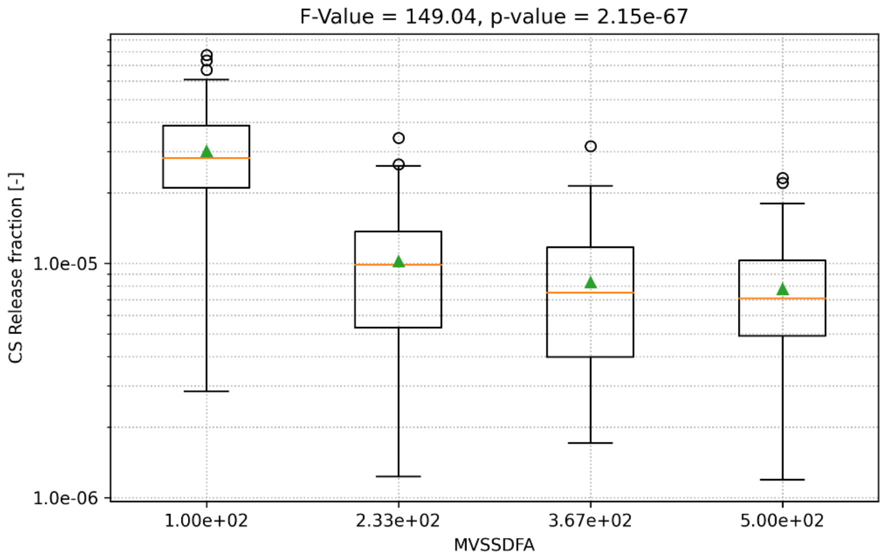

Figure 5-44 Box and whisker plot for the fraction of Cs release [-] vs. MVSSDFA [-][6]

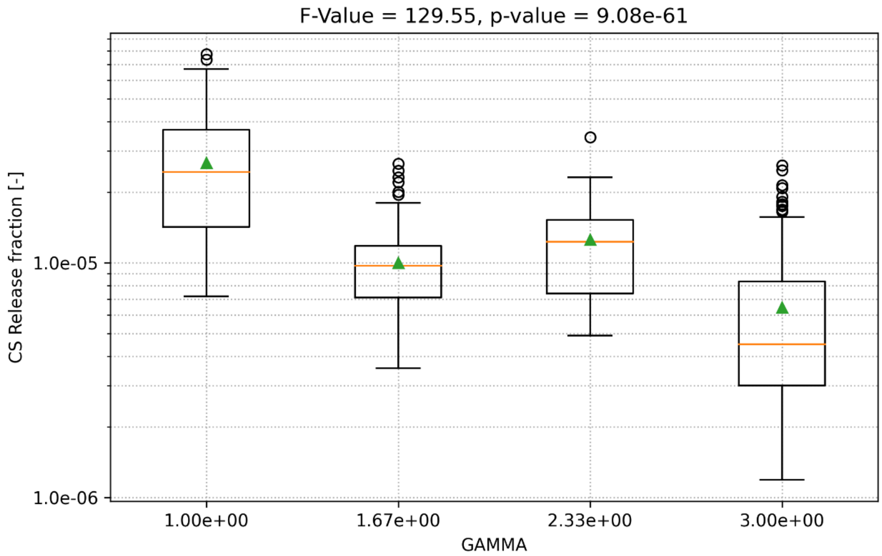

Figure 5-45 Box and whisker plot for the fraction of Cs release [-] vs. GAMMA [-][6]

[6] Whiskers' lengths are defined by IQR - the interquartile range (Q3-Q1), and the first and the third quartiles. The upper whisker will extend to last data point less than (Q3 + 1.5*IQR). Similarly, the lower whisker will extend to the first datum greater than (Q1 – 1.5*IQR). Beyond the whiskers, data points are considered as outliers and are plotted as individual points.

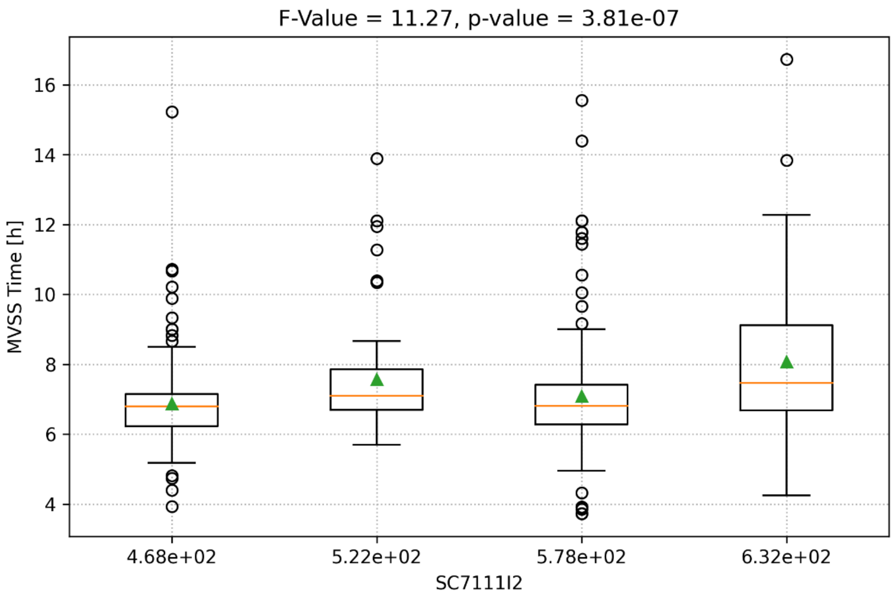

Figure 5-46 Box and whisker plot for the timing of MVSS [h] vs. SC7111I2 [] [6]

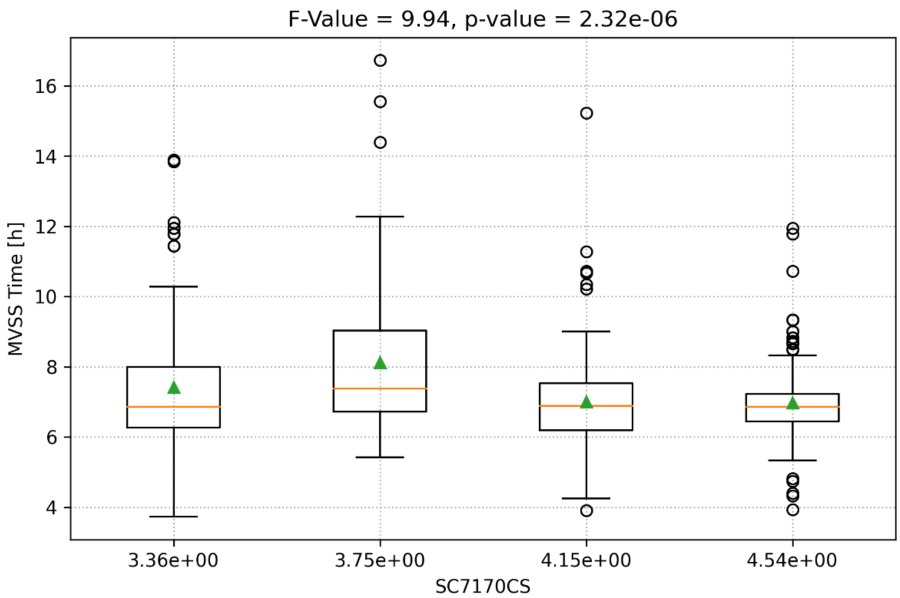

Figure 5-47 Box and whisker plot for the timing of MVSS [h] vs. SC7170CS [-] [6]

Based on the results from the Morris SA and ANOVA, 19 MELCOR code modelling parameters were selected for the uncertainty analysis. The selection is based on the 5 most influential parameters per FOM (fraction of Cs released to the environment, fraction of I released to the environment, timing of release to the environment (MVSS opening)).

Table 5-13. Parameter selection for UA for SBO-MVSS IDEJ1

N	Parameter ID	Description	Units
1	PDPor	Particulate debris porosity	-
2	SC1020	Multiplication factor for SC1020-1 and SC1020-2	-
3	STICK	Aerosol particles sticking probability	-
4	GAMMA	Aerosol agglomeration shape factor	-
5	VFALL	Velocity of falling debris	M/s
6	CORNSBLD	Control blade failure temperature	K

N	Parameter ID	Description	Units
7	HFRZSS	Refreezing heat transfer coefficient for SS	W/m2-K
8	CHI	Aerosol dynamic shape factor	-
9	DHYPDLP	Lower plenum particulate debris equivalent diameter	m
10	TZRSSINC	Temp. for Zr SS eutectic pairs	K
11	MVSSDFA	MVSS decontamination factor for radioactive aerosols	-
12	SC11312	Critical temperature at which molten materials are released from an oxide shell or local blockage	K
13	SC7111I1	Characteristic diameter of the molecule for I	Å
14	SC71551	SPARC-90 model multiplication constants in the DF factor correlations for small Stokes numbers	-
15	SC11321	Oxidized fuel rod collapse temperature	K
16	SC7111I2	Characteristic energy of interaction between the molecules divided by the Boltzmann constant for I2	K
17	SC7170CSM	Saturation solubility at high and low temperature reference for CsM	kg/kg H2O
18	SC71555	SPARC-90 model multiplication constants in the DF factor correlations for and large Stokes numbers	-
19	HFRZZR	Refreezing heat transfer coefficient for Zr	W/m2-K
20	RHONOM	Aerosol density	kg/m3
21	MVSSDFV	MVSS decontamination factor for radioactive vapours	-

5.2.2.1.2. RC7A - SBO-MVSS IDEJ0

Table 5-14 illustrates the range as well as the mean and 0.05/0.5/0.95 quantiles of the distributions of the main FOMs analyzed in sensitivity study.

Table 5-14. Summary of SA analysis results for SBO-MVSS IDEJ0 (RC7A IDEJ0)

	Range		Mean	Median	5%	95%
MVSS Time [h]	2.52	10.39	5.50	5.47	4.61	6.71
LHF Time [h]	1.44	8.62	2.56	2.42	1.72	4.04
MVSS-LHF Time[h]	0.22	4.34	2.94	3.01	1.37	3.90
H2 Mass in COR [kg]	304.09	696.80	504.01	498.77	404.77	623.49
CS Release fraction [-]	9.55E-07	5.16E-05	6.59E-06	5.23E-06	1.86E-06	1.77E-05
I Release fraction [-]	1.33E-06	1.82E-03	2.55E-04	2.96E-05	4.3E-06	1.20E-03

Figures 5-48-5-52 show the Morris diagrams, where the x-axis represents the Morris modified mean and y-axis shows the Morris standard deviation. Morris modified mean values substantially different from zero, indicate significant overall influence of the parameter, while large values of Morris standard deviation indicate possible interactions with other input parameters and non-linear behavior of the output with respect to the input.

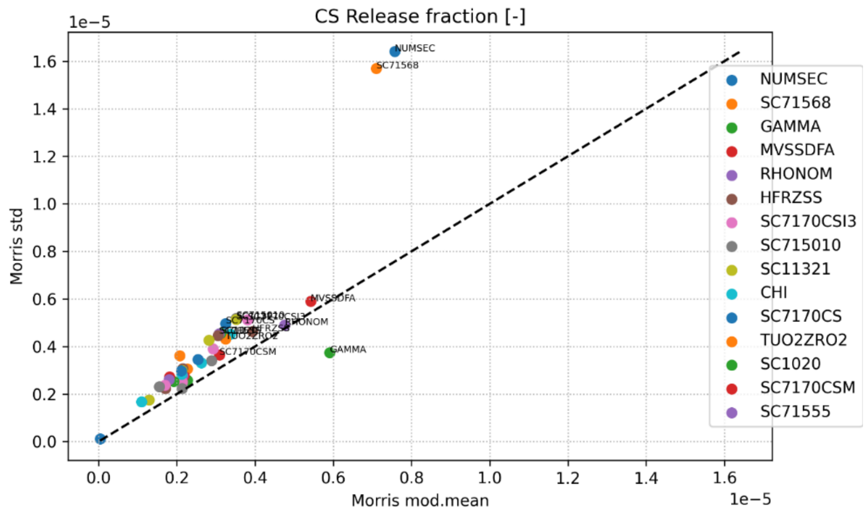

Figure 5-48 Morris diagram for the fraction of Cs released to the environment [-]

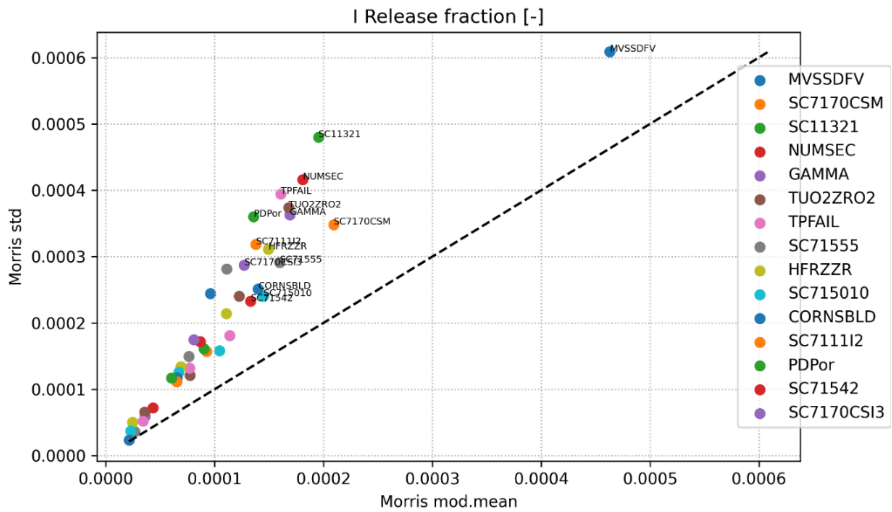

Figure 5-49 Morris diagram for the fraction of I released to the environment [-]

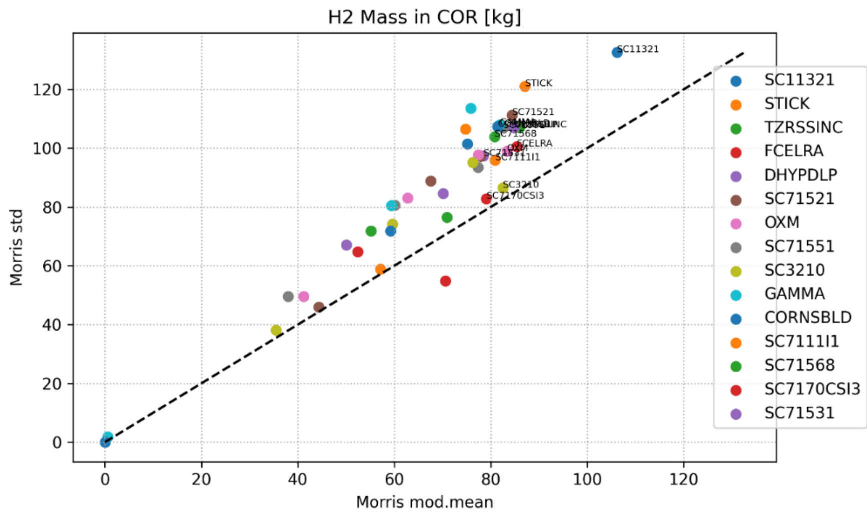

Figure 5-50 Morris diagram for the H2 mass generated in the COR package [kg]

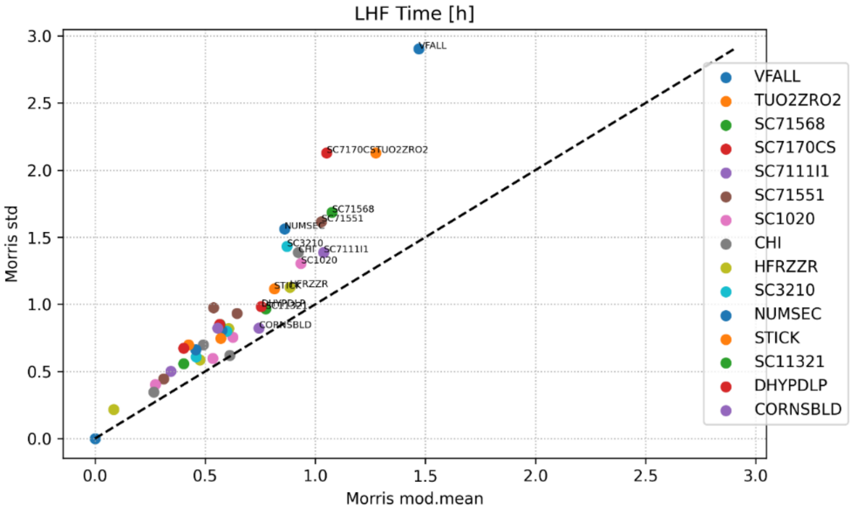

Figure 5-51 Morris diagram for the lower head failure time [h]

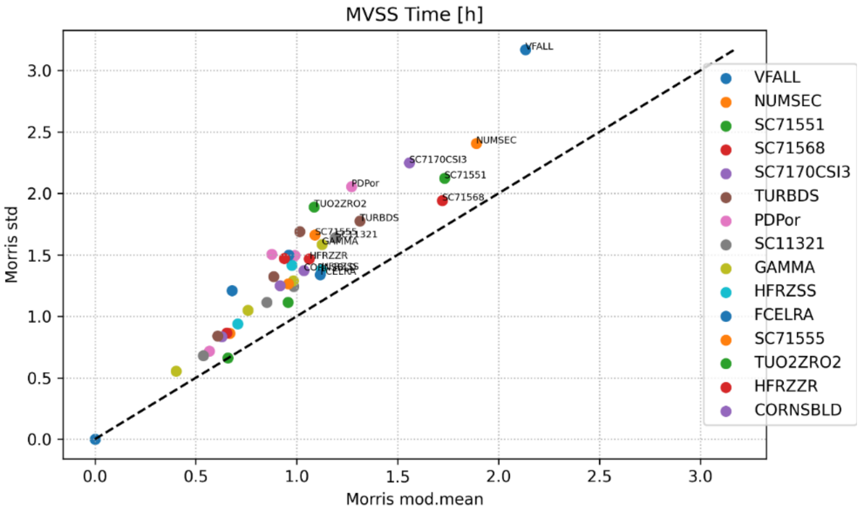

Figure 5-52 Morris diagram for MVSS opening time [h]

One-way ANOVA analysis was performed on the data set generated by the Morris method for SA, the results of the analysis are summarized in Table 5-15. Figures 5-53 - 5-56 show the box-and-whisker plots for the fraction of Cs released to the environment and timing of MVSS venting vs. the most influential parameters identified by ANOVA.

Table 5-15. One-way ANOVA results for SBO-MVSS IDEJ0

Cs release fraction [-]			**MVSS Time [h]**		
variable	**F-value**	**p-value**	**variable**	**F-value**	**p-value**
GAMMA	183.02	5.50E-78	HDBPN	16.73	2.50E-10
MVSSDFA	159.85	6.92E-71	MVSSDFA	14.82	3.18E-09
SC7111I1	56.33	5.18E-31	SC7111CS1	13.03	3.51E-08
SC71551	47.19	1.37E-26	FCELRA	11.81	1.82E-07
RHONOM	35.51	1.19E-20	SC7111I1	10.96	5.79E-07
SC7170CSM	31.71	1.22E-18	VFALL	10.55	1.01E-06
SC7111I2	31.48	1.62E-18	SC71555	10.05	2.00E-06
SC71555	29.40	2.12E-17	SC7170CSI4	9.45	4.54E-06
OXM	28.90	3.96E-17	NUMSEC	8.64	1.38E-05
SC3210	28.28	8.55E-17	SC1020	8.37	1.99E-05

Cs release fraction [-]		
variable	F-value	p-value
SC11321	24.63	8.65E-15
HDBPN	23.75	2.66E-14
VFALL	23.02	6.79E-14
MVSSDFV	22.92	7.69E-14
STICK	22.80	8.96E-14
HFRZZR	21.75	3.47E-13
SC7170CS	20.30	2.28E-12
SC71531	18.50	2.40E-11
SC7170CSI4	15.76	9.11E-10
TURBDS	15.17	2.00E-09
DHYPDLP	15.00	2.51E-09
HDBH2O	14.01	9.43E-09
SC7111CS1	13.54	1.77E-08
TPFAIL	13.16	2.95E-08
SC11312	12.59	6.34E-08
SC71521	12.31	9.34E-08
SC71542	11.70	2.12E-07
SC715010	9.17	6.68E-06
NUMSEC	8.18	2.59E-05
PDPor	7.51	6.48E-05
SC7170CSI3	6.65	2.10E-04
TZRSSINC	6.26	3.60E-04
SC71568	6.00	5.15E-04
CHI	5.92	5.73E-04
SC7111CS2	4.38	4.73E-03
CORNSBLD	4.17	6.27E-03
SC11412	4.06	7.31E-03
HFRZSS	4.05	7.37E-03
FCELRA	3.39	1.81E-02
SC1020	2.96	3.21E-02
TUO2ZRO2	0.33	8.02E-01

MVSS Time [h]		
variable	F-value	p-value
SC7170CS	6.88	1.53E-04
SC7170CSM	6.79	1.75E-04
SC715010	6.53	2.49E-04
SC11412	6.47	2.70E-04
TPFAIL	6.41	2.91E-04
SC71551	6.17	4.06E-04
SC11312	6.04	4.85E-04
SC71568	5.61	8.77E-04
PDPor	5.55	9.45E-04
SC7111I2	5.07	1.84E-03
CHI	5.02	1.96E-03
CORNSBLD	4.51	3.91E-03
HDBH2O	4.35	4.87E-03
HFRZSS	4.31	5.17E-03
SC11321	3.85	9.60E-03
SC71531	3.07	2.76E-02
STICK	2.98	3.12E-02
TUO2ZRO2	2.95	3.26E-02
TZRSSINC	2.58	5.28E-02
TURBDS	2.40	6.71E-02
GAMMA	2.30	7.61E-02
SC71521	2.23	8.40E-02
SC7170CSI3	1.99	1.15E-01
SC71542	1.94	1.22E-01
MVSSDFV	1.39	2.45E-01
RHONOM	1.27	2.84E-01
DHYPDLP	1.04	3.73E-01
SC3210	0.95	4.14E-01
SC7111CS2	0.50	6.84E-01
HFRZZR	0.44	7.26E-01
OXM	0.37	7.72E-01

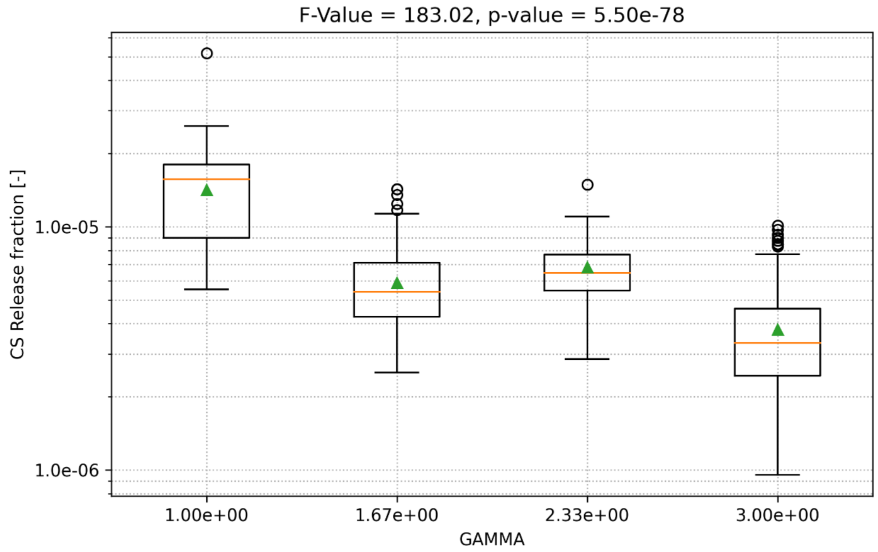

Figure 5-53 Box and whisker plot for the fraction of Cs release [-] vs. GAMMA [-][6]

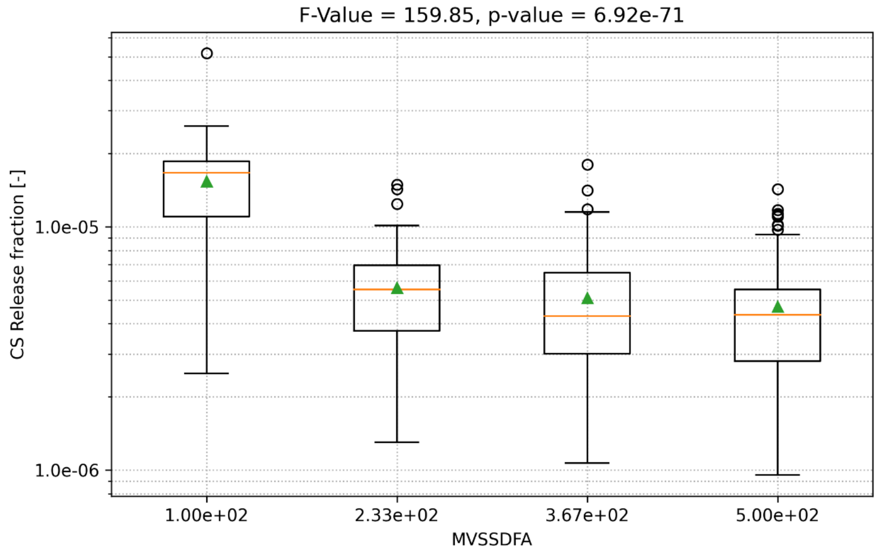

Figure 5-54 Box and whisker plot for the fraction of Cs release [-] vs. MVSSA[-] [6]

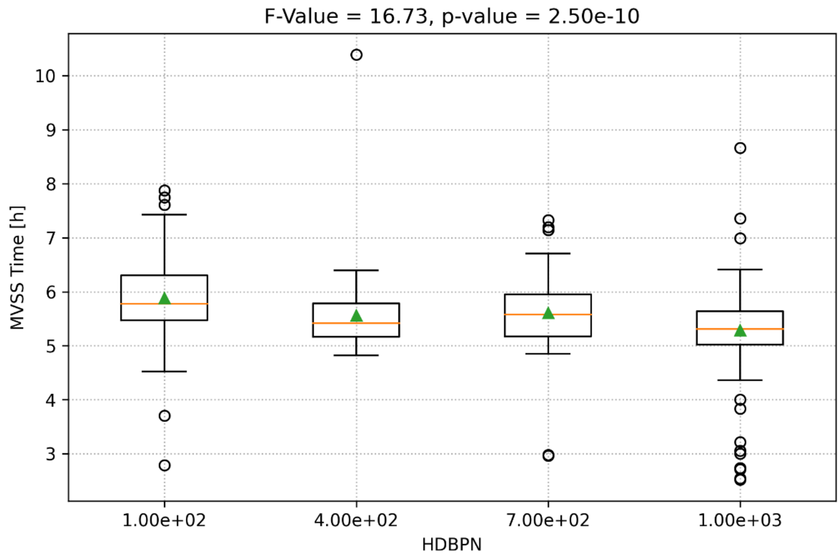

Figure 5-55 Box and whisker plot for the timing of MVSS [h] vs. HDBPN [K][6]

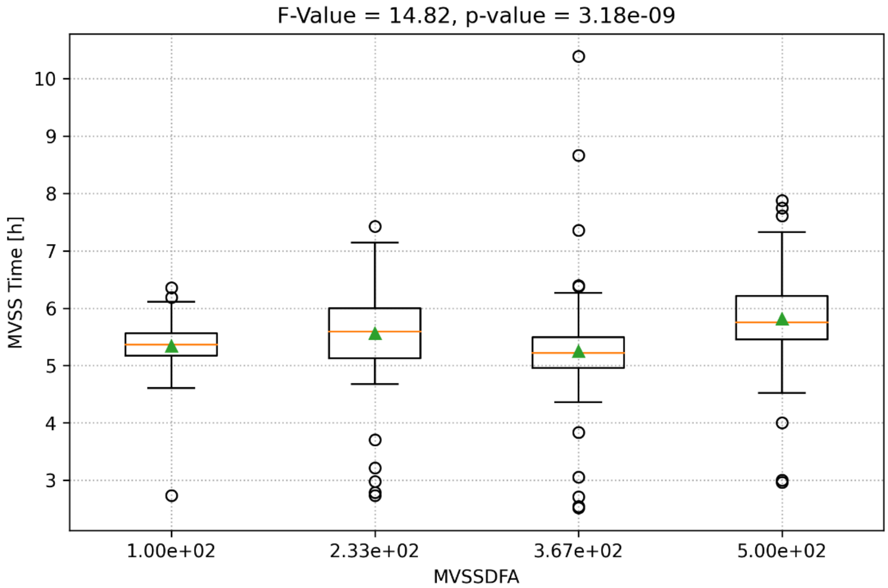

Figure 5-56 Box and whisker plot for the fraction of Cs release [-] vs. MVSSDFV [-][6]

Based on the results from the Morris SA and ANOVA, 21 MELCOR code modelling parameters were selected for the uncertainty analysis. The selection is based on the 5 most influential parameters per FOM (fraction of Cs released to the environment, fraction of I released to the environment, timing of release to the environment (MVSS opening)).

Table 5-16. Parameter selection for UA for SBO-MVSS IDEJ0

N	Parameter ID	Description	Units
1	VFALL	Velocity of falling debris	m/s
2	NUMSEC	Number of sections	-
3	SC71551	SPARC-90 model multiplication constants in the DF factor correlations for small Stokes numbers	-
4	SC71568	Multiplicative constant in a temperature correction correlation in the SPARC-90 model	-
5	SC7170CSI3	Saturation solubility at low temperature reference for CsI	kg/kg H2O
6	GAMMA	Aerosol agglomeration shape factor	-
7	MVSSDFA	MVSS decontamination factor for radioactive aerosols	-
8	RHONOM	Aerosol density	kg/m3
9	SC7170CSM	Saturation solubility at high and low temperature reference for CsM	kg/kg H2O
10	SC11321	Oxidized fuel rod collapse temperature	K
11	SC7111I1	Characteristic diameter of the molecule for I	Å
12	HDBPN	Heat transfer coefficient between particulate debris and LH penetration	W/m2-K
13	SC7111CS1	Characteristic diameter of the molecule for Cs	Å
14	FCELRA	Radiative exchange factors for radiation radially outward and upward from the cell boundary to the next adjacent cell	-
15	CHI	Aerosol dynamic shape factor	-
16	PDPor	Particulate debris porosity	-
17	HFRZZR	Refreezing heat transfer coefficient for Zr	W/m2-K
18	HFRZSS	Refreezing heat transfer coefficient for SS	W/m2-K

N	Parameter ID	Description	Units
19	STICK	Aerosol particles sticking probability	-
20	TZRSSINC	Temp. for Zr SS eutectic pairs	K
21	MVSSDFV	MVSS decontamination factor for radioactive vapours	-

5.2.2.2.Release category RC7B - LOCA-MVSS

5.2.2.2.1. RC7B – LOCA-MVSS IDEJ1

Table 5-17 illustrates the range as well as the mean and 0.05/0.5/0.95 quantiles of the distributions of the main FOMs analyzed in sensitivity study.

Table 5-17. Summary of SA analysis results for LOCA-MVSS IDEJ1 (RC7B IDEJ1)

	Range		Mean	Median	5%	95%
MVSS Time [h]	1.02	10.39	4.90	4.86	1.52	8.83
LHF Time [h]	0.68	4.44	1.46	1.34	0.84	2.52
MVSS-LHF Time[h]	-2.29	8.89	3.44	3.43	-0.44	7.63
H2 Mass in COR [kg]	349.34	801.18	555.08	553.13	427.37	693.44
CS Release fraction [-]	9.62E-05	1.58E-01	3.38E-02	7.93E-04	3.06E-04	1.33E-01
I Release fraction [-]	9.52E-05	2.16E-01	4.23E-02	9.54E-04	3.66E-04	1.72E-01

Figures 5-57 - 5-63 show the Morris diagrams, where the x-axis represents the Morris modified mean and y-axis shows the Morris standard deviation. Morris modified mean values substantially different from zero, indicate significant overall influence of the parameter, while large values of Morris standard deviation indicate possible interactions with other input parameters and non-linear behavior of the output with respect to the input.

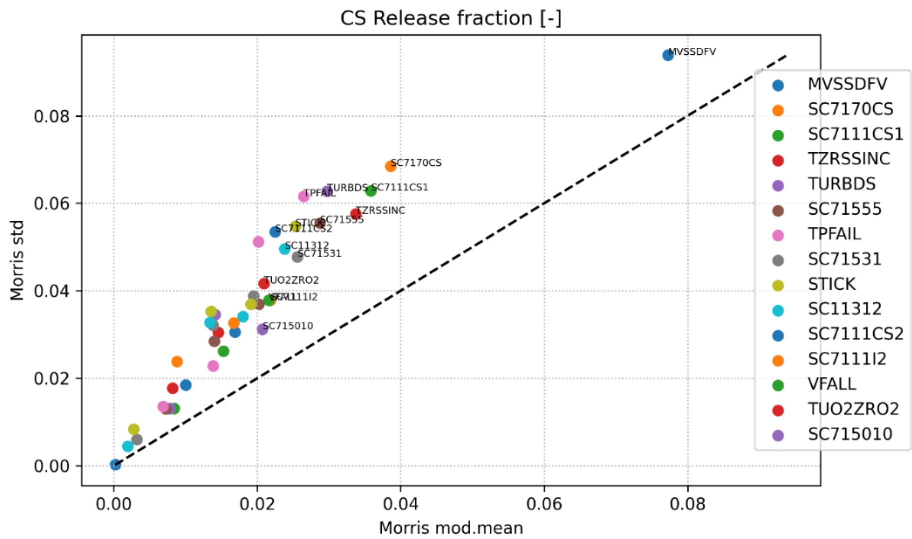

Figure 5-57 Morris diagram for the fraction of Cs released to the environment [-]

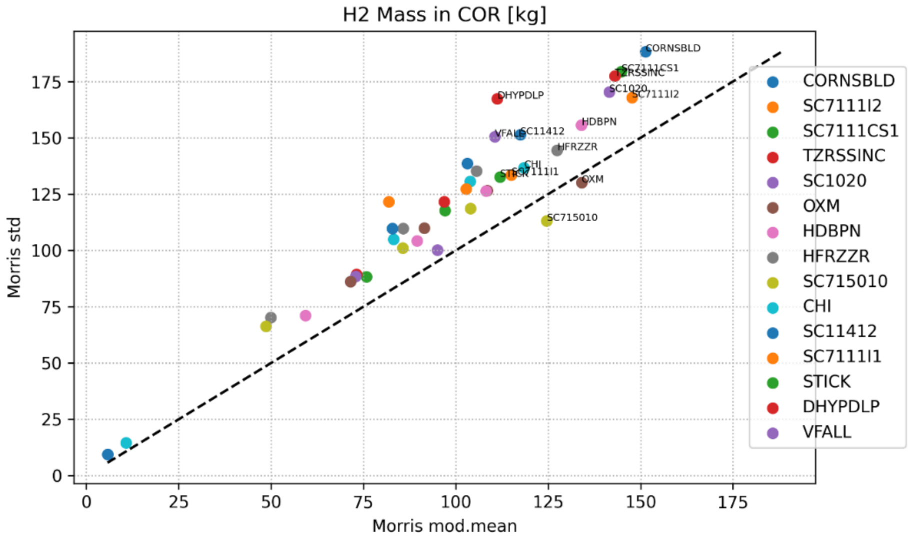

Figure 5-58 Morris diagram for the H2 mass generated in the COR package [kg]

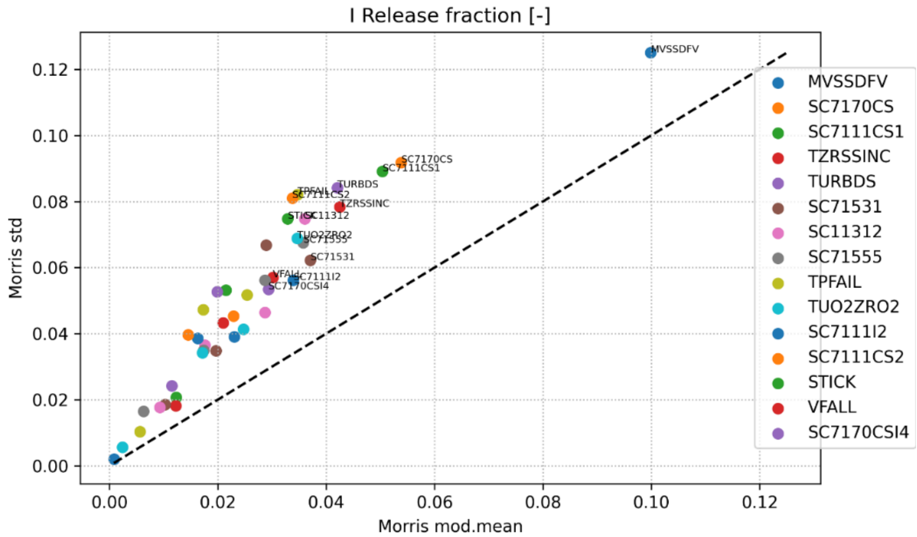

Figure 5-59 Morris diagram for the fraction of I released to the environment [-]

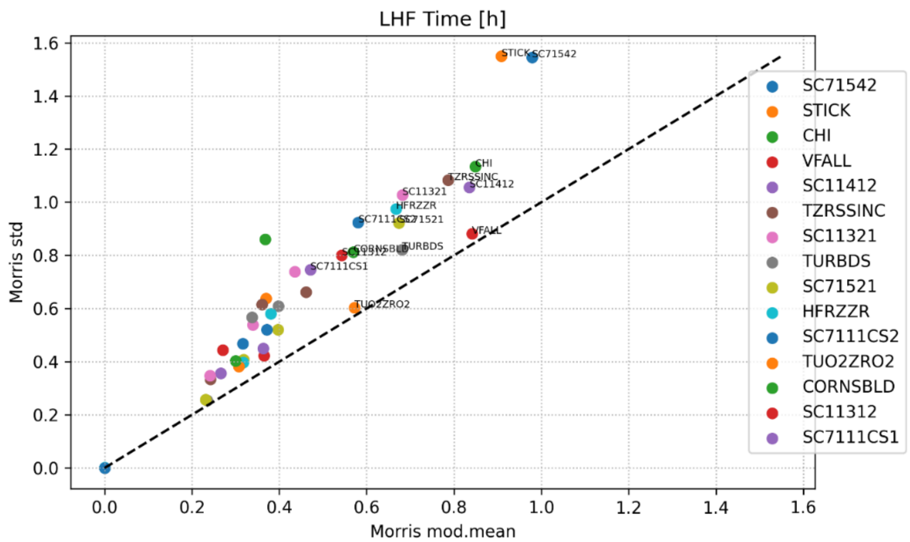

Figure 5-60 Morris diagram for the lower head failure time [h]

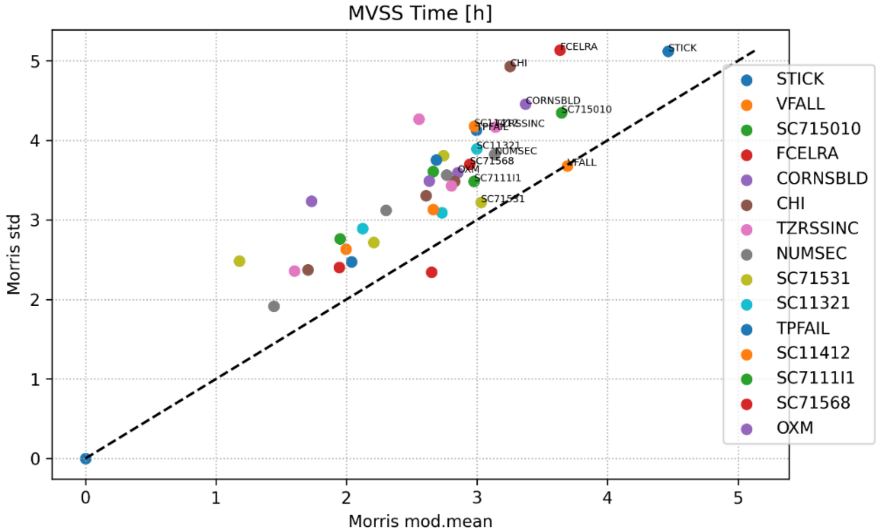

Figure 5-61 Morris diagram for MVSS opening time [h]

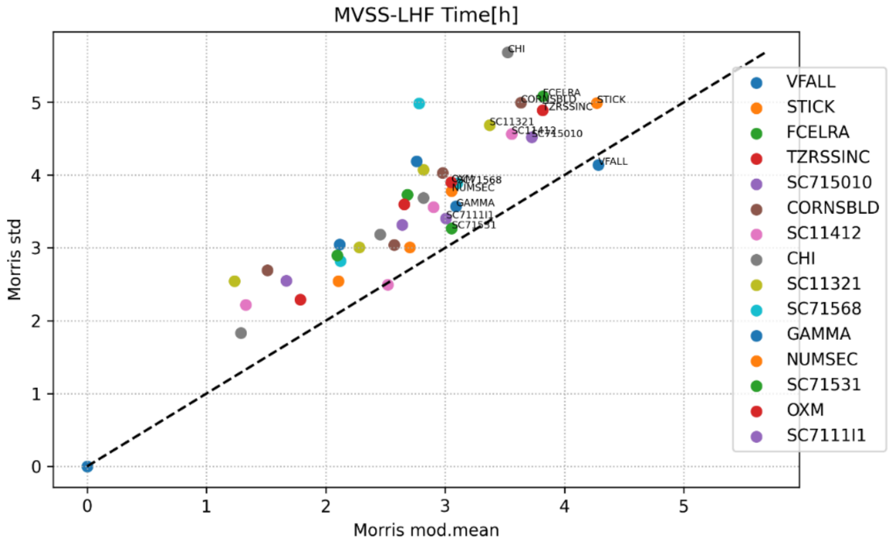

Figure 5-62 Morris diagram for the difference between the time of MVSS opening and vessel lower head failure [h]

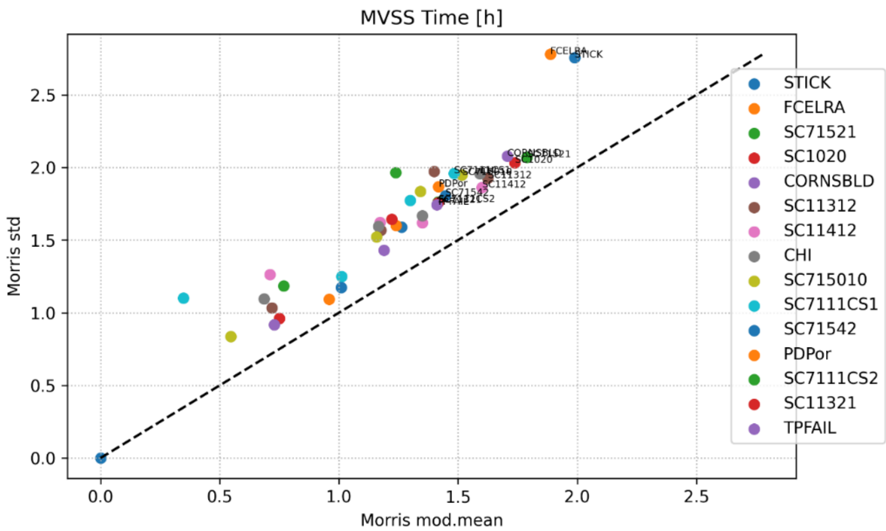

Figure 5-63 Morris diagram for MVSS opening time [h]

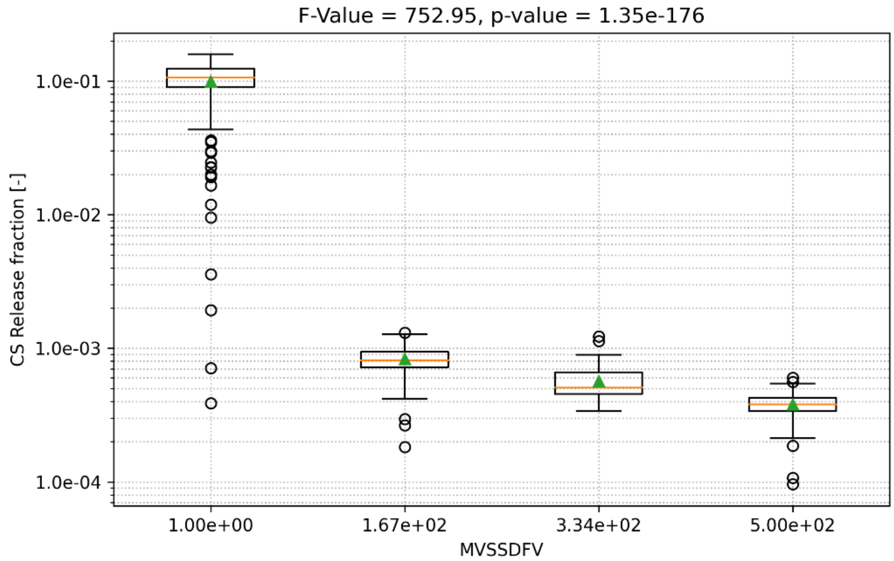

Figure 5-64 Box and whisker plot for the fraction of Cs release [-] vs. MVSSDFV [-][6]

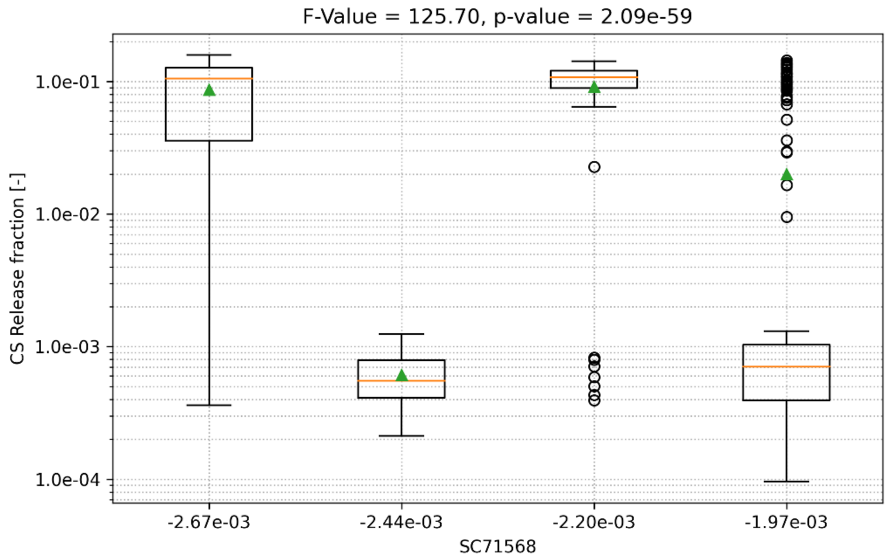

Figure 5-65 Box and whisker plot for the fraction of Cs release [-] vs. SC71568 [-] [6]

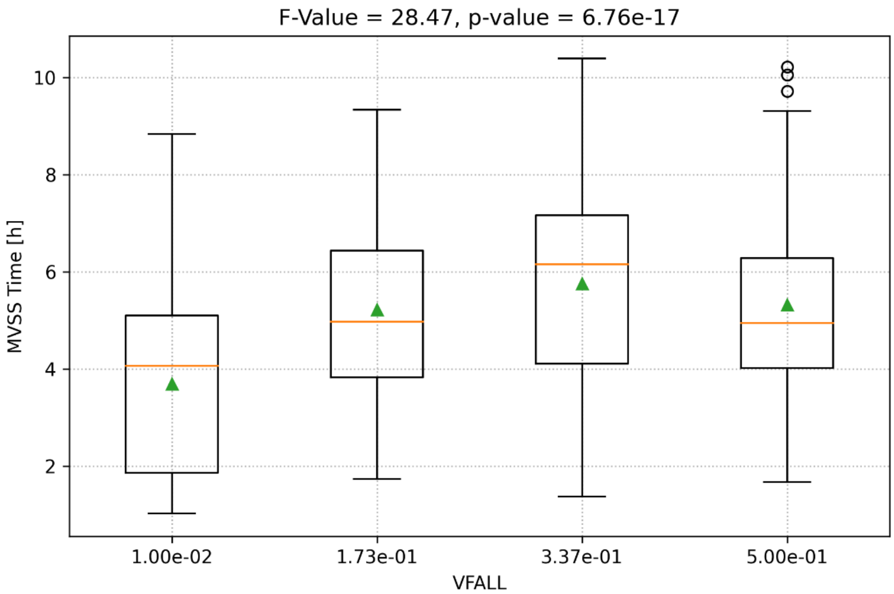

Figure 5-66 Box and whisker plot for the timing of MVSS [h] vs. VFALL [m/s] [6]

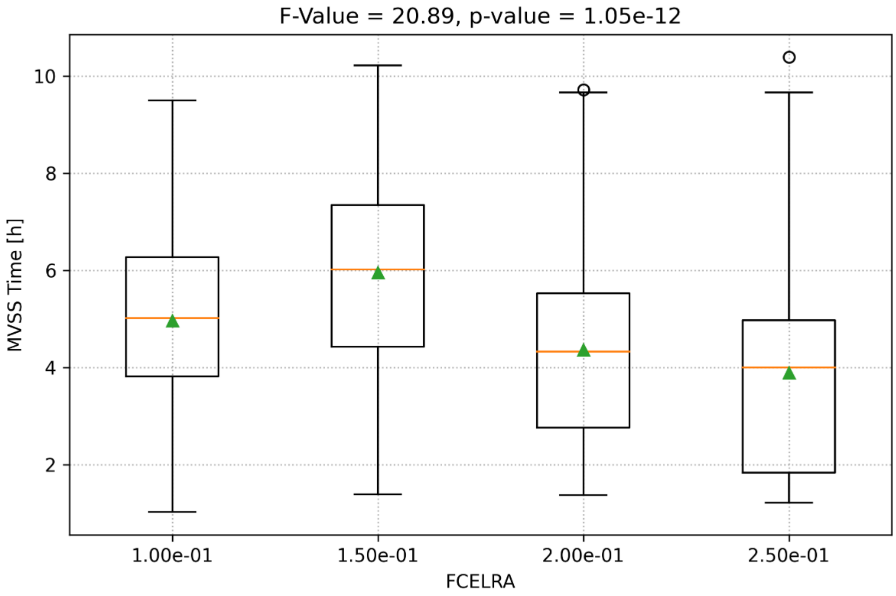

Figure 5-67 Box and whisker plot for the timing of MVSS [h] vs. FCELRA [-] [6]

One-way ANOVA analysis was performed on the data set generated by the Morris method for SA, the results of the analysis are summarized in Table 5-18. Figures 5-64 - 5-67 show the box-and-whisker plots for the fraction of Cs released to the environment and timing of MVSS venting vs. the most influential parameters identified by ANOVA.

Table 5-18. One-way ANOVA results for LOCA-MVSS IDEJ1

Cs release fraction [-]		
variable	**F-value**	**p-value**
MVSSDFV	752.95	1.35E-176
SC71568	125.70	2.09E-59
HFRZZR	71.06	9.48E-38
SC7170CS	70.45	1.76E-37
TPFAIL	68.69	1.07E-36
SC7170CSM	55.97	7.73E-31
SC3210	42.33	3.68E-24
SC11321	41.56	9.05E-24
SC71531	40.37	3.64E-23
GAMMA	39.09	1.66E-22
CORNSBLD	32.37	5.44E-19
SC7111CS2	29.15	2.88E-17
SC11312	24.22	1.45E-14
SC7111CS1	21.45	5.15E-13
TUO2ZRO2	20.76	1.26E-12
SC71542	17.74	6.53E-11
MVSSDFA	17.67	7.20E-11
SC1020	17.11	1.51E-10
SC7111I2	15.35	1.57E-09
SC71555	14.89	2.89E-09
SC7111I1	14.71	3.66E-09
OXM	14.15	7.75E-09

MVSS Time [h]		
variable	**F-value**	**p-value**
VFALL	28.47	6.76E-17
FCELRA	20.89	1.05E-12
SC7111I1	18.52	2.36E-11
SC71555	16.19	5.10E-10
RHONOM	12.77	5.00E-08
CORNSBLD	12.17	1.12E-07
PDPor	12.07	1.28E-07
CHI	11.77	1.93E-07
SC715010	11.18	4.29E-07
GAMMA	10.86	6.65E-07
SC3210	10.49	1.10E-06
SC7170CS	9.72	3.13E-06
HDBH2O	9.07	7.68E-06
HDBPN	9.04	7.93E-06
SC7111I2	8.61	1.44E-05
SC7111CS1	8.57	1.51E-05
TPFAIL	7.70	5.01E-05
TUO2ZRO2	7.07	1.19E-04
STICK	6.23	3.76E-04
SC71521	5.86	6.23E-04
SC7170CSM	5.83	6.52E-04
HFRZZR	4.35	4.90E-03

Cs release fraction [-]		
variable	F-value	p-value
NUMSEC	13.64	1.54E-08
CHI	12.76	5.04E-08
FCELRA	11.79	1.88E-07
SC11412	11.14	4.53E-07
HDBPN	10.45	1.16E-06
SC7170CSI3	9.08	7.58E-06
VFALL	8.34	2.06E-05
STICK	7.82	4.20E-05
PDPor	6.99	1.32E-04
TURBDS	6.19	3.97E-04
RHONOM	5.26	1.42E-03
SC715010	4.87	2.41E-03
SC71551	4.80	2.64E-03
HFRZSS	4.66	3.23E-03
SC7170CSI4	4.08	7.06E-03
TZRSSINC	2.55	5.53E-02
HDBH2O	1.75	1.56E-01
SC71521	1.57	1.95E-01
DHYPDLP	0.76	5.19E-01

MVSS Time [h]		
variable	F-value	p-value
SC11412	4.29	5.31E-03
SC11321	3.46	1.64E-02
DHYPDLP	3.32	1.99E-02
SC71542	3.06	2.80E-02
SC71531	3.03	2.93E-02
OXM	3.02	2.96E-02
HFRZSS	2.82	3.84E-02
SC71568	2.51	5.79E-02
SC1020	2.40	6.72E-02
SC7170CSI4	2.36	7.06E-02
SC11312	2.21	8.63E-02
TZRSSINC	2.14	9.41E-02
SC7111CS2	2.06	1.05E-01
SC71551	1.66	1.75E-01
MVSSDFA	1.59	1.90E-01
SC7170CSI3	1.01	3.90E-01
TURBDS	0.98	4.03E-01
MVSSDFV	0.76	5.20E-01
NUMSEC	0.62	6.02E-01

Based on the results from the Morris SA and ANOVA, 16 MELCOR code modelling parameters were selected for the uncertainty analysis. The selection is based on the 5 most influential parameters per FOM (fraction of Cs released to the environment, fraction of I released to the environment, timing of release to the environment (MVSS opening)).

Table 5-19. Parameter selection for UA for LOCA-MVSS IDEJ1

N	Parameter ID	Description	Units
1	STICK	Particle sticking probability	-
2	VFALL	Velocity of falling debris	m/s
3	SC715010	Scaling factor for SPARC-90 model vent exit condensation decontamination factor	-
4	FCELRA	Radiative exchange factors for radiation radially outward and upward from the cell boundary to the next adjacent cell	-
5	CORNSBLD	NS failure temperature threshold	K
6	MVSSDFV	MVSS decontamination factor for radioactive vapours	-
7	SC7170CS	Saturation solubility at low/high temperature reference for Cs	kg/kg H2O
8	SC7111CS1	Characteristic diameter of the molecule for Cs	Å
9	TZRSSINC	Solidus temperatures for ZR/SS and ZR/INC eutectic pairs	K
10	TURBDS	Turbulence dissipation rate	m2/s3
11	SC71568	Multiplicative constant in a temperature correction correlation in the SPARC-90 model	-
12	HFRZZR	Refreezing heat transfer coefficient for Zr	W/m2-K
13	TPFAIL	Penetration failure temperature	K

N	Parameter ID	Description	Units
14	SC7111I1	Characteristic diameter of the molecule for I	Å
15	SC71555	SPARC-90 model multiplication constants in the DF factor correlations for and large Stokes numbers	-
16	RHONOM	Aerosol density	kg/m3
17	HFRZSS	Refreezing heat transfer coefficient for SS	W/m2-K
18	CHI	Aerosol dynamic shape factor	-
19	GAMMA	Aerosol agglomeration shape factor	-
20	PDPor	Particulate debris porosity	-
21	MVSSDFV	MVSS decontamination factor for radioactive vapours	-

5.2.2.2.2. RC7B – LOCA-MVSS IDEJ0

Table 5-20 illustrates the range as well as the mean and 0.05/0.5/0.95 quantiles of the distributions of the main FOMs analyzed in sensitivity study.

Table 5-20. Summary of SA analysis results for LOCA-MVSS IDEJ1 (RC7B IDEJ0)

	Range		**Mean**	**Median**	**5%**	**95%**
MVSS Time [h]	0.88	6.49	2.99	3.04	1.48	8.83
LHF Time [h]	0.68	4.44	1.47	1.34	0.84	2.60
MVSS-LHF Time[h]	-2.29	3.82	1.52	1.81	-0.47	2.92
H2 Mass in COR [kg]	285.64	760.94	477.48	468.69	330.44	643.47
CS Release fraction [-]	3.19E-05	3.23E-03	2.98E-04	1.03E-04	4.22E-05	1.32E-03
I Release fraction [-]	3.57E-05	1.91E-03	2.32E-04	1.14E-04	4.76E-05	8.50E-04

Figures 5-68 - 5-72 show the Morris diagrams, where the x-axis represents the Morris modified mean and y-axis shows the Morris standard deviation. Morris modified mean values substantially different from zero, indicate significant overall influence of the parameter, while large values of Morris standard deviation indicate possible interactions with other input parameters and non-linear behavior of the output with respect to the input.

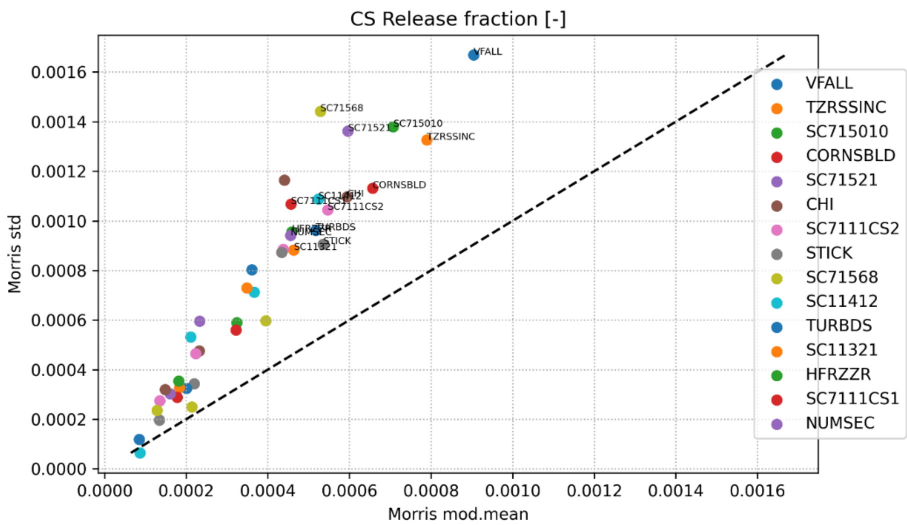

Figure 5-68 Morris diagram for the fraction of Cs released to the environment [-]

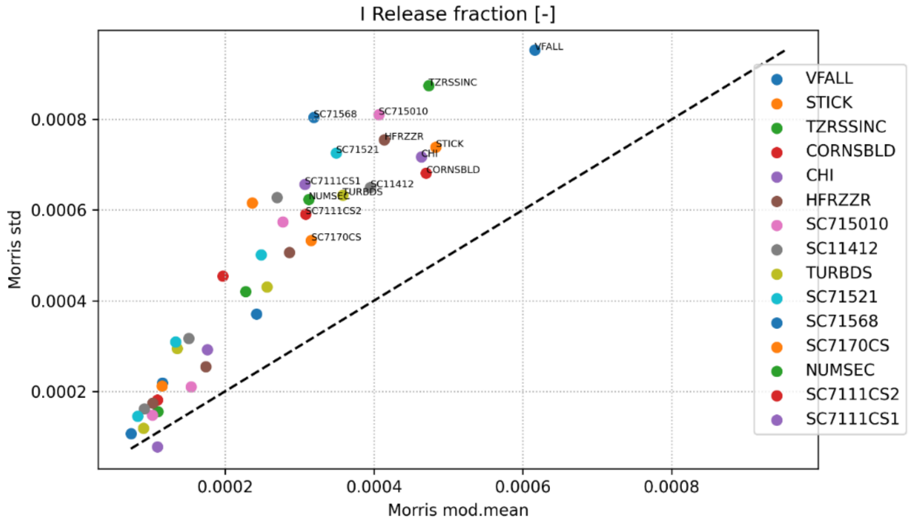

Figure 5-69 Morris diagram for the fraction of I released to the environment [-]

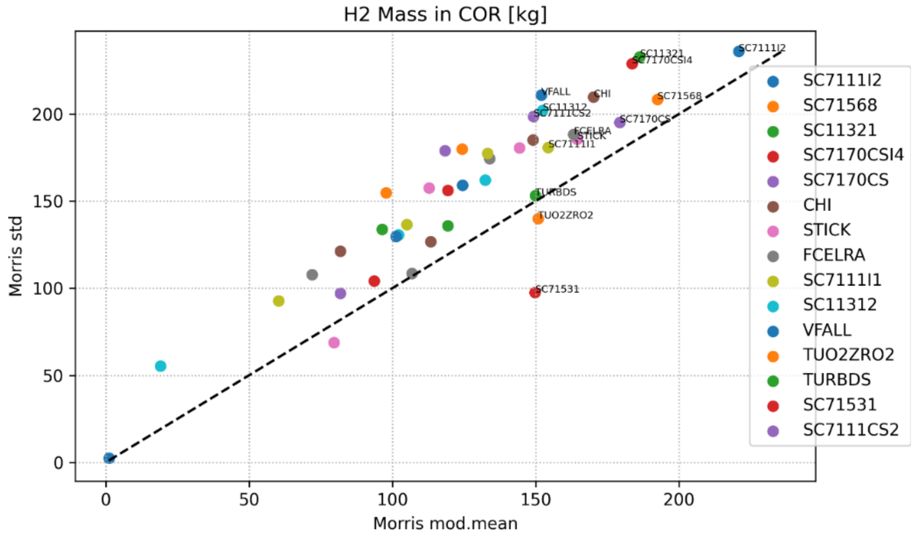

Figure 5-70 Morris diagram for the H2 mass generated in the COR package [kg]

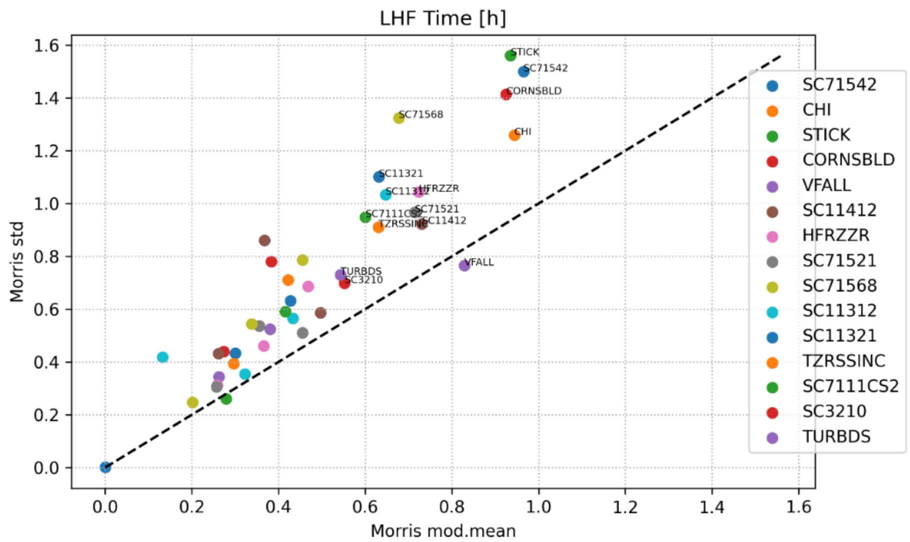

Figure 5-71 Morris diagram for the lower head failure time [h]

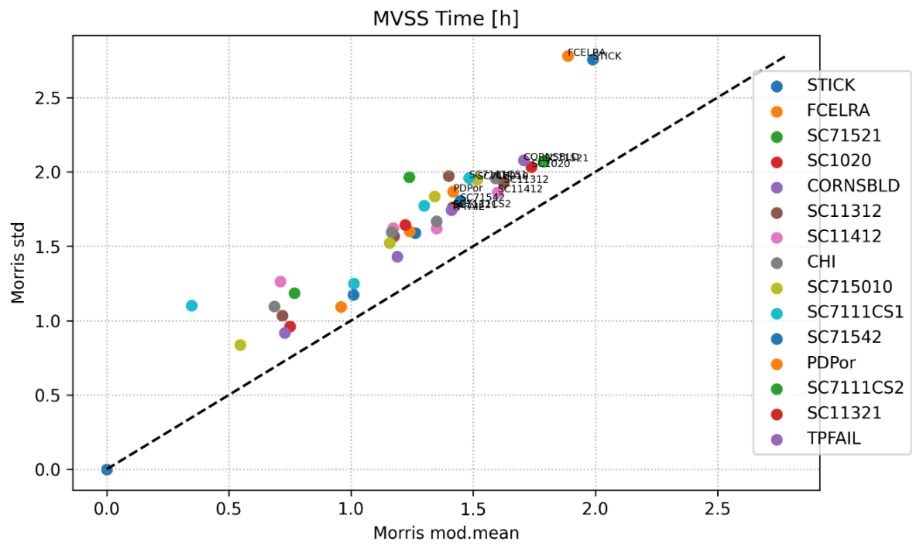

Figure 5-72 Morris diagram for MVSS opening time [h]

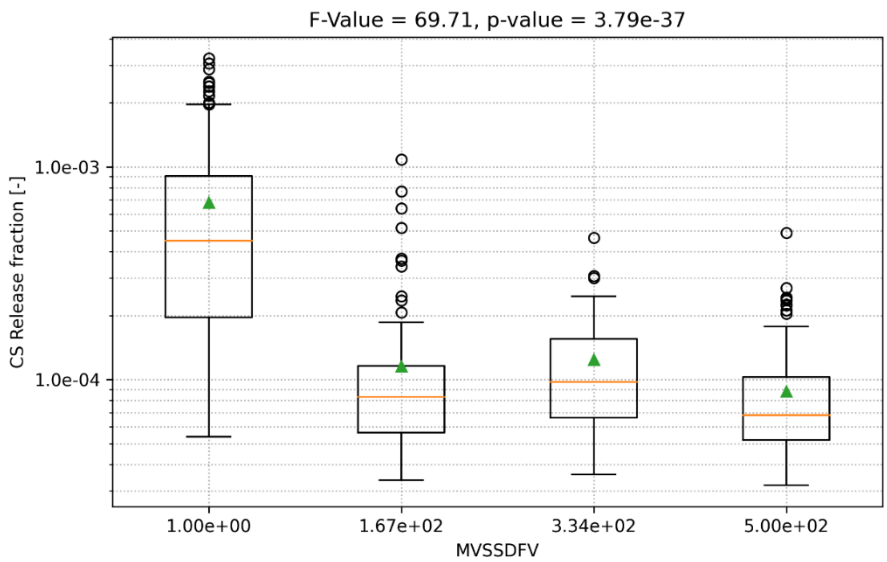

Figure 5-73 Box and whisker plot for the fraction of Cs release [-] vs. MVSSDFV [-][6]

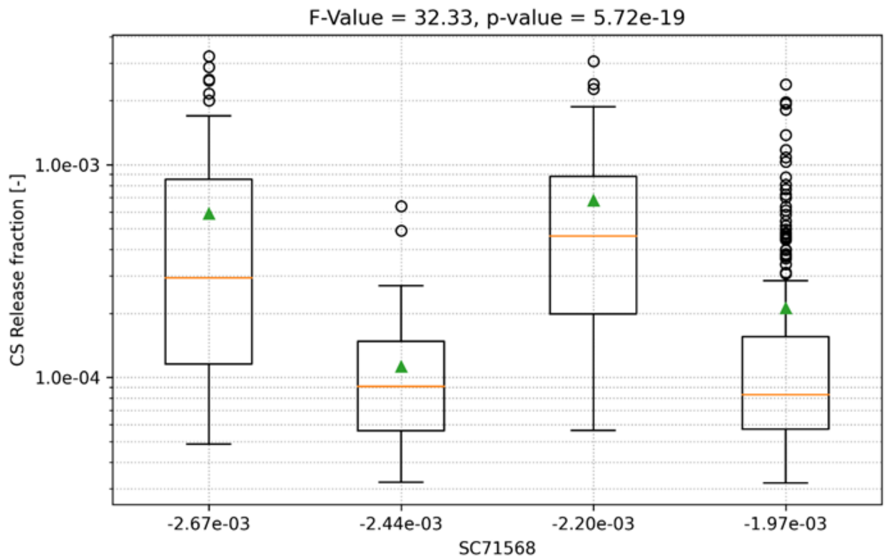

Figure 5-74 Box and whisker plot for the fraction of Cs release [-] vs. SC71568[6]

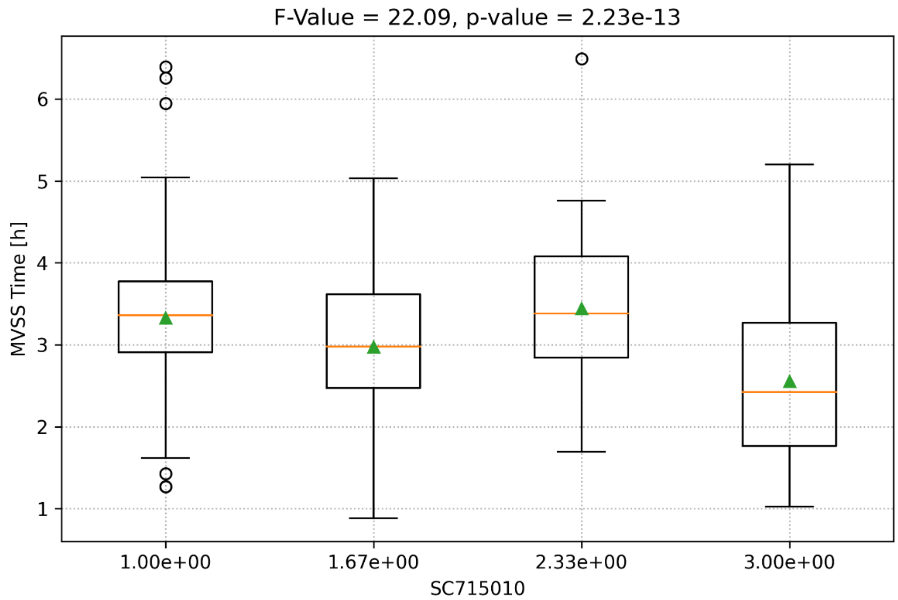

Figure 5-75 Box and whisker plot for the timing of MVSS [h] vs. SC105010 [] [6]

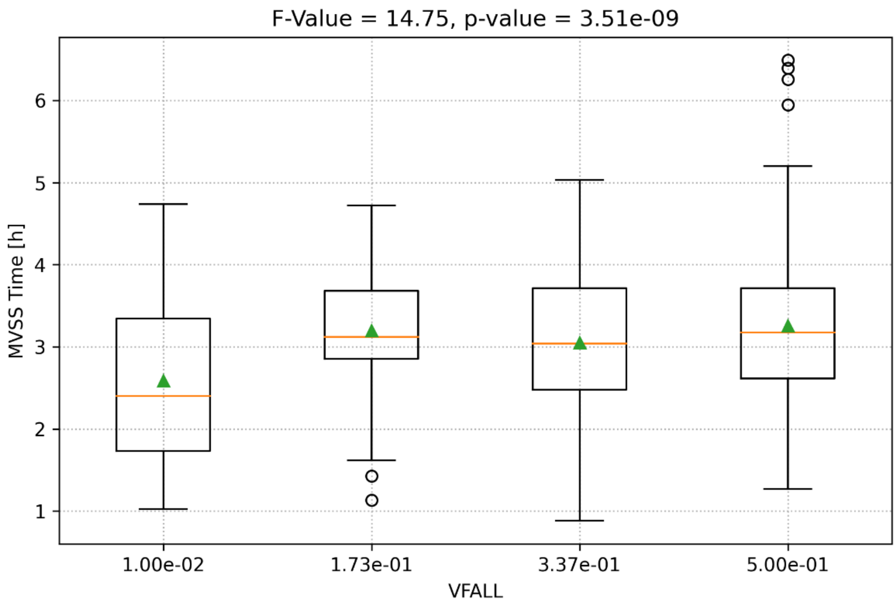

Figure 5-76 Box and whisker plot for the timing of MVSS [h] vs. VFALL [m/s] [6]

One-way ANOVA analysis was performed on the data set generated by the Morris method for SA, the results of the analysis are summarized in Table 5-21. Figures 5-73 - 5-76 show the box-and-whisker plots for the fraction of Cs released to the environment and timing of MVSS venting vs. the most influential parameters identified by ANOVA.

Table 5-21. One-way ANOVA results for LOCA-MVSS IDEJ0

Cs release fraction [-]		
variable	**F-value**	**p-value**
MVSSDFV	69.71	3.79E-37
SC71568	32.33	5.72E-19
TPFAIL	26.78	5.65E-16
HFRZZR	23.38	4.25E-14
SC7170CSM	18.12	3.96E-11
SC3210	15.61	1.11E-09

MVSS Time [h]		
variable	**F-value**	**p-value**
SC715010	22.09	2.23E-13
VFALL	14.75	3.51E-09
SC71555	11.84	1.75E-07
RHONOM	11.58	2.50E-07
SC7111CS2	10.65	8.83E-07
SC3210	10.32	1.39E-06

Cs release fraction [-]		
variable	F-value	p-value
SC11321	13.56	1.71E-08
SC71531	12.81	4.70E-08
CORNSBLD	12.24	1.03E-07
SC7111CS2	12.15	1.15E-07
MVSSDFA	11.97	1.47E-07
00GAMMA	11.20	4.17E-07
NUMSEC	10.84	6.80E-07
SC7170CS	10.30	1.43E-06
SC11412	9.68	3.33E-06
FCELRA	8.52	1.62E-05
TURBDS	7.15	1.07E-04
SC11312	7.11	1.13E-04
SC71542	6.88	1.54E-04
TUO2ZRO2	6.49	2.61E-04
CHI	6.09	4.56E-04
SC7111I2	6.08	4.60E-04
SC7111CS1	5.77	7.03E-04
SC1020	5.67	8.09E-04
SC7170CSI4	5.09	1.79E-03
OXM	5.07	1.84E-03
SC7111I1	5.07	1.85E-03
TZRSSINC	4.80	2.65E-03
PDPor	4.17	6.29E-03
HDBPN	4.03	7.54E-03
SC715010	3.52	1.51E-02
SC71521	3.25	2.17E-02
VFALL	3.19	2.37E-02
SC7170CSI3	3.13	2.54E-02
SC71555	2.98	3.13E-02
SC71551	2.78	4.07E-02
HDBH2O	2.76	4.17E-02
STICK	2.00	1.14E-01
RHONOM	1.78	1.50E-01
DHYPDLP	1.02	3.85E-01
HFRZSS	0.59	6.24E-01

MVSS Time [h]		
variable	F-value	p-value
HDBH2O	10.30	1.42E-06
CORNSBLD	9.30	5.55E-06
FCELRA	8.81	1.10E-05
STICK	8.11	2.86E-05
SC71531	8.10	2.88E-05
SC7170CS	7.96	3.51E-05
SC71521	7.09	1.16E-04
PDPor	6.81	1.69E-04
SC7111CS1	6.42	2.88E-04
TUO2ZRO2	6.26	3.58E-04
TPFAIL	5.59	8.98E-04
HDBPN	5.44	1.10E-03
HFRZSS	5.41	1.15E-03
SC7170CSM	5.25	1.44E-03
SC7170CSI4	5.13	1.70E-03
SC7111I2	4.82	2.60E-03
OXM	4.59	3.55E-03
SC7111I1	4.04	7.49E-03
SC1020	3.98	8.06E-03
GAMMA	3.89	9.14E-03
SC11412	3.77	1.08E-02
TZRSSINC	3.43	1.70E-02
TURBDS	3.03	2.93E-02
SC71542	2.89	3.51E-02
CHI	2.87	3.59E-02
NUMSEC	2.75	4.26E-02
SC71568	1.89	1.31E-01
DHYPDLP	1.64	1.79E-01
SC7170CSI3	1.27	2.85E-01
SC11312	1.17	3.20E-01
SC71551	1.11	3.46E-01
HFRZZR	0.50	6.85E-01
MVSSDFV	0.35	7.92E-01
MVSSDFA	0.31	8.15E-01
SC11321	0.15	9.31E-01

Based on the results from Morris SA and ANOVA, 17 MELCOR code modelling parameters were selected for uncertainty analysis. The selection is based on 5 most influential parameters per FOM (fraction of Cs released to the environment, fraction of I released to the environment, timing of release to the environment (MVSS opening)).

Table 5-22. Parameter selection for UA for LOCA-MVSS IDEJ0

N	Parameter ID	Description	Units
1	STICK	Particle sticking probability	-
2	FCELRA	Radiative exchange factors for radiation radially outward and upward from the cell boundary to the next adjacent cell	-
3	SC71521	Initial bubble diameter correlation coefficient in SPARC-90 model	m
4	SC1020	Multiplication factor for time constant for radial solid and molten debris relocation	-
5	CORNSBLD	NS failure temperature threshold	K
6	VFALL	Velocity of falling debris	m/s
7	TZRSSINC	Solidus temperatures for ZR/SS and ZR/INC eutectic pairs	K
8	SC715010	Scaling factor for SPARC-90 model vent exit condensation decontamination factor	-
9	CHI	Aerosol dynamic shape factor	-
10	MVSSDFV	MVSS decontamination factor for radioactive vapours	-
11	SC71568	Multiplicative constant in a temperature correction correlation in the SPARC-90 model	-
12	TPFAIL	Penetration failure temperature	K
13	HFRZZR	Refreezing heat transfer coefficient for Zr	W/m2-K
14	SC7170CSM	Saturation solubility at high and low temperature reference for CsM	kg/kg H2O
15	SC71555	SPARC-90 model multiplication constants in the DF factor correlations for and large Stokes numbers	-
16	RHONOM	Aerosol density	kg/m3
17	SC7111CS2	Characteristic energy of interaction between the molecules divided by the Boltzmann constant for CsI/CsM	K
18	GAMMA	Aerosol agglomeration shape factor	-
19	HFRZSS	Refreezing heat transfer coefficient for SS	W/m2-K
20	PDPor	Particulate debris porosity	-
21	MVSSDFV	MVSS decontamination factor for radioactive vapours	-

5.2.3. Summary of sensitivity analysis results for RC7

Sensitivity analysis showed that different MELCOR code modelling parameters have different importance depending on the accident scenario (SBO-MVSS vs. LOCA-MVSS), modelling assumptions (IDEJ) as well as FOMs considered in the study.

In case of RC7A (SBO-MVSS) release category, the influence of the modelling of debris ejection from the vessel (IDEJ switch) has relatively small importance compared to other MELCOR modelling parameters. Based on the results the most influential parameters are MVSSDFA – aerosol decontamination factor of MVSS, and GAMMA - Aerosol agglomeration shape factor, in case of the fractions of Cs and I released to the environment.

In case of RC7B (LOCA-MVSS) release category, the mode of debris ejection from the vessel (IDEJ switch) has the dominant effect on the code predictions of the fractions of Cs and I released to the environment. Furthermore, the results show that MVSSDFV – MVSS decontamination factor for radioactive vapors has significant effect on the magnitude of Cs and I released, which can be explained by (i) early opening of MVSS in case of LOCA; (ii) in case of LOCA the fission products are released directly to the containment, bypassing scrubbing (and condensation for radioactive vapors) inside the condensation pool. The effect of the mode of debris ejection from the vessel (IDEJ) is explained in section 7.3.3 in [23].

From the quantitative perspective, the sensitivity analysis results are summarized in Figures 5-77 - 5-81.

The results show that the spread in the opening time of MVSS is quite significant, and it is larger in case of IDEJ1 compared to scenarios with IDEJ0. The difference between IDEJ0 and 1 can be explained by the rate of debris ejection from the vessel, where scenarios simulated with IDEJ0 have rather gradual release of in-vessel debris over time, while in case of IDEJ1 the debris is ejected in a dripping mode initially, followed by a massive relocation to the cavity due to creep-rupture of the vessel lower head [24][25].

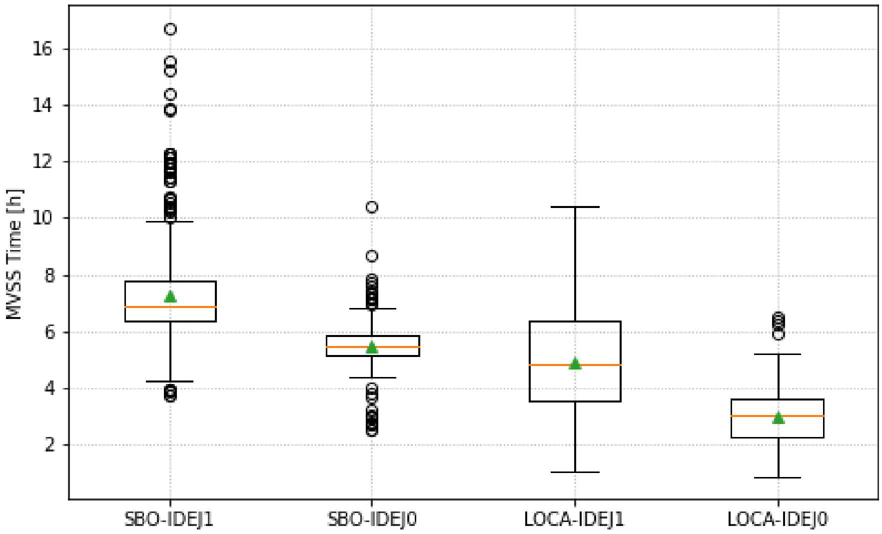

Figure 5-77 Box and whisker plot for the timing of MVSS [h]

Based on the results, the vessel lower head failure occurs ~2.5 hours after the initiating event in case of unmitigated SBO and ~1.5 hours in case of LOCA. Furthermore, the results show that in case of SBO the opening of the MVSS happens after the vessel lower head failure, while in case of LOCA there is a quite significant fraction of simulations that predict the MVSS opening before the vessel lower head failure (up to ~2 hours).

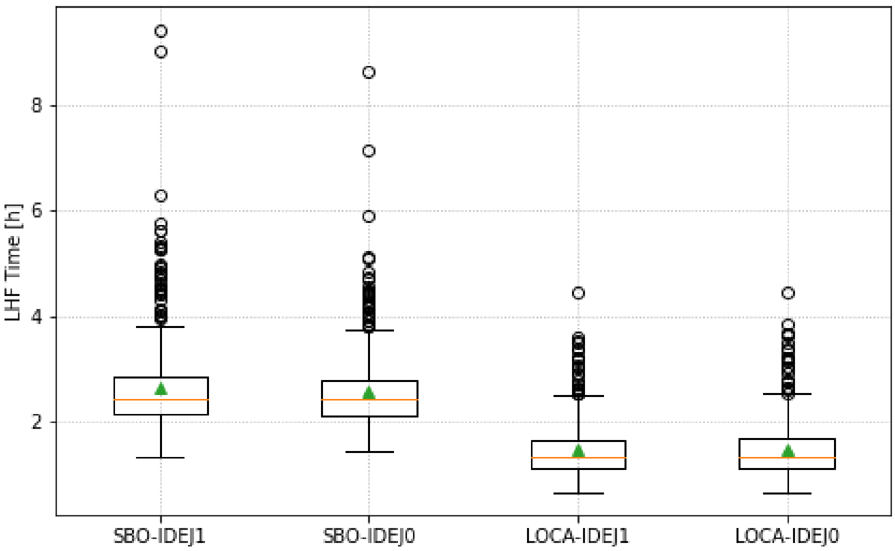

Figure 5-78 Box and whisker plot for the timing of LHF [h].

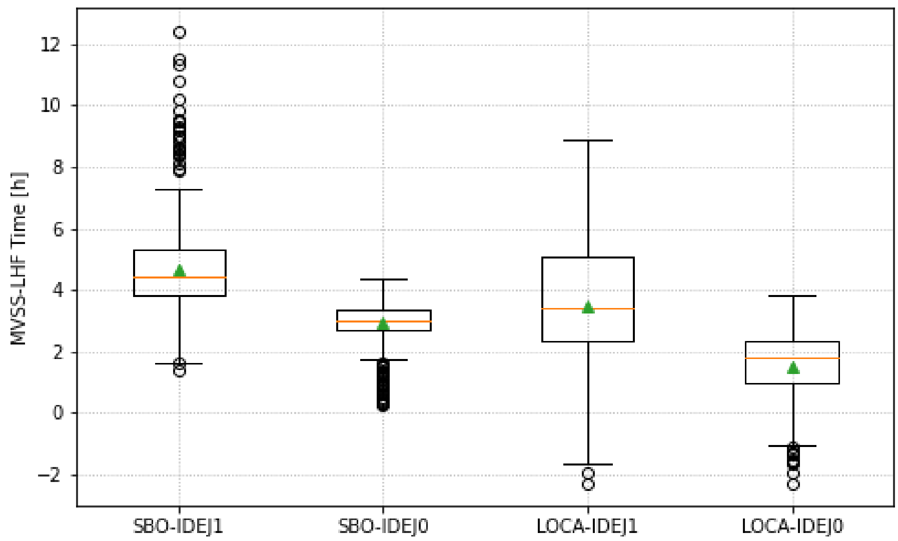

Figure 5-79 Box and whisker plot for the timing of MVSS – LHF [h]

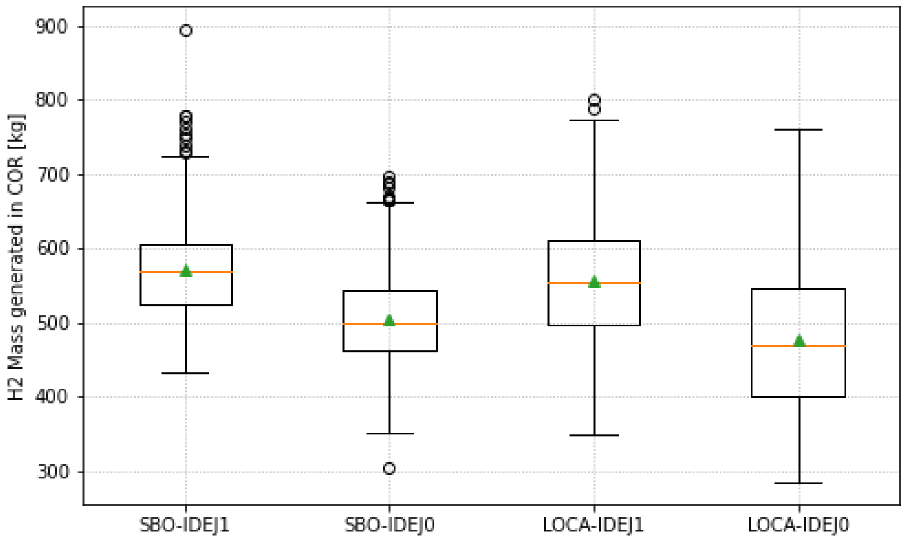

Figure 5-80 Box and whisker plot for the hydrogen mass generated in COR package [kg]

The fraction of Cs released to the environment in case of SBO is well below the acceptance criterion for the acceptable release[7] and, judging by the results, the effect of the mode of debris ejection from the vessel has relatively low effect on the results. In case of LOCA there is a quite significant fraction of simulations where the fraction of Cs released exceeds the acceptable release boundary. Furthermore, the mode of debris ejection from the vessel has the dominant effect on the fraction of Cs released to the environment. In case of IDEJ1 the fraction of Cs released to the environment is approximately two orders of magnitude larger then in case of IDEJ0.

[7] Releases over 0,1 % of the inventory of the caesium isotopes Cs-134 and Cs-137 in a core of 1800 MW_{Th}, excluding noble gases, which corresponds to a release of 160 TBq of Cs-134 and of 103 TBq of Cs-137.

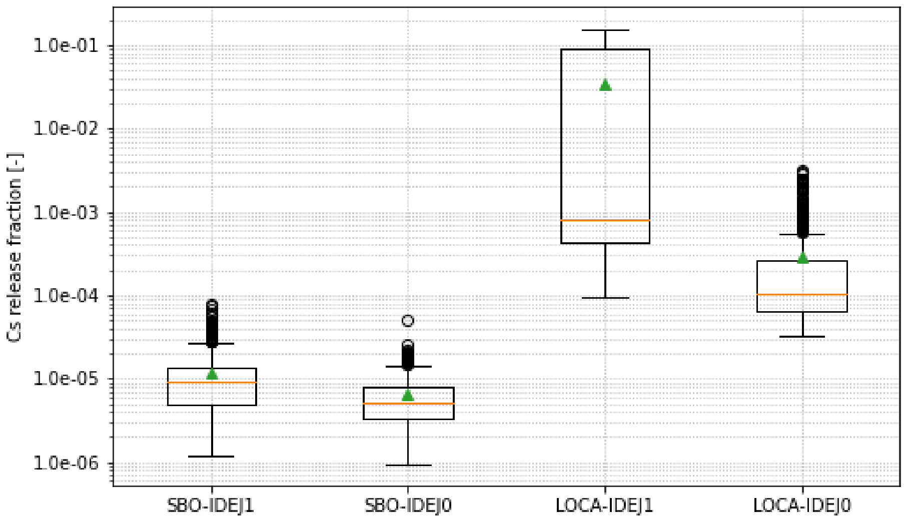

Figure 5-81 Box and whisker plot for the fraction of Cs released to the environment [-].

5.3. Sensitivity analysis RC7 SBO – Finnish plant configuration

During the first and second phases of the project, VTT studied scenario RC7 – filtered containment venting in the case of SBO. In the first phase a bounding analysis with two additional "middle values" was performed and the results were compared to the best estimate case. Two figures of merit were studied: the integral cesium release to the environment and the start time of the filtered venting. From the results multiple parameters potentially affecting the MELCOR calculation results were identified. However, in some irregular cases, erosion of the reactor cavity and production hydrogen was observed, which was assumed to be affecting the calculation results. In order to minimize the effect of hydrogen production, the erosion of the reactor cavity will be switched off during the sensitivity and uncertainty studies.

In the second part of the project, the parameters highlighted during the first part are used to perform a sensitivity analysis. The results from the sensitivity analysis are further used in determining the parameter set for the uncertainty analysis. In both tasks sampling, running the calculations, extracting the data and running the analyses are performed with SNAP and its Dakota plug-in.

5.3.1. Parameter selection

During the first part of the project, it was observed that quite many of the studied parameters seemed to influence the simulation results. However, due to limitations on the computational resources, the number of parameters chosen for the sensitivity study needed to be reduced significantly. Because the effect of parameter variations on FCV opening times was quite small compared to the effect on cesium release, more weight was put on cesium release during the parameter selection process.

The irregularly appearing hydrogen generation was assumed to influence especially the cesium release, which might have distorted the final results. For this reason, the appearance of hydrogen production was taken into an account when highlighting interesting parameters. Because hydrogen was produced in the "best estimate" case as well, the results from each parameter variation were not compared to that case but rather the results from each parameter variation case were compared to each other. Parameters that seemed to have only a small effect on the FOM's were excluded from the sensitivity study. Such excluded parameters included, for example, SC710611, SC710621, SC710651, HDBH2O, TPFAIL, HDBPN, CHI, NUMSEC and SC71572 – SC715714.

Additionally, if some parameter showed very strong influence on the results, it was excluded. The best example of this is MVSSDF, whose effect on simulation results was so evident that including it in the OAT sensitivity studies might have been unnecessary. Additionally, some parameters showing less influence than others were excluded in order to reduce computational burden.

Out of the initial 49 parameters, the following 22 parameters were selected for the sensitivity studies:

Table 5-23. Selected parameters for RC7 SBO SA.

N	Parameter name	Default	Range	Units
1	SC710641	3.814E5	[2.41E5, 3.814E5]	J/kg-mole
2	FCELRA	0.1	[0.1, 0.25]	-
3	CORNSBLD	1520	[1520, 1700]	K

4	VFALL	1.0	[0.01, 0.1]	m/s
5	SC10201	360	[180, 720]	s
6	SC10202	60	[30, 120]	s
7	HFRZSS	2500	[1000, 2500]	W/m2-K
8	HFRZZR	7500	[1000, 7500]	W/m2-K
9	SC11412	1.0	[0.2, 2.0]	kg/m-s
10	GAMMA	1	[1.0, 3.0]	-
11	STICK	1	[0.5, 1]	-
12	SC7111I1	4.982	[4.2347, 5.7293]	Å
13	SC7111CS1	3.617	[3.0745,4.1595]	Å
14	SC7111CS2	97	[82.450,111.550]	K
15	SC715010	1	[1,3]	-
16	SC715111	3.45	[2.9325, 3.9675]	-
17	SC71521	0.007	[5.E-3, 8.E-3]	m
18	SC71531	7.876	[6.6946, 9.0574]	cm/s
19	SC71551	1.79182	[1.5230, 2.0606]	-
20	SC71555	1.13893	[0.9681, 1.3098]	-
21	SC71568	-2.321E-3	[-2.6691e-03, -1.9728e-03]	-
22	DECAYH	1	0.96 – 1.04	-

Parameters descriptions and justification of the ranges used in the analysis can be found in Section 5 of the final report for the first phase of the NKS-STATUS project [23].

The OAT sensitivity analysis was performed in SNAP using the Dakota plug-in. The minimum number of samples (22) per parameter was calculated by Dakota according to the user input (90% probability and confidence limit, LHS). The distributions of all the parameters were assumed uniform. Only IDEJ0 was considered in these calculations.

5.3.2. Results

Figure 5-82 and Figure 5-83 present the simple and simple rank correlation coefficients in the case of cesium release and FCV opening time respectively. As mentioned in chapter 4.2, simple and simple rank correlation coefficients indicate the linear correlation between two variables such as a parameter and a FOM. The higher the absolute value of the coefficient is, the stronger the correlation. If the coefficient is positive, it is called positive correlation, and if it's negative, it's called negative correlation.

In the case of cesium release (Figure 5-82) four notable correlations can be observed. FCELRA (positive correlation), and CORNSBLD, GAMMA and SC71555 (negative correlations). Some correlation can be also observed in HFRZZR, SC10201 (only simple correlation), SC710641, SC7111CS2, SC7111I1, SC715111, SC71521, STICK, and SC715010. As for FCV opening time, Figure 5-83 shows that the correlation coefficients are in general higher than with Cs release. This indicates better correlation, and it would seem that the FCV opening time is more sensitive to the parameter changes than Cs release. However, it should be remembered that OAT is a very robust method, and the indicated linear correlations might not actually exist in the model itself.

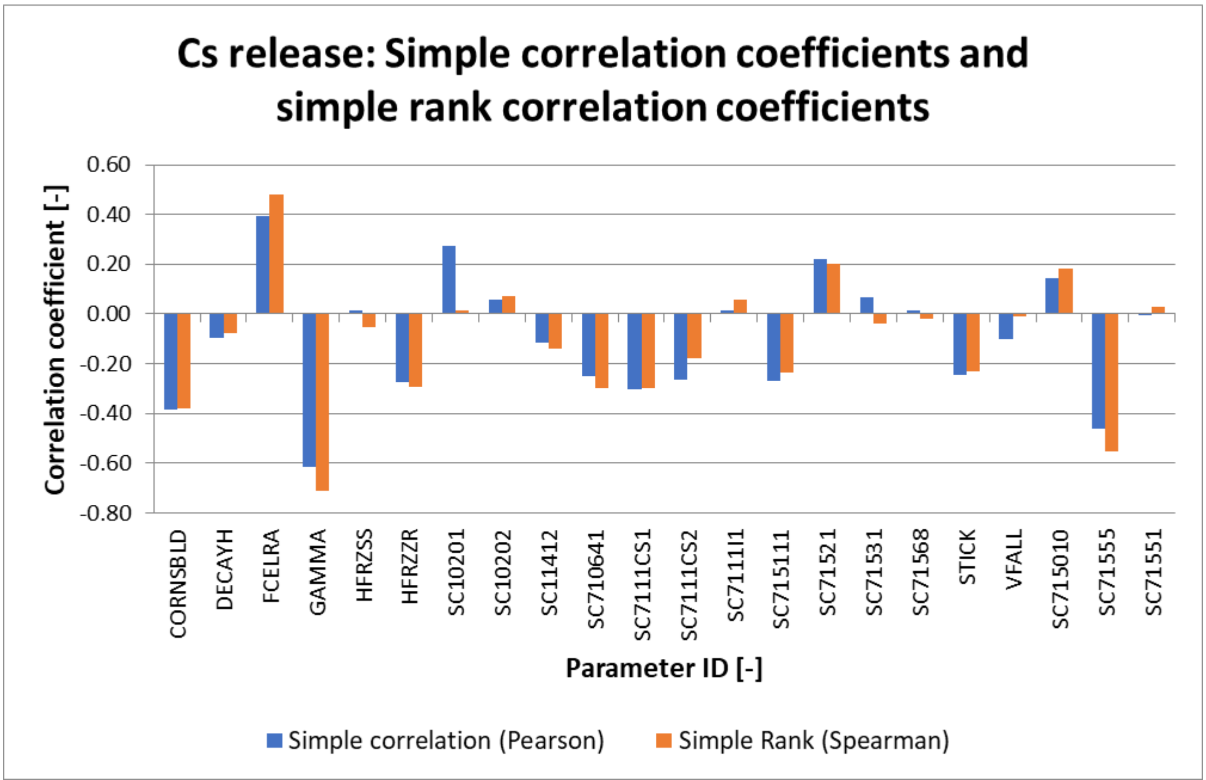

Figure 5-82. Cs release - simple correlation coefficients (Pearson) and simple rank correlation coefficients (Spearman).

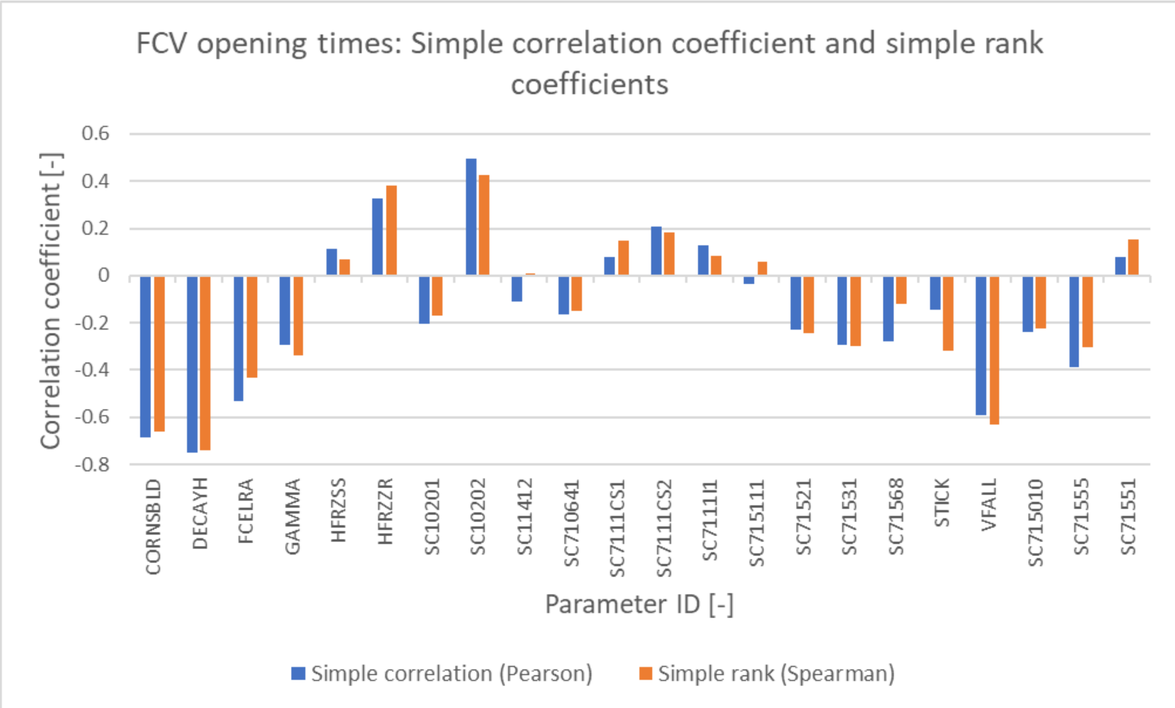

Figure 5-83. FCV opening times - simple correlation coefficients (Pearson) and simple rank correlation coefficients (Spearman).

Table 5-24 presents the minimum, maximum and mean values of both FOMs in each calculation round.

Table 5-24. Minimum, maximum and mean values of the FOMs in each calculation round.

	Cs release [-]			FCV opening time [s]		
ID	**Min value**	**Max value**	**Mean**	**Min value**	**Max value**	**Mean**
CORNSBLD	1.71E-07	3.92E-05	2.35E-05	5431	6796	6090
DECAYH	1.46E-09	4.21E-05	2.22E-05	5729	6558	6198
FCELRA	6.94E-09	4.85E-05	3.05E-05	5737	6487	6149
GAMMA	4.82E-10	3.97E-05	1.62E-05	5958	6455	6160
HFRZSS	0.00E+00	5.02E-05	2.91E-05	5856	6331	6078
HFRZZR	1.21E-08	4.05E-05	2.54E-05	5854	6642	6213
SC10201	1.45E-07	3.18E-05	2.27E-05	6006	6360	6179
SC10202	3.61E-09	3.68E-05	2.21E-05	6210	6340	6287
SC11412	5.27E-09	4.47E-05	2.84E-05	5650	6336	5992
SC710641	0.00E+00	5.26E-05	2.92E-05	6053	6864	6358
SC7111CS1	7.00E-09	4.50E-05	2.57E-05	6122	6564	6254

	Cs release [-]			FCV opening time [s]		
ID	**Min value**	**Max value**	**Mean**	**Min value**	**Max value**	**Mean**
SC7111CS2	1.25E-07	3.61E-05	2.09E-05	5864	6366	6146
SC7111I1	2.43E-09	3.32E-05	2.28E-05	6028	6424	6197
SC715111	1.70E-08	4.38E-05	2.18E-05	5971	6325	6178
SC71521	1.72E-05	4.08E-05	2.61E-05	6010	6390	6215
SC71531	7.79E-10	2.79E-05	1.88E-05	6019	6425	6203
SC71568	2.89E-09	4.61E-05	2.39E-05	6053	6351	6232
STICK	4.08E-09	4.81E-05	2.25E-05	5972	6411	6211
VFALL	0.00E+00	3.68E-05	1.81E-05	5193	10439	6090
SC715010	1.27E-08	5.03E-05	2.31E-05	6033	6404	6218
SC71555	4.35E-07	3.83E-05	2.08E-05	5901	6313	6174
SC71551	7.76E-09	3.51E-05	2.21E-05	6047	6396	6208

While the mean values on both sides and the minimum values on the FCV opening time -side stay quite consistent without many outliers, the minimum values of Cs release seem to fluctuate quite a bit between the parameter cases. These outliers appearing in almost every parameter case are caused by the crashed simulations that were very common during the study. Because there didn't seem to be a way to run Dakota plug-in on its own, dealing with the crashes was quite difficult without replacing Dakota as post-processor.

5.4. Uncertainty analysis RC4 – Swedish plant configuration

The uncertainty analysis was performed by both parametric and non-parametric methods. A procedure similar to the deterministic-realistic hybrid methodology [32] is applied to calculate the uncertainty ranges. Firstly, N number of runs for each accident scenario is performed. For the sampling of N trials Monte Carlo (MC) random sampling or Latin Hyper Cube (LHS) sampling methods can be used in Dakota. 95th percentiles from the empirical cumulative distribution functions can be obtained for each of the FOMs. A subset of these N trials can be sampled for Wilks' 95/95 estimates. As was discussed in Section 4.1.2.2, for 1st, 2nd and 3rd order Wilks' non-parametric method that reconstructs distribution of the uncertain quantities from the data, 59, 93 and 124 trials are necessary. The 59th, 92nd and 122nd value in the set of ordered output gives the conservative 95/95 value. Out of N trials, 59, 93 and 124 samples are randomly selected, and Wilks' values are calculated. Correspondingly, for the parametric method the distribution of these randomly selected sets can be identified by a goodness-of-fit test. If the samples follow a normal distribution, the population mean (μ_p) and population standard deviation (σ_p) under a confidence level (say 95%), can be estimated as,

$$\mu_p \le \left[\mu_s + t_\alpha(n-1) * \frac{\sigma_s}{\sqrt{n}}\right] \tag{6}$$

$$\sigma_p^2 \le \frac{(n-1) * \sigma_s^2}{\chi_{1-\alpha}^2(n-1)} \tag{7}$$

Where μ_s is the sample mean, σ_s is the sample standard deviation, $t_\alpha(n-1)$ is the student t variable at $(1-\alpha)$ confidence level under $(n-1)$ degrees of freedom and $\chi_{1-\alpha}^2(n-1)$ is the χ^2 variable at $(1-\alpha)$ confidence level under $(n-1)$ degrees of freedom [32]. The 95/95 coverage ($Y_{95/95}$) can then be expressed as,

$$Y_{95/95} = \mu_{p,95\%} + 1.645 * \sigma_{p,95\%} \tag{8}$$

To determine the goodness-of-fit for a distribution, Pearson χ^2 test, Kolmogorov-Smirnov test [33] and Anderson-Darling test [34] are performed, which tests the hypothesis that the given distribution can be defined by a normal distribution. In the event that the distribution does not follow a normal distribution, the test is performed by fitting Weibull and Extreme Value distributions. In the latter two cases, the 95/95 confidence interval can be determined by means of probability box methods, log-likelihood ratio test, Wald test and Lagrange multiplier test [35]. An alternative is using bootstrap method to obtain approximate confidence intervals for 95% limits [36]. The idea is to repeatedly sample random 59, 93 and 124 samples from the original N trials and perform the goodness-of-fit test and determine the 95th percentile for each of the distributions. In this work, N = 150 trials were performed for LOCA and SBO each (300 each, considering IDEJ0 and IDEJ1) and 500 sets of bootstraps for each order were used for estimation.

5.4.1. Parameter and distribution selection

The same parameters were used for the uncertainty analysis as sensitivity analysis. PDF types for the selected parameters were considered to be uniform distribution within the respective ranges. The parameters, their ranges, and PDF types are listed in Table 5-25.

Table 5-25. MELCOR parameters for UA and their distributions.

No	Model	Parameter name	Range	Units	Distribution	Scenario
1	Fission product release from fuel	SC710641	241000 - 381400	J/kg-mole	Uniform	LOCA/SBO
2		SC710651	0.000006 - 0.00001	M	Uniform	SBO
3	Core degradation and relocation	TUO2ZRO2	2450 - 2800	K	Uniform	LOCA
4		FCELRA	0.1 - 0.25		Uniform	LOCA
5		HFRZSS	1000 - 2500	W/m2-K	Uniform	LOCA
6		SC11312	2100 - 2500	K	Uniform	LOCA/SBO
7	RPV lower head failure	TPFAIL	1273 - 1600	K	Uniform	SBO
8		HDBPN	100 - 1000	W/m2-K	Uniform	LOCA/SBO
9	Fission product and aerosol dynamics	GAMMA	1 - 3		Uniform	LOCA/SBO
10		STICK	0.5 - 1		Uniform	LOCA
11		RHONOM	1000 - 4900	kg/m3	Uniform	SBO
12		TURBDS	0.00075 - 0.00125	m2/s3	Uniform	LOCA/SBO
13		SC7111I1	4.2347 - 5.7293	A	Uniform	LOCA
14		SC7111I2	467.5 - 632.5	K	Uniform	LOCA/SBO
15		SC7111CS1	3.0745 - 4.1595	A	Uniform	SBO
16		SC7111CS2	82.45 - 111.55	K	Uniform	LOCA
17		SC7170CS	3.3575 - 4.5425	kg/kg H2O	Uniform	SBO
18		SC7170CSI3	0.374 - 0.506	kg/kg H2O	Uniform	SBO
19		SC7170CSI4	1.9125 - 2.5875	kg/kg H2O	Uniform	LOCA
20		SC7170CSM	0.5695 - 0.7705	kg/kg H2O	Uniform	LOCA/SBO
21	Spray and pool scrubbing, and filters trapping	SC71521	0.005 - 0.008	m	Uniform	LOCA
22		SC71531	6.6946 - 9.0574	cm/s	Uniform	LOCA
23		SC71551	1.523 - 2.0606		Uniform	LOCA
24		SC71555	0.9681 - 1.3098		Uniform	SBO
25		SC71542	0.0025593 - 0.0034626	I-s/cm2	Uniform	LOCA/SBO
26		SC3210	1 - 1.15		Uniform	LOCA

5.4.2. Results

5.4.2.1.Empirical results

The boxplots for the CS release fractions during LOCA and SBO is shown in Figure 5-84. The boxplots for the I2 release fractions are shown in Figure 5-85. The values of mean, standard deviation, 5th/95th percentiles, minimum and maximum for all the scenarios of CS and I2 releases is presented in Table 5-26 and Table 5-25. These values are computed at 72h after the initiating event. The time evolution of release fractions for the 4 scenarios is provided in Appendix B.

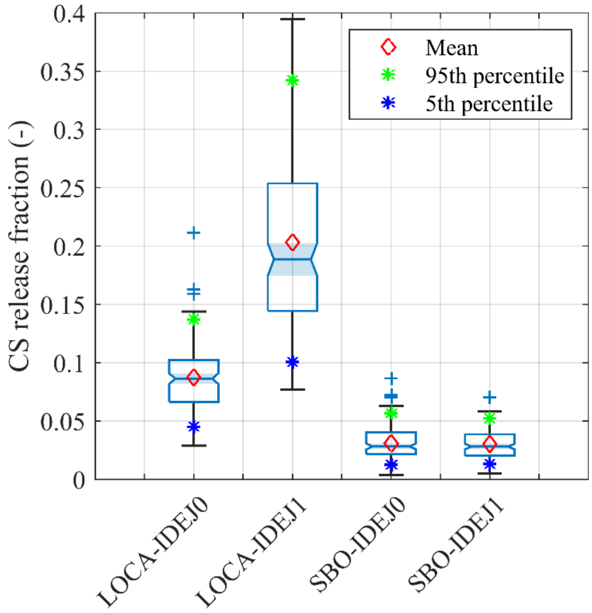

Figure 5-84 CS release fractions to the environment during LOCA and SBO (150 runs each for IDEJ0 and IDEJ1).

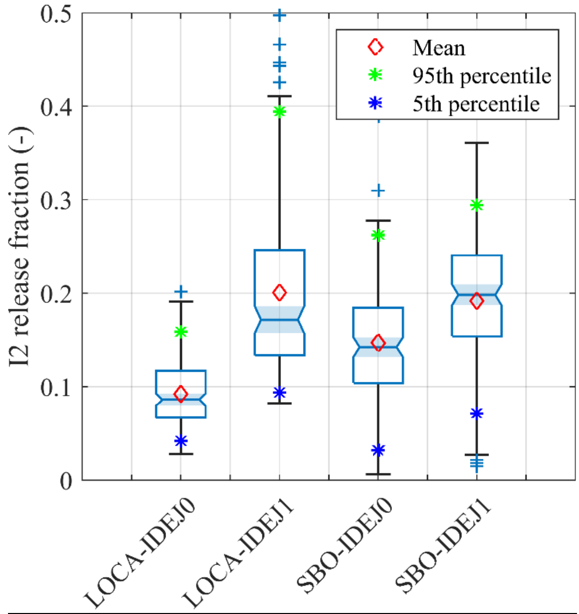

Figure 5-85 I2 release fractions to the environment during LOCA and SBO (150 runs each for IDEJ0 and IDEJ1).

Table 5-26 Summary of UA results.

	Sample size	min	max	μ	σ	95^{th} %
CS release fraction						
LOCA-IDEJ0	150	0.0287	0.2115	0.0875	0.0286	0.1372
LOCA-IDEJ1	150	0.0768	0.3948	0.2032	0.0781	0.342
SBO-IDEJ0	150	0.0037	0.0869	0.0311	0.0147	0.0567
SBO-IDEJ1	150	0.0053	0.0706	0.0303	0.0124	0.0523

I2 release fraction						
LOCA-IDEJ0	150	0.028	0.2018	0.092	0.0338	0.1588
LOCA-IDEJ1	150	0.082	0.4977	0.2008	0.093	0.3945
SBO-IDEJ0	150	0.0064	0.3896	0.147	0.0663	0.2623
SBO-IDEJ1	150	0.0149	0.3606	0.1918	0.0681	0.2942

The distributions of CS release fraction during LOCA, together with distribution fits are presented in Figure 5-86. The hypothesis testing metric is shown in the figure. A value of 0 implies acceptance of null hypothesis (a good fit for a particular distribution) and 1 implies rejection of null hypothesis (a poor fit for a particular distribution). The goodness-of-fit test is performed for normal, Weibull and extreme value (EV: Gumbel-minimum and flipped extreme value EV-rev: Gumbel-maximum) distributions. χ^2 refers to Pearson χ^2 test, KS refers to Kolmogorov-Smirnov test and AD refers to Anderson-Darling test. Similarly, distributions for CS release fractions during SBO, I2 release fractions during LOCA and I2 release fractions during SBO are presented in Figure 5-87, Figure 5-88 and Figure 5-89 respectively.

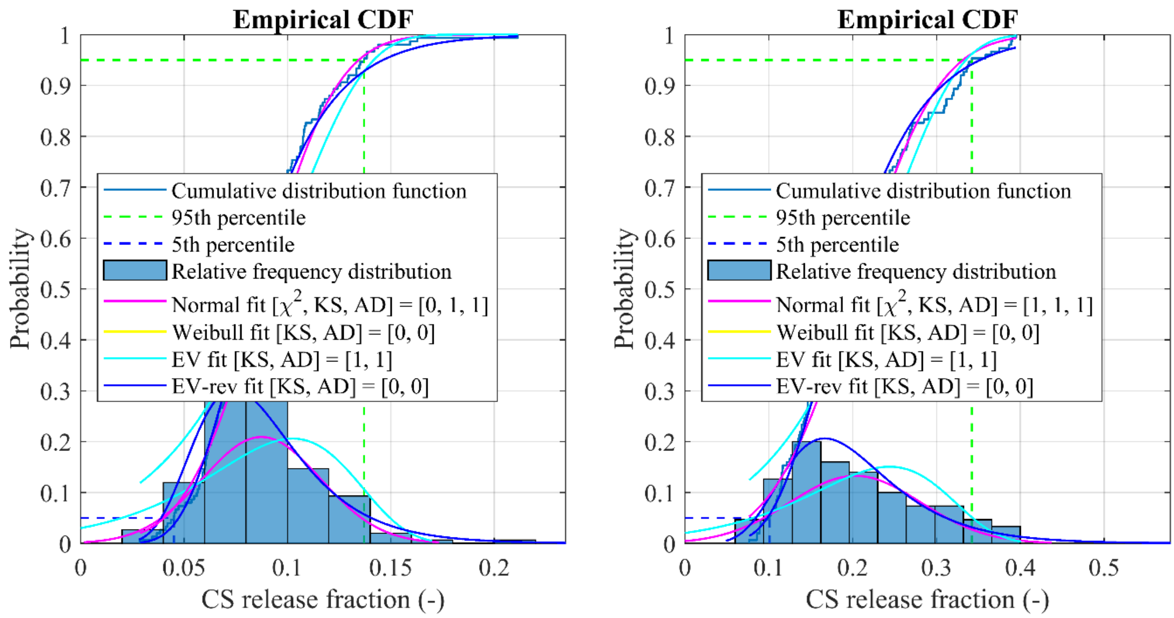

Figure 5-86 Cumulative distributions of CS release fractions during LOCA-IDEJ0 (left) and LOCA-IDEJ1 (right).

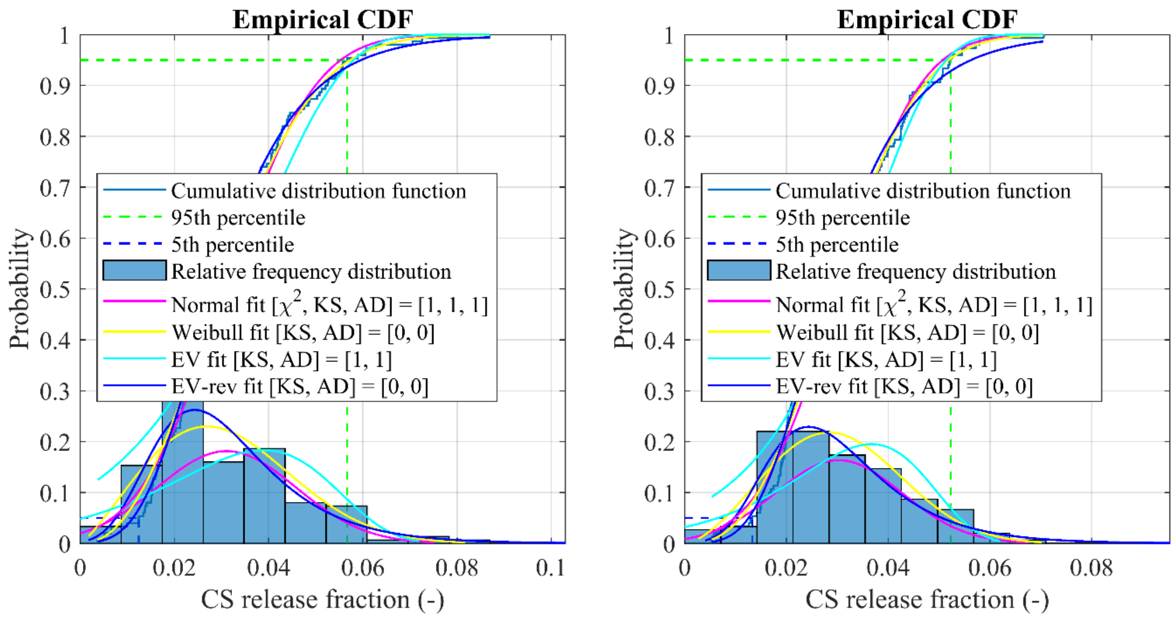

Figure 5-87 Cumulative distributions of CS release fractions during SBO-IDEJ0 (left) and SBO-IDEJ1 (right).

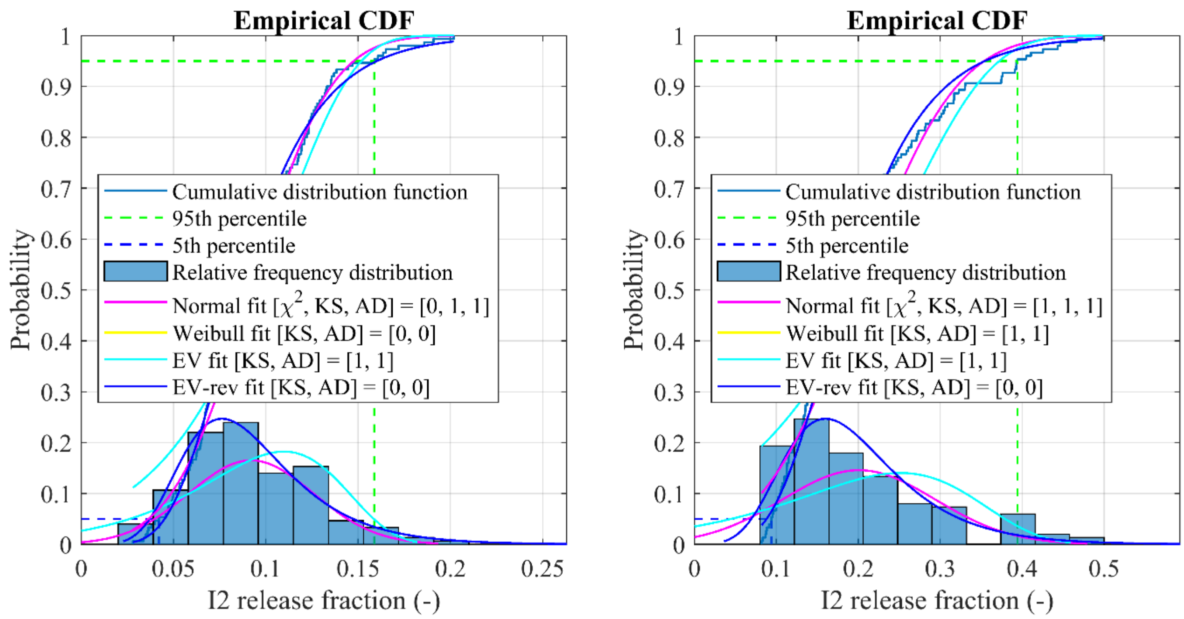

Figure 5-88 Cumulative distributions of I2 release fractions during LOCA-IDEJ0 (left) and LOCA-IDEJ1 (right).

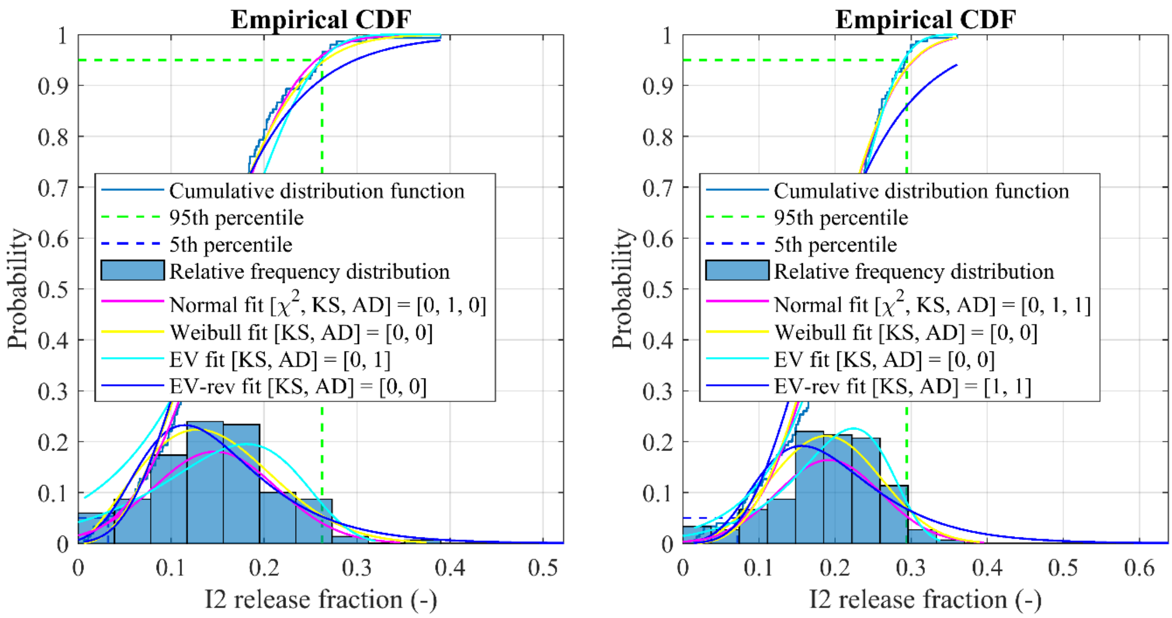

Figure 5-89 Cumulative distributions of I2 release fractions during SBO-IDEJ0 (left) and SBO-IDEJ1 (right).

The goodness-of-fit tests show that the distributions can be represented by any one of these distributions. For the parametric method, a sample distribution is assumed to be a good fit if either of the test is satisfied for a specific distribution.

5.4.2.2.Non-parametric method results

Considering each FOM independently, the Wilks' non-parametric estimates for the first 3 orders of one sided 95/95 is calculated. These are then repeatedly calculated for 500 different, random selections of samples for each order and the mean and standard deviation of the resulting distributions is presented in Table 5-27.

Table 5-27 Wilks' non-parametric 95/95 estimates.

	Sample size	min	max	μ	σ
CS release fraction					
LOCA-IDEJ0	59	0.1333	0.2115	0.1755	0.0298
	93	0.1347	0.1629	0.1555	0.009
	124	0.1372	0.1593	0.1528	0.0081
LOCA-IDEJ1	59	0.3325	0.3948	0.3885	0.0102
	93	0.3387	0.389	0.3867	0.0051
	124	0.3582	0.389	0.3867	0.0051
SBO-IDEJ0	59	0.0556	0.0869	0.0754	0.0101
	93	0.0557	0.0705	0.067	0.0042
	124	0.0589	0.0705	0.067	0.0042
SBO-IDEJ1	59	0.0471	0.0706	0.0625	0.0069
	93	0.0518	0.0579	0.0573	0.0011
	124	0.0526	0.0579	0.0573	0.0011

	Sample size	min	max	μ	σ
I2 release fraction					
LOCA-IDEJ0	59	0.1353	0.2018	0.1882	0.0145
	93	0.147	0.1857	0.179	0.0082
	124	0.1607	0.1857	0.179	0.0082
LOCA-IDEJ1	59	0.3746	0.4977	0.4703	0.0289
	93	0.3945	0.4468	0.443	0.0078
	124	0.4048	0.4468	0.443	0.0078
SBO-IDEJ0	59	0.2390	0.3896	0.3262	0.0531
	93	0.2515	0.278	0.2747	0.0041
	124	0.2623	0.278	0.2747	0.0041
SBO-IDEJ1	59	0.2802	0.3606	0.3298	0.0271
	93	0.29	0.3062	0.3032	0.0036
	124	0.2944	0.3062	0.3032	0.0036

5.4.2.3.Parametric method results

Based on the goodness-of-fit tests, the 95/95 estimates for a normal distribution are calculated for 500 bootstraps of each statistical order using the Equation (8) mentioned earlier. The boxplots of the resulting distribution in CS release fraction during LOCA and SBO, and in I2 release fraction during LOCA and SBO are shown in Figure 5-90, Figure 5-91, Figure 5-92 and Figure 5-93 respectively. The 95th percentiles are calculated only for those instances which passes the respective tests. In addition to estimation by normal distribution fit, estimations by Weibull and EV distributions are also shown in the figures. The 95th percentile estimates for the initial 150 trials are shown as horizontal line. Note that since the distributions of CS and I2 release fractions did not pass the test for Weibull fit, the estimate is not shown. However, for CS release during LOCA-IDEJ1, SBO-IDEJ0, SBO-IDEJ1 and I2 release during LOCA-IDEJ1 do not pass the test for normal fit, nevertheless the 95th percentile is estimated for reference purposes.

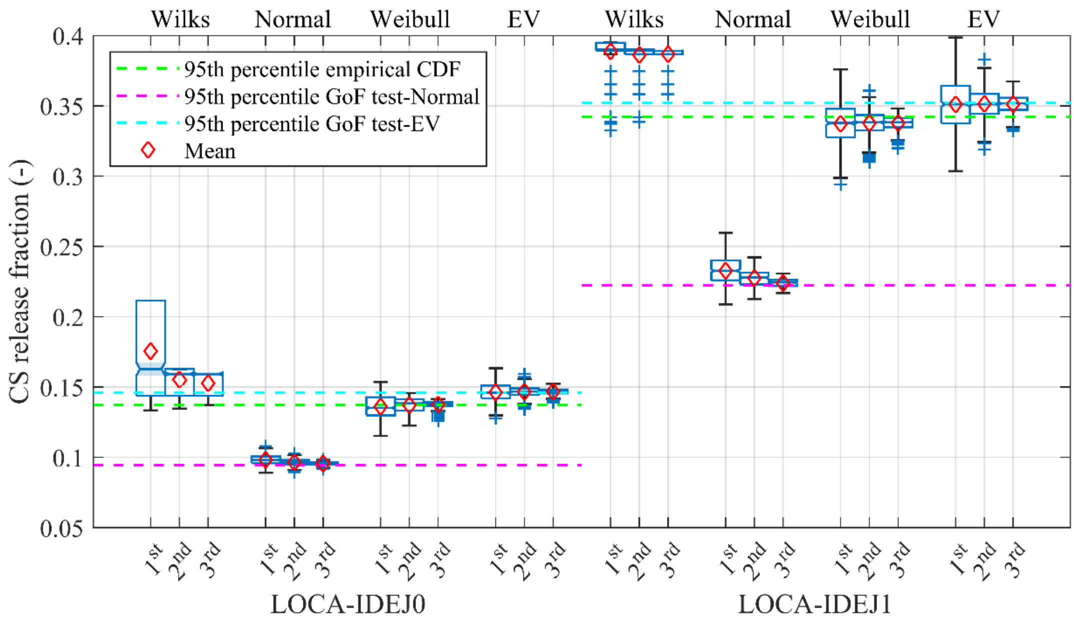

Figure 5-90 Boxplots for the 95/95 estimates by goodness-of-fit tests for CS release fraction during LOCA-IDEJ0 (left) and LOCA-IDEJ1 (right).

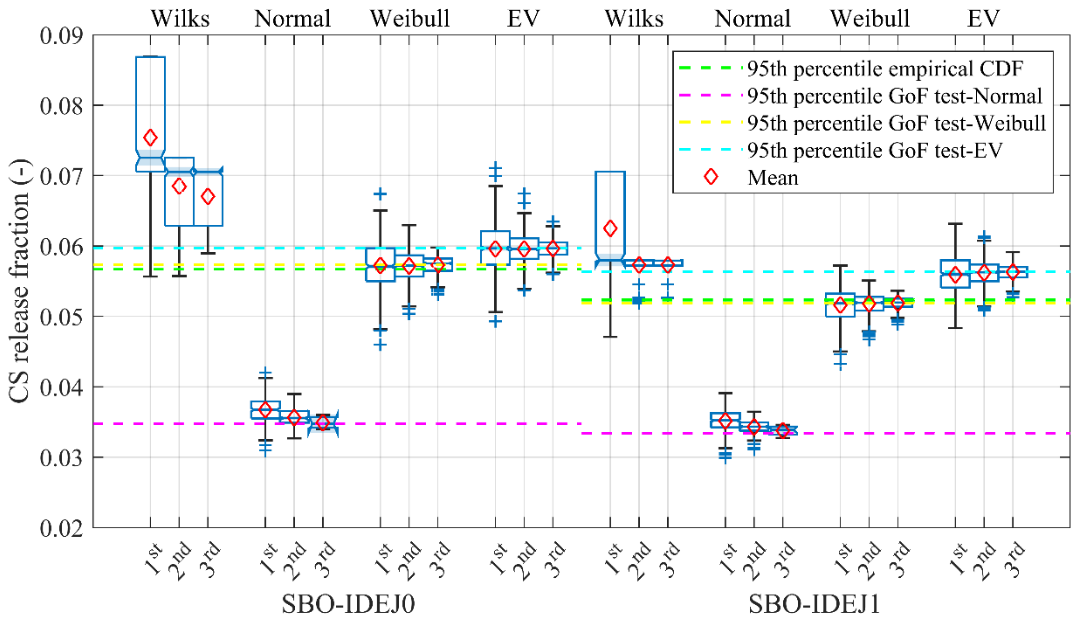

Figure 5-91 Boxplots for the 95/95 estimates by goodness-of-fit tests for CS release fraction during SBO-IDEJ0 (left) and SBO-IDEJ1 (right).

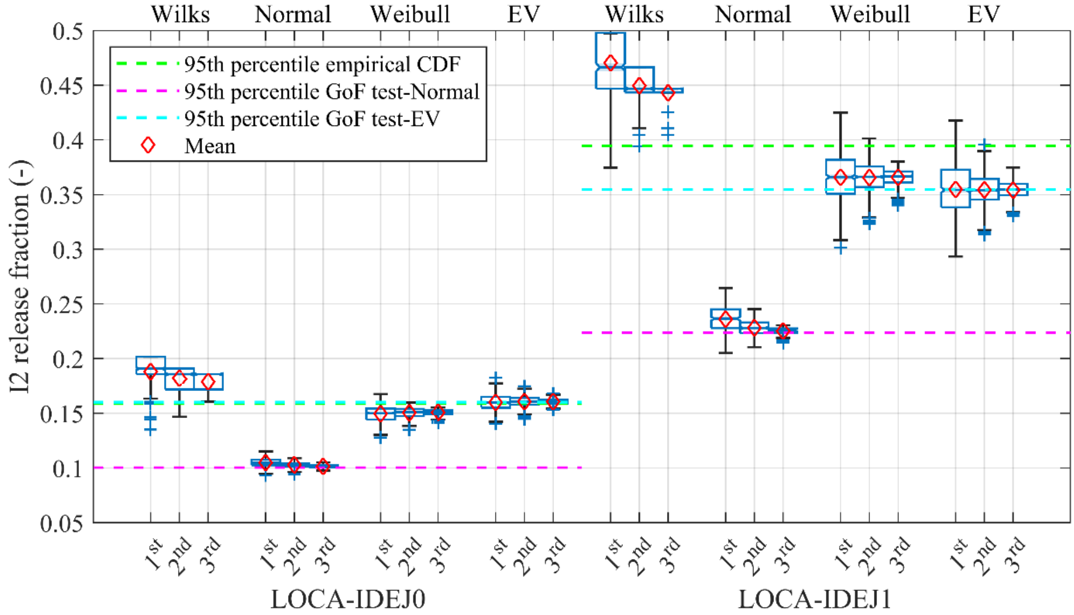

Figure 5-92 Boxplots for the 95/95 estimates by goodness-of-fit tests for I2 release fraction during LOCA-IDEJ0 (left) and LOCA-IDEJ1 (right).

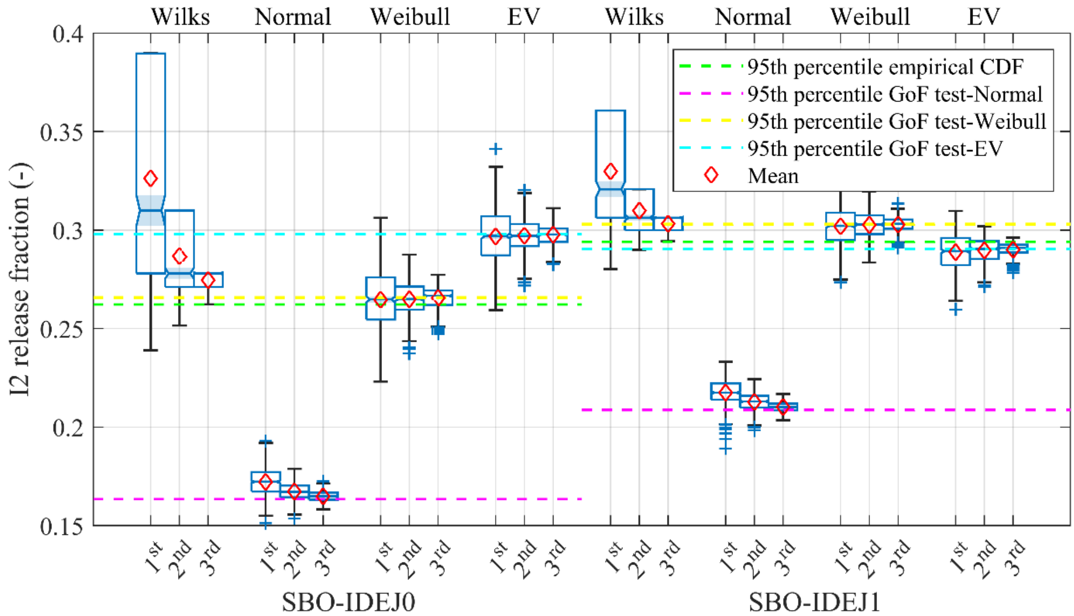

Figure 5-93 Boxplots for the 95/95 estimates by goodness-of-fit tests for I2 release fraction during SBO-IDEJ0 (left) and SBO-IDEJ1 (right).

5.5.Uncertainty analysis RC7 – Swedish plant configuration

5.5.1. Selection of parameters and sampling size

Based on the sensitivity analysis results, in total 4 sets of the most influential MELCOR modelling parameters have been identified for the RC7A and RC7B scenarios, together with the combinations of the mode of debris ejection from the vessel (IDEJ) which was considered as a phenomenological splinter[2] for every accident scenario considered in the analysis. The parameters and associated uncertainty distributions are summarized in Table 5-28.

The uncertainty distributions are based on the literature review [26][27][28][29][30][31] and, in many cases, on expert judgment, due to lack of publicly available information.

The MVSS filter decontamination factor for radioactive vapours is one of the most influential parameters for the RC7B scenario (LOCA-MVSS), especially in case of IDEJ1 (solid debris ejection off). A set of standalone calculations using the SPARC-90 model for the MVSS filter showed that it is possible to achieve DFs for gaseous forms of Cs in the order of 10-100. Furthermore, since the current MELCOR model of Nordic BWR lacks the necessary level of details regarding the MVSS structures (multi-venturi assembly, moist separator, etc., and associated heat structures) in the model, the actual decontamination factor can be even higher. For the purpose of uncertainty analysis, the decontamination factor for radioactive aerosols MVSSDFA will have a normal distribution with (μ=500,σ=250) truncated on the range between [100,1000], while the decontamination factor for radioactive vapors (except RN class 1 – noble gases) MVSSDFV will have a log-normal distribution (μ=4.6,σ=0.91) truncated on the range [10,100]]. Both parameters are assumed to be correlated. It is important note that the uncertainty distribution for the MVSSDFV used in the present study is not necessarily conservative and require further investigation, that will be addressed in the next phase of the project.

For the uncertainty analysis, the sample size of 500 MELCOR code calculations (per every accident scenario and IDEJ parameter combinations) was selected, which should produce adequate results based on the 99% tolerance/confidence levels for upper bounds (one sided), as discussed in section 4.1.2.2. The sampling will be performed using the LHS method, using the Dakota software package[10]. Management of the sampling generation and MELCOR code simulations will be performed by the pyMELCOR and pyDakota tools (see section 4.1.3).

Table 5-28. Parameter selection and associated uncertainty distributions considered in UA for RC7 release category.

Parameter name	Default value	Range	Units	Description	Proposed distribution
STICK	1	[0.5, 1]	-	Particle sticking probability (see 5.4.2 in [23])	Scaled beta (2.5, 1.0), scaled on [0.5, 1.0] [31]
FCELRA	0.25	[0.1, 0.25]	-	Radiative exchange factors for radiation radially outward and upward from the cell boundary to the next adjacent cell (see section 5.3.5 in [23])	Truncated normal (0.1, 0.035) truncated on [0.020, 0.30] [27]
SC71521	0.007	[5.E-3, 8.E-3]	m	Initial bubble diameter correlation coefficient in SPARC-90 model (see section 5.10.2 in [23])	Triangular M = 7.E-3, range [5.E-3, 8.E-3] [EJ][8]
SC1020	2	[1,4]	-	Multiplication factor for time constant for radial solid and molten debris relocation (see section 5.5.2 in [23] and section 5.2)	Scaled beta (1.33, 1.67) scaled on range [1.0, 4.0] [29]
CORNSBLD	1520	[1520, 1700]	K	NS failure temperature threshold (see section 5.5.1 in [23])	Uniform [1520-1700] [30]
VFALL	0.01	[0.01, 1.0]	m/s	Velocity of falling debris (see section 5.5.2 in [23])	Scaled beta (0.85, 1.14), scaled on range [0.01, 1.0] [29]
TZRSSINC	1210	[1210, 1700]	K	Solidus temperatures for ZR/SS and ZR/INC eutectic pairs (see section 5.3.3 in [23])	Scaled beta (2.0, 1.0), scaled on range [1210, 1700] [EJ]
SC715010	1	[1,3]	-	Scaling factor for SPARC-90 model vent exit condensation decontamination factor (see section 5.10.2 in [23])	Triangular M = 2, range [1.0, 3.0] [EJ]
CHI	1	[1.0, 5.0]	-	Aerosol dynamic shape factor (see section 5.4.1 in [23])	Scaled beta (1.0, 1.5) scaled on [1.0, 5.0] [31]
MVSSDFV	1	[10-1000]	-	MVSS decontamination factor for radioactive vapours (see section 5.10.2 in [23] and section 5.2)	Lognormal (4.6, 0.916) truncated on [10,1000], 0.99 – correlation with MVSSDFA [EJ]

[8] EJ – expert judgement.

Parameter name	Default value	Range	Units	Description	Proposed distribution
SC71568	-0.00232	[-2.6691e-03, -1.9728e-03]	-	Multiplicative constant in a temperature correction correlation in the SPARC-90 model (see 5.10.2 in [23])	Triangular M = -0.00232, [-2.6691e-03, -1.9728e-03] [EJ]
TPFAIL	1273	[1273, 1600]	K	Penetration failure temperature (see section 5.6 in [23])	Scaled beta (2.0, 2.0) scaled on [1273, 1600] [EJ]
HFRZZR	7500	[2000, 22000]	W/m2-K	Refreezing heat transfer coefficient for Zr (see section 5.5.2 in [23])	Lognormal (8.9227, 0.55962) truncate on [2000, 22000] [27]
SC7170CSM	0.67	[0.5695, 0.7705]	kg/kg H2O	Saturation solubility at high and low temperature reference for CsM (see section 5.4.7 in [23])	Triangular M = 0.67, range [0.5695, 0.7705] [EJ]
SC71555	1.13893	[0.9681, 1.3098]	-	SPARC-90 model multiplication constants in the DF factor correlations for and large Stokes numbers (see section 5.10.2 in [23])	Triangular M = 1.13893, range [0.9681, 1.3098] [EJ]
RHONOM	1000	[870,4500]	kg/m3	Aerosol density (see section 5.4.3 in [23])	Triangular M = 2000, range [870,4500] [26]
SC7111CS2	97	[82.450,111.550]	K	Characteristic energy of interaction between the molecules divided by the Boltzmann constant for CsI/CsM(see section 5.4.7 in [23])	Triangular M = 97, range [82.450,111.550] [EJ]
SC7170CS	3.95	[3.3575, 4.5425]	kg/kg H2O	Saturation solubility at low/high temperature reference for Cs (see section 5.4.7 in [23])	Triangular M = 3.95, range [3.3575, 4.5425] [EJ]
SC7111CS1	3.617	[3.0745,4.1595]	Å	Characteristic diameter of the molecule for Cs (see section 5.4.7 in [23])	Triangular M = 3.617, range [3.0745,4.1595] [EJ]
TURBDS	0.001	[7.5E-4, 1.25E-3]	m2/s3	Turbulence dissipation rate (see section 5.4.7 in [23])	Uniform [7.5E-4, 1.25E-3] [28][EJ]
SC7111I1	4.982	[4.2347, 5.7293]	Å	Characteristic diameter of the molecule for I (see section 5.4.7 in [23])	Triangular M = 4.982, range [4.2347, 5.7293] [EJ]
NUMSEC	10	[10, 20]	-	Number of sections (see section 5.4.4 in [23])	Uniform [10, 20] [EJ]
SC71551	1.79182	[1.5230, 2.0606]	-	SPARC-90 model multiplication constants in the DF factor correlations for small Stokes numbers (see section 5.10.2 in [23])	Triangular M = 1.79182, range [1.5230, 2.0606] [EJ]

Parameter name	Default value	Range	Units	Description	Proposed distribution
SC7170CSI3	0.44	[0.374, 0.5060]	kg/kg H2O	Saturation solubility at low temperature reference for CsI (see section 5.4.7 in [23])	Triangular M = 0.44, range [0.374, 0.5060] [EJ]
GAMMA	1	[1.0, 5.0]	-	Aerosol agglomeration shape factor (see section 5.4.1 in [23])	Scaled beta (1.0,1.5) scaled on range [1.0, 5.0] [31]
MVSSDFA	500	[100, 1000]	-	MVSS decontamination factor for radioactive aerosols (see 5.10.2 in [23] and section 5.2)	Truncated normal (500, 250) truncated on [100,1000], 0.99 – correlation with MVSSDFV [EJ]
SC11321	2800	[2500-2800]	K	Oxidized fuel rod collapse temperature (see section 5.2)	Scaled beta (2, 5) scaled on range [2500-2800] [EJ]
HDBPN	1000	[100, 1000]	W/m2-K	Heat transfer coefficient between particulate debris and LH penetration (see section 5.6 in [23])	Uniform [100, 1000] [EJ]
PDPor	0.3	[0.25, 0.50]	-	Particulate debris porosity (see section 5.5.1 in [23])	Truncated normal(0.38, 0.1) truncated on [0.25, 0.50] [27][EJ]
HFRZSS	1000	[1000, 5000]	W/m2-K	Refreezing heat transfer coefficient for SS (see section 5.5.2 in [23])	Lognormal (7.824, 0.40547), truncated on [1000, 5000] [27]
DHYPDLP	0.002	[0.002, 0.005]	m	Lower plenum particulate debris equivalent diameter (see section 5.5.2 and 5.5.3 in [23])	Truncated normal (0.0035, 0.001) truncated on [0.002, 0.005] [EJ]
SC11312	2400	[2100, 2500]	K	Critical temperature at which molten materials are released from an oxide shell or local blockage (see section 5.5.2 in [23])	Triangular M = 2400, range [2100, 2500] [27]
SC7111I2	550	[467.50, 632.50]	K	Characteristic energy of interaction between the molecules divided by the Boltzmann constant for I2 (see section 5.4.7 in [23])	Triangular M = 550, range [467.50, 632.50] [EJ]

5.5.2. Uncertainty analysis for RC7A – SBO-MVSS IDEJ1

5.5.2.1.Parameter selection

The selection of the parameters for the uncertainty analysis for the RC7A – SBO-MVSS IDEJ1 scenario is based on the sensitivity analysis results and presented in Table 5-13. The ranges and uncertainty distributions are summarized in Table 5-28.

5.5.2.2.Uncertainty analysis results

The uncertainty analysis results for the RC7A-SBO-MVSS-IDEJ1 are summarized in Table 5-29 and Figures 5-94-5-103.

Table 5-29. Descriptive statistics of the main figures of merit for RC7A – SBO-MVSS-IDEJ1.

	MVSS Time (h)	LHF Time (h)	CSP Failure Time (h)	Max temp in WW (K)	Debris ejected from RPV [kg]	Cs release fraction [-]	I release fraction [-]
Mean	7.67	3.21	3.16	393	237790	5.44E-06	4.23E-05
5%	6.1	2.37	2.32	387	195986	1.50E-06	2.11E-06
25%	6.72	2.62	2.58	390	230745	2.86E-06	1.98E-05
50%	7.36	2.97	2.92	392	240754	4.46E-06	3.37E-05
75%	8.27	3.46	3.42	394	247505	6.79E-06	5.45E-05
95%	10.05	5.46	5.41	400	272294	1.24E-05	1.15E-04
Min	5	1.71	1.63	384	183855	9.30E-07	1.25E-06
Max	15.22	8.06	8.01	408	297251	3.69E-05	3.83E-04

Figures 5-94-5-99 show the distributions of the fractions of Cs released from the fuel and deposited in the different control volumes of the MELCOR model of Nordic BWR, where *Cs_F/DB* – denote the fraction of Cs (fraction of total core inventory) retained in the fuel/in-vessel debris (COR package) and cavity debris (CAV package); *CS_RCS* – fraction of Cs deposited in the reactor coolant system (control volumes and heat structures representing the reactor pressure vessel, steam lines, etc.); *CS_DW* – fraction of Cs deposited in the drywell (upper drywell, lower drywell and associated heat structures); *CS_WW* – fraction of Cs deposited in the wetwell (wetwell and associated control volumes and heat structures), *CS_MVSS* – fraction of Cs deposited in the MVSS filter (MVSS filter and associated control volumes), *CS_ENV* – fraction of Cs released to the environment (sum of filtered release, unfiltered release (containment overpressure protection line and due to rupture) and diffuse leakage; *CS_ENV_DL* – fraction of Cs released to the environment due to diffuse leakage.

The results indicate that the fraction of Cs released to the environment during the first 6 hours after the initiating event is dominated by diffuse leakage from the containment. After MVSS opening, the contribution of MVSS release start to increase and becomes dominant after 16-24 hours after the initiating event.

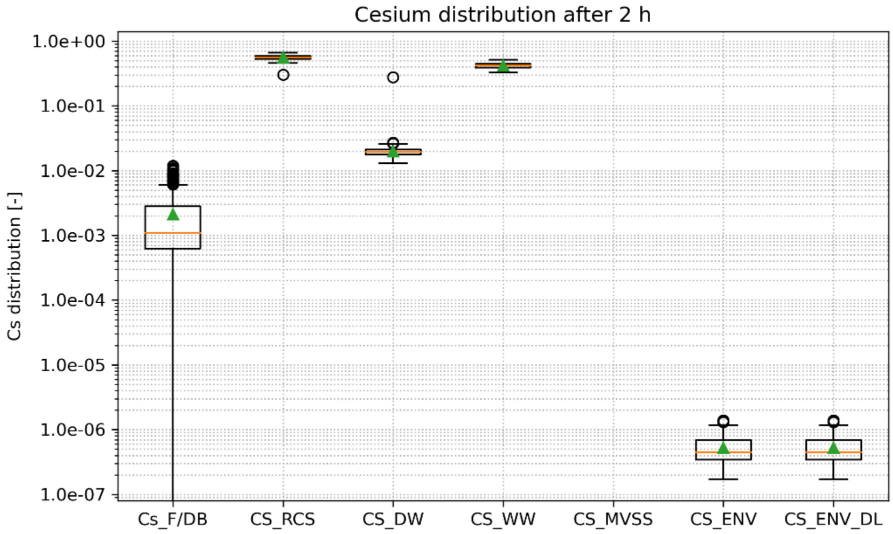

Figure 5-94 Box and whisker plot of the fraction of Cs [-] deposited in the containment and environment after 2h after the initiating event[6]

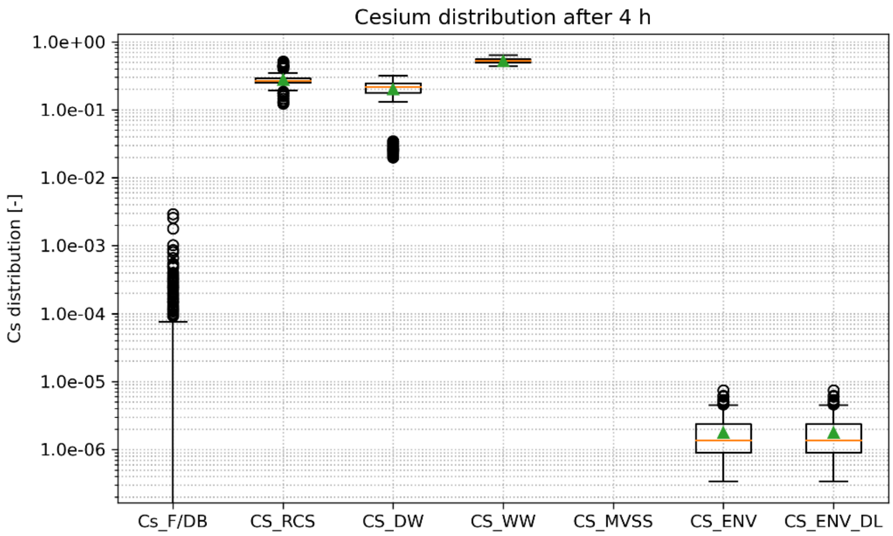

Figure 5-95 Box and whisker plot of the fraction of Cs [-] deposited in the containment and environment after 4h after the initiating event[6]

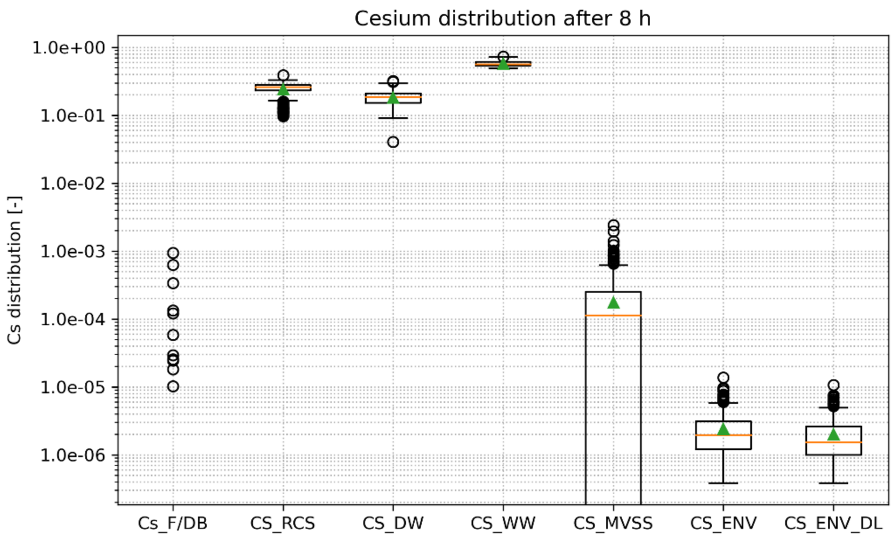

Figure 5-96 Box and whisker plot of the fraction of Cs [-] deposited in the containment and environment after 8h after the initiating event[6]

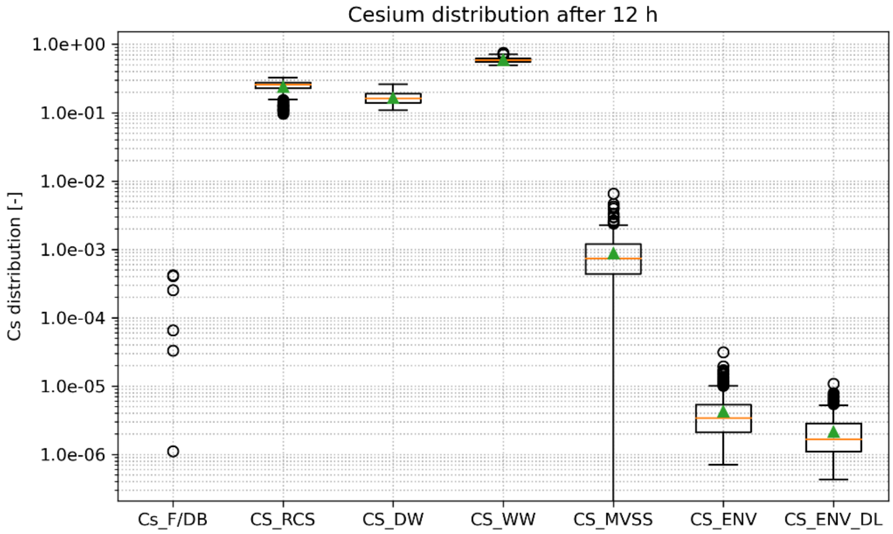

Figure 5-97 Box and whisker plot of the fraction of Cs [-] deposited in the containment and environment after 12h after the initiating event[6]

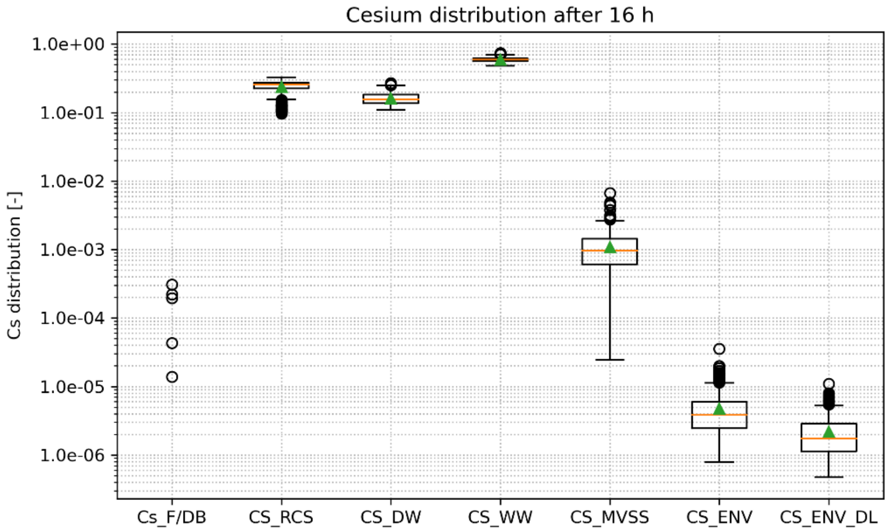

Figure 5-98 Box and whisker plot of the fraction of Cs [-] deposited in the containment and environment after 16h after the initiating event[6]

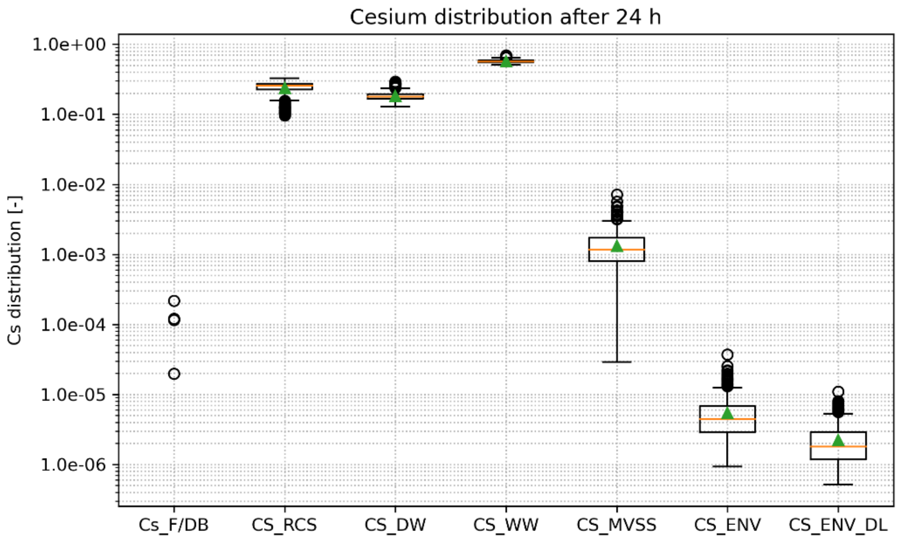

Figure 5-99 Box and whisker plot of the fraction of Cs [-] deposited in the containment and environment after 24h after the initiating event[6]

Furthermore, the results indicate that in case of SBO, the major part of Cs released from the fuel/debris is deposited in the wetwell.

Figure 5-100 and Figure 5-101 show that the results agree with the main findings from the sensitivity analysis results for the RC7A release category. In particular, the most influential parameters are MVSSDFA – MVSS filter decontamination factor for radioactive aerosols [-], and GAMMA – aerosol shape factor [-], where in both cases, the fraction of Cs released to the environment decrease with increase of these parameters. While higher values of MVSSDFA lead to improved retention of radioactive aerosols in the filter, the higher values GAMMA parameter increase retention of the aerosol fission products in the containment, as illustrated in Figure 5-102, where the fraction of Cs deposited in the DW increase from approximately 20 to 35%.

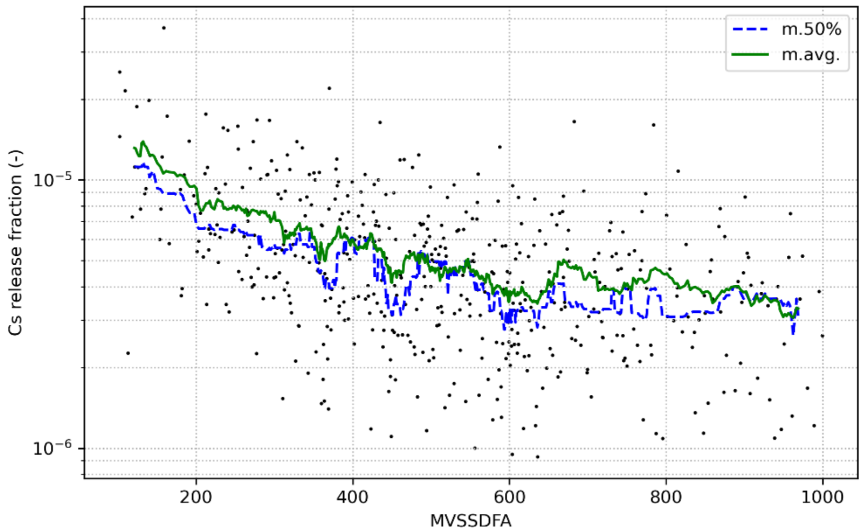

Figure 5-100 Scatter plot and moving average (green)/median(dashed blue) of the fraction of Cs released to the environment as a function of MVSSDFA [-]

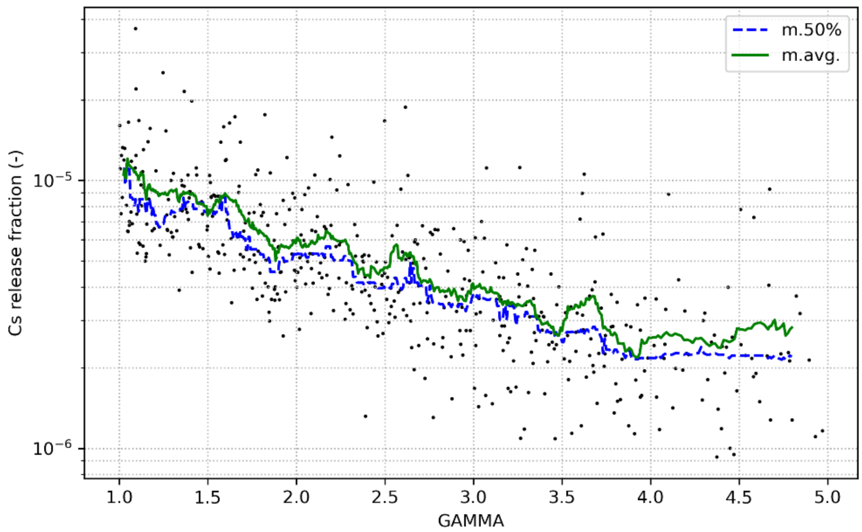

Figure 5-101 Scatter plot and moving average (green)/median(dashed blue) of the fraction of Cs released to the environment as a function of GAMMA [-]

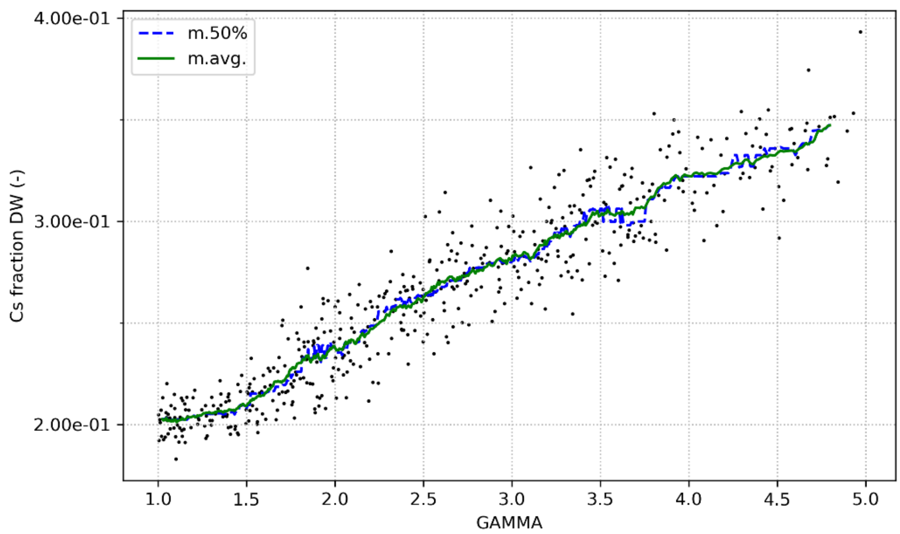

Figure 5-102 Scatter plot and moving average (green)/median(dashed blue) of the fraction of Cs deposited in the drywell as a function of GAMMA [-]

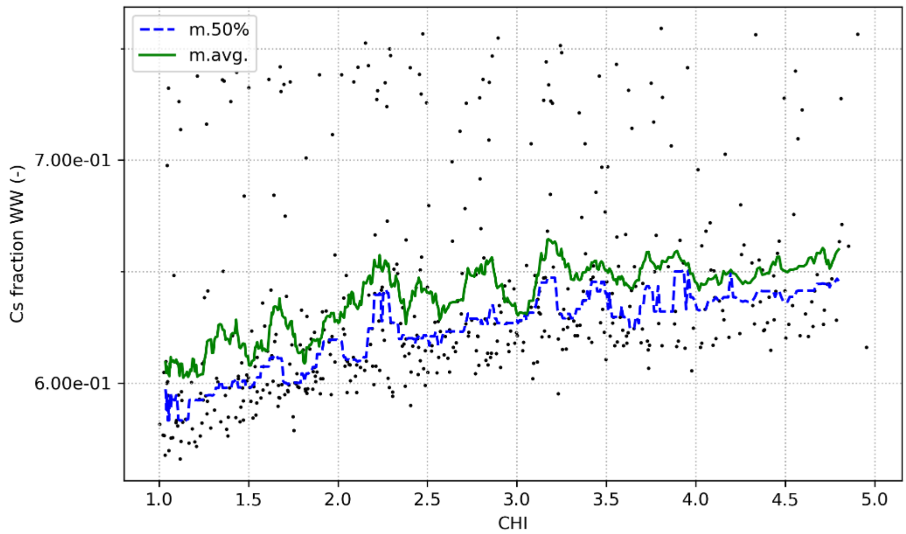

Figure 5-103 Scatter plot and moving average (green)/median(dashed blue) of the fraction of Cs deposited in the wetwell as a function of CHI [-]

Furthermore, the results indicate that the fraction of Cs deposited in the WW increases with increase of CHI – Aerosol dynamic shape factor [-].

5.5.3. Uncertainty analysis for RC7A – SBO-MVSS IDEJ0

5.5.3.1.Parameter selection

The selection of the parameters for the uncertainty analysis for RC7A – SBO-MVSS IDEJ0 scenario is based on the results of the sensitivity analysis and presented in Table 5-16. The ranges and uncertainty distributions are summarized in Table 5-28.

5.5.3.2.Uncertainty analysis results

The results of the uncertainty analysis for the RC7A-SBO-MVSS-IDEJ1 are summarized in Table 5-30 and Figures 5-104-5-113.

Table 5-30. Descriptive statistics of the main figures of merit for RC7A – SBO-MVSS-IDEJ0

	MVSS Time (h)	LHF Time (h)	CSP Failure Time (h)	Max temp in WW (K)	Debris ejected from RPV [kg]	Cs release fraction [-]	I release fraction [-]
Mean	5.62	2.8	2.73	401	293560	3.60E-06	1.64E-05
5%	4.9	2.19	2.14	398	277004	1.42E-06	5.23E-06
25%	5.48	2.44	2.36	399	293148	2.10E-06	9.30E-06
50%	5.65	2.71	2.66	400	295559	2.98E-06	1.30E-05
75%	5.85	3.01	2.96	401	297627	4.58E-06	1.99E-05
95%	6.35	3.68	3.64	406	301440	7.55E-06	3.94E-05
Min	2.64	1.61	1.55	395	251127	5.73E-07	6.88E-07
Max	10.06	8.19	8.14	417	306653	1.48E-05	1.04E-04

The results indicate that the fraction of Cs released to the environment during the first 6 hours after the initiating event is dominated by diffuse leakage from the containment. After MVSS opening, the contribution of MVSS release start to increase and becomes dominant after 16-24 hours the after the initiating event. Furthermore, in both cases SBO-IDEJ1 (see section 5.5.2.2) and IDEJ0 the accident progression prior to RPV failure is expected to be similar. After PRV failure, typically due the failure and ejection of RPV lower head penetrations, the in-vessel debris can be ejected from the vessel to the water-flooded cavity located under the RPV. The analysis performed in [22][24], showed that in case of IDEJ=0 (solid debris ejection – ON), it is expected that the in-vessel debris is gradually ejected to the cavity directly after RPV failure, while in case of IDEJ=1 (solid debris ejection – OFF) it expected that the in-vessel debris is ejected in a dripping mode initially (through failed LH penetrations), followed by massive debris ejection, typically due to creep-rupture of the vessel lower head.

The different modes of debris ejection (IDEJ) lead to different containment pressurization patterns in case of IDEJ1 and 0, where IDEJ0, typically leads to a more gradual and rapid pressurization of the containment after RPV failure and earlier activation of the MVSS filter, but smaller releases to the environment.

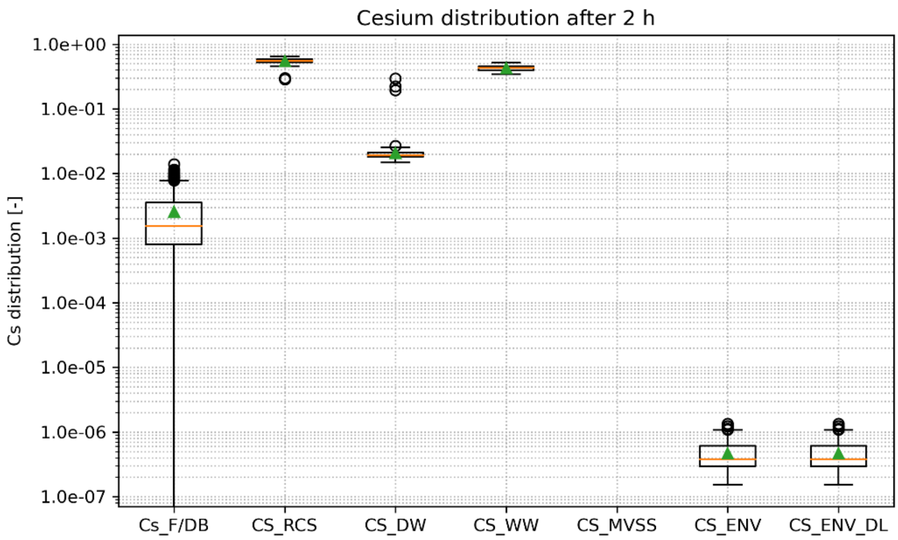

Figure 5-104 Box and whisker plot of the fraction of Cs [-] deposited in the containment and environment after 2h after the initiating event[6]

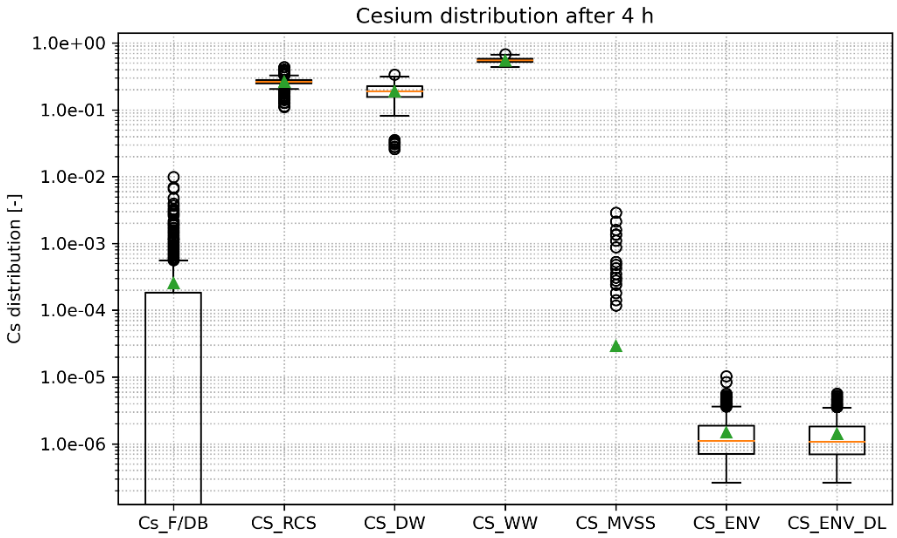

Figure 5-105 Box and whisker plot of the fraction of Cs [-] deposited in the containment and environment after 4h after the initiating event[6]

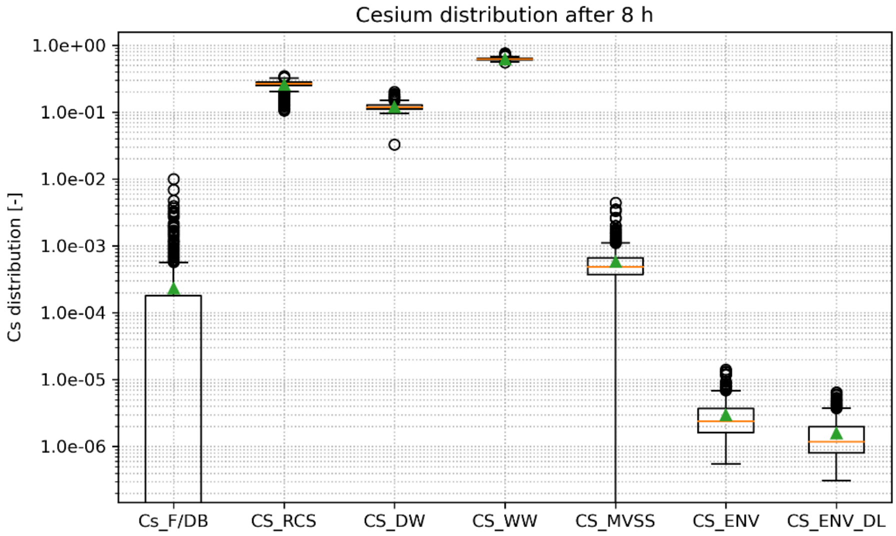

Figure 5-106 Box and whisker plot of the fraction of Cs [-] deposited in the containment and environment after 8h after the initiating event[6]

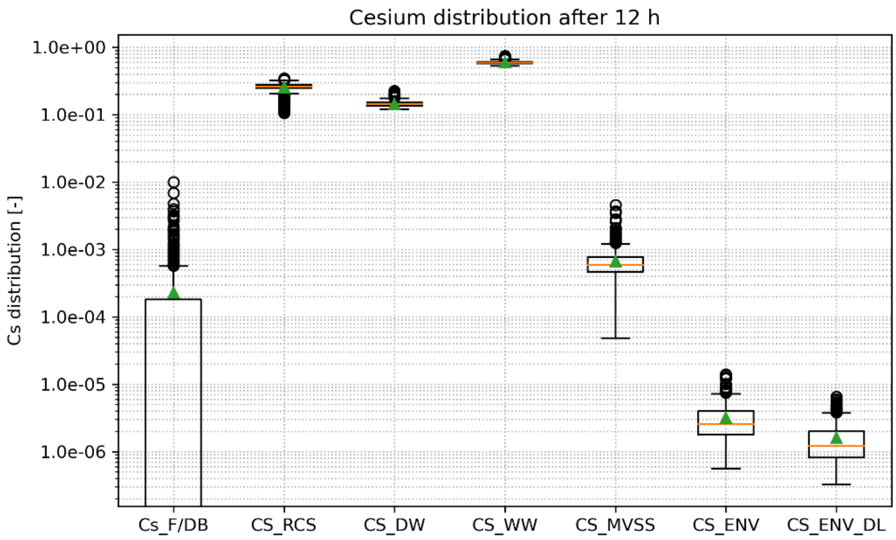

Figure 5-107 Box and whisker plot of the fraction of Cs [-] deposited in the containment and environment after 12h after the initiating event[6]

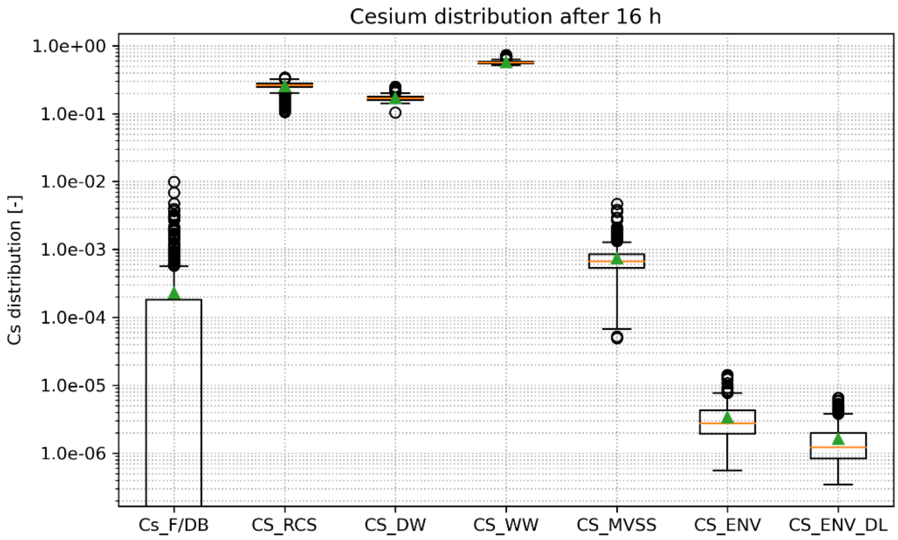

Figure 5-108 Box and whisker plot of the fraction of Cs [-] deposited in the containment and environment after 16h after the initiating event[6]

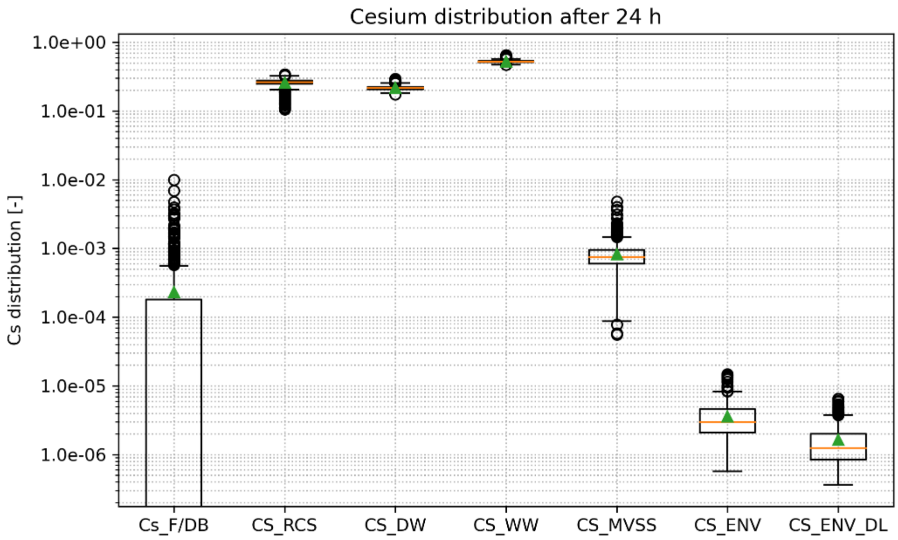

Figure 5-109 Box and whisker plot of the fraction of Cs [-] deposited in the containment and environment after 24h after the initiating event[6]

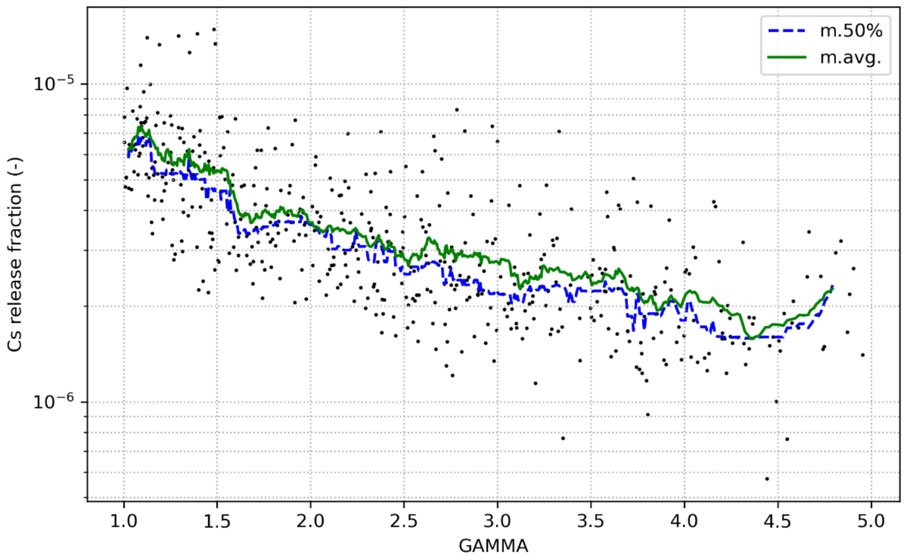

Figure 5-110 Scatter plot and moving average (green)/median(dashed blue) of the fraction of Cs released to the environment as a function of GAMMA [-]

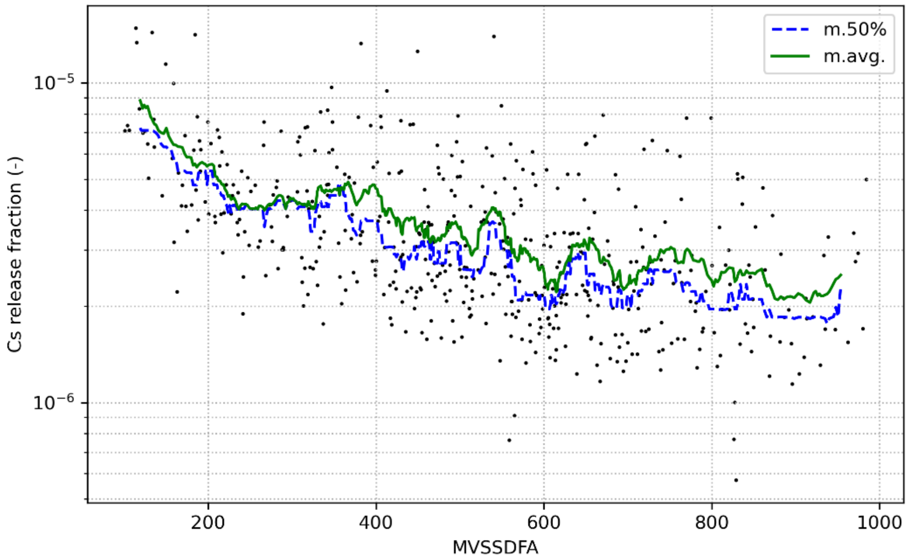

Figure 5-111 Scatter plot and moving average (green)/median(dashed blue) of the fraction of Cs released to the environment as a function of MVSSDFA [-]

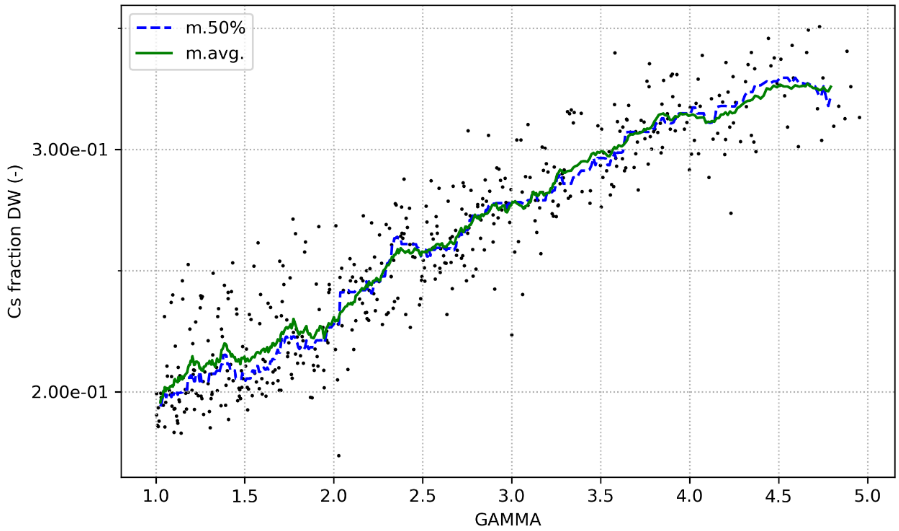

Figure 5-112 Scatter plot and moving average (green)/median(dashed blue) of the fraction of Cs deposited in the drywell as a function of GAMMA [-]

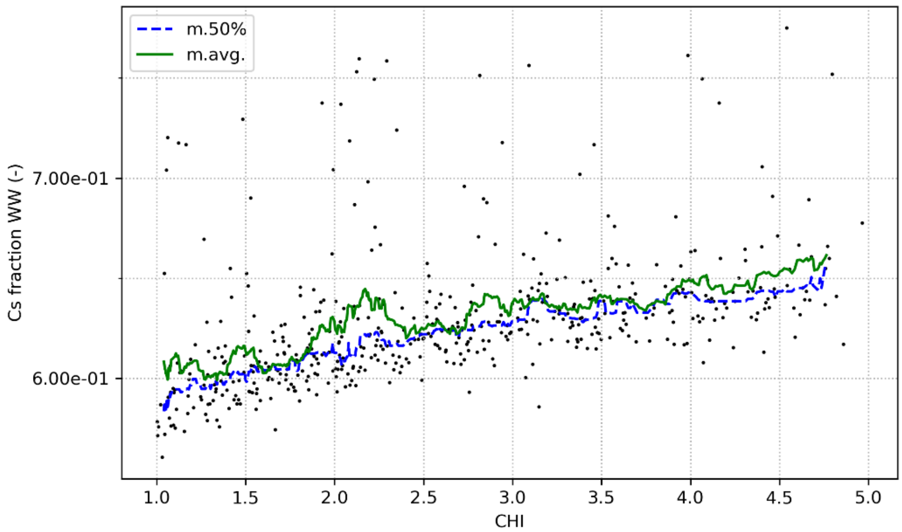

Figure 5-113 Scatter plot and moving average (green)/median(dashed blue) of the fraction of Cs deposited in the wetwell as a function of CHI [-]

As in case of SBO-IDEJ1 (see section 5.5.2.2), the major part of Cs released from the fuel/debris is deposited in the wetwell. The most influential parameters are MVSSDFA – MVSS filter decontamination factor for radioactive aerosols [-], and GAMMA – aerosol shape factor [-], where in both cases, the fraction of Cs released to the environment decrease with increase of these parameters. While higher values of MVSSDFA lead to improved retention of radioactive aerosols in the filter, the higher values GAMMA parameter increase retention of the aerosol fission products in the containment, as illustrated in Figure 5-102, where the fraction of Cs deposited in the DW increase from approximately 20 to 30%. The fraction of Cs deposited in the WW increases with increase of CHI – Aerosol dynamic shape factor [-] from approximately 60 to 65%.

5.5.4. Uncertainty analysis for RC7B – LOCA-MVSS IDEJ1

5.5.4.1.Parameter selection

The selection of the parameters for the uncertainty analysis for the RC7B – LOCA-MVSS IDEJ1 scenario is based on the results of sensitivity analysis and presented in Table 5-19. The ranges and uncertainty distributions are summarized in Table 5-28.

5.5.4.2.Uncertainty analysis results

The results of the uncertainty analysis for RC7B-LOCA-MVSS-IDEJ1 are summarized in Table 5-31 and Figures 5-114-Figure 5-122.

Table 5-31. Descriptive statistics of the main figures of merit for RC7B – LOCA-MVSS-IDEJ1

	MVSS Time (h)	LHF Time (h)	CSP Failure Time (h)	Max temp in WW (K)	Debris ejected from RPV [kg]	Cs release fraction [-]	I release fraction [-]
Mean	6.61	2.18	2.12	371	211343	9.70E-04	1.26E-03
5%	4.11	1.21	1.16	366	169742	2.39E-04	2.91E-04
25%	5.25	1.47	1.41	369	188517	4.18E-04	5.26E-04
50%	6.69	1.73	1.66	371	199727	6.62E-04	8.80E-04
75%	7.48	2.48	2.41	374	238681	1.12E-03	1.45E-03
95%	9.67	5.24	5.1	377	275633	2.33E-03	3.20E-03
Min	2.23	0.95	0.86	358	119419	1.33E-04	1.70E-04
Max	15.56	7.59	7.54	382	287093	1.91E-02	2.46E-02

The results indicate that the fraction of Cs released to the environment during the first 4 hours after the initiating event is dominated by diffuse leakage from the containment. After MVSS opening, the contribution of the MVSS release start to increase and becomes dominant after 8-24 hours after the initiating event.

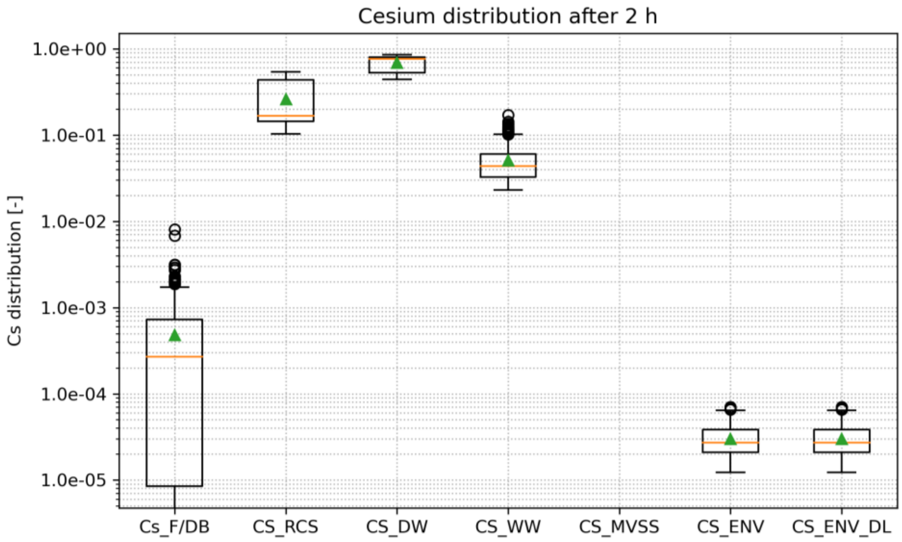

Figure 5-114 Box and whisker plot of the fraction of Cs [-] deposited in the containment and environment after 2h after the initiating event[6]

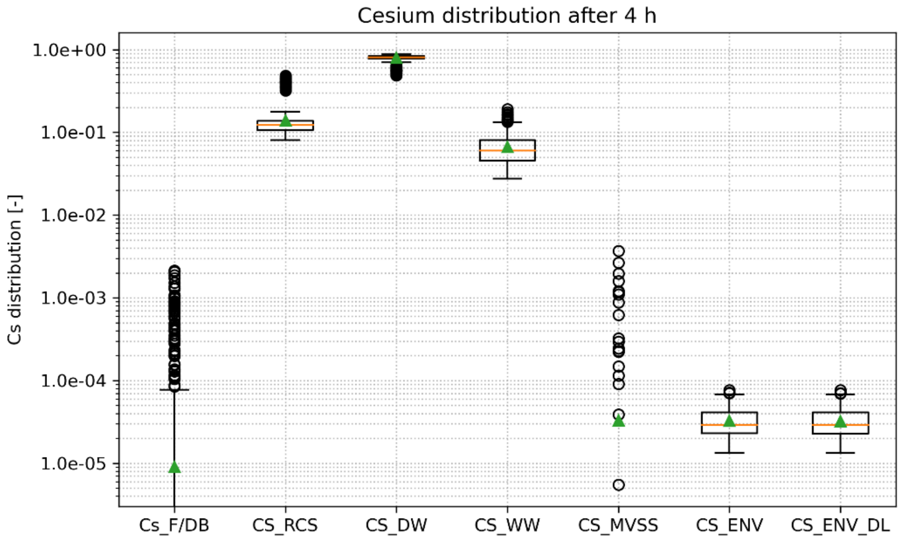

Figure 5-115 Box and whisker plot of the fraction of Cs [-] deposited in the containment and environment after 4h after the initiating event[6]

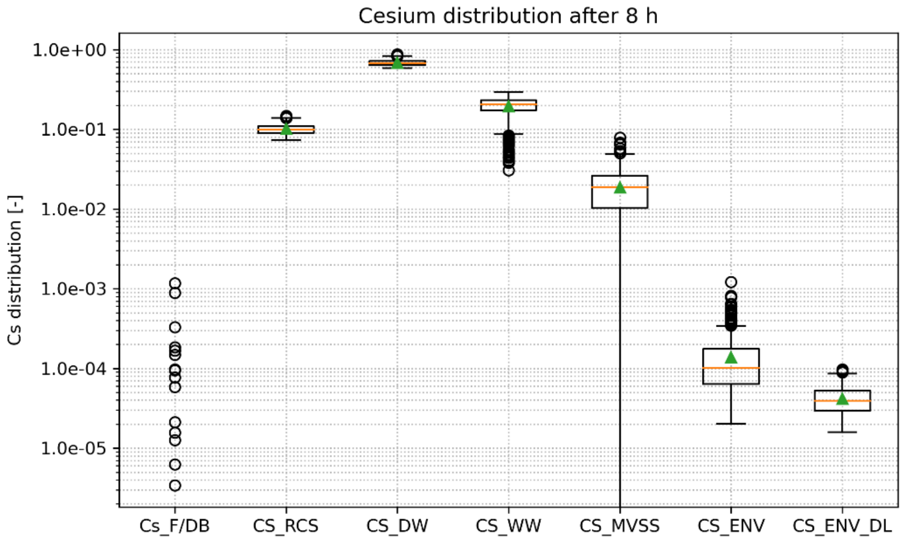

Figure 5-116 Box and whisker plot of the fraction of Cs [-] deposited in the containment and environment after 8h after the initiating event[6]

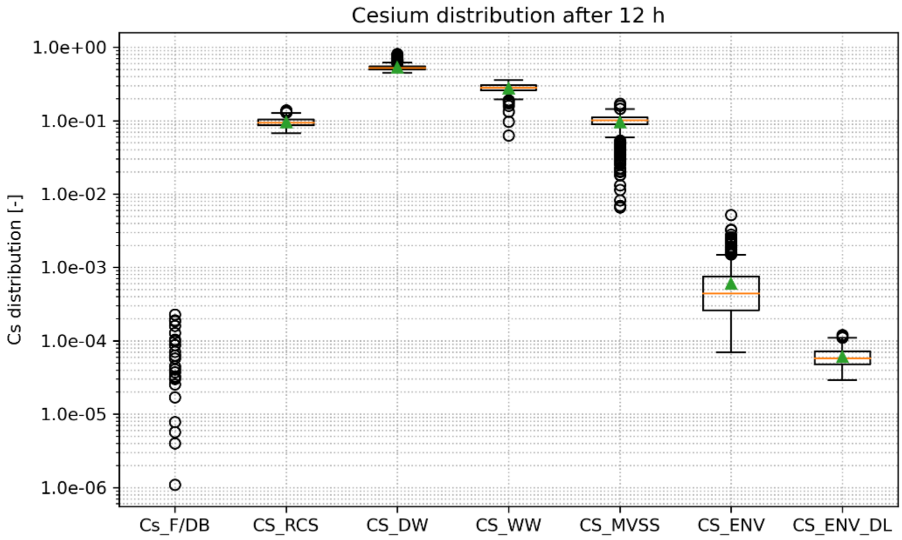

Figure 5-117 Box and whisker plot of the fraction of Cs [-] deposited in the containment and environment after 12h after the initiating event[6]

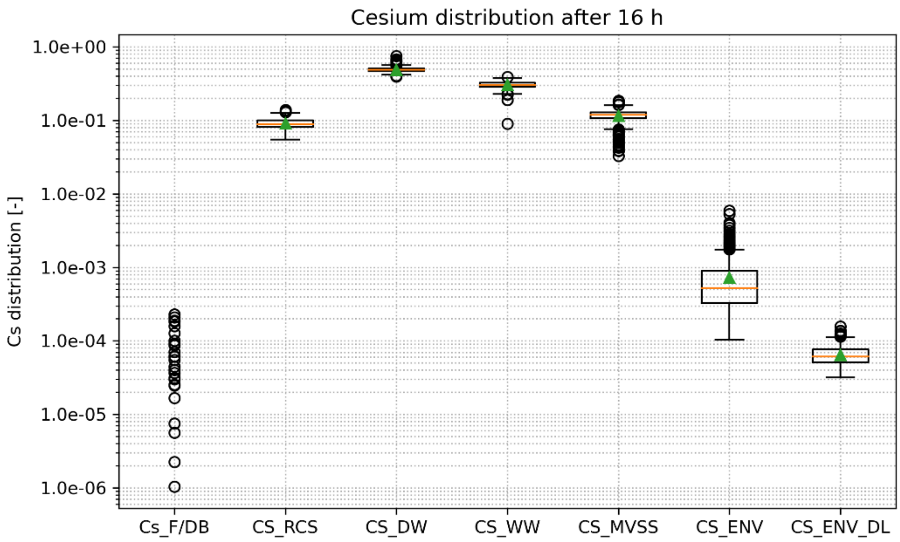

Figure 5-118 Box and whisker plot of the fraction of Cs [-] deposited in the containment and environment after 16h after the initiating event[6]

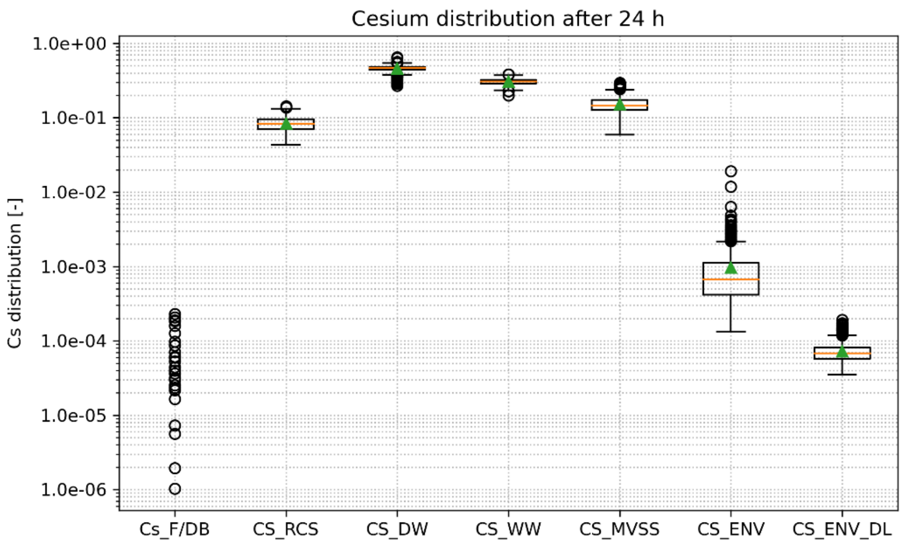

Figure 5-119 Box and whisker plot of the fraction of Cs [-] deposited in the containment and environment after 24h after the initiating event[6]

The results show that the uncertainty in the fraction of Cs released to the environment in case of RC7B-LOCA-MVSS-IDEJ1 is dominated by MVSSDFV - MVSS filter decontamination factor for radioactive vapors [-] – which is in agreement with the results of sensitivity analysis presented in section 5.2.2.2.1.

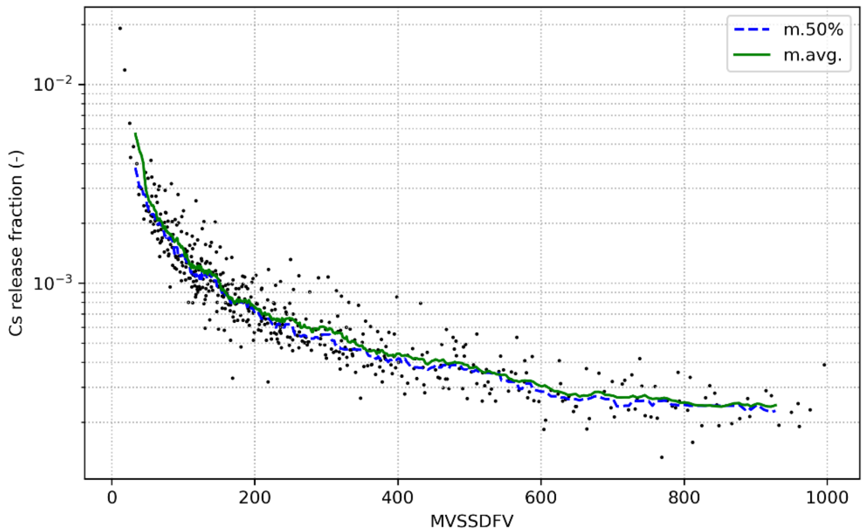

Figure 5-120 Scatter plot and moving average (green)/median(dashed blue) of the fraction of Cs released to the environment as a function of MVSSDFV [-]

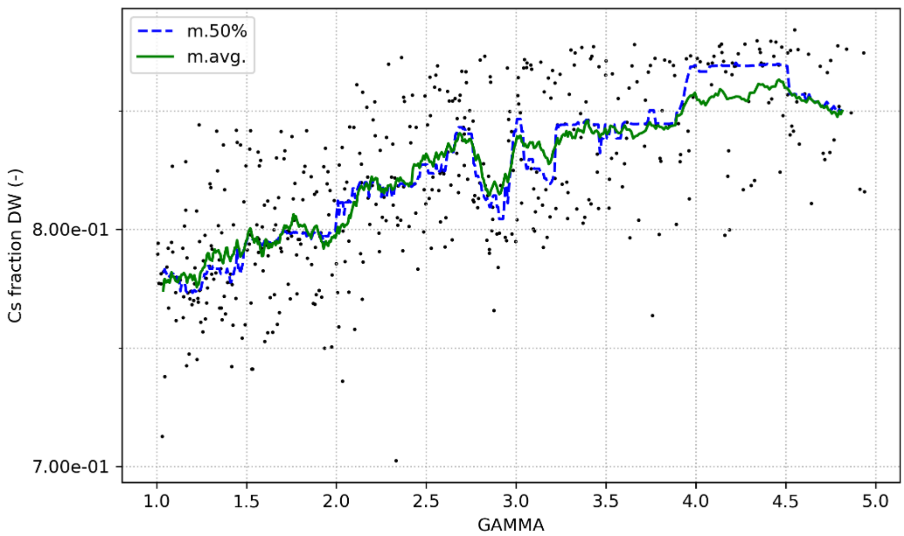

Figure 5-121 Scatter plot and moving average (green)/median(dashed blue) of the fraction of Cs deposited in the drywell as a function of GAMMA [-]

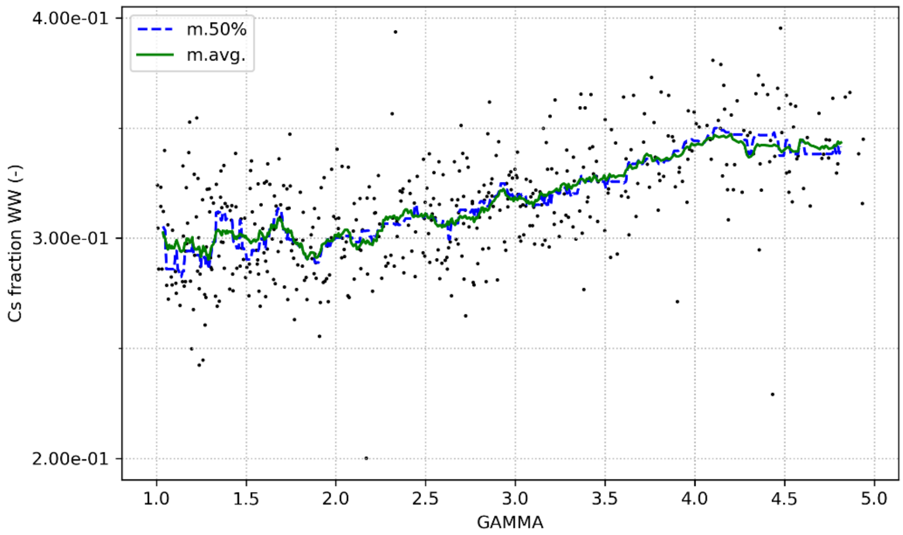

Figure 5-122 Scatter plot and moving average (green)/median(dashed blue) of the fraction of Cs deposited in the wetwell as a function of GAMMA [-]

The major fraction of Cs released from the fuel is deposited in the drywell, ranging from 77 to 85%, where GAMMA – aerosol shape factor [-] is the most influential parameter. The fraction of Cs deposited in the WW is around 30%.

5.5.5. Uncertainty analysis for RC7B – LOCA-MVSS IDEJ0

5.5.5.1. Parameter selection

The selection of the parameters for the uncertainty analysis for RC7B – LOCA-MVSS IDEJ0 scenario is based on the results of the sensitivity analysis and presented in Table 5-22. The ranges and uncertainty distributions are summarized in Table 5-28.

5.5.5.2. Uncertainty analysis results

The results of the uncertainty analysis for RC7B-LOCA -MVSS-IDEJ are summarized in Table 5-32 and Figures 5-123-5-132.

Table 5-32. Descriptive statistics of the main figures of merit for RC7B – LOCA-MVSS-IDEJ0

	MVSS Time (h)	LHF Time (h)	CSP Failure Time (h)	Max temp in WW (K)	Debris ejected from RPV [kg]	Cs release fraction [-]	I release fraction [-]
Mean	3.69	2.09	2.02	390	290452	1.67E-04	1.79E-04
5%	2.15	1.26	1.22	383	263653	4.86E-05	5.10E-05
25%	3.05	1.52	1.46	389	289281	7.10E-05	7.52E-05
50%	3.76	1.75	1.69	391	294022	1.05E-04	1.09E-04
75%	4.18	2.36	2.3	393	296722	1.75E-04	1.82E-04
95%	5.24	3.86	3.75	395	301176	4.52E-04	5.19E-04
Min	1.76	0.87	0.84	375	240138	2.74E-05	2.62E-05
Max	6.78	6.52	6.46	402	313737	1.78E-03	2.05E-03

The results indicate that the fraction of Cs released to the environment during the first 6 hours after the initiating event is dominated by the diffuse leakage from the containment. After MVSS opening, the contribution of MVSS release start to increase and becomes dominant after 8 hours after the initiating event.

Furthermore, in both cases LOCA-IDEJ1 and IDEJ0 the accident progression prior to RPV failure is expected to be similar. After PRV failure, typically due the failure and ejection of RPV lower head penetrations, the in-vessel debris can be ejected from the vessel to the water-flooded cavity located under the RPV. The analysis performed in [22][24], showed that in case of IDEJ=0 (solid debris ejection – ON), it is expected that the in-vessel debris is gradually ejected to the cavity directly after RPV failure, while in case of IDEJ=1 (solid debris ejection – OFF) it expected that the in-vessel debris is ejected in a dripping mode initially (through failed LH penetrations), followed by massive debris ejection, typically due to creep-rupture of the vessel lower head.

The different modes of debris ejection (IDEJ) lead to different containment pressurization patterns in case of IDEJ1 and 0, where IDEJ0, typically leads to a more gradual and rapid pressurization of the containment after RPV failure and earlier activation of MVSS.

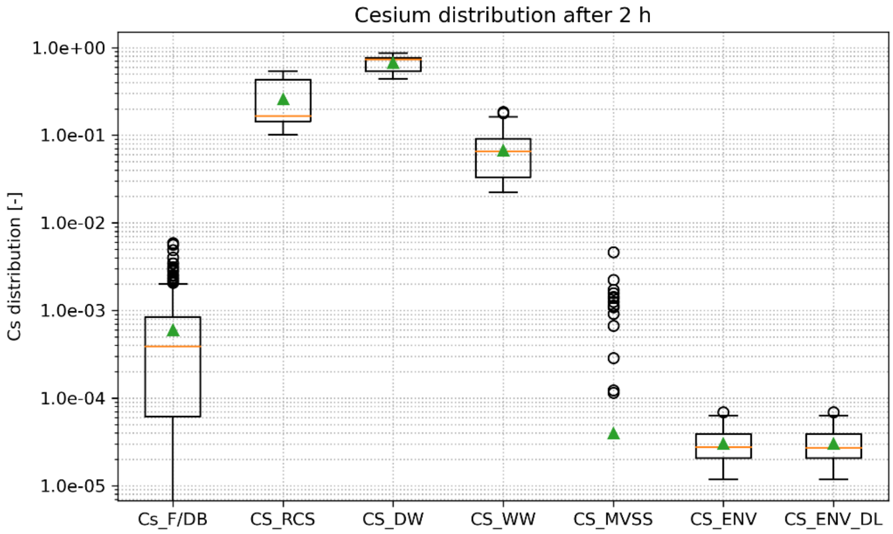

Figure 5-123 Box and whisker plot of the fraction of Cs [-] deposited in the containment and environment after 2h after the initiating event[6]

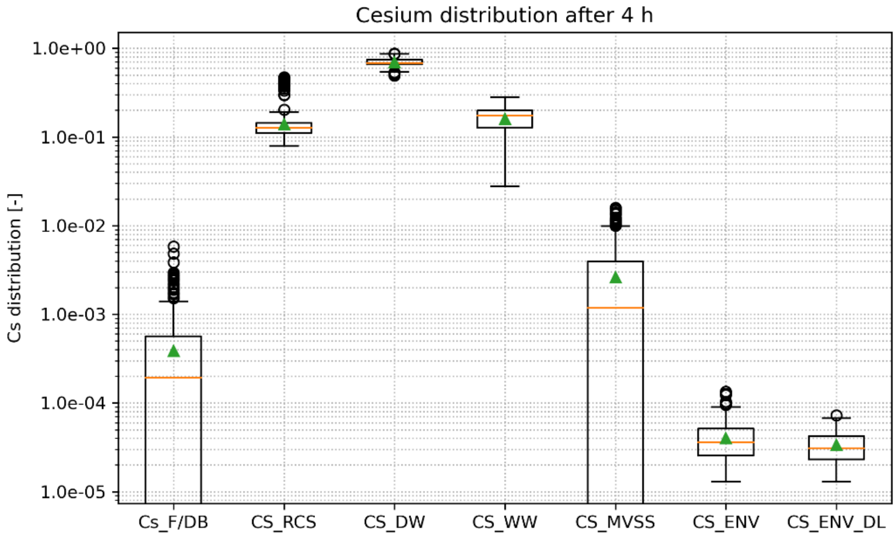

Figure 5-124 Box and whisker plot of the fraction of Cs [-] deposited in the containment and environment after 4h after the initiating event[6]

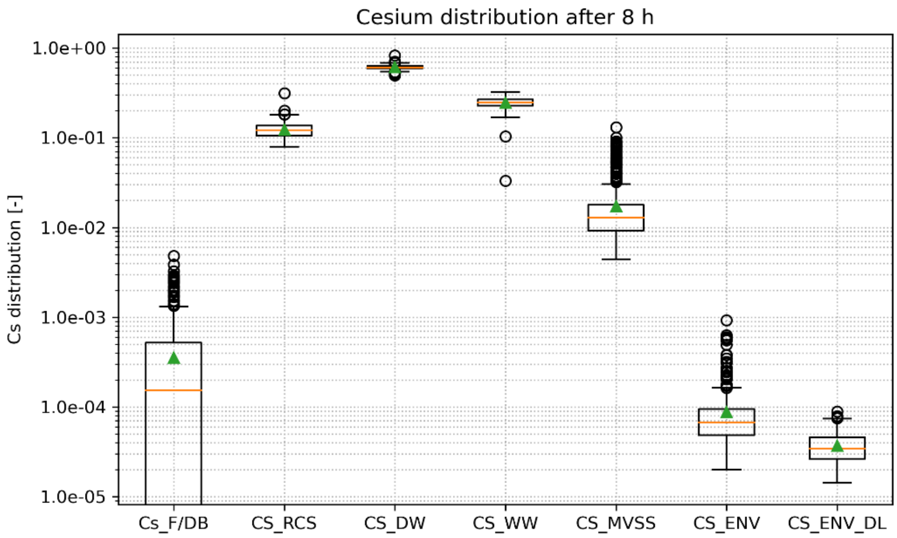

Figure 5-125 Box and whisker plot of the fraction of Cs [-] deposited in the containment and environment after 8h after the initiating event[6]

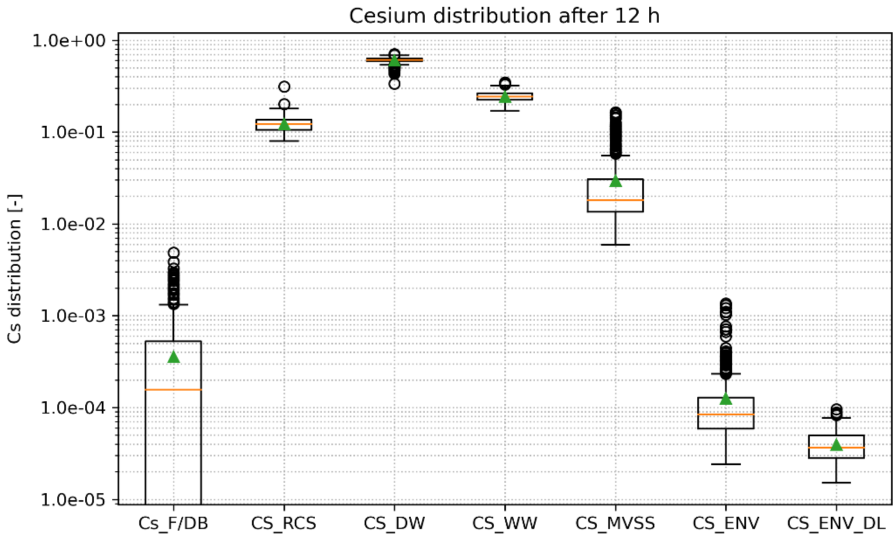

Figure 5-126 Box and whisker plot of the fraction of Cs [-] deposited in the containment and environment after 12h after the initiating event[6]

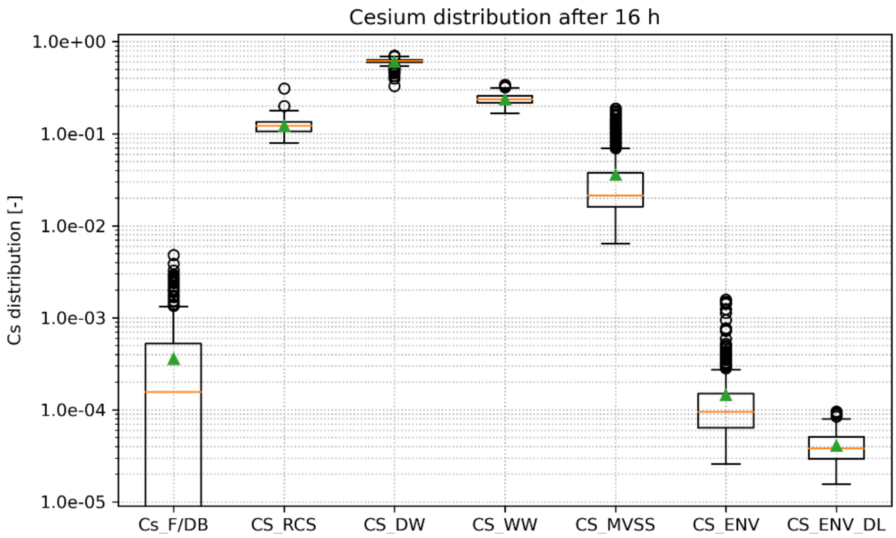

Figure 5-127 Box and whisker plot of the fraction of Cs [-] deposited in the containment and environment after 16h after the initiating event[6]

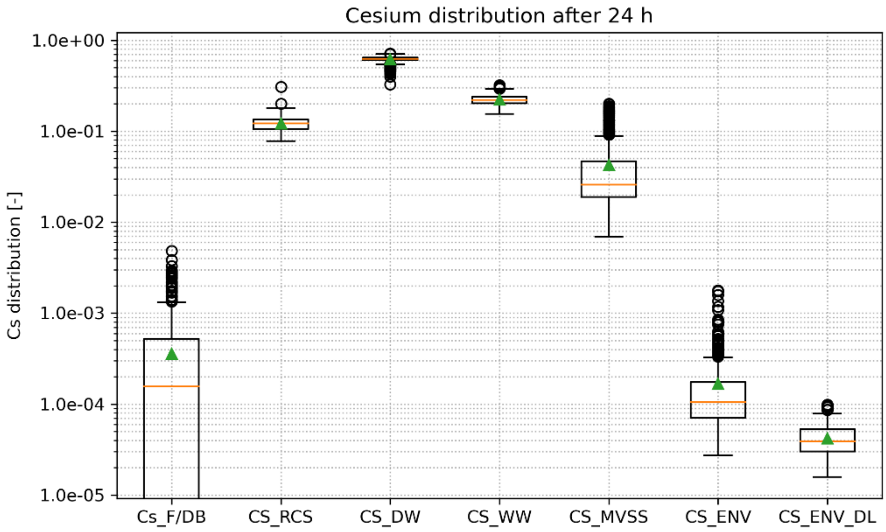

Figure 5-128 Box and whisker plot of the fraction of Cs [-] deposited in the containment and environment after 24h after the initiating event[6]

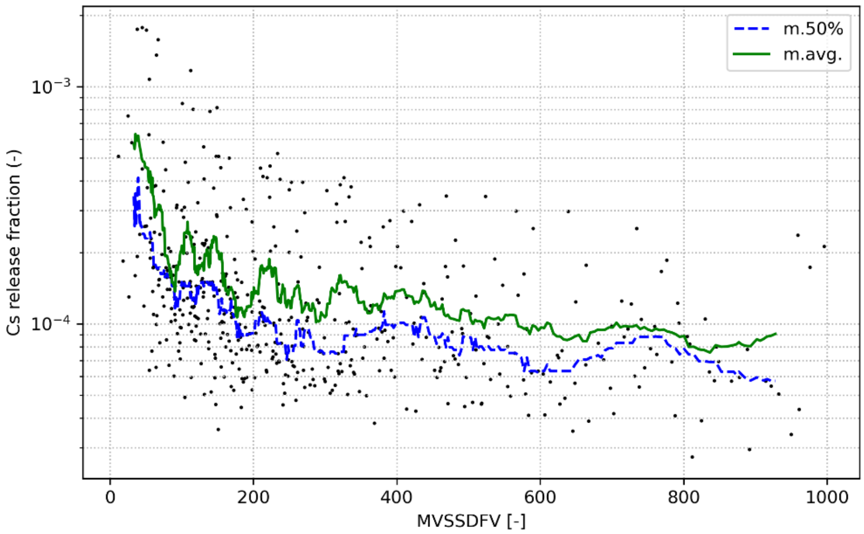

Figure 5-129 Scatter plot and moving average (green)/median(dashed blue) of the fraction of Cs released to the environment as a function of MVSSDFV [-]

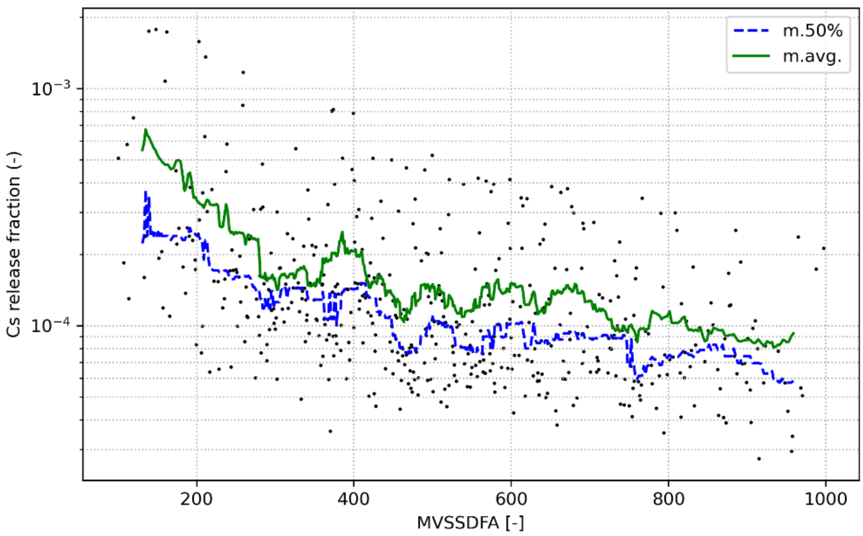

Figure 5-130 Scatter plot and moving average (green)/median(dashed blue) of the fraction of Cs released to the environment as a function of MVSSDFA [-]

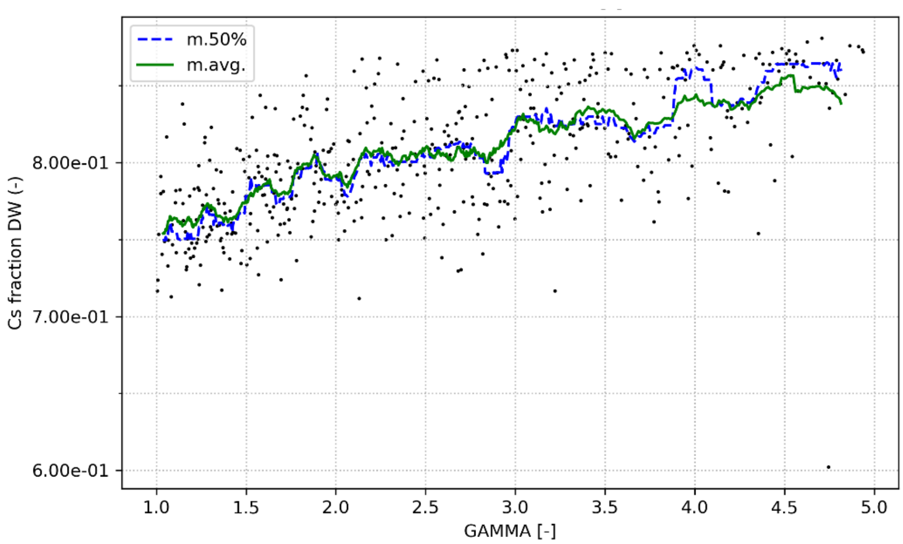

Figure 5-131 Scatter plot and moving average (green)/median(dashed blue) of the fraction of Cs deposited in the drywell as a function of GAMMA [-]

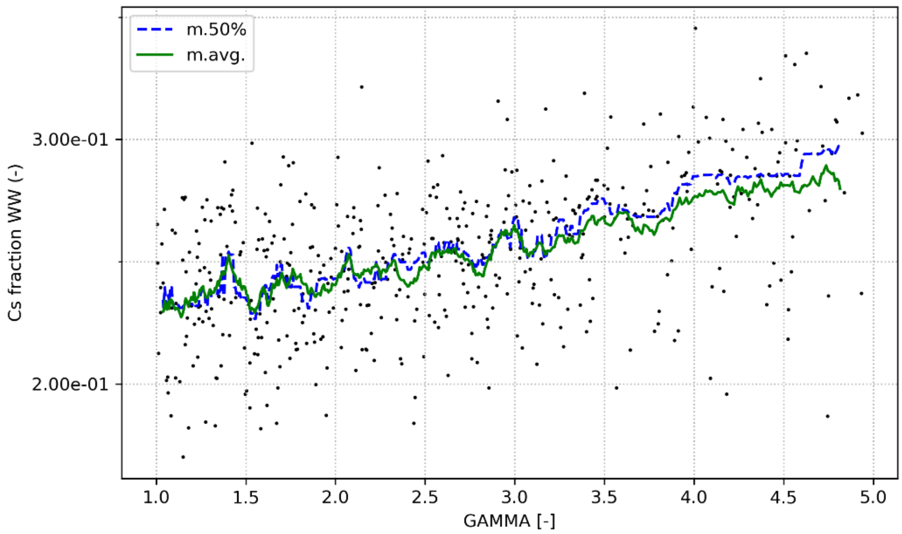

Figure 5-132 Scatter plot and moving average (green)/median(dashed blue) of the fraction of Cs deposited in the wetwell as a function of GAMMA [-]

The results show that the uncertainty in the fraction of Cs released to the environment in case of RC7B-LOCA-MVSS-IDEJ0 is dominated by MVSSDFV and MVSSDFA - MVSS filter decontamination factor for radioactive vapors (V) and aerosols (A) [-] – which is in agreement with the results of sensitivity analysis presented in section 5.2.2.2.2. Note that these parameters were considered as correlated, thus larger values of MVSSDFV typically have larger values of MVSSDFA.

In case of LOCA-MVSS, the major part of Cs released from the fuel/debris is deposited in the drywell, ranging from 75 to 85% in case of RC7B-LOCA-MVSS-IDEJ0, where GAMMA – Aerosol shape factor [-] is the major contributor to the uncertainty. The fraction of Cs deposited in the wetwell is around 30%.

5.5.6. Summary for RC7 release category

Figures 5-133-5-141 show the comparison of the main figures of merit for the uncertainty analysis of the RC7 release category. Appendix A show the uncertainty analysis results for all MELCOR radionuclide groups.

The results show that the pressure in the containment reaches the MVSS rupture disk setpoint (5.5 Bar(abs)) at approximately 4-7h after the initiating event. The mode of debris ejection from the vessel (IDEJ) has one of the major contributions to the uncertainty in the timing of MVSS release, where IDEJ=1 (solid debris ejection – OFF), typically, leads to a slower rate of pressurization of the containment and delayed activation of the MVSS, compared to IDEJ=0 cases. This difference can be explained by the effect of IDEJ switch on the process of debris ejection from the vessel. In case of IDEJ=1 the debris ejection is limited to the molten materials, up until the global failure of the vessel lower head due to creep-rupture. This effectively limits (delays) in-vessel materials relocation from the RPV to the water-filled cavity; and, as a result, limits (delays) steam generation due to FCI/debris coolability.

Table 5-33. RC7 - distribution of MVSS activation time (h)

	SBO-MVSS-IDEJ1 (h)	SBO-MVSS-IDEJ0 (h)	LOCA-MVSS-IDEJ1 (h)	LOCA-MVSS-IDEJ0 (h)
Mean	7.67	5.62	6.61	3.69
5%	6.1	4.9	4.11	2.15
25%	6.72	5.48	5.25	3.05
50%	7.36	5.65	6.69	3.76
75%	8.27	5.85	7.48	4.18
95%	10.05	6.35	9.67	5.24
Min	5	2.64	2.23	1.76
Max	15.22	10.06	15.56	6.78

In case of LOCA, the MVSS activation is distributed (i) between 1.76 and 6.78 h, with mean/median values equal to 3.69/3.76 h in case of IDEJ0; and (ii) between 2.23 and 15.56h with mean/median values equal to 6.61/6.69 h in case of IDE1.

In case of SBO, the MVSS activation is distributed (i) between 2.64 and 10.06 h, with mean/median values equal to 5.62/5.65 h in case of IDEJ0; and (ii) between 5 and 15.22h with mean/median values equal to 7.67/7.36 h in case of IDE1.

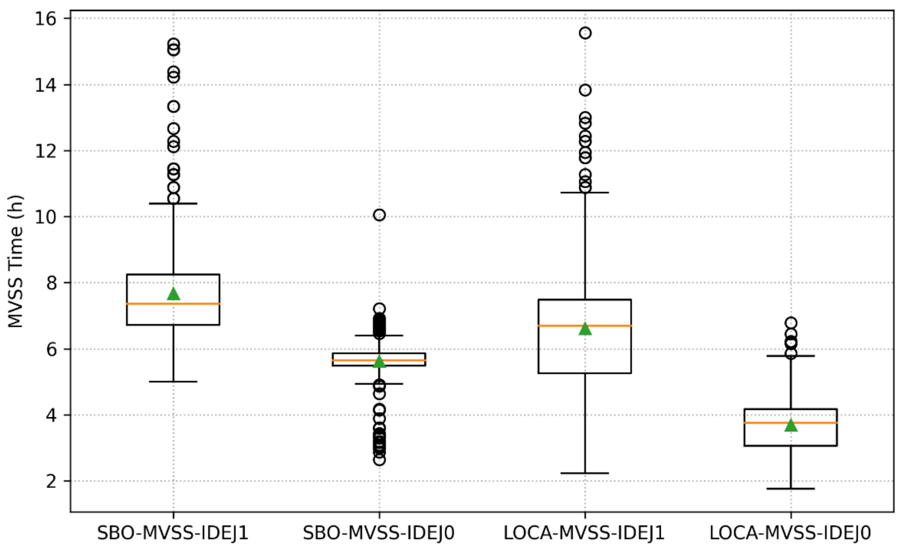

Figure 5-133 Box and whisker plot of the timing of MVSS opening[6]

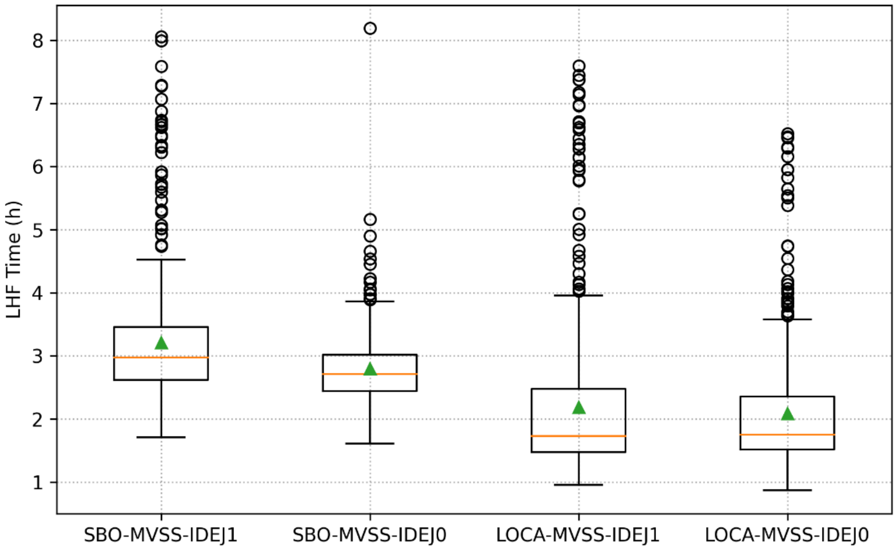

Figure 5-134 Box and whisker plot of the timing of LH failure[6]

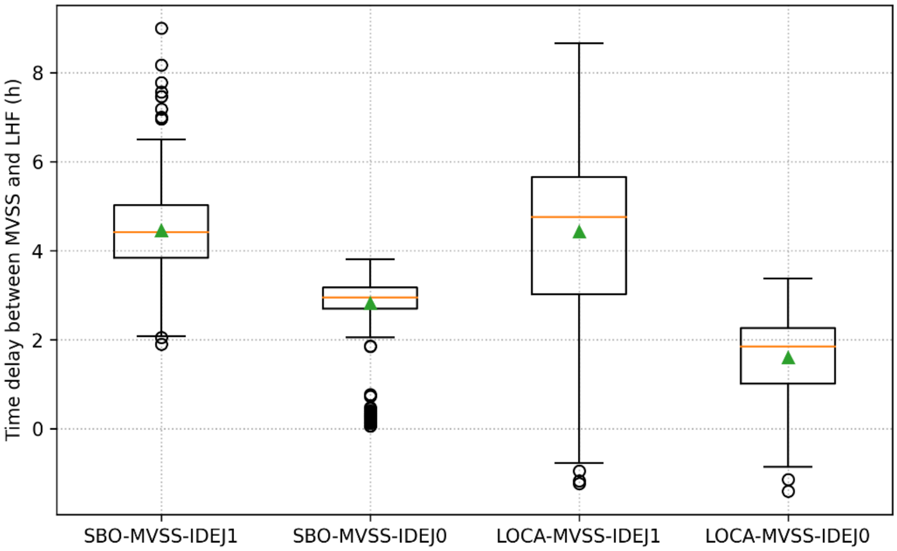

Figure 5-135 Box and whisker plot of the time delay between MVSS and LHF (h)[6]

Furthermore, the results indicate that the MVSS rupture disk opening typically occurs 2-5 hours after failure of the vessel lower head (Figure 5-135), with a very few exceptions in case of LOCA.

Figures 5-136-5-141 show the fraction of Cs released to the environment after 2,4,8,12,16 and 24 hours after the initiating event.

The results indicate that the fraction of Cs released to the environment is significantly larger in case of LOCA compared to SBO scenario. This difference can be explained by the effect of condensation pool scrubbing. Thus, it is expected that the fraction of Cs deposited in the wetwell will be larger in case of SBO compared to LOCA scenarios (see the results presented in sections 5.5.2.2, 5.5.3.2 (SBO) vs. 5.5.4.2, 5.5.5.2 (LOCA)).

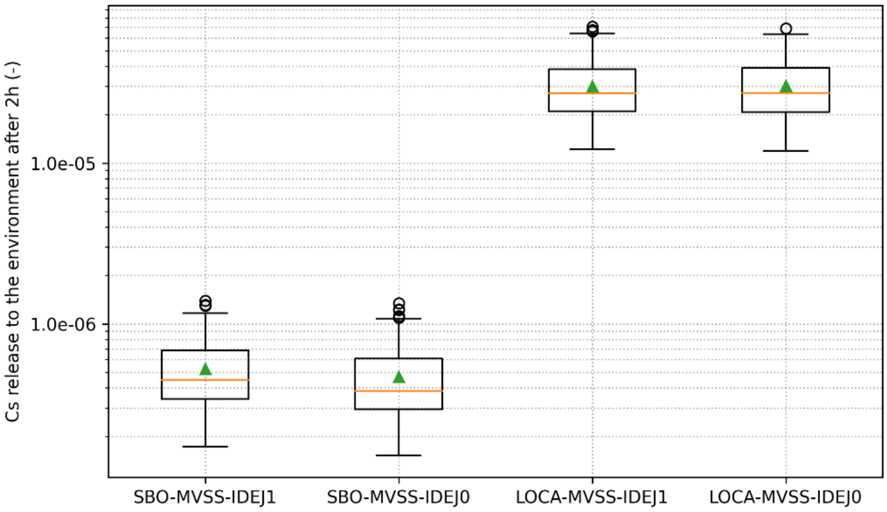

Figure 5-136 Box and whisker plot of the fraction of Cs [-] released to the environment after 2h after the initiating event[6]

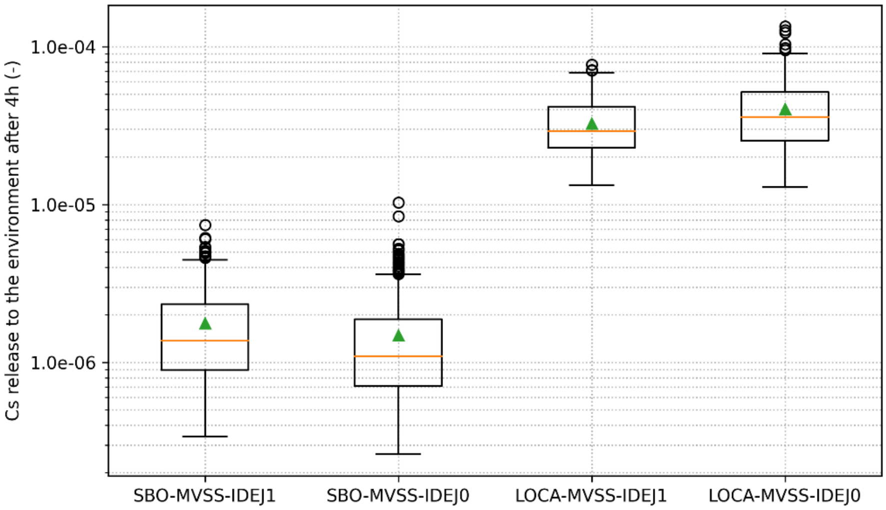

Figure 5-137 Box and whisker plot of the fraction of Cs [-] released to the environment after 4h after the initiating event[6]

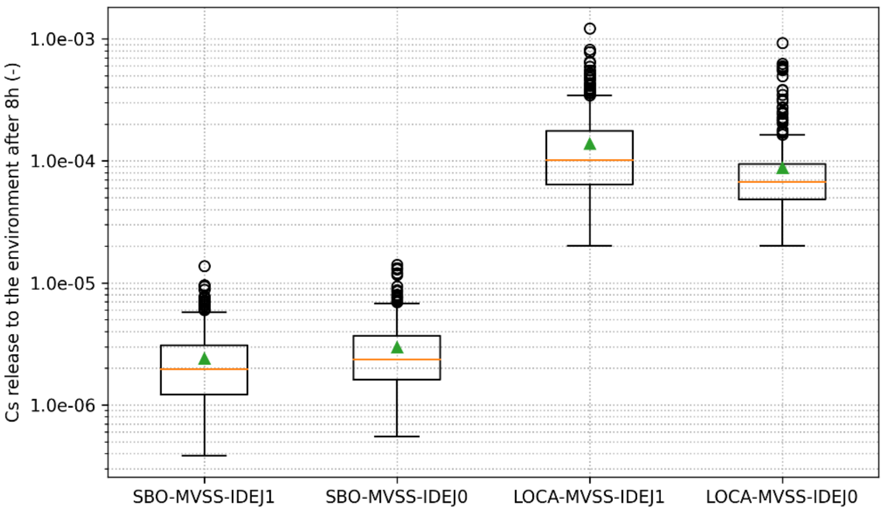

Figure 5-138 Box and whisker plot of the fraction of Cs [-] released to the environment after 8h after the initiating event[6]

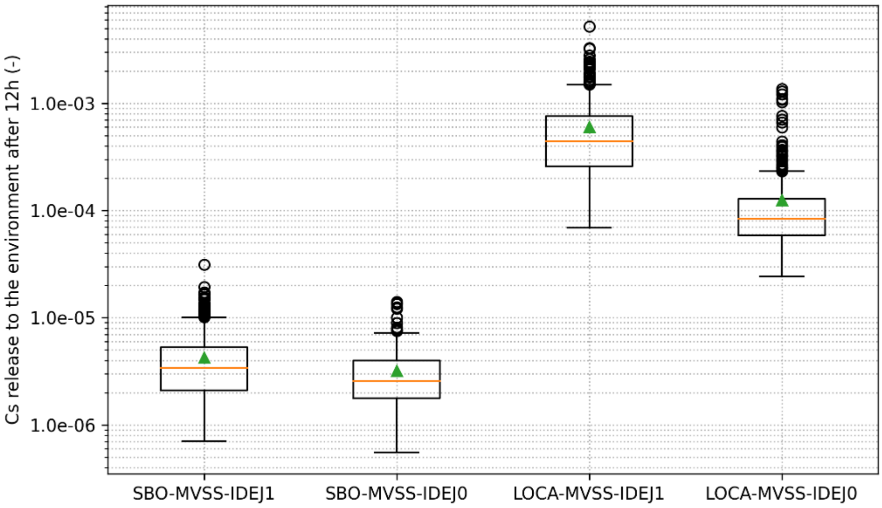

Figure 5-139 Box and whisker plot of the fraction of Cs [-] released to the environment after 12h after the initiating event[6]

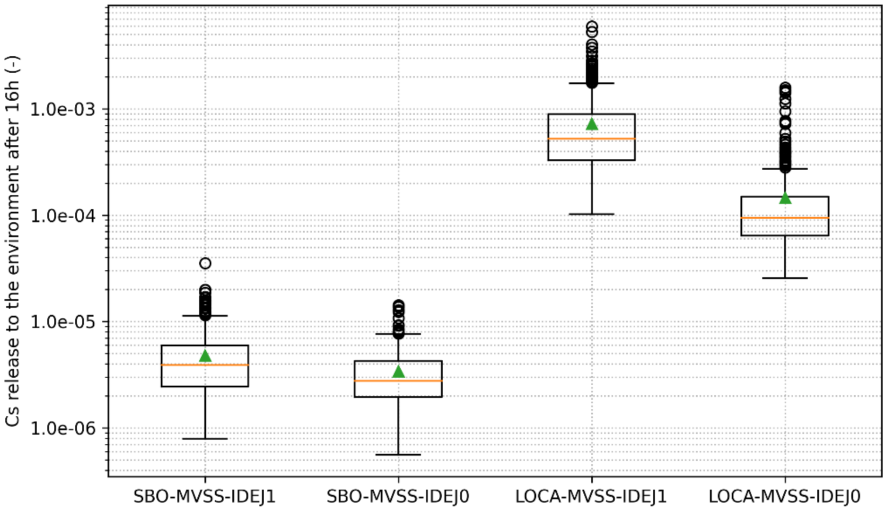

Figure 5-140 Box and whisker plot of the fraction of Cs [-] released to the environment after 16h after the initiating event[6]

In case of SBO, the uncertainty in the fraction of Cs released to the environment is majorly driven by the MVSSDFA (MVSS decontamination factor for radioactive aerosols [-]) and GAMMA (aerosol shape factor [-]), and it is distributed between (9.30E-7, 3.69E-5) with mean/median values equal to 5.44E-6/4.46E-6 in case of IDE1; and (5.73E-7, 1.48E-5) with mean/median values equal to 3.60E-6/2.98E-6 in case of IDEJ0.

In case of LOCA, the uncertainty in the fraction of Cs released to the environment is majorly driven by the mode of debris ejection from the vessel (IDEJ=1 – solid debris ejection – OFF; IDEJ=0 – solid debris ejection – ON), and MVSSDFV (MVSS decontamination factor for radioactive vapors [-]), and it is distributed between (1.33E-4, 1.92E-2) with mean/median values equal to 9.7E-4/6.62E-4 in case of IDE1; and (2.74E-5,1.78E-3) with mean/median values equal to 1.67E-4/1.05E-4 in case of IDEJ0.

The IDEJ is the modelling switch that limits the mode of debris ejection from the vessel (see section 5.7 in [23] for more details) to (i) in case of IDEJ = 1 - only molten materials; (ii) in case of IDEJ = 0 (default) – both molten and solid materials. Effectively it means that in case of IDEJ =1 the UO2/ZrO2 debris will remain in vessel until either complete remelting or vessel lower head failure due to creep-rupture. The exposed debris in the vessel will heat-up the atmosphere inside the vessel and the containment which can lead to revaporization of the aerosols suspended in the vessel/containment atmosphere.

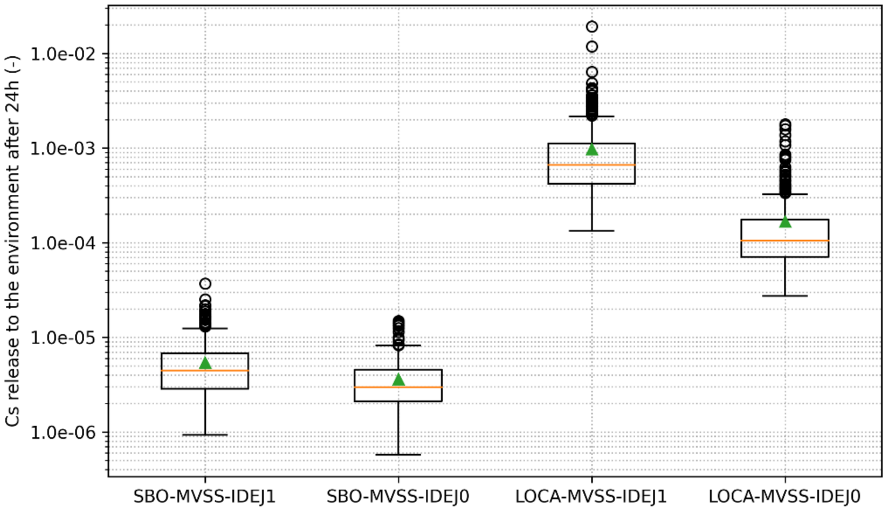

Figure 5-141 Box and whisker plot of the fraction of Cs [-] released to the environment after 24h after the initiating event[6]

5.6. Uncertainty analysis RC7 SBO – Finnish plant configuration

The uncertainty analysis was performed in a very similar way as the sensitivity study. SNAP and Dakota plug-in were used in the analysis and their practical applicability was tested. Both Dakota and Excel were used in post-processing the output data. The two FOMs used in sensitivity analysis, Cs release fraction and FCV opening times, were studied here as well.

The LHS sampling were done in SNAP with Dakota plugin. The target probability and confidence levels were increased to 95%, and two cases with different number of samples (59 and 93) were run. Unfortunately, the maximum number of samples and the number of UA cases was greatly limited by the computational resources. Two input parameter sets were chosen for the uncertainty analysis: a complete set with all the parameters used in the sensitivity study (22) and a smaller set consisting of nine parameters showing notable linear correlation with the FOMs (Table 5-34). Initially DECAYH and VFALL were supposed to be included as well since they seemed to have a significant impact on FCV opening times, but it seems they were accidentally dropped from the sampling process. The first parameter set was run with 59 and 93 samples, and the second one only with 59 samples. Uniform distribution was assumed in all parameters.

Table 5-34. The most significant parameters from the sensitivity study used in uncertainty analysis.

N	Parameter name	Default	Range	Units
1	FCELRA	0.1	[0.1, 0.25]	-
2	CORNSBLD	1520	[1520, 1700]	K
3	SC10201	360	[180, 720]	s
4	SC10202	60	[30, 120]	s
5	HFRZZR	7500	[1000, 7500]	W/m2-K
6	GAMMA	1	[1.0, 3.0]	-
7	SC7111CS1	3.617	[3.0745,4.1595]	Å
8	SC715111	3.45	[2.9325, 3.9675]	-
9	SC71555	1.13893	[0.9681, 1.3098]	-

5.6.1. Results

The issue with random crashes continued in the uncertainty analysis. The number of crashed samples in each case were 9 (ALL_59, 59 samples, all parameters), 7 (SIGN_59, 59 samples, the most correlating parameters) and 8 (ALL_93, 93 samples, all parameters). In the following analysis, the failed datapoints are replaced by the median of the FOM in question. It should be noted, that since the share of the replaced datapoints is quite significant (up to 15 %) especially in the two cases with 59 total samples, this approach will inevitably cause some bias in the results. This imputation will also affect the probability distribution of the input parameters, and the confidence and probability levels. It is very likely that the levels set during the sampling do not hold true anymore.

Table 5-35 presents some key numbers related to the FOMs in each case.

Table 5-35. Key results from the uncertainty analysis.

		Min	Max	Mean	Median	Standard deviation	Skewness	Kurtosis
Cs release fraction (-)	ALL_59	1.80E-06	9.23E-05	2.38E-05	2.09E-05	1.47E-05	2.19	7.76
	SIGN_59	7.96E-06	8.12E-05	2.86E-05	2.43E-05	1.48E-05	1.82	3.75
	All_93	4.81E-09	7.10E-05	2.21E-05	2.07E-05	1.16E-05	1.09	2.88
FCV opening time (s)	ALL_59	5 248	17 526	6 773	6 324	1 965	4.19	18.85
	SIGN_59	5 956	11 008	6 968	6 618	1 206	2.42	4.84
	All_93	4 926	14 263	6 476	6 233	1 147	4.21	24.80

Variations in minimum and maximum values of each FOM are mostly caused by outliers. When comparing those values to mean and median, it can be seen that in these cases, outliers observed in Cs release data seem to be on the small side, whereas in the case of FCV opening time, the outliers seem to be on the larger side. The mean, median and standard deviation values seem to be very close to each other. However, it should be noted that a part of this similarity is due the imputation of the failed data points. The standard deviations are almost the same in the cases consisting of 59 samples. In the case consisting of 93 cases, it is smaller, which means the majority of the outputs are closer to each other than in the other cases.

In all the cases the FOMs seem to have some positive skewness, which means that when plotted, the probability distributions are leaning on the left. The cases also have some positive kurtosis, which means that the shape of the distribution is more peaked. This is also most likely caused by the imputation.

Table 5-36 presents the percentiles of the FOMs in all three cases.

Table 5-36. Percentiles in each case.

Percentiles		5 %	10 %	25 %	50 %	75 %	90 %	95 %
Cs release fraction (-)	ALL_59	4.88E-06	7.94E-06	1.76E-05	2.09E-05	2.60E-05	4.07E-05	4.94E-05
	SIGN_59	1.70E-07	1.11E-05	2.44E-05	3.74E-05	5.32E-05	6.03E-05	6.48E-05
	All_93	1.35E-05	1.59E-05	1.93E-05	2.43E-05	3.23E-05	4.23E-05	6.52E-05
FCV opening time (s)	ALL_59	5595	5729	6022	6324	6670	7257	7989
	SIGN_59	5430	5491	5816	6141	6822	10027	12199
	All_93	6098	6150	6351	6618	6887	7844	10205

Values at each percentile around the middle 50% are very similar, but towards the lower and upper boundaries there seem to be some variation in the results between the cases. Especially in the case of SIGN_59, it can be seen that the distribution of the values is somewhat larger than in the other two cases.

Histograms in Figure 5-142 and Figure 5-143 present the distribution of the Cs release fraction and FCV opening times in case ALL_59. In all following histograms the number of bins is limited to 30.

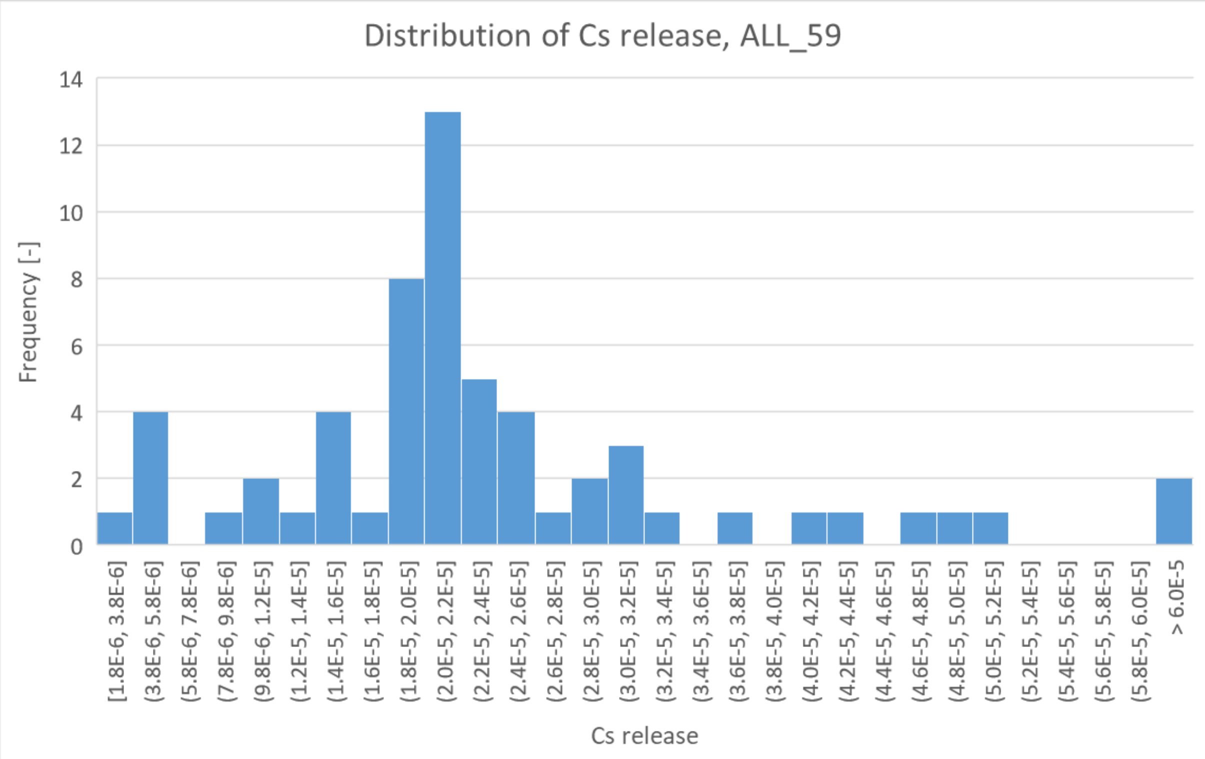

Figure 5-142 Distribution of Cs release in ALL_59.

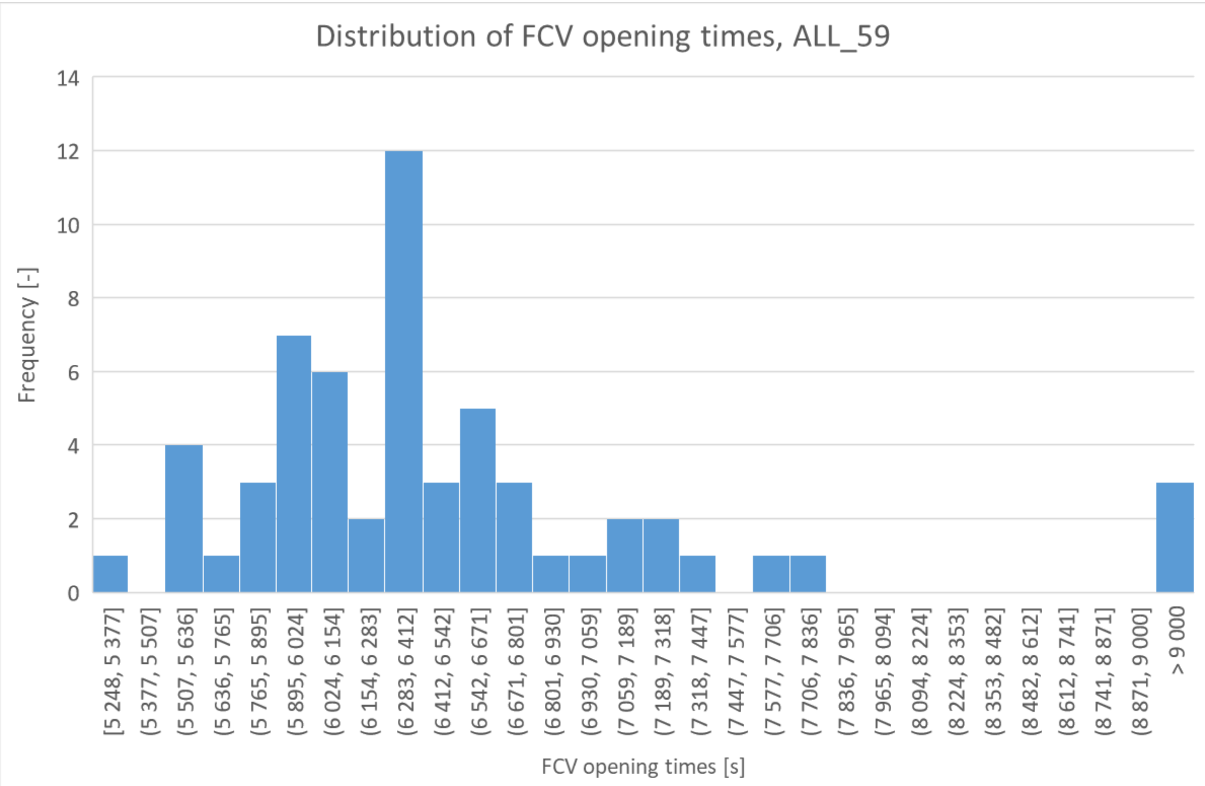

Figure 5-143 Distribution of FCV opening times in ALL_59.

Figure 5-144 and Figure 5-145 present the distribution of the Cs release fraction and FCV opening times in case SIGN_59.

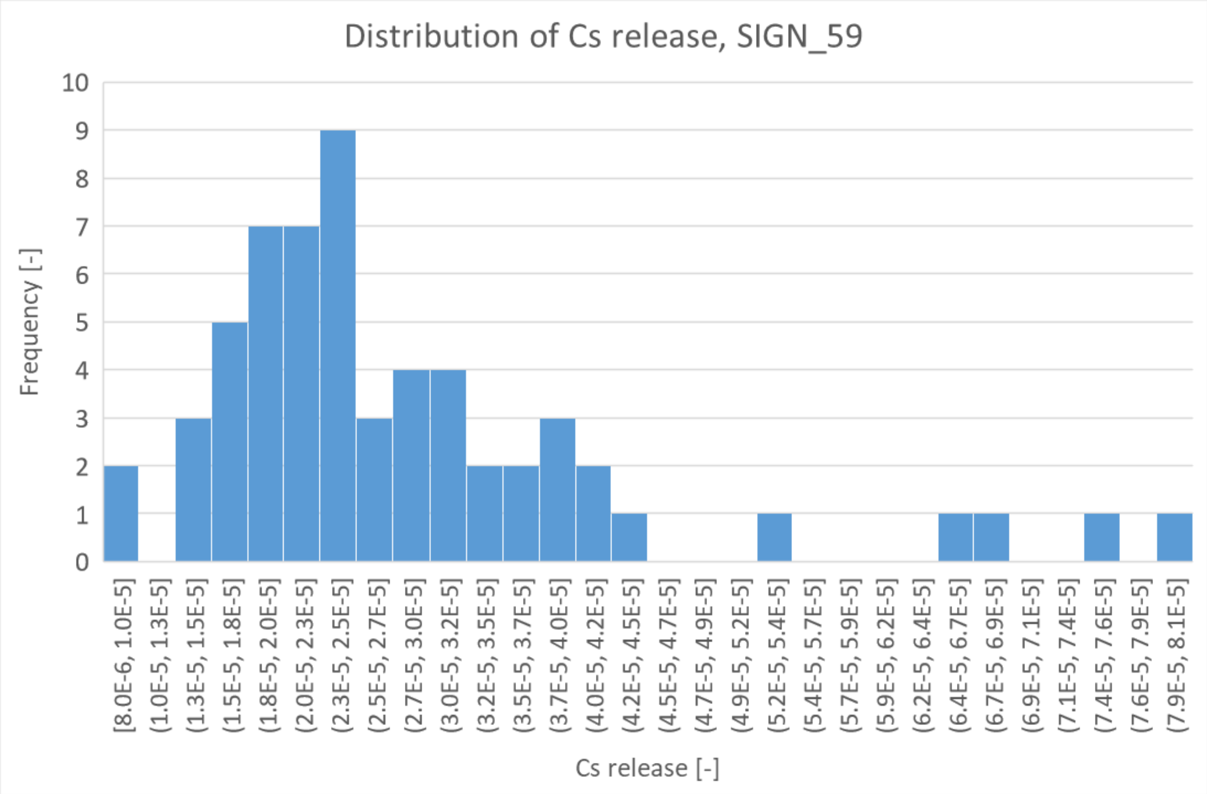

Figure 5-144 Distribution of Cs release in SIGN_59.

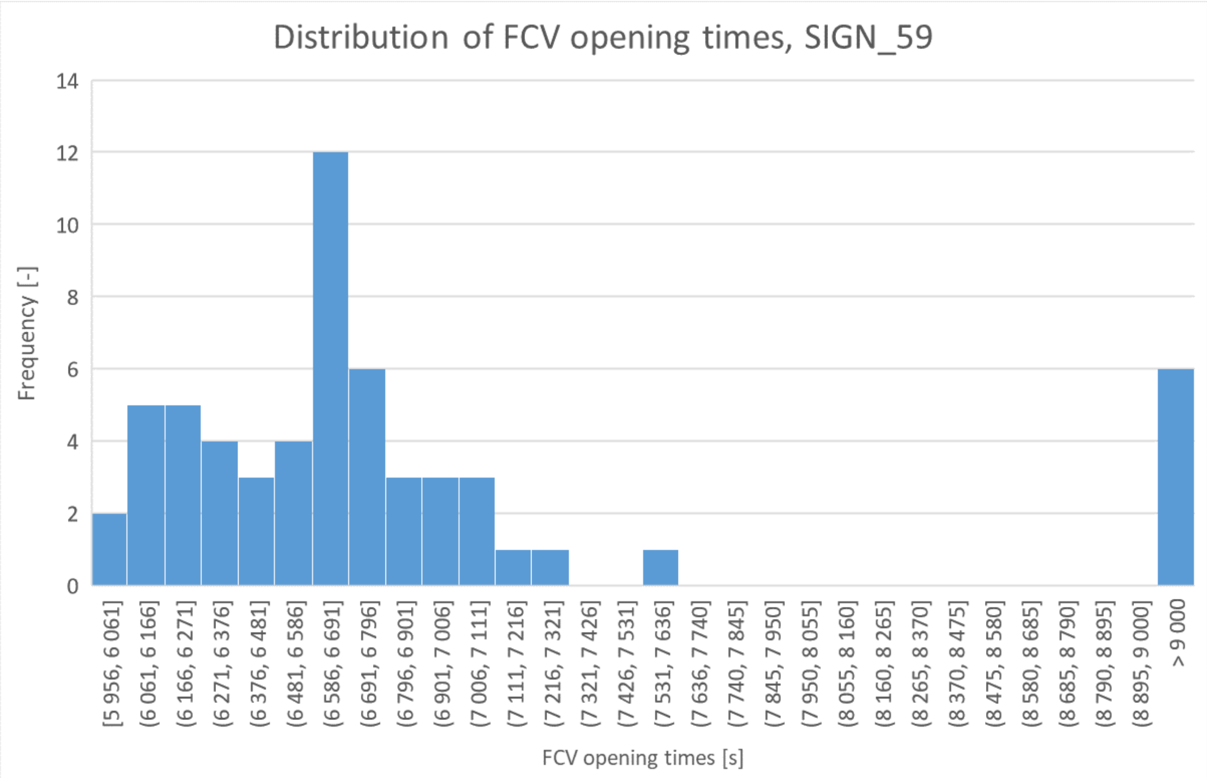

Figure 5-145 Histogram plot for FCV opening times in SIGN_59.

Figure 5-146 and Figure 5-147 present the distribution of the Cs release fraction and FCV opening times in case ALL_93.

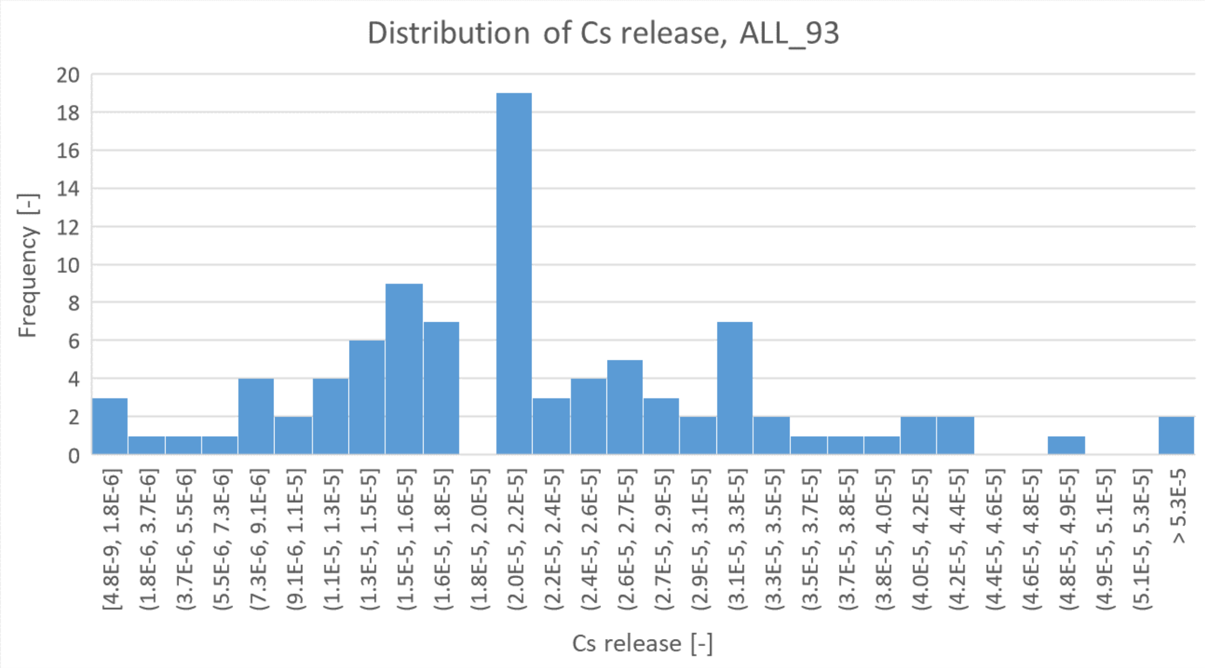

Figure 5-146 Distribution of Cs release in ALL_93.

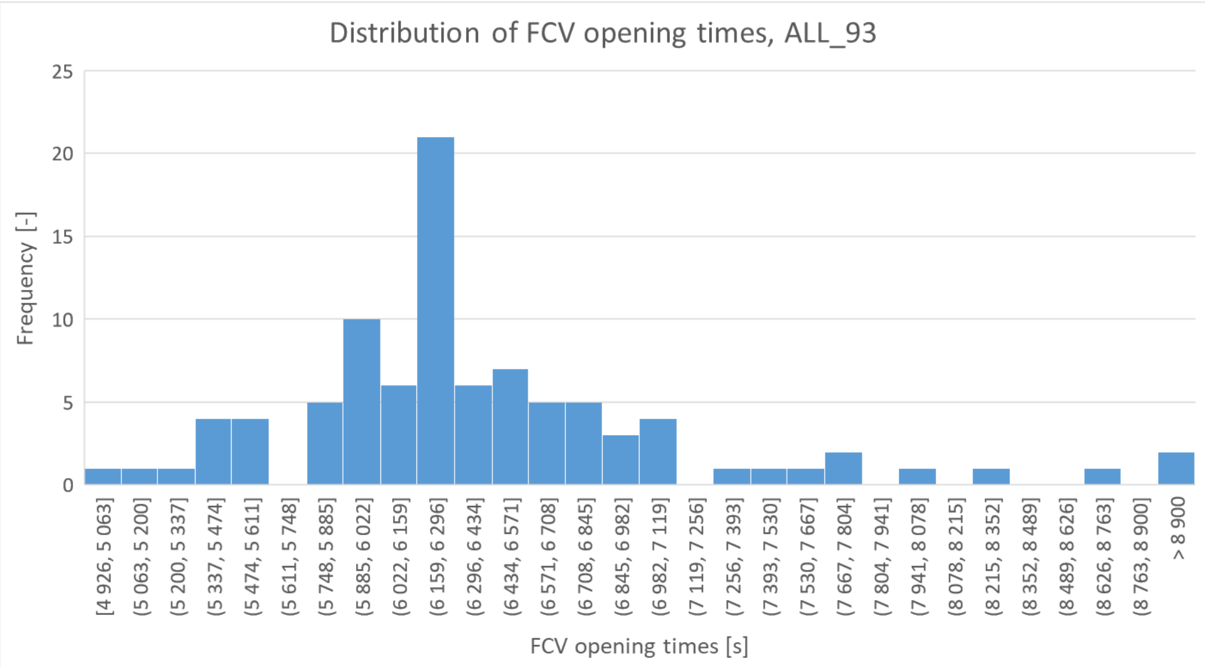

Figure 5-147 Histogram plot for FCV opening times in ALL_93.

Despite the uniform probability distribution of the input parameters, the distributions of the FOMs seem to show some resemblance to normal distribution. However, due to high skewness and kurtosis, distributions can’t really be considered normal but rather asymmetric. Having more samples doesn’t seem to influence histogram shapes, at least on low sample sizes. Based on a single case, limiting the number of input parameters seems to be affecting the distribution by making it more uniform. It may be, that some of the excluded parameters have a larger, probably non-linear effect on the distribution than initially thought, thus the more uniform distribution in SIGN_59. Confirming this would probably need more extensive sensitivity analyses.

The effect of imputation can be seen in the histograms shown above: increasing the data points around the median value causes the bar around the median value to increase which adds to the kurtosis of the distribution. The results would imply that replacing failed cases with median might not be the best approach since it seems to have a significant effect on the probability distribution. The best method would be to ensure the simulations run successfully to the end, but that is not always possible. If the number of the failed cases is relatively low, they could be rerun by hand. However, this would probably need adjustments in the time steps or the parameters, which might affect sampling and cause some bias in the uncertainty results. The failed cases could also be excluded altogether, but that might affect the pre-defined probability and confidence levels, and cause gaps in the samples.

6. Discussion and conclusions

Continuing with the preliminary screening and best estimate plus bounding analysis performed during the last phase of the project, KTH performed sensitivity analysis and uncertainty quantification for source term releases during RC4A (LOCA) and RC4B (SBO). 19 parameters were identified that were significant to LOCA, and 15 parameters to SBO. Sensitivity analysis using Morris method identified the most important parameters, these results can be seen in conjunction with Pearson and Spearman rank correlation coefficients, and with ANOVA F-statistic. The releases obtained for CS and I2 releases are conservative, with a large number of trials resulting in more than the acceptance criterion for acceptable release. Following the sensitivity studies, the results have been analyzed by parametric and non-parametric methods to determine 95/95 bounds. As the analysis with MELCOR simulations is computationally expensive, bootstrap approach to calculate the bounds of 95/95 estimate is employed in the present study. The non-parametric Wilks' method presents a very conservative approach for the first 3 statistical orders. With increasing the order of the statistics, the Wilks' method seems to converge to the empirical 95th percentile. The parametric goodness-of-fit test approach with normal fit to the distribution presents least conservative estimates. The analysis with Weibull and EV distributions shows that the 95/95 estimate bounds are dependent on the distribution selected for study. These distributions show a larger estimate bound than normal fit calculated using the equations.

Sensitivity analysis results for the RC7 release category (acceptable release through the MVSS filter in case of LOCA - RC7A, and a transient (SBO) - RC7B (SBO)) has been performed using the Morris method for sensitivity analysis, considering the mode of debris ejection from the vessel (IDEJ) as a phenomenological splinter[2], thus resulting in two separate sets of calculations for every accident scenario considered in the study. The analysis showed that the uncertainties in the source estimates are majorly driven by the mode of debris ejection from the vessel in the RC7B(LOCA) scenario. Furthermore, the results show that MVSSDFV – MVSS decontamination factor for radioactive vapors has significant effect on the magnitude of Cs and I release, which can be explained by (i) early opening of the MVSS in case of LOCA; (ii) in case of LOCA the fission products are released directly to the containment, bypassing scrubbing (and condensation for radioactive vapors) inside the condensation pool.

On the other hand, for the RC7A (SBO) scenario, the influence of the modelling of debris ejection from the vessel (IDEJ switch) is relatively small compared to other MELCOR modelling parameters. Based on the results the most influential parameters on the fractions of Cs and I released to the environment are MVSSDFA – aerosol decontamination factor of MVSS (increase deposition of radioactive aerosols in the scrubber), and GAMMA - Aerosol agglomeration shape factor (promotes agglomeration and deposition of aerosols).

For the timing of the MVSS release (time when the pressure in the containment exceed the MVSS rupture disk pressure setpoint of 5.5 Bar (abs)), the results for the RC7 release category show that there is no single MELCOR modeling parameter that dominates the uncertainty in the results, except the mode of debris ejection from the vessel (IDEJ), where IDEJ=1 (solid debris ejection OFF) typically leads to a more delayed release of the in-vessel debris to the water-filled cavity under the reactor pressure vessel, and, thus, slower pressurization rate of the containment and delayed activation of the MVSS.

The uncertainty analysis results for RC7 show that the pressure in the containment reaches the MVSS rupture disk setpoint (5.5 Bar(abs)) on average at approximately 4-7h after the initiating event. The mode of debris ejection from the vessel (IDEJ) has one of the major contributions to the uncertainty in the timing of MVSS release.

The results indicate that the fraction of Cs released to the environment is significantly larger in case of RC7B (LOCA) compared to RC7A (SBO) scenario. This difference can be explained by the effect of condensation pool scrubbing, since in case of a transient, up until the vessel lower head failure, the fission products released from the fuel will be transported and scrubbed in the wetwell, before entering the drywell and being released to the environment. In case of RC7A (SBO) the release fraction of Cs released to the environment is well below the MVSS acceptance criterion for acceptable release[7], and the average value is equal to 5.44E-6/3.60E-6 for IDEJ1/0. In case of RC7B (LOCA) the fraction of Cs released to the environment exceed the MVSS acceptance criterion[7] for some parameter combinations, the average value is equal to 9.7E-4/1.67E-4 for IDEJ1/0. The uncertainty for the RC7B (LOCA) scenario is dominated by the mode of debris ejection from the vessel (IDEJ) and MVSS decontamination factor for radioactive vapors.

VTT studied release category RC7 – filtered containment venting with a SBO transient using SNAP and Dakota plug-in. The results from the first phase of project were used to determine possibly influential parameters for sensitivity an uncertainty analysis. A total of 22 parameters were chosen for further study. Partially due to the limited features on Dakota plug-in, the sensitivity studies were done with a robust OAT method – each parameter was varied one at time 22 times. Their individual and linear correlations to the FOMs, Cs release fraction and FCV opening time, were assessed. Influences between the input parameters were not studied, which, combined with the bad data points from crashed calculations might have caused some bias in the results. In the light of the analysis, parameters CORNSBLD, FCELRA, GAMMA, HFRZZR, SC10201, SC10202, SC7111CS1, SC71551 and SC71555 were chosen to be studied in the uncertainty analysis.

Uncertainty analysis was done similarly in SNAP with Dakota plug-in. Post-processing was done in both Dakota and Excel. Three cases were ran: 59 samples and all 22 parameters, 59 samples and the nine most influential parameters, and 93 samples with all 22 parameters. The results from all three cases were quite consistent, although some rather large differences were observed near the upper and lower boundaries. Increasing sample size seemed to decrease the standard deviation and the range of the output values. Despite the uniform distribution in input parameters, the model outputs seemed to cluster close to each other, i.e., the probability distribution functions resembled normal distribution, although the PDFs had significant skewness and kurtosis. In the case of limited number of parameters, the distribution moved slightly towards uniform distribution visually. It is very possible, that some of the excluded parameters had larger influence than initially thought and excluding them also canceled their effect on the output.

Multiple crashes were encountered during the calculations in both sensitivity and uncertainty analysis, and in the uncertainty analysis the failed data points were decided to be replaced with median values. This likely was not the best method since it added kurtosis in probability distribution functions. Special care should thus be put into choosing the proper method to deal with crashes.

7. Outlook

Having addressed the sensitivity and uncertainty in the source term arisiing from the phenomena, the effect of MELCOR code predictions of melt and debris ejection from the vessel in case of unmitigated SBO or LOCA, obtained during the second phase of the project, on ex-vessel steam explosion loads on the containemnt using stand alone codes and models developed by KTH may be performed in the coming studies. Based on the information obtained during the review of available information regarding the structures in the Nordic BWR reactor building and definition of possible release pathways from the containment to the environment, the MELCOR model of Nordic BWR will be updated to account for possible break sizes in the containment and the effect of the volumes and structures outside the contaiment. The source term calculations will be performed using updated MELCOR model of Nordic BWR.

Sensitivity and uncertainty calculations for the RC7 release category (filtered release via MVSS in case of a transient or LOCA) showed that the fraction of Cs released to the environment is well below the acceptance criterion for acceptable release[7] in case of RC7A – SBO (transient) but it exceeds this criterion for some MELCOR code parameters combinations in case of RC7B-LOCA. In case of RC7B-LOCA the most influential parameters are the mode of debris ejection from the vessel (IDEJ) and the MVSS decontamination factor for radioactive vapor.

Current MELCOR model of Nordic BWR lacks the necessary level of details regarding the MVSS and employs this system as a simple filter with constant decontamination factors for radioactive aerosols and vapors. Thus, it is proposed to address different aspects of the modelling of MVSS, such as injection paths and associated heat structures, scrubbing in the pool, etc., in the next phase of the project. Another important aspect is the effect of the independent spray system, which is an important part of the SAMG for the Nordic BWR. The effect of containment sprays will be address in the next phase of the project.

During the project it was observed that SNAP and Dakota plug-in might be lacking at some aspects when it comes to sensitivity and uncertainty studies. The tools for sensitivity analysis were a bit too few in SNAP, and while there were initially no problems with the initial Dakota report generation, there didn't seem to be a simple way to regenerate a report after fixing and rerunning the crashed cases without rerunning the whole job stream. The crashes themselves and the methods to deal with them caused issues, too. In the future uncertainty studies, the whole process of post-processing should be improved, and some better consideration on model crashes should be done.

Acknowledgements

NKS conveys its gratitude to all organizations and persons who by means of financial support or contributions in kind have made the work presented in this report possible.

The work performed by VG was performed with additional support from the Swedish Radiation Protection Authority (SSM).

Disclaimer

The views expressed in this document remain the responsibility of the author(s) and do not necessarily reflect those of NKS. In particular, neither NKS nor any other organization or body supporting NKS activities can be held responsible for the material presented in this report.

References

[1] Preparedness and Response for a Nuclear or Radiological Emergency, INTERNATIONAL ATOMIC ENERGY AGENCY, 2015

[2] Actions to Protect the Public in an Emergency due to Severe Conditions at a Light Water Reactor, INTERNATIONAL ATOMIC ENERGY AGENCY, 2013

[3] Störningshandboken – BWR, SKI Rapport 03:02, 2003

[4] Nilsson L., Development of an Input Model to MELCOR 1.8.5 for Oskarshamn 3 BWR, SKI Report 2007:05, May 2006.

[5] Strandberg, M., Hydrogen Fire Risk in BWR Simulations with MELCOR. Research Report VTT-R-00669-17, 2017.

[6] L.L. Humphries, B.A. Beeny, F. Gelbard, T. Haskin, D.L. Louie, J. Phillips, R.C. Schmidt, MELCOR Computer Code Manuals Vol. 2: Reference Manual Version 2.2.18019, SAND2021-0241 O, 2021.

[7] L.L. Humphries, B.A. Beeny, F. Gelbard, D.L. Louie, J. Phillips, MELCOR Computer Code Manuals Vol. 1: Primer and Users' Guide Version 2.2.19018, SAND2021-0252 O, 2021.

[8] A. Saltelli, S. Tarantola, F. Campolongo and M. Ratto, "Sensitivity Analysis in Practice. A Guide to assessing scientific models". John Wiley & Sons Ltd, The Atrium, Southern Gate, Chichester, West Sussex PO19 8SQ, England. 2004.

[9] F. Campolongo, J. Cariboni, A. Saltelli, An effective screening design for sensitivity analysis of large models, Environmental Modelling & Software, Volume 22, Issue 10, 2007, Pages 1509-1518, ISSN 1364-8152. 2007.

[10] Adams, B.M., et al., Dakota, A Multilevel Parallel Object-Oriented Framework for Design Optimization, Parameter Estimation, Uncertainty Quantification, and Sensitivity Analysis: Version 6.0 Reference Manual. 2014, Sandia National Laboratories. (2014).

[11] Troy C. Haskin, The MELCOR Plot File Format, SAND2018-9566, 2018.

[12] Bertrand Ioos, Paul Lemaitre, A review on global sensitivity analysis methods.

[13] S. Galushin, D. Grishchenko, P. Kudinov, "Implementation of Framework for Assessment of Severe Accident Management Effectiveness in Nordic BWR", Reliability Engineering & System Safety, Vol 203, Article 107049, https://doi.org/10.1016/j.ress.2020.107049, November 2020

[14] Jon C. Helton , Jay D. Johnson , William L. Oberkampf & Cédric J. Sallaberry Representation of analysis results involving aleatory and epistemic uncertainty, International Journal of General Systems, 39:6, 605-646, (2010)

[15] Grishchenko D., Basso S., Kudinov P., "Development of a surrogate model for analysis of ex-vessel steam explosion in Nordic type BWRs," Nuclear Engineering and Design, Volume 310, Pages 311-327, 2016

[16] Dmitry Grishchenko, Sergey Galushin, Pavel Kudinov, "Failure Domain Analysis and Uncertainty Quantification using Surrogate Models for Steam Explosion in a Nordic type BWR", Nuclear Engineering and Design, Volume 343, Pages 63-75, 2019.

[17] Galushin and P. Kudinov "Uncertainty Analysis of Vessel Failure Mode and Melt Release in Station Blackout Scenario in Nordic BWR Using MELCOR Code." 18th International Topical Meeting on Nuclear Reactor Thermal Hydraulics (NURETH-18), no. Portland, OR, USA, August 18-22, (2019).

[18] S. Galushin S., Kudinov P., "Sensitivity Analysis of the Vessel Lower Head Failure in Nordic BWR using MELCOR Code", Probabilistic Safety Assessment and Management PSAM 14, September 2018, Los Angeles, CA. (2018).

[19] N. W. Porter, Wilks' Formula Applied to Computational Tools: A Practical Discussion and Verification, SAND2019-1901J

[20] T. G. Theofanous, "On Proper Formulation of Safety Goals and Assessment of Safety Margins for Rare and High-Consequence Hazards," Reliability Engineering and System Safety, 54, pp.243-257, (1996).

[21] SARNET Technical Report, In-Vessel Core Degradation in Water-Cooled Reactor Severe Accidents, State-of-the-Art Report Update, (CoreSOAR), 1996-2018, SARNET Report No. SARNET-CoreSOAR-D3, 2018.

[22] Galushin, S., and P. Kudinov. "Sensitivity and Uncertainty Analysis of the Vessel Lower Head Failure Mode and Melt Release Conditions in Nordic BWR Using MELCOR Code." Annals of Nuclear Energy, Volume 135, 2020, ISSN 0306-4549.

[23] Sergey Galushin, Anders Riber Marklund, Dmitry Grishchenko, Pavel Kudinov, Tuomo Sevón, Sara Ojalehto, Ilona Lindholm, Patrick Isaksson, Elisabeth Tengborn, Naeem Ul-Syed, Source Term And Timing Uncertainty in Severe Accidents (NKS-STATUS), NKS-461, 978-87-7893-554-0, 01 Jul 2022.

[24] S. Galushin, P Kudinov "Uncertainty Analysis of Vessel Failure Mode and Melt Release in Station Blackout Scenario in Nordic BWR Using MELCOR Code." 18th International Topical Meeting on Nuclear Reactor Thermal Hydraulics (NURETH-18), Portland, OR, USA, August 18-22, (2019).

[25] Sergey Galushin, Pavel Kudinov, Sensitivity and uncertainty analysis of the vessel lower head failure mode and melt release conditions in Nordic BWR using MELCOR code, Annals of Nuclear Energy, Volume 135, 2020, 106976, ISSN 0306-4549, https://doi.org/10.1016/j.anucene.2019.106976.

[26] Rafael Bocanegra, Luis E. Herranz, CIEMAT's outcomes from the PHEBUS-FPT1 uncertainty analysis in the framework of the EU-MUSA project, The 10th European Review Meeting on Severe Accident Research (ERMSAR2022), Karlsruhe, Germany, May 16-19, 2022

[27] Darnowski, P.; Mazgaj, P.; Włostowski, M. Uncertainty and Sensitivity Analysis of the In-Vessel Hydrogen Generation for Gen-III PWR and Phebus FPT-1 with MELCOR 2.2. Energies 2021, 14, 4884

[28] Rafael Bocanegra, Luis Enrique Herranz, The importance of characterizing input uncertainties in severe accident analyses. The effect on pool scrubbing modeling in a Fukushima Unit 1 sequence, Sociedad Nuclear Española, Reunion Virtual, 2020.

[29] Fukushima Daiichi Unit 1 Accident Progression Uncertainty Analysis and Implications for Decommissioning of Fukushima Reactors – Volume I, SAND2016-0232,Sandia National Laboratories

[30] Lucas I. Albright, Nathan Andrews, Larry L. Humphries, David L. Luxat, Tatjana Jevremovic, Material Interactions in Severe Accidents – Benchmarking the MELCOR V2.2 Eutectics Model for a BWR-3 Mark-I Station, Nuclear Engineering and Design Volume 383, November 2021, 111398 Blackout: Part II – Uncertainty Analysis.

[31] F. Mascari, M. Massone, G. Agnello, M. Angelucci, S. Paci, M. D'Onorio, F. Giannetti, Comparison of PHEBUS FPT1 uncertainty applications using MELCOR 2.2 with three different methodologies The 13th Meeting of the "European MELCOR and MACCS User Group" 27th –29th April 2022

[32] T.K.S. Liang, L,Y, Chou, Z. Zhang, H.Y. Hsueh, and M. Lee. "Development and application of a deterministic-realistic hybrid methodology for LOCA licensing analysis," Nuclear Engineering and Design, 241 (5), pp. 1857-1863, (2011).

[33] I.M. Chakravarti, R.G. Laha, and J. Roy. "Handbook of Methods of Applied Statistics, Volume I," John Wiley and Sons, pp. 392-394, (1967).

[34] T.W. Anderson, and D.A. Darling. "Asymptotic theory of certain "goodness-of-fit" criteria based on stochastic processes," Annals of Mathematical Statistics, 23 (2), pp. 193-212, (1952).

[35] A. Buse. "The Likelihood Ratio, Wald, and Lagrange Multiplier Tests: An Expository Note," The American Statistician, 36 (3-1), pp. 153-157, (1982).

[36] B. Efron, and R.J. Tibshirani. An Introduction to the Bootstrap. Chapman and Hall/CRC, (1994).

[37] Applied Programming Technology, Inc., "Symbolic Nuclear Analysis Package (SNAP): User's Manual, Version 3.1.9," Bloomsburg, 2021.

[38] B. M. Adams, W. J. Bohnhoff, K. R. Dalbey and Et.al., "Dakota, A Multilevel Parallel Object-Oriented Framework for Design Optimization, Parameter Estimation, Uncertainty Quantification, and Sensitivity Analysis: Version 6.16 User's Manual," Sandia National Laboratories, Albuquerque,, 2022

[39] A. Saltelli and P. Annoni, "How to avoid a perfunctory sensitivity analysis," *Environmental Modelling & Software,* vol. 25, no. 12, pp. 1508-1517, 2010. DOI: https://doi.org/10.1016/j.envsoft.2010.04.012.

Appendix A. Uncertainty analysis results - RC7

Table A-1. Release fractions RC7A SBO-MVSS-IDEJ1

RN group	Mean Percentiles Range	Release fraction after 2h	Release fraction after 4h	Release fraction after 8h	Release fraction after 12h	Release fraction after 16h	Release fraction after 24h
CS_ENV	mean	5.23E-07	1.77E-06	2.40E-06	4.25E-06	4.80E-06	5.44E-06
	5%	2.35E-07	5.48E-07	7.49E-07	1.14E-06	1.33E-06	1.50E-06
	25%	3.41E-07	8.96E-07	1.22E-06	2.10E-06	2.44E-06	2.86E-06
	50%	4.49E-07	1.37E-06	1.95E-06	3.41E-06	3.88E-06	4.46E-06
	75%	6.87E-07	2.34E-06	3.08E-06	5.29E-06	5.97E-06	6.79E-06
	95%	9.85E-07	4.17E-06	5.34E-06	1.05E-05	1.14E-05	1.24E-05
	min	1.72E-07	3.40E-07	3.85E-07	7.03E-07	7.92E-07	9.30E-07
	max	1.39E-06	7.41E-06	1.37E-05	3.14E-05	3.55E-05	3.69E-05
I_ENV	mean	6.20E-07	2.26E-06	6.00E-06	2.64E-05	3.34E-05	4.23E-05
	5%	2.36E-07	5.65E-07	8.32E-07	1.26E-06	1.32E-06	2.11E-06
	25%	3.39E-07	9.44E-07	2.10E-06	9.78E-06	1.42E-05	1.98E-05
	50%	4.62E-07	1.48E-06	4.38E-06	1.99E-05	2.63E-05	3.37E-05
	75%	8.27E-07	3.04E-06	7.93E-06	3.32E-05	4.31E-05	5.45E-05
	95%	1.39E-06	6.37E-06	1.66E-05	8.16E-05	9.28E-05	1.15E-04
	min	1.70E-07	3.60E-07	4.62E-07	6.43E-07	7.69E-07	1.25E-06
	max	2.14E-06	1.23E-05	7.03E-05	2.23E-04	2.51E-04	3.83E-04
Class 1 Noble Gases (Xe)	mean	6.02E-05	2.75E-04	2.16E-01	4.37E-01	4.88E-01	4.99E-01
	5%	4.71E-05	2.34E-04	6.83E-04	3.44E-01	4.13E-01	4.20E-01
	25%	5.50E-05	2.55E-04	8.20E-04	3.89E-01	4.55E-01	4.68E-01
	50%	5.97E-05	2.75E-04	2.29E-01	4.45E-01	4.89E-01	5.00E-01
	75%	6.57E-05	2.93E-04	3.83E-01	4.91E-01	5.23E-01	5.29E-01
	95%	7.30E-05	3.20E-04	4.73E-01	5.57E-01	5.72E-01	5.74E-01
	min	4.14E-05	2.05E-04	5.72E-04	1.26E-03	2.34E-01	3.56E-01
	max	8.11E-05	3.80E-04	6.20E-01	6.56E-01	6.73E-01	6.75E-01
Class 2 Alkali Metals (Cs)	mean	4.57E-07	1.52E-06	1.77E-06	1.85E-06	1.86E-06	1.88E-06
	5%	2.06E-07	4.55E-07	5.07E-07	5.08E-07	5.22E-07	5.50E-07
	25%	2.94E-07	7.73E-07	8.52E-07	8.67E-07	8.75E-07	8.94E-07
	50%	3.93E-07	1.17E-06	1.32E-06	1.33E-06	1.35E-06	1.35E-06
	75%	6.01E-07	2.00E-06	2.30E-06	2.35E-06	2.37E-06	2.42E-06
	95%	8.57E-07	3.59E-06	4.23E-06	4.57E-06	4.60E-06	4.62E-06
	min	1.51E-07	2.90E-07	3.09E-07	3.13E-07	3.41E-07	3.57E-07
	max	1.20E-06	6.31E-06	1.09E-05	1.15E-05	1.16E-05	1.16E-05
Class 3 Alkaline Earths (Ba)	mean	1.28E-09	9.76E-08	1.15E-06	4.42E-06	5.49E-06	6.72E-06
	5%	6.22E-10	7.21E-09	1.06E-07	8.77E-07	1.44E-06	1.68E-06
	25%	8.97E-10	3.44E-08	3.56E-07	2.06E-06	2.70E-06	3.08E-06
	50%	1.17E-09	6.92E-08	7.48E-07	3.30E-06	4.15E-06	4.69E-06
	75%	1.53E-09	1.33E-07	1.54E-06	5.15E-06	6.36E-06	8.11E-06
	95%	2.31E-09	2.75E-07	3.18E-06	1.08E-05	1.32E-05	1.70E-05

RN group	Mean Percentiles Range	Release fraction after 2h	Release fraction after 4h	Release fraction after 8h	Release fraction after 12h	Release fraction after 16h	Release fraction after 24h
	min	3.39E-10	2.27E-09	1.85E-08	1.91E-07	5.77E-07	6.96E-07
	max	4.42E-09	5.63E-07	8.10E-06	4.63E-05	6.78E-05	7.06E-05
Class 4 Halogens (I)	mean	5.75E-13	7.71E-10	5.57E-07	3.38E-06	5.08E-06	8.02E-06
	5%	2.18E-13	1.72E-12	6.74E-11	1.25E-08	2.37E-08	7.67E-08
	25%	3.73E-13	5.48E-11	2.10E-08	8.95E-07	1.50E-06	2.46E-06
	50%	4.12E-13	3.28E-10	2.30E-07	2.00E-06	3.10E-06	4.92E-06
	75%	4.48E-13	9.69E-10	6.52E-07	4.18E-06	6.32E-06	9.80E-06
	95%	4.98E-13	2.24E-09	2.21E-06	1.07E-05	1.52E-05	2.46E-05
	min	1.11E-13	1.01E-12	5.11E-12	3.71E-09	4.26E-09	9.39E-09
	max	8.86E-11	4.95E-08	1.33E-05	5.45E-05	8.56E-05	1.56E-04
Class 5 Chalcogens (Te)	mean	1.26E-07	4.32E-07	3.07E-06	1.37E-05	1.88E-05	2.17E-05
	5%	6.08E-08	1.56E-07	2.98E-07	9.19E-07	1.15E-06	1.16E-06
	25%	8.71E-08	2.43E-07	7.15E-07	5.31E-06	8.56E-06	1.09E-05
	50%	1.14E-07	3.57E-07	1.75E-06	1.02E-05	1.47E-05	1.73E-05
	75%	1.55E-07	5.42E-07	3.97E-06	1.70E-05	2.28E-05	2.68E-05
	95%	2.24E-07	9.47E-07	9.97E-06	3.70E-05	4.90E-05	5.48E-05
	min	4.08E-08	7.75E-08	1.35E-07	1.94E-07	1.95E-07	2.06E-07
	max	3.66E-07	2.27E-06	3.12E-05	1.77E-04	2.05E-04	2.08E-04
Class 6 Platinoids (Ru)	mean	1.44E-09	5.33E-09	1.93E-08	9.27E-08	1.14E-07	1.32E-07
	5%	4.87E-10	1.29E-09	2.81E-09	1.19E-08	1.73E-08	2.16E-08
	25%	8.23E-10	2.42E-09	6.77E-09	2.91E-08	3.75E-08	4.52E-08
	50%	1.24E-09	3.94E-09	1.26E-08	5.42E-08	6.80E-08	7.98E-08
	75%	1.86E-09	6.98E-09	2.41E-08	9.58E-08	1.24E-07	1.47E-07
	95%	3.01E-09	1.33E-08	5.94E-08	3.06E-07	3.45E-07	3.97E-07
	min	3.16E-10	5.90E-10	1.17E-09	3.80E-09	5.31E-09	6.56E-09
	max	4.92E-09	3.35E-08	1.74E-07	1.83E-06	2.24E-06	2.62E-06
Class 7 Early Transition Elements (Mo)	mean	5.85E-10	5.34E-08	2.66E-07	6.16E-07	6.49E-07	6.59E-07
	5%	1.79E-10	1.80E-09	1.38E-08	5.40E-08	6.31E-08	6.34E-08
	25%	3.16E-10	1.13E-08	6.52E-08	2.13E-07	2.36E-07	2.40E-07
	50%	4.66E-10	3.28E-08	1.49E-07	4.00E-07	4.23E-07	4.38E-07
	75%	7.13E-10	6.90E-08	3.47E-07	7.99E-07	8.23E-07	8.49E-07
	95%	1.22E-09	1.60E-07	9.14E-07	1.85E-06	1.94E-06	1.94E-06
	min	9.36E-11	6.06E-10	3.56E-09	6.32E-09	8.09E-09	9.61E-09
	max	1.78E-08	6.28E-07	2.00E-06	5.27E-06	5.61E-06	5.71E-06
Class 8 Tetravalent (Ce)	mean	5.59E-11	1.17E-09	9.04E-09	4.15E-08	4.86E-08	5.48E-08
	5%	2.53E-11	1.16E-10	5.89E-10	5.34E-09	8.12E-09	9.25E-09
	25%	3.89E-11	3.71E-10	2.23E-09	1.41E-08	1.83E-08	2.05E-08
	50%	5.24E-11	7.69E-10	5.53E-09	2.83E-08	3.40E-08	3.81E-08
	75%	7.07E-11	1.65E-09	1.13E-08	4.99E-08	5.92E-08	6.75E-08
	95%	9.66E-11	3.25E-09	2.81E-08	1.15E-07	1.29E-07	1.41E-07
	min	1.58E-11	3.39E-11	1.63E-10	1.29E-09	1.93E-09	2.37E-09

RN group	Mean Percentiles Range	Release fraction after 2h	Release fraction after 4h	Release fraction after 8h	Release fraction after 12h	Release fraction after 16h	Release fraction after 24h
	max	1.23E-10	6.30E-09	9.58E-08	4.95E-07	5.53E-07	6.28E-07
Class 9 Trivalents (La)	mean	5.55E-11	1.14E-09	8.69E-09	4.07E-08	4.79E-08	5.41E-08
	5%	2.51E-11	1.16E-10	5.93E-10	5.33E-09	7.91E-09	9.19E-09
	25%	3.86E-11	3.68E-10	2.22E-09	1.40E-08	1.82E-08	2.03E-08
	50%	5.21E-11	7.64E-10	5.42E-09	2.72E-08	3.30E-08	3.77E-08
	75%	7.02E-11	1.60E-09	1.06E-08	4.79E-08	5.79E-08	6.67E-08
	95%	9.61E-11	3.16E-09	2.69E-08	1.15E-07	1.30E-07	1.37E-07
	min	1.56E-11	3.35E-11	1.62E-10	1.25E-09	1.92E-09	2.36E-09
	max	1.23E-10	6.30E-09	8.85E-08	4.95E-07	5.53E-07	6.19E-07
Class 10 Uranium (U)	mean	2.96E-10	4.30E-08	3.81E-07	1.90E-06	2.20E-06	2.44E-06
	5%	1.18E-10	7.04E-10	1.93E-08	2.16E-07	3.56E-07	3.95E-07
	25%	1.85E-10	1.31E-08	8.85E-08	6.89E-07	8.39E-07	9.51E-07
	50%	2.59E-10	2.94E-08	2.22E-07	1.25E-06	1.52E-06	1.69E-06
	75%	3.60E-10	5.67E-08	4.84E-07	2.25E-06	2.55E-06	2.85E-06
	95%	5.76E-10	1.33E-07	1.33E-06	5.66E-06	6.22E-06	6.68E-06
	min	6.98E-11	2.46E-10	1.36E-09	3.96E-08	1.02E-07	1.27E-07
	max	2.27E-09	3.01E-07	2.85E-06	1.63E-05	2.33E-05	2.42E-05
Class 11 More Volatile Main Group (Cd)	mean	9.94E-08	2.87E-07	7.18E-07	1.88E-06	2.51E-06	3.27E-06
	5%	4.86E-08	1.05E-07	1.79E-07	4.41E-07	5.25E-07	6.48E-07
	25%	7.18E-08	1.78E-07	3.39E-07	8.06E-07	1.04E-06	1.29E-06
	50%	9.51E-08	2.51E-07	5.43E-07	1.26E-06	1.67E-06	2.09E-06
	75%	1.23E-07	3.65E-07	8.66E-07	2.02E-06	2.70E-06	3.56E-06
	95%	1.65E-07	5.58E-07	1.78E-06	4.38E-06	6.52E-06	9.75E-06
	min	3.12E-08	6.75E-08	8.13E-08	1.95E-07	2.29E-07	3.10E-07
	max	2.14E-07	7.72E-07	5.88E-06	3.97E-05	5.79E-05	5.96E-05
Class 12 Less Volatile Main Group (Ag)	mean	8.63E-08	2.30E-07	4.81E-07	8.07E-07	8.99E-07	9.68E-07
	5%	4.03E-08	8.17E-08	1.62E-07	2.91E-07	3.12E-07	3.21E-07
	25%	6.13E-08	1.38E-07	2.71E-07	4.38E-07	4.69E-07	4.92E-07
	50%	8.16E-08	2.04E-07	4.08E-07	6.53E-07	7.04E-07	7.46E-07
	75%	1.07E-07	3.02E-07	5.59E-07	9.46E-07	1.03E-06	1.10E-06
	95%	1.49E-07	4.65E-07	1.09E-06	1.80E-06	2.35E-06	2.53E-06
	min	2.48E-08	4.28E-08	6.82E-08	1.07E-07	1.11E-07	1.17E-07
	max	1.97E-07	7.65E-07	3.20E-06	4.67E-06	5.89E-06	6.17E-06
Class 16 Cesium Iodide (CsI)	mean	6.25E-07	2.28E-06	5.49E-06	2.32E-05	2.85E-05	3.46E-05
	5%	2.37E-07	5.69E-07	8.28E-07	1.22E-06	1.30E-06	2.05E-06
	25%	3.41E-07	9.51E-07	1.97E-06	8.64E-06	1.25E-05	1.62E-05
	50%	4.67E-07	1.49E-06	3.99E-06	1.78E-05	2.31E-05	2.86E-05
	75%	8.33E-07	3.06E-06	7.36E-06	2.92E-05	3.63E-05	4.54E-05
	95%	1.41E-06	6.43E-06	1.44E-05	7.09E-05	7.85E-05	9.01E-05
	min	1.72E-07	3.63E-07	4.42E-07	6.18E-07	7.37E-07	1.16E-06

RN group	Mean Percentiles Range	Release fraction after 2h	Release fraction after 4h	Release fraction after 8h	Release fraction after 12h	Release fraction after 16h	Release fraction after 24h
	max	2.16E-06	1.24E-05	5.76E-05	1.97E-04	2.20E-04	2.34E-04
Class 17 Cesium Molybdate (Cs2MoO4)	mean	7.51E-08	3.05E-07	8.80E-07	2.49E-06	2.94E-06	3.54E-06
	5%	4.07E-08	1.33E-07	2.53E-07	6.38E-07	7.94E-07	8.85E-07
	25%	5.55E-08	2.15E-07	4.80E-07	1.08E-06	1.31E-06	1.45E-06
	50%	7.34E-08	2.94E-07	6.80E-07	1.62E-06	1.99E-06	2.31E-06
	75%	9.16E-08	3.78E-07	1.07E-06	2.65E-06	3.37E-06	4.19E-06
	95%	1.18E-07	5.03E-07	2.14E-06	6.40E-06	7.26E-06	9.21E-06
	min	2.34E-08	6.47E-08	1.34E-07	2.65E-07	3.07E-07	3.75E-07
	max	1.73E-07	7.32E-07	5.50E-06	4.68E-05	5.66E-05	5.76E-05

Table A-2. Release fractions RC7A SBO-MVSS-IDEJ0

RN group	Mean Percentiles Range	Release fraction after 2h	Release fraction after 4h	Release fraction after 8h	Release fraction after 12h	Release fraction after 16h	Release fraction after 24h
CS_ENV	mean	4.68E-07	1.48E-06	2.98E-06	3.20E-06	3.39E-06	3.60E-06
	5%	2.20E-07	4.61E-07	1.10E-06	1.22E-06	1.33E-06	1.42E-06
	25%	2.95E-07	7.08E-07	1.61E-06	1.77E-06	1.95E-06	2.10E-06
	50%	3.82E-07	1.09E-06	2.36E-06	2.56E-06	2.76E-06	2.98E-06
	75%	6.11E-07	1.87E-06	3.70E-06	3.99E-06	4.25E-06	4.58E-06
	95%	9.35E-07	3.81E-06	6.59E-06	6.96E-06	7.29E-06	7.55E-06
	min	1.52E-07	2.62E-07	5.51E-07	5.55E-07	5.57E-07	5.73E-07
	max	1.34E-06	1.03E-05	1.41E-05	1.41E-05	1.42E-05	1.48E-05
I_ENV	mean	5.47E-07	1.87E-06	6.81E-06	8.83E-06	1.17E-05	1.64E-05
	5%	2.21E-07	4.63E-07	2.06E-06	2.89E-06	3.77E-06	5.23E-06
	25%	2.95E-07	7.15E-07	3.68E-06	5.07E-06	6.95E-06	9.30E-06
	50%	3.88E-07	1.16E-06	5.46E-06	7.27E-06	9.56E-06	1.30E-05
	75%	7.18E-07	2.38E-06	8.56E-06	1.08E-05	1.41E-05	1.99E-05
	95%	1.28E-06	5.43E-06	1.56E-05	1.98E-05	2.69E-05	3.94E-05
	min	1.55E-07	2.71E-07	6.01E-07	6.13E-07	6.21E-07	6.88E-07
	max	2.06E-06	1.43E-05	3.90E-05	4.40E-05	6.48E-05	1.04E-04
Class 1 Noble Gases (Xe)	mean	5.94E-05	1.33E-02	3.82E-01	3.84E-01	3.85E-01	3.85E-01
	5%	4.75E-05	2.45E-04	3.34E-01	3.39E-01	3.40E-01	3.40E-01
	25%	5.39E-05	2.73E-04	3.57E-01	3.59E-01	3.59E-01	3.60E-01
	50%	5.93E-05	2.95E-04	3.76E-01	3.78E-01	3.78E-01	3.78E-01
	75%	6.48E-05	3.15E-04	3.93E-01	3.94E-01	3.94E-01	3.94E-01
	95%	7.11E-05	3.50E-04	4.44E-01	4.46E-01	4.46E-01	4.47E-01
	min	4.18E-05	2.14E-04	6.56E-04	2.67E-01	2.82E-01	2.82E-01
	max	7.81E-05	5.54E-01	6.64E-01	6.64E-01	6.64E-01	6.64E-01
Class 2 Alkali Metals (Cs)	mean	4.09E-07	1.25E-06	2.05E-06	2.11E-06	2.15E-06	2.18E-06
	5%	1.91E-07	3.84E-07	6.92E-07	7.42E-07	7.72E-07	7.88E-07
	25%	2.57E-07	5.96E-07	1.05E-06	1.09E-06	1.12E-06	1.13E-06

RN group	Mean Percentiles Range	Release fraction after 2h	Release fraction after 4h	Release fraction after 8h	Release fraction after 12h	Release fraction after 16h	Release fraction after 24h
	50%	3.31E-07	9.01E-07	1.50E-06	1.57E-06	1.60E-06	1.62E-06
	75%	5.39E-07	1.56E-06	2.56E-06	2.67E-06	2.71E-06	2.75E-06
	95%	8.15E-07	3.26E-06	4.91E-06	5.03E-06	5.06E-06	5.13E-06
	min	1.32E-07	2.14E-07	4.52E-07	4.52E-07	4.53E-07	4.62E-07
	max	1.17E-06	8.06E-06	1.13E-05	1.13E-05	1.13E-05	1.13E-05
Class 3 Alkaline Earths (Ba)	mean	1.07E-09	1.28E-07	5.22E-07	5.64E-07	5.99E-07	7.22E-07
	5%	4.85E-10	1.59E-08	8.72E-08	1.01E-07	1.21E-07	1.77E-07
	25%	7.07E-10	3.65E-08	1.68E-07	1.87E-07	2.16E-07	2.95E-07
	50%	9.09E-10	6.74E-08	2.87E-07	3.16E-07	3.47E-07	4.55E-07
	75%	1.22E-09	1.34E-07	5.73E-07	6.15E-07	6.55E-07	8.04E-07
	95%	1.68E-09	3.19E-07	1.85E-06	1.99E-06	2.01E-06	2.13E-06
	min	2.70E-10	4.07E-09	1.35E-08	4.36E-08	5.23E-08	7.71E-08
	max	2.71E-08	4.58E-06	8.79E-06	9.24E-06	9.45E-06	9.79E-06
Class 4 Halogens (I)	mean	1.71E-12	3.00E-09	2.58E-07	5.50E-07	1.47E-06	4.10E-06
	5%	3.12E-13	7.32E-11	4.72E-08	9.02E-08	2.09E-07	5.05E-07
	25%	3.91E-13	5.89E-10	8.97E-08	1.96E-07	5.02E-07	1.36E-06
	50%	4.20E-13	1.55E-09	1.56E-07	3.33E-07	8.97E-07	2.56E-06
	75%	4.54E-13	2.82E-09	2.90E-07	6.41E-07	1.70E-06	4.87E-06
	95%	4.98E-13	1.02E-08	7.50E-07	1.56E-06	4.05E-06	1.21E-05
	min	1.12E-13	1.39E-12	3.93E-12	2.66E-09	3.49E-09	7.52E-09
	max	5.67E-10	8.81E-08	3.67E-06	9.08E-06	2.31E-05	5.56E-05
Class 5 Chalcogens (Te)	mean	1.10E-07	5.06E-07	3.36E-06	4.56E-06	7.30E-06	9.73E-06
	5%	5.04E-08	1.49E-07	6.62E-07	1.35E-06	2.54E-06	3.28E-06
	25%	7.42E-08	2.42E-07	1.34E-06	2.23E-06	4.09E-06	5.43E-06
	50%	9.65E-08	3.56E-07	2.39E-06	3.48E-06	5.64E-06	7.56E-06
	75%	1.37E-07	5.82E-07	4.23E-06	5.55E-06	8.76E-06	1.18E-05
	95%	2.03E-07	1.22E-06	8.98E-06	1.12E-05	1.69E-05	2.28E-05
	min	3.63E-08	7.79E-08	3.71E-07	6.25E-07	9.10E-07	1.04E-06
	max	4.73E-07	7.80E-06	4.52E-05	4.73E-05	5.12E-05	6.04E-05
Class 6 Platinoids (Ru)	mean	1.49E-09	4.94E-09	1.20E-08	1.24E-08	1.25E-08	1.25E-08
	5%	4.85E-10	1.10E-09	1.17E-09	1.18E-09	1.18E-09	1.18E-09
	25%	8.26E-10	2.04E-09	2.39E-09	2.40E-09	2.40E-09	2.40E-09
	50%	1.19E-09	3.53E-09	4.72E-09	4.75E-09	4.76E-09	4.77E-09
	75%	1.92E-09	6.09E-09	9.70E-09	1.00E-08	1.01E-08	1.01E-08
	95%	3.16E-09	1.31E-08	4.17E-08	4.18E-08	4.18E-08	4.18E-08
	min	2.92E-10	5.73E-10	5.88E-10	5.88E-10	5.88E-10	5.88E-10
	max	1.79E-08	4.47E-08	8.16E-07	8.31E-07	8.32E-07	8.32E-07
Class 7 Early Transition Elements (Mo)	mean	6.20E-10	6.07E-08	8.95E-08	9.00E-08	9.00E-08	9.00E-08
	5%	1.56E-10	5.01E-09	1.08E-08	1.09E-08	1.09E-08	1.09E-08
	25%	2.50E-10	1.64E-08	2.61E-08	2.62E-08	2.62E-08	2.62E-08
	50%	3.54E-10	3.02E-08	4.73E-08	4.80E-08	4.80E-08	4.80E-08

RN group	Mean Percentiles Range	Release fraction after 2h	Release fraction after 4h	Release fraction after 8h	Release fraction after 12h	Release fraction after 16h	Release fraction after 24h
	75%	5.26E-10	5.99E-08	9.72E-08	9.74E-08	9.74E-08	9.74E-08
	95%	9.62E-10	2.00E-07	2.88E-07	2.93E-07	2.93E-07	2.93E-07
	min	7.77E-11	6.91E-10	1.33E-09	2.40E-09	2.40E-09	2.40E-09
	max	6.66E-08	2.13E-06	2.28E-06	2.28E-06	2.28E-06	2.28E-06
Class 8 Tetravalent (Ce)	mean	4.93E-11	1.05E-09	1.99E-09	2.01E-09	2.02E-09	2.02E-09
	5%	2.16E-11	1.59E-10	2.28E-10	2.29E-10	2.29E-10	2.29E-10
	25%	3.28E-11	3.45E-10	5.35E-10	5.41E-10	5.41E-10	5.41E-10
	50%	4.48E-11	6.45E-10	9.84E-10	9.99E-10	1.00E-09	1.00E-09
	75%	6.21E-11	1.25E-09	1.92E-09	1.96E-09	1.97E-09	1.97E-09
	95%	8.94E-11	2.87E-09	4.99E-09	5.09E-09	5.10E-09	5.10E-09
	min	1.39E-11	3.82E-11	4.94E-11	4.94E-11	4.94E-11	4.94E-11
	max	2.16E-10	3.82E-08	9.93E-08	9.95E-08	9.95E-08	9.95E-08
Class 9 Trivalents (La)	mean	4.89E-11	9.82E-10	1.90E-09	1.92E-09	1.93E-09	1.93E-09
	5%	2.14E-11	1.43E-10	2.07E-10	2.09E-10	2.09E-10	2.09E-10
	25%	3.25E-11	3.31E-10	5.00E-10	5.01E-10	5.01E-10	5.01E-10
	50%	4.45E-11	5.90E-10	9.12E-10	9.16E-10	9.16E-10	9.17E-10
	75%	6.18E-11	1.20E-09	1.80E-09	1.84E-09	1.84E-09	1.86E-09
	95%	8.89E-11	2.71E-09	4.82E-09	4.96E-09	4.96E-09	4.96E-09
	min	1.37E-11	3.80E-11	5.09E-11	5.09E-11	5.09E-11	5.09E-11
	max	2.14E-10	3.60E-08	9.48E-08	9.50E-08	9.50E-08	9.50E-08
Class 10 Uranium (U)	mean	2.65E-10	3.24E-08	6.06E-08	6.12E-08	6.12E-08	6.13E-08
	5%	1.01E-10	3.25E-09	4.97E-09	5.12E-09	5.12E-09	5.12E-09
	25%	1.56E-10	9.39E-09	1.34E-08	1.34E-08	1.34E-08	1.34E-08
	50%	2.10E-10	1.82E-08	2.75E-08	2.77E-08	2.77E-08	2.77E-08
	75%	3.07E-10	3.72E-08	5.87E-08	5.94E-08	5.94E-08	5.94E-08
	95%	4.93E-10	9.94E-08	1.89E-07	1.90E-07	1.90E-07	1.90E-07
	min	5.99E-11	5.79E-10	6.92E-10	6.92E-10	6.92E-10	6.92E-10
	max	7.56E-09	1.23E-06	2.24E-06	2.25E-06	2.25E-06	2.25E-06
Class 11 More Volatile Main Group (Cd)	mean	8.92E-08	3.05E-07	7.85E-07	8.19E-07	8.70E-07	1.18E-06
	5%	4.12E-08	9.74E-08	1.56E-07	1.61E-07	1.93E-07	3.08E-07
	25%	6.17E-08	1.56E-07	2.74E-07	2.82E-07	3.29E-07	5.48E-07
	50%	8.26E-08	2.34E-07	4.42E-07	4.53E-07	5.18E-07	7.92E-07
	75%	1.10E-07	3.61E-07	7.62E-07	7.84E-07	8.42E-07	1.29E-06
	95%	1.56E-07	7.54E-07	2.57E-06	2.65E-06	2.71E-06	2.99E-06
	min	2.64E-08	5.42E-08	8.14E-08	8.28E-08	9.07E-08	1.43E-07
	max	2.14E-07	2.37E-06	1.42E-05	1.48E-05	1.50E-05	1.56E-05
Class 12 Less Volatile Main Group (Ag)	mean	7.76E-08	2.14E-07	4.99E-07	5.06E-07	5.06E-07	5.09E-07
	5%	3.41E-08	6.89E-08	1.18E-07	1.19E-07	1.19E-07	1.20E-07
	25%	5.20E-08	1.16E-07	2.18E-07	2.20E-07	2.20E-07	2.23E-07
	50%	7.06E-08	1.79E-07	3.49E-07	3.53E-07	3.53E-07	3.55E-07
	75%	9.73E-08	2.70E-07	5.58E-07	5.65E-07	5.65E-07	5.68E-07

RN group	Mean Percentiles Range	Release fraction after 2h	Release fraction after 4h	Release fraction after 8h	Release fraction after 12h	Release fraction after 16h	Release fraction after 24h
	95%	1.40E-07	4.64E-07	1.29E-06	1.31E-06	1.31E-06	1.31E-06
	min	2.09E-08	3.83E-08	5.14E-08	5.14E-08	5.15E-08	5.21E-08
	max	1.92E-07	2.08E-06	6.14E-06	6.15E-06	6.16E-06	6.16E-06
Class 16 Cesium Iodide (CsI)	mean	5.53E-07	1.89E-06	6.63E-06	8.37E-06	1.04E-05	1.24E-05
	5%	2.24E-07	4.67E-07	2.01E-06	2.70E-06	3.58E-06	4.38E-06
	25%	2.99E-07	7.22E-07	3.59E-06	4.85E-06	6.27E-06	7.59E-06
	50%	3.92E-07	1.17E-06	5.31E-06	6.95E-06	8.63E-06	1.04E-05
	75%	7.26E-07	2.40E-06	8.32E-06	1.02E-05	1.23E-05	1.50E-05
	95%	1.29E-06	5.47E-06	1.51E-05	1.93E-05	2.27E-05	2.73E-05
	min	1.57E-07	2.71E-07	6.02E-07	6.12E-07	6.18E-07	6.82E-07
	max	2.09E-06	1.44E-05	3.57E-05	3.90E-05	4.66E-05	5.42E-05
Class 17 Cesium Molybdate (Cs2MoO4)	mean	7.04E-08	3.93E-07	1.93E-06	2.00E-06	2.01E-06	2.06E-06
	5%	3.55E-08	1.53E-07	3.76E-07	3.83E-07	3.89E-07	4.18E-07
	25%	5.30E-08	2.40E-07	7.23E-07	7.47E-07	7.53E-07	7.93E-07
	50%	6.52E-08	3.09E-07	1.29E-06	1.33E-06	1.34E-06	1.36E-06
	75%	8.43E-08	4.14E-07	2.28E-06	2.38E-06	2.39E-06	2.43E-06
	95%	1.13E-07	7.79E-07	5.68E-06	6.01E-06	6.06E-06	6.11E-06
	min	1.92E-08	8.37E-08	1.04E-07	1.04E-07	1.05E-07	1.07E-07
	max	3.07E-07	5.69E-06	2.47E-05	2.56E-05	2.58E-05	2.59E-05

Table A-3. Release fractions RC7B LOCA-MVSS-IDEJ1

RN group	Mean Percentiles Range	Release fraction after 2h	Release fraction after 4h	Release fraction after 8h	Release fraction after 12h	Release fraction after 16h	Release fraction after 24h
CS_ENV	mean	3.00E-05	3.26E-05	1.38E-04	6.02E-04	7.25E-04	9.70E-04
	5%	1.54E-05	1.66E-05	3.34E-05	1.51E-04	1.97E-04	2.39E-04
	25%	2.10E-05	2.30E-05	6.40E-05	2.59E-04	3.26E-04	4.18E-04
	50%	2.72E-05	2.92E-05	1.01E-04	4.41E-04	5.24E-04	6.62E-04
	75%	3.85E-05	4.14E-05	1.76E-04	7.56E-04	8.92E-04	1.12E-03
	95%	5.16E-05	5.55E-05	3.45E-04	1.57E-03	1.88E-03	2.33E-03
	min	1.22E-05	1.33E-05	2.02E-05	6.89E-05	1.03E-04	1.33E-04
	max	7.03E-05	7.68E-05	1.21E-03	5.19E-03	5.93E-03	1.91E-02
I_ENV	mean	3.56E-05	3.83E-05	1.65E-04	8.13E-04	9.69E-04	1.26E-03
	5%	1.91E-05	2.04E-05	3.90E-05	1.89E-04	2.50E-04	2.91E-04
	25%	2.58E-05	2.74E-05	7.16E-05	3.45E-04	4.34E-04	5.26E-04
	50%	3.28E-05	3.53E-05	1.12E-04	5.82E-04	6.92E-04	8.80E-04
	75%	4.47E-05	4.80E-05	2.03E-04	1.01E-03	1.17E-03	1.45E-03
	95%	5.75E-05	6.30E-05	4.40E-04	2.18E-03	2.50E-03	3.20E-03
	min	1.53E-05	1.58E-05	2.40E-05	9.59E-05	1.27E-04	1.70E-04
	max	7.45E-05	7.89E-05	1.70E-03	7.40E-03	8.31E-03	2.46E-02
Class 1 No ble	mean	3.89E-04	8.51E-03	4.04E-01	6.15E-01	6.60E-01	6.69E-01

RN group	Mean Percentiles Range	Release fraction after 2h	Release fraction after 4h	Release fraction after 8h	Release fraction after 12h	Release fraction after 16h	Release fraction after 24h
	5%	3.52E-04	4.52E-04	1.30E-03	4.45E-01	5.61E-01	5.79E-01
	25%	3.72E-04	6.68E-04	2.52E-01	5.82E-01	6.24E-01	6.35E-01
	50%	3.88E-04	8.00E-04	4.86E-01	6.44E-01	6.76E-01	6.83E-01
	75%	4.05E-04	8.59E-04	6.01E-01	6.88E-01	7.02E-01	7.07E-01
	95%	4.31E-04	9.24E-04	6.49E-01	7.18E-01	7.28E-01	7.31E-01
	min	2.65E-04	3.84E-04	5.28E-04	1.56E-03	2.89E-01	4.70E-01
	max	4.68E-04	5.75E-01	7.26E-01	7.39E-01	7.57E-01	7.57E-01
Class 2 Alkali Metals (Cs)	mean	2.39E-05	2.50E-05	1.11E-04	5.12E-04	6.14E-04	8.25E-04
	5%	1.26E-05	1.30E-05	2.58E-05	1.23E-04	1.57E-04	1.91E-04
	25%	1.69E-05	1.78E-05	4.84E-05	2.13E-04	2.70E-04	3.38E-04
	50%	2.17E-05	2.28E-05	7.65E-05	3.74E-04	4.35E-04	5.59E-04
	75%	3.04E-05	3.17E-05	1.41E-04	6.32E-04	7.49E-04	9.47E-04
	95%	4.06E-05	4.24E-05	2.92E-04	1.36E-03	1.61E-03	2.06E-03
	min	1.01E-05	1.04E-05	1.60E-05	5.31E-05	8.19E-05	1.08E-04
	max	5.41E-05	5.60E-05	1.06E-03	4.55E-03	5.17E-03	1.70E-02
Class 3 Alkaline Earths (Ba)	mean	2.67E-06	6.84E-06	3.23E-05	6.58E-05	8.19E-05	1.08E-04
	5%	9.77E-07	2.87E-06	9.86E-06	2.08E-05	2.74E-05	3.47E-05
	25%	1.52E-06	4.13E-06	1.72E-05	3.60E-05	4.47E-05	5.75E-05
	50%	2.25E-06	5.64E-06	2.72E-05	5.49E-05	6.56E-05	8.27E-05
	75%	3.64E-06	9.04E-06	3.91E-05	8.11E-05	9.85E-05	1.23E-04
	95%	5.49E-06	1.36E-05	7.35E-05	1.41E-04	1.75E-04	2.33E-04
	min	7.77E-07	2.22E-06	5.68E-06	1.12E-05	1.29E-05	1.46E-05
	max	8.29E-06	2.20E-05	1.85E-04	3.91E-04	6.70E-04	1.71E-03
Class 4 Halogens (I)	mean	9.06E-08	1.90E-07	5.47E-07	6.55E-07	6.68E-07	6.91E-07
	5%	2.35E-08	5.49E-08	1.19E-07	1.36E-07	1.39E-07	1.48E-07
	25%	3.63E-08	8.16E-08	1.96E-07	2.38E-07	2.41E-07	2.58E-07
	50%	5.80E-08	1.22E-07	3.27E-07	4.12E-07	4.20E-07	4.33E-07
	75%	1.10E-07	2.15E-07	5.44E-07	6.85E-07	7.14E-07	7.50E-07
	95%	2.65E-07	5.20E-07	1.50E-06	2.00E-06	2.03E-06	2.08E-06
	min	7.55E-09	3.35E-08	8.25E-08	9.16E-08	9.17E-08	9.47E-08
	max	8.53E-07	3.89E-06	1.78E-05	1.79E-05	1.79E-05	1.79E-05
Class 5 Chalcogens (Te)	mean	1.74E-05	2.09E-05	2.46E-05	1.10E-04	3.49E-04	6.15E-04
	5%	7.43E-06	9.37E-06	1.00E-05	2.11E-05	3.66E-05	4.45E-05
	25%	1.04E-05	1.25E-05	1.43E-05	3.85E-05	7.55E-05	1.28E-04
	50%	1.49E-05	1.71E-05	1.99E-05	5.87E-05	1.73E-04	3.56E-04
	75%	2.24E-05	2.73E-05	3.15E-05	1.09E-04	3.78E-04	8.27E-04
	95%	3.65E-05	4.41E-05	5.47E-05	3.28E-04	1.20E-03	2.02E-03
	min	6.04E-06	7.73E-06	7.87E-06	1.17E-05	1.38E-05	1.45E-05
	max	5.01E-05	6.27E-05	1.10E-04	4.29E-03	7.87E-03	9.38E-03
Class 6 Platinoids (Ru)	mean	9.07E-08	2.61E-07	8.62E-07	1.65E-06	2.41E-06	3.70E-06
	5%	1.31E-08	3.17E-08	1.44E-07	3.61E-07	5.95E-07	9.58E-07

RN group	Mean Percentiles Range	Release fraction after 2h	Release fraction after 4h	Release fraction after 8h	Release fraction after 12h	Release fraction after 16h	Release fraction after 24h
	25%	2.81E-08	7.69E-08	3.50E-07	7.29E-07	1.15E-06	1.85E-06
	50%	5.80E-08	1.83E-07	6.06E-07	1.25E-06	1.84E-06	2.77E-06
	75%	1.31E-07	3.29E-07	9.93E-07	2.03E-06	3.06E-06	4.55E-06
	95%	2.62E-07	7.97E-07	2.15E-06	4.23E-06	6.04E-06	9.29E-06
	min	5.71E-09	1.19E-08	5.77E-08	1.65E-07	2.19E-07	2.26E-07
	max	6.12E-07	1.79E-06	1.39E-05	1.67E-05	1.90E-05	2.33E-05
Class 7 Early Transition Elements (Mo)	mean	3.74E-06	5.86E-06	1.49E-05	1.98E-05	2.13E-05	2.23E-05
	5%	7.15E-07	1.07E-06	1.93E-06	2.85E-06	3.20E-06	3.31E-06
	25%	1.39E-06	2.06E-06	4.50E-06	6.72E-06	7.22E-06	7.54E-06
	50%	2.60E-06	3.91E-06	9.22E-06	1.33E-05	1.41E-05	1.50E-05
	75%	5.38E-06	8.20E-06	1.92E-05	2.49E-05	2.62E-05	2.75E-05
	95%	1.00E-05	1.65E-05	4.21E-05	5.34E-05	6.07E-05	6.46E-05
	min	4.22E-07	5.74E-07	8.02E-07	1.28E-06	1.30E-06	1.35E-06
	max	1.84E-05	3.00E-05	2.53E-04	3.22E-04	3.26E-04	3.29E-04
Class 8 Tetravalent (Ce)	mean	1.87E-08	4.67E-08	2.34E-07	4.86E-07	6.80E-07	9.54E-07
	5%	4.27E-09	1.21E-08	4.18E-08	1.26E-07	1.95E-07	2.56E-07
	25%	7.54E-09	2.18E-08	9.16E-08	2.20E-07	3.25E-07	4.71E-07
	50%	1.31E-08	3.46E-08	1.69E-07	3.82E-07	5.25E-07	7.32E-07
	75%	2.69E-08	6.46E-08	2.89E-07	5.88E-07	8.22E-07	1.17E-06
	95%	4.89E-08	1.15E-07	6.07E-07	1.14E-06	1.68E-06	2.36E-06
	min	2.11E-09	7.62E-09	2.04E-08	3.36E-08	3.42E-08	3.46E-08
	max	7.99E-08	1.97E-07	2.68E-06	4.72E-06	7.03E-06	1.14E-05
Class 9 Trivalents (La)	mean	1.85E-08	4.61E-08	2.33E-07	4.84E-07	6.76E-07	9.44E-07
	5%	4.20E-09	1.18E-08	4.08E-08	1.24E-07	1.92E-07	2.55E-07
	25%	7.33E-09	2.12E-08	9.05E-08	2.20E-07	3.24E-07	4.68E-07
	50%	1.28E-08	3.41E-08	1.69E-07	3.82E-07	5.23E-07	7.19E-07
	75%	2.64E-08	6.41E-08	2.87E-07	5.88E-07	8.24E-07	1.16E-06
	95%	4.88E-08	1.15E-07	6.08E-07	1.13E-06	1.67E-06	2.33E-06
	min	2.02E-09	7.44E-09	2.02E-08	3.27E-08	3.33E-08	3.36E-08
	max	7.96E-08	1.96E-07	2.72E-06	4.68E-06	6.70E-06	1.10E-05
Class 10 Uranium (U)	mean	8.66E-07	2.10E-06	1.08E-05	2.20E-05	3.01E-05	4.05E-05
	5%	1.74E-07	4.78E-07	1.74E-06	5.31E-06	8.58E-06	1.14E-05
	25%	3.22E-07	8.87E-07	3.95E-06	1.02E-05	1.46E-05	2.04E-05
	50%	5.93E-07	1.51E-06	7.80E-06	1.67E-05	2.36E-05	3.12E-05
	75%	1.25E-06	2.97E-06	1.43E-05	2.90E-05	3.85E-05	5.07E-05
	95%	2.37E-06	5.67E-06	2.81E-05	5.37E-05	7.05E-05	9.96E-05
	min	7.85E-08	2.33E-07	6.31E-07	1.53E-06	1.54E-06	1.54E-06
	max	3.84E-06	1.00E-05	9.24E-05	1.32E-04	1.46E-04	2.69E-04
Class 11 More Volatile Main Group	mean	1.01E-05	1.57E-05	4.78E-05	9.41E-05	1.15E-04	1.26E-04
	5%	3.31E-06	4.73E-06	1.49E-05	2.10E-05	2.28E-05	2.46E-05
	25%	5.27E-06	7.58E-06	2.50E-05	4.09E-05	4.46E-05	4.88E-05

RN group	Mean Percentiles Range	Release fraction after 2h	Release fraction after 4h	Release fraction after 8h	Release fraction after 12h	Release fraction after 16h	Release fraction after 24h
	50%	8.39E-06	1.35E-05	3.91E-05	6.80E-05	7.55E-05	8.59E-05
	75%	1.37E-05	2.15E-05	5.77E-05	1.25E-04	1.51E-04	1.64E-04
	95%	2.22E-05	3.45E-05	1.12E-04	2.55E-04	3.21E-04	3.51E-04
	min	2.54E-06	3.60E-06	8.05E-06	1.28E-05	1.32E-05	1.33E-05
	max	3.33E-05	4.83E-05	2.72E-04	4.89E-04	1.20E-03	1.22E-03
Class 12 Less Volatile Main Group (Ag)	mean	6.71E-06	9.04E-06	2.31E-05	4.78E-05	7.33E-05	1.24E-04
	5%	1.89E-06	2.70E-06	6.16E-06	1.09E-05	1.28E-05	1.34E-05
	25%	3.02E-06	4.38E-06	1.09E-05	2.21E-05	2.85E-05	3.15E-05
	50%	4.84E-06	6.86E-06	1.89E-05	3.61E-05	5.14E-05	7.90E-05
	75%	9.47E-06	1.22E-05	3.01E-05	6.18E-05	9.66E-05	1.81E-04
	95%	1.62E-05	2.20E-05	5.16E-05	1.24E-04	2.14E-04	3.80E-04
	min	1.35E-06	1.96E-06	3.88E-06	6.06E-06	6.21E-06	6.34E-06
	max	2.70E-05	3.73E-05	1.95E-04	2.16E-04	3.75E-04	7.23E-04
Class 16 Cesium Iodide (CsI)	mean	3.56E-05	3.82E-05	1.65E-04	8.15E-04	9.71E-04	1.26E-03
	5%	1.91E-05	2.04E-05	3.89E-05	1.89E-04	2.50E-04	2.92E-04
	25%	2.58E-05	2.73E-05	7.16E-05	3.46E-04	4.35E-04	5.27E-04
	50%	3.28E-05	3.52E-05	1.12E-04	5.84E-04	6.93E-04	8.82E-04
	75%	4.48E-05	4.80E-05	2.03E-04	1.01E-03	1.17E-03	1.45E-03
	95%	5.77E-05	6.26E-05	4.41E-04	2.19E-03	2.51E-03	3.21E-03
	min	1.53E-05	1.58E-05	2.38E-05	9.57E-05	1.28E-04	1.70E-04
	max	7.47E-05	7.90E-05	1.70E-03	7.42E-03	8.34E-03	2.47E-02
Class 17 Cesium Molybdate (Cs2MoO4)	mean	1.34E-05	1.86E-05	5.90E-05	1.02E-04	1.32E-04	1.77E-04
	5%	5.58E-06	8.54E-06	1.43E-05	2.49E-05	2.89E-05	2.97E-05
	25%	7.74E-06	1.19E-05	2.53E-05	4.39E-05	5.76E-05	7.65E-05
	50%	1.10E-05	1.58E-05	4.75E-05	8.10E-05	9.57E-05	1.35E-04
	75%	1.76E-05	2.40E-05	8.10E-05	1.35E-04	1.73E-04	2.35E-04
	95%	2.77E-05	3.63E-05	1.48E-04	2.54E-04	3.39E-04	4.68E-04
	min	4.22E-06	6.52E-06	9.89E-06	1.34E-05	1.46E-05	1.49E-05
	max	4.10E-05	5.85E-05	2.56E-04	4.74E-04	9.59E-04	1.09E-03

Table A-4. – Release fractions RC7B LOCA-MVSS-IDEJ0

RN group	Mean Percentiles Range	Release fraction after 2h	Release fraction after 4h	Release fraction after 8h	Release fraction after 12h	Release fraction after 16h	Release fraction after 24h
CS_ENV	mean	3.03E-05	4.02E-05	8.78E-05	1.25E-04	1.46E-04	1.67E-04
	5%	1.55E-05	1.78E-05	3.41E-05	4.04E-05	4.38E-05	4.86E-05
	25%	2.07E-05	2.54E-05	4.85E-05	5.85E-05	6.41E-05	7.10E-05
	50%	2.74E-05	3.60E-05	6.72E-05	8.35E-05	9.44E-05	1.05E-04
	75%	3.90E-05	5.16E-05	9.44E-05	1.28E-04	1.50E-04	1.75E-04
	95%	5.48E-05	6.89E-05	2.06E-04	3.26E-04	3.89E-04	4.52E-04
	min	1.19E-05	1.29E-05	2.01E-05	2.43E-05	2.57E-05	2.74E-05

RN group	Mean Percentiles Range	Release fraction after 2h	Release fraction after 4h	Release fraction after 8h	Release fraction after 12h	Release fraction after 16h	Release fraction after 24h
	max	6.87E-05	1.34E-04	9.23E-04	1.36E-03	1.58E-03	1.78E-03
I_ENV	mean	3.58E-05	4.78E-05	1.04E-04	1.43E-04	1.61E-04	1.79E-04
	5%	1.93E-05	2.10E-05	3.78E-05	4.39E-05	4.76E-05	5.10E-05
	25%	2.57E-05	2.97E-05	5.54E-05	6.57E-05	7.05E-05	7.52E-05
	50%	3.33E-05	4.31E-05	7.60E-05	9.32E-05	1.01E-04	1.09E-04
	75%	4.48E-05	6.08E-05	1.11E-04	1.40E-04	1.60E-04	1.82E-04
	95%	6.07E-05	8.35E-05	2.15E-04	3.78E-04	4.52E-04	5.19E-04
	min	1.44E-05	1.59E-05	2.28E-05	2.43E-05	2.52E-05	2.62E-05
	max	7.49E-05	1.85E-04	1.31E-03	1.72E-03	1.94E-03	2.05E-03
Class 1 Noble Gases (Xe)	mean	2.41E-03	2.12E-01	5.20E-01	5.20E-01	5.20E-01	5.20E-01
	5%	3.53E-04	4.72E-04	4.63E-01	4.63E-01	4.63E-01	4.63E-01
	25%	3.76E-04	7.27E-04	5.02E-01	5.02E-01	5.02E-01	5.02E-01
	50%	3.96E-04	1.43E-01	5.20E-01	5.20E-01	5.20E-01	5.20E-01
	75%	4.15E-04	4.42E-01	5.34E-01	5.34E-01	5.34E-01	5.34E-01
	95%	4.48E-04	5.42E-01	5.84E-01	5.84E-01	5.84E-01	5.85E-01
	min	3.37E-04	3.90E-04	3.59E-01	3.59E-01	3.59E-01	3.90E-01
	max	1.35E-01	6.39E-01	6.92E-01	6.92E-01	6.92E-01	6.92E-01
Class 2 Alkali Metals (Cs)	mean	2.41E-05	2.96E-05	7.11E-05	1.05E-04	1.24E-04	1.44E-04
	5%	1.26E-05	1.36E-05	2.61E-05	3.24E-05	3.49E-05	3.80E-05
	25%	1.67E-05	1.89E-05	3.79E-05	4.65E-05	5.13E-05	5.90E-05
	50%	2.19E-05	2.65E-05	5.15E-05	6.80E-05	7.62E-05	8.83E-05
	75%	3.07E-05	3.76E-05	7.47E-05	1.05E-04	1.23E-04	1.48E-04
	95%	4.29E-05	5.18E-05	1.80E-04	2.87E-04	3.37E-04	4.01E-04
	min	9.40E-06	1.03E-05	1.50E-05	1.69E-05	1.82E-05	1.99E-05
	max	5.31E-05	9.81E-05	8.02E-04	1.22E-03	1.43E-03	1.61E-03
Class 3 Alkaline Earths (Ba)	mean	2.88E-06	1.12E-05	1.52E-05	1.58E-05	1.63E-05	1.67E-05
	5%	9.81E-07	2.50E-06	3.49E-06	3.71E-06	3.74E-06	3.79E-06
	25%	1.54E-06	4.37E-06	6.68E-06	6.78E-06	6.85E-06	6.90E-06
	50%	2.48E-06	7.56E-06	1.12E-05	1.14E-05	1.15E-05	1.16E-05
	75%	3.79E-06	1.36E-05	1.93E-05	2.01E-05	2.03E-05	2.08E-05
	95%	5.94E-06	3.43E-05	3.76E-05	4.01E-05	4.01E-05	4.08E-05
	min	7.53E-07	1.58E-06	1.85E-06	1.95E-06	1.95E-06	1.95E-06
	max	2.36E-05	1.43E-04	1.45E-04	1.46E-04	1.46E-04	2.18E-04
Class 4 Halogens (I)	mean	8.66E-08	3.85E-07	6.41E-07	6.43E-07	6.44E-07	6.45E-07
	5%	2.40E-08	6.95E-08	1.16E-07	1.16E-07	1.16E-07	1.18E-07
	25%	3.80E-08	1.08E-07	2.18E-07	2.19E-07	2.19E-07	2.20E-07
	50%	5.43E-08	1.82E-07	3.44E-07	3.45E-07	3.46E-07	3.46E-07
	75%	9.48E-08	3.54E-07	6.10E-07	6.11E-07	6.15E-07	6.19E-07
	95%	2.69E-07	1.17E-06	1.87E-06	1.87E-06	1.87E-06	1.88E-06
	min	1.31E-08	4.77E-08	5.02E-08	5.03E-08	5.03E-08	5.04E-08

RN group	Mean Percentiles Range	Release fraction after 2h	Release fraction after 4h	Release fraction after 8h	Release fraction after 12h	Release fraction after 16h	Release fraction after 24h
	max	2.36E-06	1.02E-05	1.02E-05	1.02E-05	1.02E-05	1.02E-05
Class 5 Chalcogens (Te)	mean	1.75E-05	2.91E-05	3.43E-05	3.62E-05	3.71E-05	3.77E-05
	5%	7.29E-06	9.57E-06	1.09E-05	1.17E-05	1.20E-05	1.21E-05
	25%	1.03E-05	1.39E-05	1.69E-05	1.86E-05	1.89E-05	1.91E-05
	50%	1.49E-05	2.14E-05	2.54E-05	2.67E-05	2.73E-05	2.77E-05
	75%	2.21E-05	3.70E-05	4.18E-05	4.32E-05	4.46E-05	4.53E-05
	95%	3.67E-05	7.03E-05	7.84E-05	8.59E-05	8.86E-05	9.09E-05
	min	5.11E-06	7.15E-06	8.18E-06	8.28E-06	8.32E-06	8.33E-06
	max	6.10E-05	3.74E-04	3.79E-04	3.80E-04	3.82E-04	3.84E-04
Class 6 Platinoids (Ru)	mean	8.24E-08	2.30E-07	4.21E-07	6.13E-07	7.16E-07	8.06E-07
	5%	1.31E-08	2.41E-08	3.40E-08	3.41E-08	3.42E-08	3.43E-08
	25%	2.56E-08	5.96E-08	9.12E-08	9.16E-08	9.16E-08	9.30E-08
	50%	5.24E-08	1.41E-07	2.12E-07	2.15E-07	2.15E-07	2.16E-07
	75%	1.12E-07	3.03E-07	4.24E-07	4.43E-07	4.49E-07	4.52E-07
	95%	2.57E-07	6.25E-07	1.07E-06	1.41E-06	1.64E-06	1.64E-06
	min	5.85E-09	1.03E-08	1.14E-08	1.19E-08	1.19E-08	1.19E-08
	max	4.46E-07	3.74E-06	1.66E-05	5.47E-05	6.87E-05	7.27E-05
Class 7 Early Transition Elements (Mo)	mean	3.81E-06	4.56E-06	4.85E-06	4.86E-06	4.86E-06	4.86E-06
	5%	7.22E-07	9.63E-07	1.07E-06	1.07E-06	1.07E-06	1.07E-06
	25%	1.40E-06	1.68E-06	1.83E-06	1.83E-06	1.83E-06	1.83E-06
	50%	2.60E-06	3.16E-06	3.50E-06	3.50E-06	3.50E-06	3.50E-06
	75%	5.44E-06	6.29E-06	6.65E-06	6.65E-06	6.65E-06	6.65E-06
	95%	1.08E-05	1.25E-05	1.28E-05	1.28E-05	1.28E-05	1.28E-05
	min	2.16E-07	4.31E-07	4.37E-07	4.37E-07	4.37E-07	4.37E-07
	max	1.79E-05	2.66E-05	2.80E-05	2.80E-05	2.80E-05	2.80E-05
Class 8 Tetravalent (Ce)	mean	1.88E-08	4.34E-08	7.61E-08	9.85E-08	1.15E-07	1.31E-07
	5%	4.36E-09	1.08E-08	1.29E-08	1.30E-08	1.31E-08	1.31E-08
	25%	7.23E-09	1.82E-08	2.48E-08	2.49E-08	2.49E-08	2.50E-08
	50%	1.32E-08	3.24E-08	4.20E-08	4.33E-08	4.33E-08	4.35E-08
	75%	2.55E-08	5.39E-08	7.17E-08	7.24E-08	7.32E-08	7.47E-08
	95%	5.19E-08	1.12E-07	1.89E-07	2.13E-07	2.36E-07	2.36E-07
	min	2.65E-09	5.89E-09	5.93E-09	5.93E-09	5.93E-09	5.93E-09
	max	8.56E-08	2.92E-07	1.85E-06	6.33E-06	1.00E-05	1.33E-05
Class 9 Trivalents (La)	mean	1.86E-08	4.28E-08	7.49E-08	9.72E-08	1.13E-07	1.30E-07
	5%	4.22E-09	1.06E-08	1.23E-08	1.25E-08	1.26E-08	1.26E-08
	25%	7.12E-09	1.78E-08	2.41E-08	2.45E-08	2.45E-08	2.46E-08
	50%	1.30E-08	3.18E-08	4.17E-08	4.27E-08	4.27E-08	4.28E-08
	75%	2.53E-08	5.36E-08	7.13E-08	7.21E-08	7.31E-08	7.39E-08
	95%	5.17E-08	1.09E-07	1.85E-07	2.13E-07	2.32E-07	2.32E-07
	min	2.53E-09	5.59E-09	5.63E-09	5.63E-09	5.63E-09	5.63E-09

RN group	Mean Percentiles Range	Release fraction after 2h	Release fraction after 4h	Release fraction after 8h	Release fraction after 12h	Release fraction after 16h	Release fraction after 24h
	max	8.53E-08	2.89E-07	1.85E-06	6.33E-06	1.00E-05	1.33E-05
Class 10 Uranium (U)	mean	8.68E-07	1.68E-06	2.15E-06	2.18E-06	2.20E-06	2.23E-06
	5%	1.73E-07	3.24E-07	3.61E-07	3.61E-07	3.61E-07	3.61E-07
	25%	3.16E-07	6.13E-07	7.43E-07	7.49E-07	7.49E-07	7.54E-07
	50%	5.95E-07	1.21E-06	1.48E-06	1.48E-06	1.50E-06	1.50E-06
	75%	1.16E-06	2.19E-06	2.64E-06	2.64E-06	2.64E-06	2.64E-06
	95%	2.45E-06	4.96E-06	5.85E-06	6.27E-06	6.60E-06	6.60E-06
	min	8.15E-08	1.30E-07	1.30E-07	1.30E-07	1.30E-07	1.30E-07
	max	4.05E-06	1.30E-05	2.35E-05	2.43E-05	2.48E-05	2.54E-05
Class 11 More Volatile Main Group (Cd)	mean	1.07E-05	2.98E-05	3.64E-05	3.73E-05	3.78E-05	3.82E-05
	5%	3.33E-06	4.62E-06	5.82E-06	5.93E-06	5.96E-06	6.00E-06
	25%	5.55E-06	8.37E-06	1.21E-05	1.23E-05	1.24E-05	1.25E-05
	50%	8.91E-06	1.94E-05	2.50E-05	2.57E-05	2.59E-05	2.65E-05
	75%	1.49E-05	3.88E-05	4.79E-05	4.82E-05	4.86E-05	4.87E-05
	95%	2.26E-05	8.70E-05	9.83E-05	9.98E-05	9.99E-05	1.01E-04
	min	2.20E-06	3.00E-06	3.71E-06	3.73E-06	3.73E-06	3.73E-06
	max	6.17E-05	4.54E-04	4.55E-04	4.55E-04	4.55E-04	4.55E-04
Class 12 Less Volatile Main Group (Ag)	mean	7.15E-06	1.08E-05	1.25E-05	1.25E-05	1.25E-05	1.25E-05
	5%	1.97E-06	3.26E-06	3.63E-06	3.66E-06	3.66E-06	3.66E-06
	25%	3.17E-06	5.40E-06	6.59E-06	6.67E-06	6.71E-06	6.71E-06
	50%	5.36E-06	8.44E-06	1.01E-05	1.02E-05	1.02E-05	1.02E-05
	75%	9.92E-06	1.47E-05	1.61E-05	1.62E-05	1.62E-05	1.62E-05
	95%	1.81E-05	2.25E-05	2.52E-05	2.52E-05	2.52E-05	2.55E-05
	min	1.07E-06	2.24E-06	2.40E-06	2.40E-06	2.40E-06	2.40E-06
	max	2.64E-05	1.42E-04	1.43E-04	1.43E-04	1.43E-04	1.43E-04
Class 16 Cesium Iodide (CsI)	mean	3.59E-05	4.76E-05	1.04E-04	1.42E-04	1.61E-04	1.79E-04
	5%	1.93E-05	2.08E-05	3.78E-05	4.39E-05	4.76E-05	5.08E-05
	25%	2.57E-05	2.94E-05	5.52E-05	6.53E-05	7.04E-05	7.52E-05
	50%	3.34E-05	4.31E-05	7.53E-05	9.30E-05	1.01E-04	1.09E-04
	75%	4.49E-05	6.04E-05	1.10E-04	1.40E-04	1.60E-04	1.81E-04
	95%	6.08E-05	8.32E-05	2.14E-04	3.79E-04	4.53E-04	5.21E-04
	min	1.44E-05	1.58E-05	2.29E-05	2.44E-05	2.52E-05	2.62E-05
	max	7.51E-05	1.84E-04	1.31E-03	1.73E-03	1.95E-03	2.05E-03
Class 17 Cesium Molybdate (Cs2MoO4)	mean	1.38E-05	2.84E-05	3.52E-05	3.55E-05	3.56E-05	3.57E-05
	5%	5.65E-06	9.38E-06	1.19E-05	1.20E-05	1.21E-05	1.21E-05
	25%	7.88E-06	1.59E-05	2.07E-05	2.11E-05	2.11E-05	2.11E-05
	50%	1.17E-05	2.51E-05	3.16E-05	3.19E-05	3.22E-05	3.22E-05
	75%	1.80E-05	3.56E-05	4.51E-05	4.52E-05	4.52E-05	4.53E-05
	95%	2.94E-05	5.85E-05	7.23E-05	7.26E-05	7.26E-05	7.26E-05
	min	4.29E-06	6.33E-06	6.85E-06	6.85E-06	6.85E-06	6.85E-06

RN group	Mean Percentiles Range	Release fraction after 2h	Release fraction after 4h	Release fraction after 8h	Release fraction after 12h	Release fraction after 16h	Release fraction after 24h
	max	3.78E-05	1.83E-04	2.03E-04	2.03E-04	2.03E-04	2.03E-04

Appendix B. Sensitivity and uncertainty analysis results - RC4

Appendix B.1. SA results

Appendix B.2. Release fractions during LOCA

The Morris indices (modified mean and standard deviation) for CS release fraction during LOCA-IDEJ0 is shown in Figure B-1 and during LOCA-IDEJ1 is shown in Figure B-2. First release here is when the earliest LHF (among 400 runs) is detected, and FP is released to the environment.

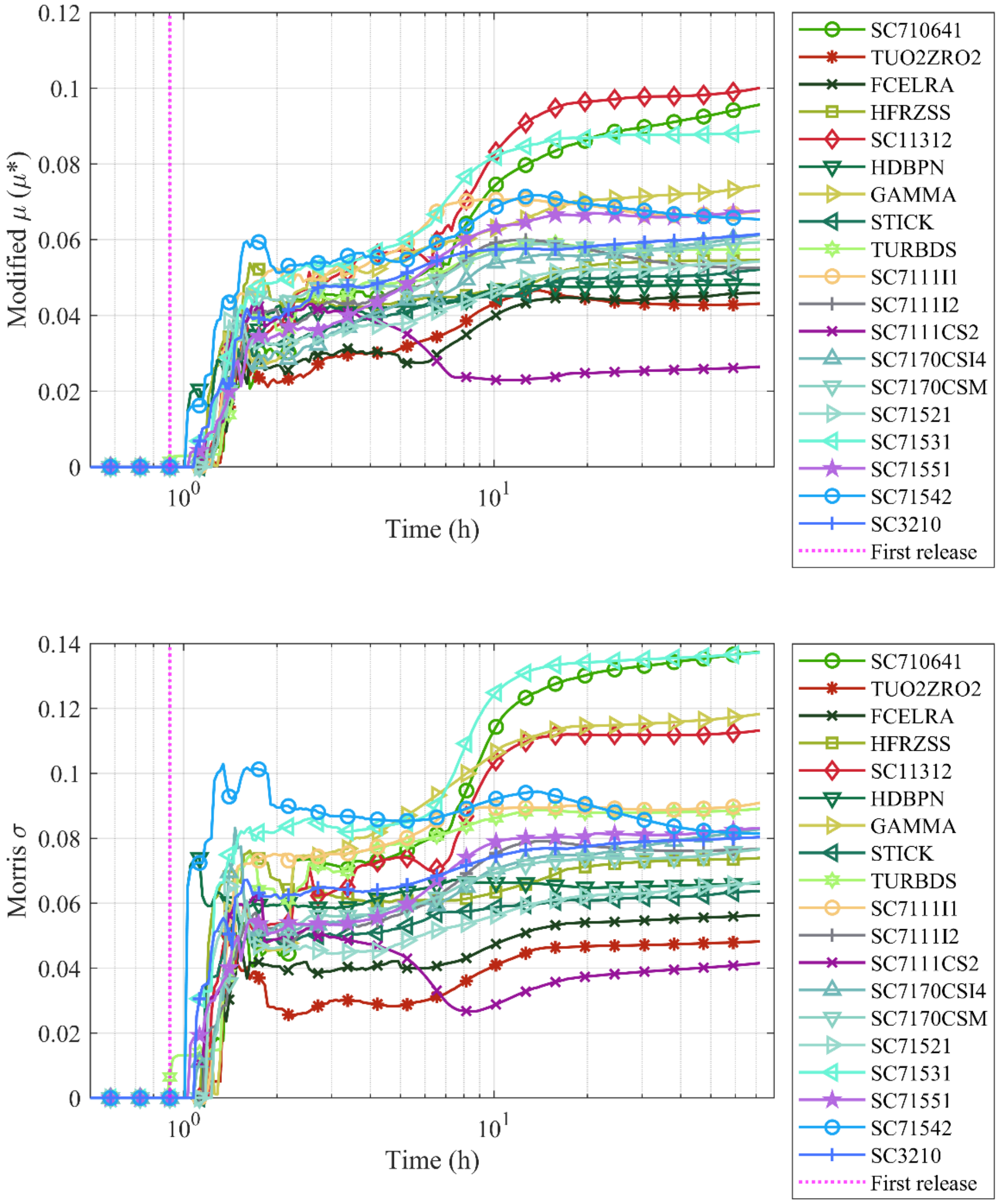

Figure B-1 Evolution of Morris sensitivity indices for CS release fraction (LOCA-IDEJ0).

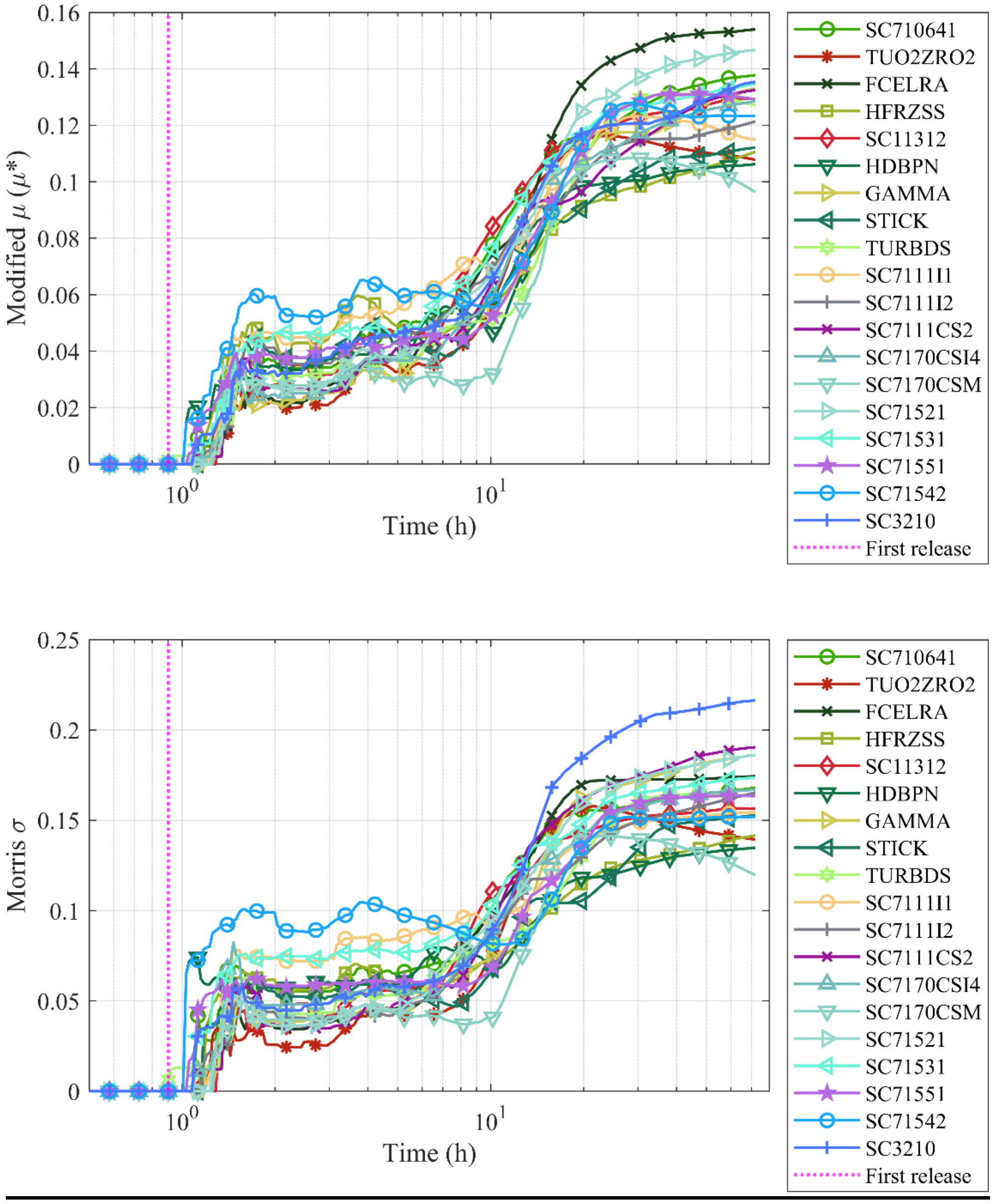

Figure B-2 Evolution of Morris sensitivity indices for CS release fraction (LOCA-IDEJ1).

The Morris indices for I2 release fraction during LOCA-IDEJ0 is shown in Figure B-3 and during LOCA-IDEJ1 is shown in Figure B-4.

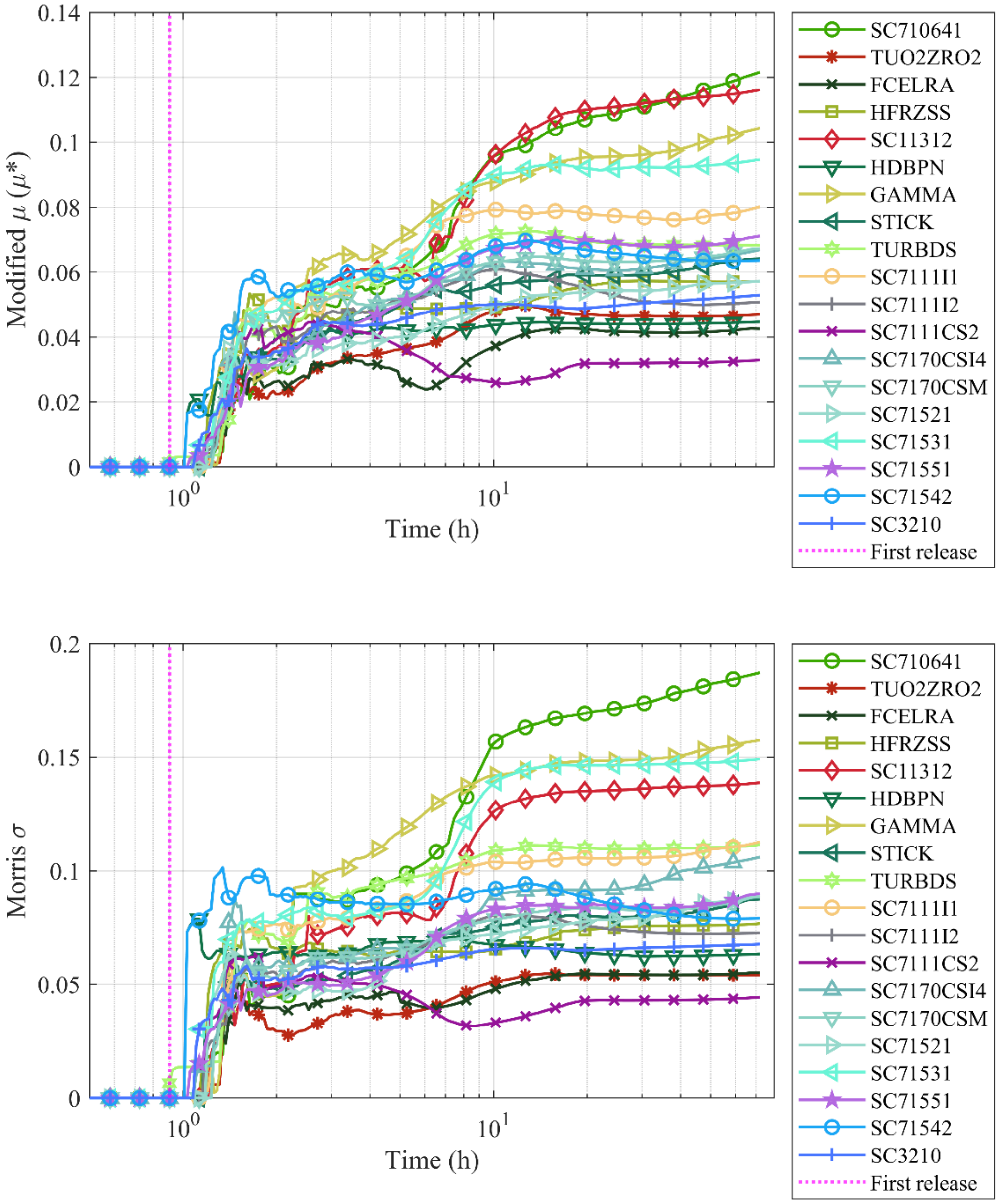

Figure B-3 Evolution of Morris sensitivity indices for I2 release fraction (LOCA-IDEJ0).

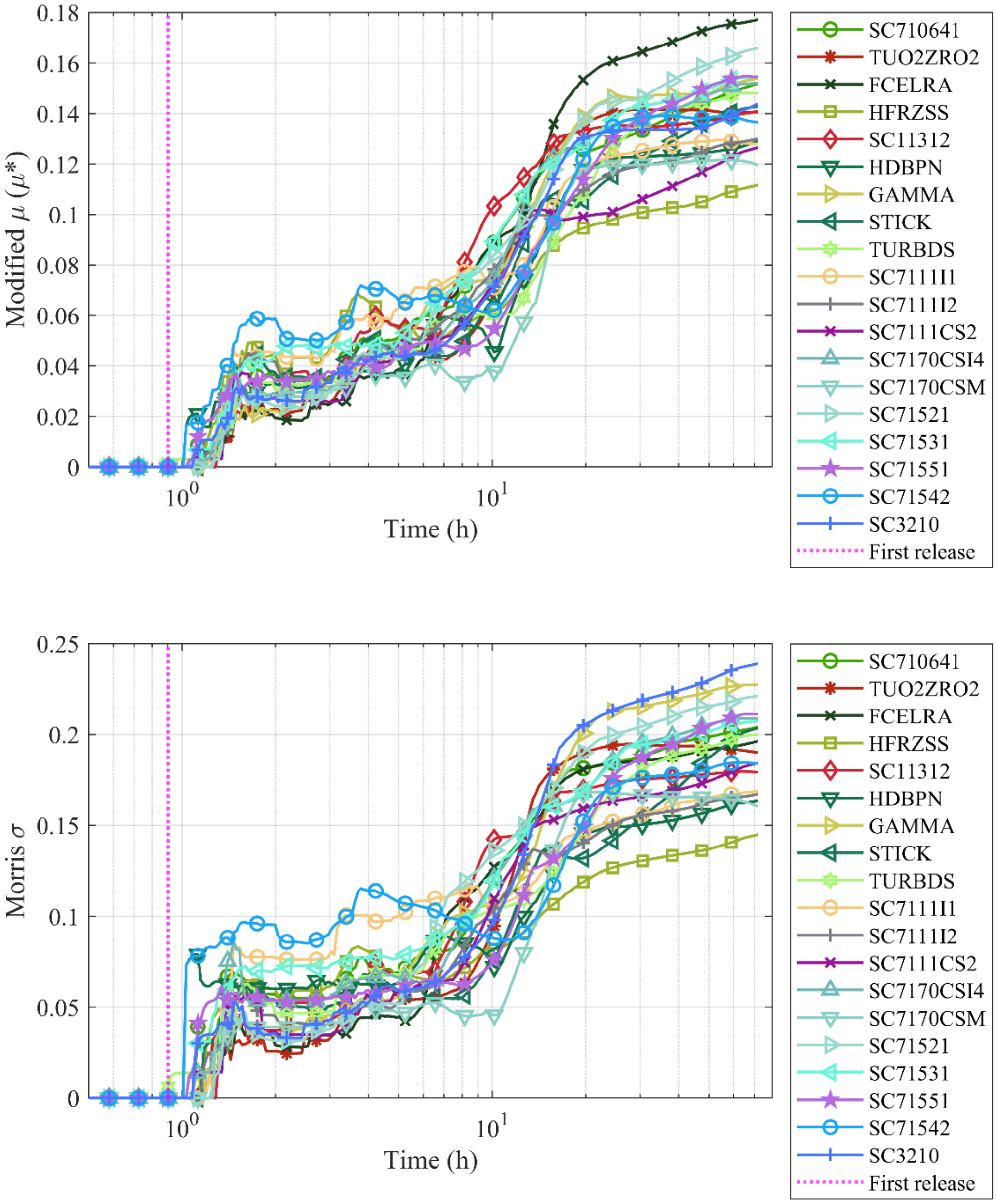

Figure B-4 Evolution of Morris sensitivity indices for I2 release fraction (LOCA-IDEJ1).

Release fractions during SBO

The Morris indices (modified mean and standard deviation) for CS release fraction during SBO-IDEJ0 is shown in Figure B-5 and during SBO-IDEJ1 is shown in Figure B-6.

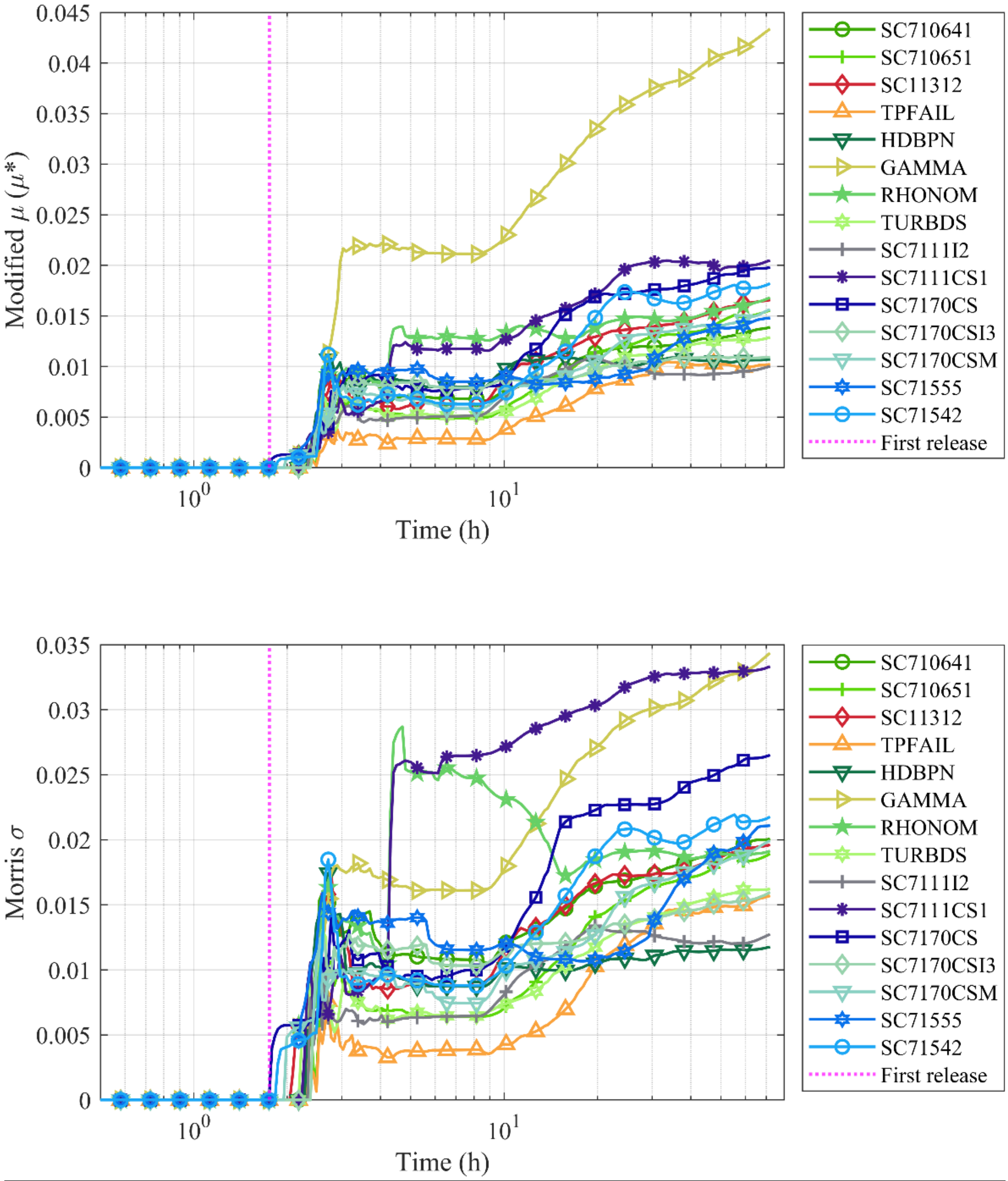

Figure B-5 Evolution of Morris sensitivity indices for CS release fraction (SBO-IDEJ0).

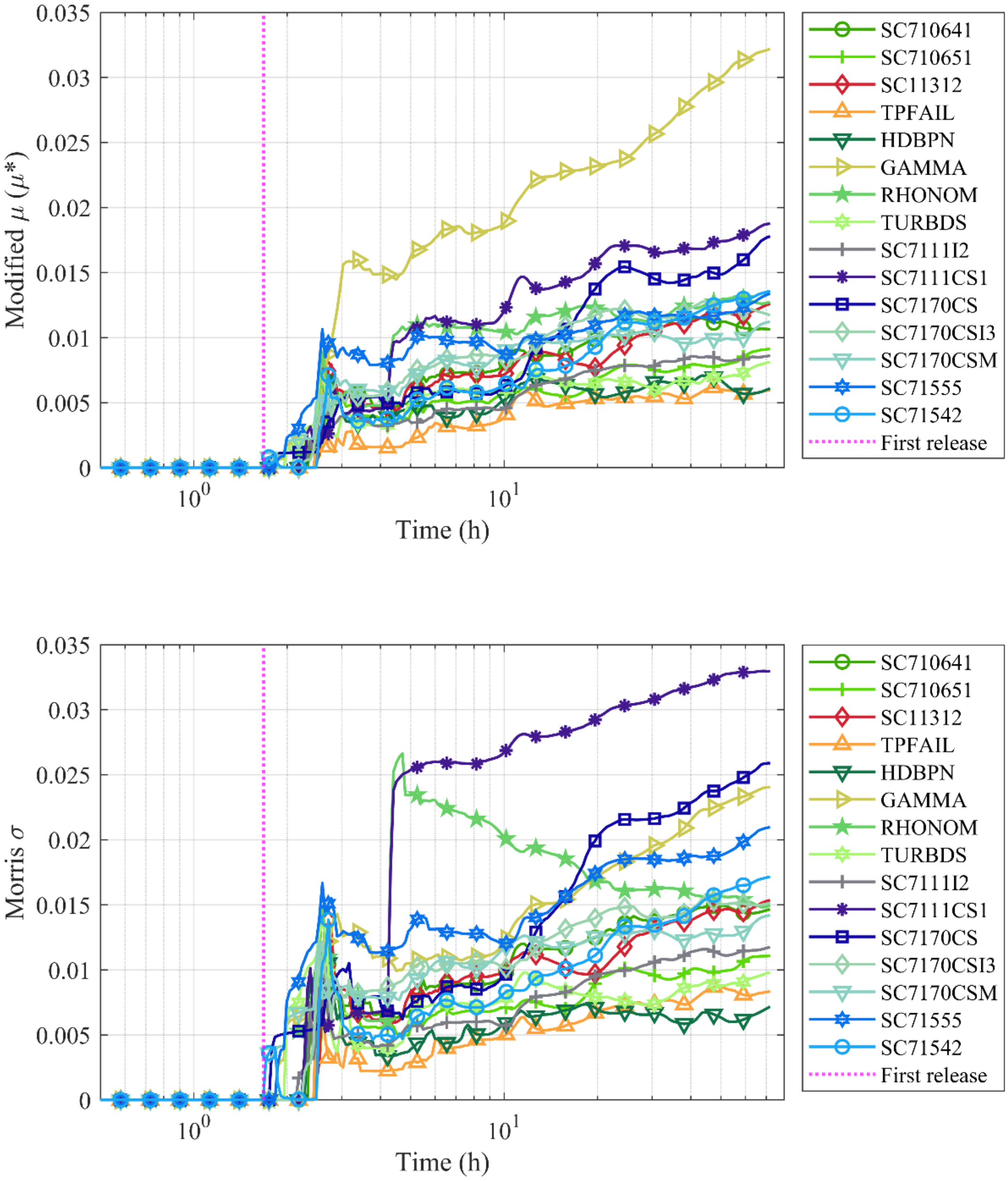

Figure B-6 Evolution of Morris sensitivity indices for CS release fraction (SBO-IDEJ1).

The Morris indices (modified mean and standard deviation) for I2 release fraction during SBO-IDEJ0 is shown in Figure B-7 and during SBO-IDEJ1 is shown in Figure B-8.

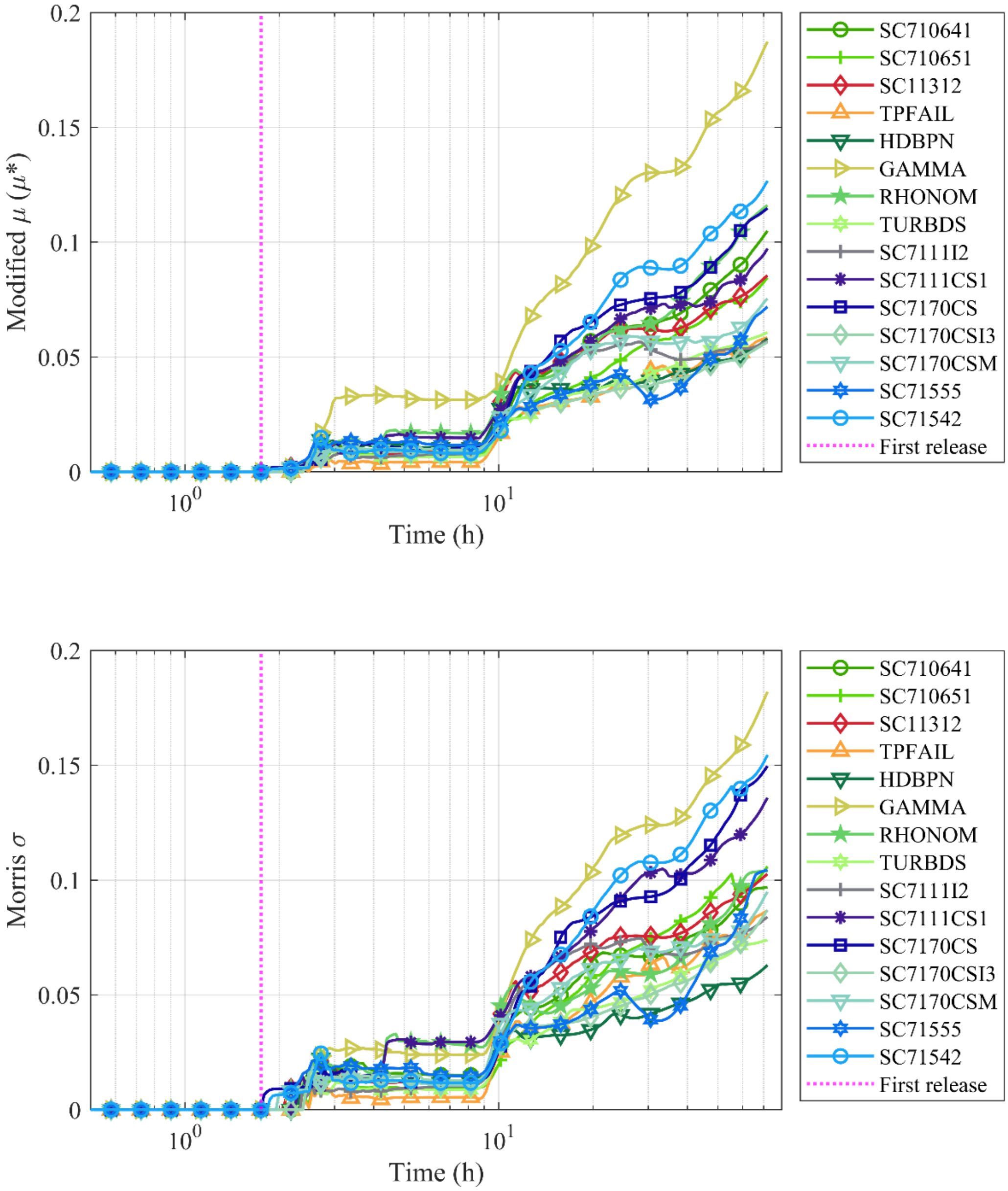

Figure B-7 Evolution of Morris sensitivity indices for I2 release fraction (SBO-IDEJ0).

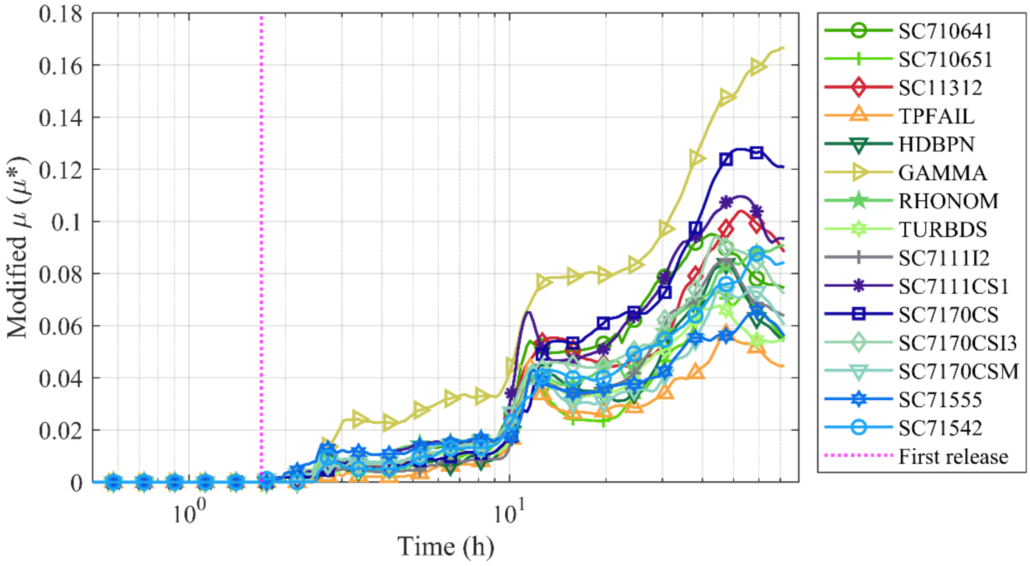

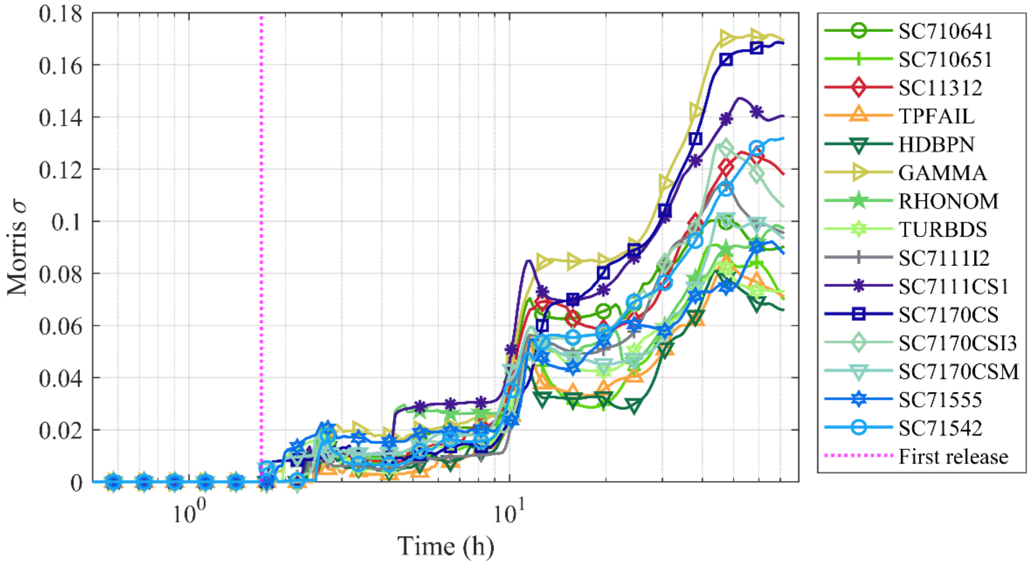

Figure B-8 Evolution of Morris sensitivity indices for I2 release fraction (SBO-IDEJ1).

Appendix B.3. UA results

CS release fractions during LOCA and SBO

The CS release fractions obtained during the 150 trials of LOCA-IDEJ0 and LOCA-IDEJ1 are shown in Figure B-9 and Figure B-10, and of SBO-IDEJ0 and SBO-IDEJ1 in Figure B-11 and Figure B-12. The 5th/95th percentiles and the mean, along with the 95% confidence intervals of the mean are also presented in the figures (neon blue lines represent the upper and lower whisker lengths in each figure).

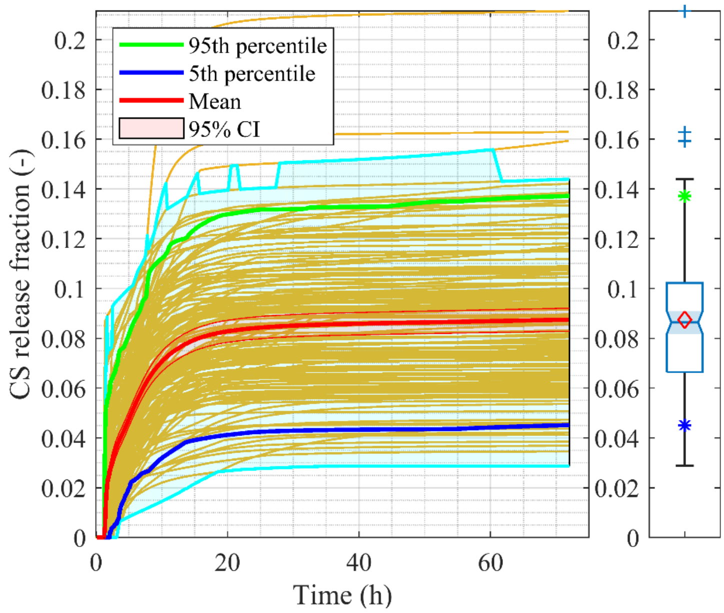

Figure B-9 CS release fractions to the environment during LOCA-IDEJ0.

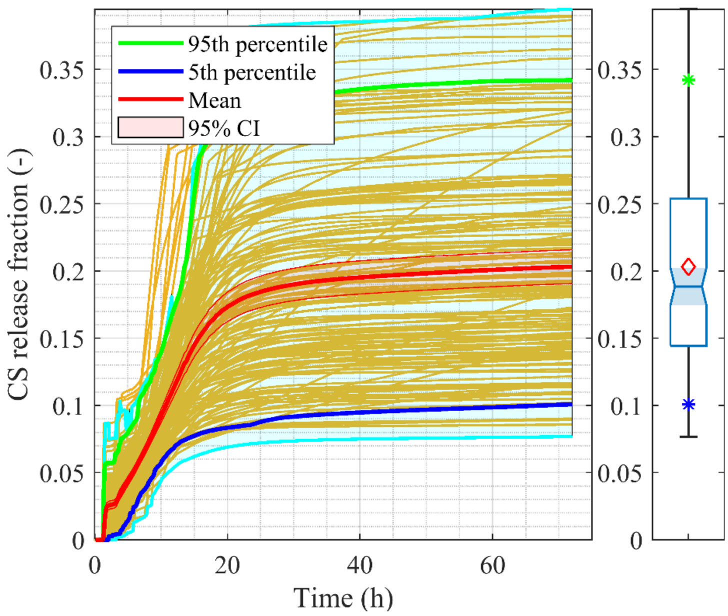

Figure B-10 CS release fractions to the environment during LOCA-IDEJ1.

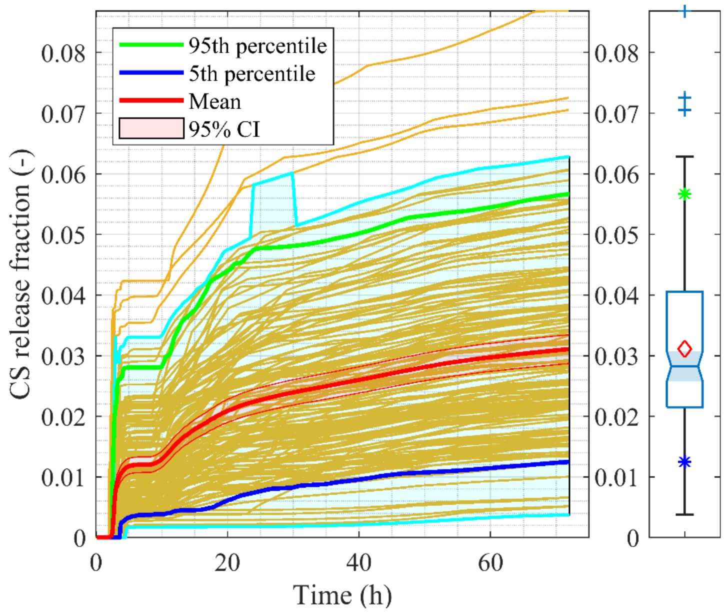

Figure B-11 CS release fractions to the environment during SBO-IDEJ0.

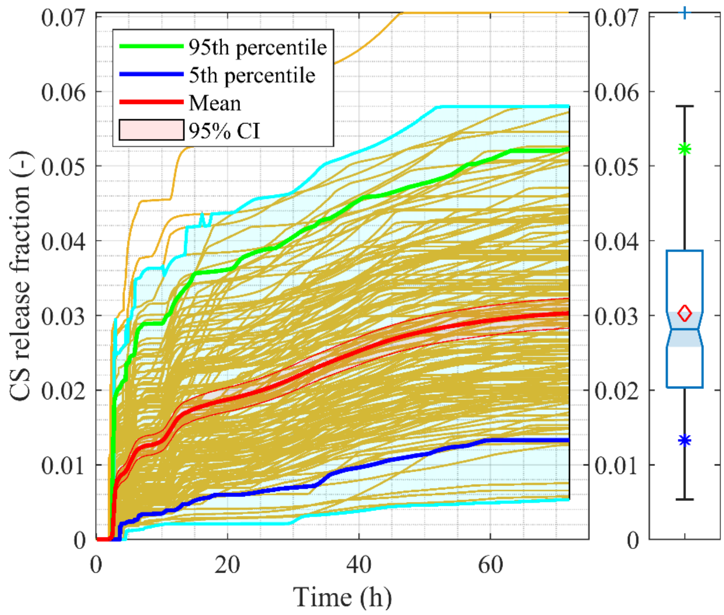

Figure B-12 CS release fractions to the environment during SBO-IDEJ1.

I2 release fractions during LOCA and SBO

The I2 release fractions obtained during the 150 trials of LOCA-IDEJ0 and LOCA-IDEJ1 are shown in Figure B-13 and Figure B-14, and of SBO-IDEJ0 and SBO-IDEJ1 in Figure B-15 and Figure B-16. The $5^{th}/95^{th}$ percentiles and the mean, along with the 95% confidence intervals of the mean are also presented in the figures.

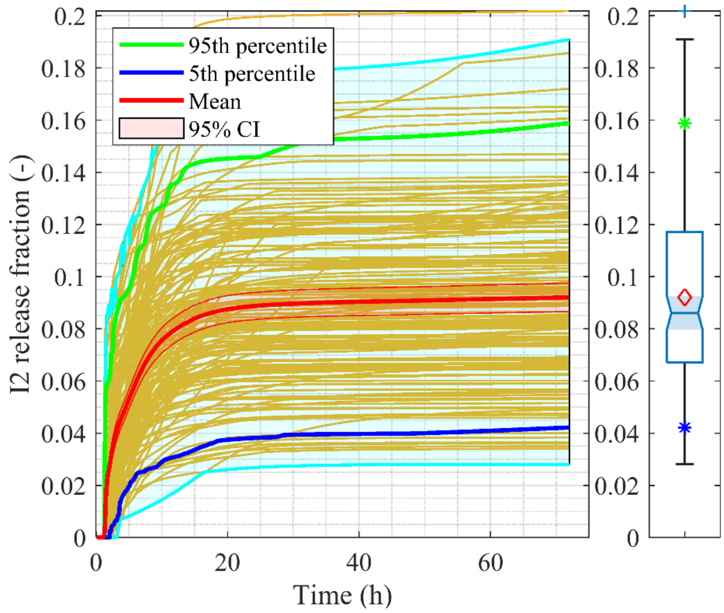

Figure B-13 I2 release fractions to the environment during LOCA-IDEJ0.

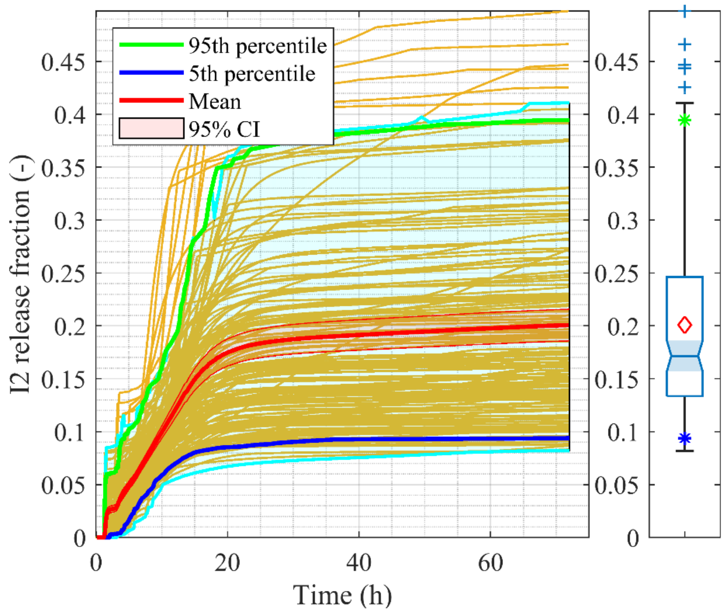

Figure B-14 I2 release fractions to the environment during LOCA-IDEJ1.

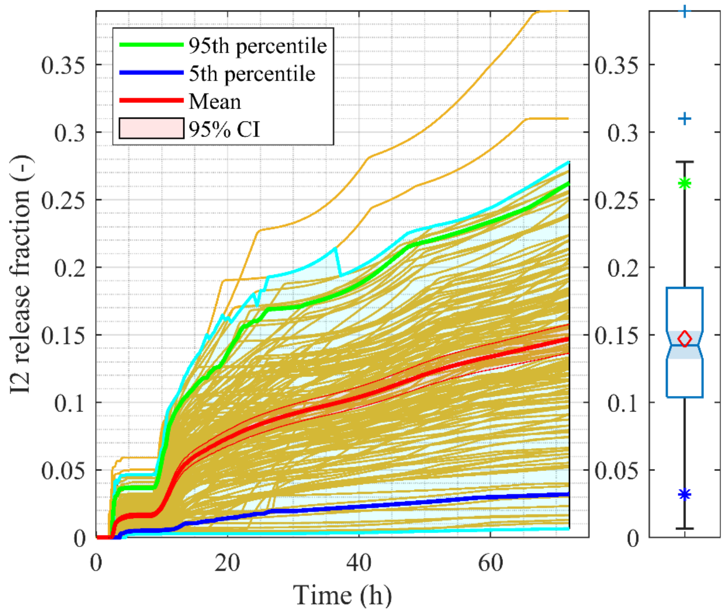

Figure B-15 I2 release fractions to the environment during SBO-IDEJ0.

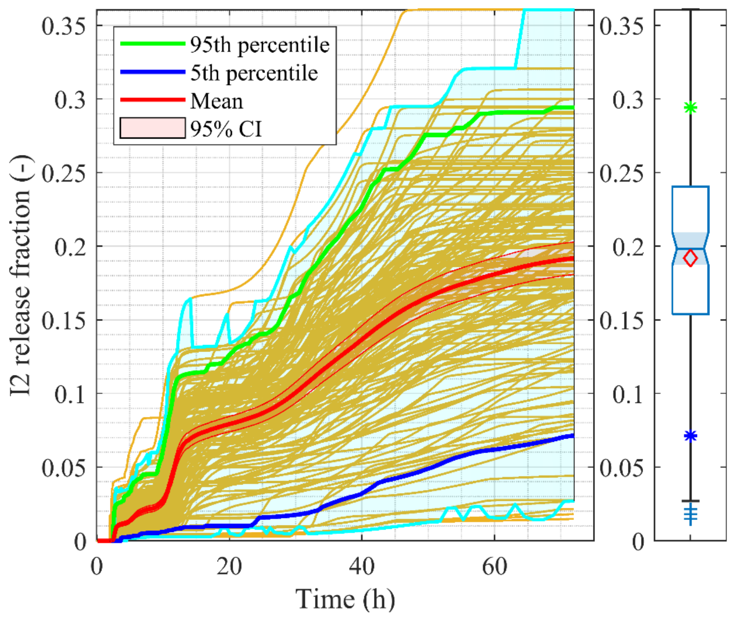

Figure B-16 I2 release fractions to the environment during SBO-IDEJ1.

Bibliographic Data Sheet	**NKS-475**

Title	Source Term and Timing Uncertainty in Severe accidents NKS-STATUS Phase 2 report
Author(s)	Sergey Galushin[1], Govatsa Acharya[2], Dmitry Grischenko[2], Pavel Kudinov[2] Sara Ojalehto[3], Tuomo Sevón[3], Ilona Lindholm[3] Patrick Isaksson[4], Elisabeth Tengborn[4] Naeem Ul-Syed[5]
Affiliation(s)	[1] Vysus Sweden AB [2] KTH Royal Institute of Technology [3] VTT Technical Research Centre of Finland Ltd [4] SSM Swedish Radiation Safety Authority [5] DSA Norwegian Radiation and Nuclear Safety Authority
ISBN	978-87-7893-570-0
Date	July 2023
Project	NKS-R / STATUS activity NKS-R(21)133/5
No. of pages	160
No. of tables	42
No. of illustrations	170
No. of references	39
Abstract max. 2000 characters	The overall goal of the project is to generate a body of knowledge regarding the uncertainty in the magnitude of fission products release in case of a potential severe accident in Nordic nuclear power plants. The work aims to provide insights into the effect of various types of uncertainty on the source term predictions. Results of the work will be useful both for probabilistic and deterministic safety assessments as well as for emergency response applications. Within the second phase of the project sensitivity and uncertainty analyses were performed for a set of risk significant accident scenarios identified by the review of PSA L2 for a typical Nordic BWR within the first phase of the project. These scenarios include accident sequences that lead to filtered containment venting in case of a transient or LOCA, and accident sequences that lead to containment failure due to ex-vessel phenomena in case of a transient or LOCA. To perform sensitivity and uncertainty analyses, a review of available methods and tools for sensitivity analysis and uncertainty

quantification was performed, selected methods were implemented in the simulation tools used in the project.

Sensitivity analysis was performed to identify the most influential MELCOR code modelling parameters for selected accident scenarios. These parameters involved in the modelling of core degradation and relocation, fission products release from fuel, debris behaviour in the core region and vessel lower head, vessel lower head failure, fission products behaviour in the RCS and the containment, as well as modelling of the filter trapping, containment sprays and pool scrubbing.

The most influential MELCOR code modelling parameters were then considered in quantification of uncertainty in the magnitude and timing of the fission products release to the environment.

Key words Severe accident, uncertainty quantification, MELCOR, Nordic BWR, fission products, source term

Available on request from the NKS Secretariat, P.O.Box 49, DK-4000 Roskilde, Denmark.
Phone (+45) 4677 4041, e-mail nks@nks.org, www.nks.org